

The Use of Polymeric Systems to Control Microenvironment and Moderate Anion Binding Affinities



Bunian A. Shareef

Department of Chemistry
The University of Sheffield

Submitted to the University of Sheffield in fulfilment
of the requirements for the degree of
Doctor of Philosophy

November 2019

Declaration

I hereby declare that the research discussed has not been submitted, either entirely or partly, for this or any other degree. All the work presented in this thesis is the original work of the author, except where other sources have been acknowledged by references. This work was carried out at the University of Sheffield between November 2015 and November 2019.

Signature:

Date:

Acknowledgments

First and foremost I would like to express my sincere gratitude to my supervisor Dr. Lance Twyman. Thank you for your on-going support and expertise throughout the course of my studies. Without your guidance, patience and encouragement, this thesis would not have been possible.

This work would not have been possible without the help of many colleagues, so I would like to express my gratitude to the following people: Dr. Sandra van Meurs and Dr. Craig Robertson for help with NMR and X-Ray crystallography, Keith Owen for Grubbs training and technical help, IT team for their computer knowledge, Simon Thorpe for Mass spectrometry, Dan Jackson for glass repair. I would also like to express my thanks to Nick Smith, Louise Brown-Leng and Denise Richards, you have all shown me such kindness, made me laugh and helped me enormously over the years and I am extremely grateful to you all.

In addition, I would like to express my gratitude to everyone on D floor for providing an enjoyable and relaxed work environment. I have made many friends over the years and my experience working on D floor has been a thoroughly enjoyable one. A special thank you must go to the research technician Heather Grievson, your expertise over the last four years has helped me hugely and I am extremely thankful. Furthermore, I would like to convey my sincere appreciation to my friends and colleagues Ammar Eid, Hamza Qasim, Devanish Singh, Fatema Aboshnaf, Talal Alghassab, Ibrahim Althobaiti, Meng Fan, Abdullah Neda and Alaa Kadhim, and my friends from Dr. Ahmad Iraqi group. Thank you all for your friendship, helping me preserve my sanity and for making my PhD a much more enjoyable experience.

My final thanks must go to my mum and dad and my brothers and sisters. Thank you for your continued love and support, without which none of this would be possible. Thank you for not only believing in me, but putting up with me through the difficult times as I know it could not have been easy. I love you all with all my heart and I am eternally grateful for all you have done for me.

Abstract

This research has examined a variety of macromolecules; including hyperbranched polymers, di-block copolymers and tri-block copolymers. The architecture of these materials has been exploited for anion binding and transportation applications. The first area of study focussed on the interior properties of hyperbranched polymers. This work looked at controlling the environment surrounding a receptor and anion binding was the tool used to probe these properties. Hyperbranched poly 3,5 diacetoxybenzoic acid of varying molecular weights was used to house an anion receptor and the effect upon binding affinities of a variety of anions was measured. The polymer had a positive effect upon binding and transporting the 4-nitrophenolate anion from one aqueous layer to another through organic media. However, a different observation was made for the polymeric receptors than the free receptor. For the small and medium sized polymers (3,000 and 6,000 Mw respectively), the binding was higher than the free receptor only, although, binding dropped significantly for the highest molecular weight studied (14,000 Mw). For a water-soluble anion receptor system a different approach was employed. This consisted of a biocompatible di-block copolymer micelle composed of poly (ethylene glycol) and poly (ϵ -caprolactone) (mPEG-*b*-PCLn). The free receptor and medium hyperbranched polymer (6,000 Mw) was encapsulated within micelles. Encapsulation and stability of complexes was verified by UV/Vis spectroscopy. The next area studied continued the theme of encapsulation using di-block polymers. This work involved tethering mPEG with a receptor and co-micellized with di-block copolymers, where the co-micellization properties of complexes were probed using fluorescence spectroscopy. The final area involved covalently incorporate binding sites as co-monomers during controlled synthesis of amphiphilic terpolymers using atom transfer radical polymerisation (ATRP). This polymer would consist of a PEG block and a second block containing both the copolymer of methyl methacrylate and an anion receptor. For binding characterisation, displacement approach was conducted using Uiv-Vis measurements.

Table of Contents

Declaration.....	i
Acknowledgments	ii
Abstract.....	iii
Abbreviations	x
Chapter One: Introduction	1
1.1 Introduction	2
1.1.1 Anion Coordination Chemistry	5
1.1.2 Biological Anion Receptors.....	17
1.1.3 Receptors for radioactive anions and decontamination.....	21
Chapter Two: Functionalisation of HBP for Controlled Microenvironment of Isophthalamide Anion Receptor.....	25
2.1. Introduction	26
2.1.1 Hyperbranched polymers: Structures and properties.....	26
2.1.2. Synthesis of HBPs	28
2.1.3. Applications of HBPs	29
2.1.4. Use of HBPs in anion recognition	30
2.1.5. The optimum molecular weight of HBPs for anionic interaction	31
2.1.6. Principles of anion binding receptor.....	32
2.2. Aim and Objectives	34
2.2.1 Synthetic approach and consideration.....	35

2.2.3. Transportation of anion within an organic soluble environment.....	39
2.3. Results and Discussion	41
2.3.1. Synthesis of N,N'-bis-(3-acetoxyphenyl) isophthalamide.....	41
2.3.2. Synthesis of monomer unit 3,5-diacetoxybenzoic acid.....	46
2.3.3. Homo polymerisation of 3,5-diacetoxybenzoic acid.....	48
2.3.4. Synthesis of core functionalised HBP 1:15	52
2.3.5. Synthesis of core functionalised HBP 1:5	56
2.3.6. Synthesis of core functionalised HBP 1:25	57
2.3.7. Anion binding assay using ¹ HNMR titration analysis.....	61
2.3.8. UV-Vis anion transportation study.....	64
2.4. Conclusion.....	69
2.5. Experimental.....	71
2.5.1 Chemicals and Instrumentation	71
2.5.2. Synthesis of N,N'-bis-(3-hydroxyphenyl)-isophthalamide (2).....	73
2.5.3. Acetylation of N, N'-bis-(3-actoxyphenyl)-isophthalamide (R1).....	73
2.5.4. Synthesis of 3,5-diacetoxybenzoic acid (3).....	74
2.5.5. General procedure for polymerisation of 3,5-diacetoxybenzoic acid.....	76
Chapter Three: Incorporated Hydrophobic Anion Binding Receptors within Water-Soluble Diblock Polymers	82
3.1 Introduction	83
3.1.1 Diblock copolymers: Structures and properties.....	83

3.1.2 Synthesis of diblock copolymers	84
3.1.3 Self-assembly of diblock copolymers	86
3.1.4 Exploiting the encapsulation properties of polymeric micelles	89
3.2 Aim and Objectives	91
3.3 Results and Discussion	94
3.3.1 Synthesis of mPEG ₄₅ - <i>b</i> -PCL _n diblock copolymers	94
3.3.2 Aggregation of Diblock Copolymers into Micelle Structures	96
3.3.3 Determination of critical micelle concentration (CMC).....	98
3.3.4 Non-covalent encapsulation of anion receptor	102
3.4 Conclusion	107
3.5 Experimental.....	108
3.5.1 Chemicals and Instrumentation	108
3.5.2. General procedure for the synthesis of di-block copolymers	110
3.5.3 Micelle formation	112
3.5.4 Encapsulation of HBP within polymeric micelles.....	112
Chapter Four: Co-micellization of mPEG-Amide Anion Binding Receptor with Water-Soluble Diblock Polymers	113
4.1 Introduction	114
4.1.1 Amide based receptors.....	116
4.2 Aim and Objectives	119
4.3 Results and Discussion	121

4.3.1. Synthetic strategies for designing a functionalised mPEG.....	121
4.3.2. Anion binding assay using NMR titration.....	128
4.3.3. Co-micellization of receptor R2 within micelles (Host formation).....	129
4.3.4. Stability of co-micelle system during extraction.....	134
4.3.5. Anion binding studies of the co-micelle host system.....	134
4.4 Conclusion.....	138
4.5 Experimental.....	139
4.5.1. Chemicals and Instrumentation.....	139
4.5.2 Synthesis of 3,5-bis(benzoylamino) benzoic acid (1).....	140
4.5.3 Synthesis of methoxy polyethylene glycol tosylate (2).....	141
Chapter Five: Synthesis of Amphiphilic Anion Sensors Using ATRP.....	143
5.1 Introduction.....	144
5.1.1. Anion sensors.....	144
5.1.2. Polymer based anion receptors.....	147
5.1.3 Controlled polymerisation.....	149
5.1.4. AGET ATRP.....	151
5.2 Aim and Objectives.....	154
5.3 Results and Discussion.....	157
5.3.1 Synthesis of mPEG macroinitiator.....	157
5.3.2 Synthesis of acryloyloxy-based isophthalamide monomers.....	159
5.3.3 Acylation of 5-amino isophthalic acid with methacryloyl chloride.....	164

5.3.4 Synthesis of 5-methacrylamide-N,N'-dipropyl isophthalamide or N-(3,5-dipropylamine isophthaloyl)-2-methylprop-2-enamide (R4)	165
5.3.5. Anion binding assay using ¹ HNMR titration.....	168
5.3.6 Displacement approach using UV-Vis spectroscopy	170
5.3.7 Copolymerisation of methyl methacrylate and receptor R4 using ATRP.....	172
5.5.4 Conclusion.....	175
5.5 Experimental.....	176
5.5.1 Chemicals and Instrumentation	176
5.5.2 Synthesis of mPEG macroinitiator (5).....	178
5.5.3 Synthesis of 5-methacryloyloxy isophthalic acid (1)	179
5.5.4 Synthesis of 5-methacryloyloxy isophthaloy-N,N'-diphenyl amine monomer (R3).	179
5.5.5 Synthesis of 5-methacrylamide isophthalic acid (2).....	180
5.5.6 Synthesis of 5-methacrylamide-N,N'-dipropyl isophthalamide (R4).....	180
5.5.7 ATRP (General procedure).....	181
5.5.8 AGET ATRP (General procedure).....	182
References	184

Abbreviations

Stander Abbreviations

¹³C-NMR - Carbon Nuclear Magnetic Resonance Spectrometry

¹H-NMR - Proton Nuclear Magnetic Resonance Spectrometry

FTIR - Fourier Transform Infrared Spectroscopy

IR - Infrared Spectroscopy

DLS - Dynamic Light Scattering

GPC - Gel Permeation Chromatography

ES MS - Electrospray Ionisation Mass Spectrometry

MALDI-TOF-MS - Matrix Assisted Laser Desorption Ionisation Time of Flight Mass Spectroscopy

UV/Vis - Ultraviolet-visible

CMC - Critical Micelle Concentration

DB - Degree of Branching

M_n - Number Average Molecular Weight

M_w - Weight Average Molecular Weight

PD – Polydispersity

HBP - Hyperbranched Polymer

MMA - Methyl methacrylate

mPEG- methoxy Polyethylene Glycol

PCL - Poly (ε-caprolactone)

ppm - part per million

ATRP - Atomic Transfer Radical Polymerisation

ROP - Ring Opening Polymerisation

NMR Abbreviations

δ – Chemical Shift

s – singlet

d – doublet

t – triplet

q – quartet

m – multiplet

br – broad

o – *ortho*

m – *meta*

p – *para*

Chapter One: Introduction

1.1 Introduction

Research into anion recognition chemistry began around fifty years ago when Lehn reported on cryptand cation coordination chemistry and Pedersen published his study describing the coordination chemistry and synthesis of crown ethers. By the 1970s, most of the research interest was focused upon group 1 and 2 metal and ammonium cation coordination chemistry. By the twenty-first century, the cation recognition area of supramolecular chemistry has become well established. However, besides a handful of exceptions, anion coordination chemistry had largely been neglected (until about twenty years ago). It is only within these last two decades that the innate problems of binding anions has been given mainstream consideration.¹ The surge in interest in this aspect of coordination chemistry can be attributed to a number of factors, including being universal in biological systems. For example, DNA is a polyanion and most enzyme co-factors and substrates are anions. The protease, carboxypeptidase A, hydrolyses the peptide bond of the carboxylate group at the C-terminal in polypeptides by forming an arginine–aspartate salt bridge.² Salt-bridge binding motifs are implicated in the interactions between protein and the stem loop of RNA and in zinc finger/DNA complexes.^{3,4}

These examples highlight the key contribution of anions to many different aspects of biology. However, not all anion interactions are beneficial to life. For example, the diseases epilepsy, myotonia and cystic fibrosis are attributed, in part, to the dysregulation of chloride ion flux.⁵⁻⁷ Polluting anions are harmful to the environment, for example, the excessive use of fertilisers containing phosphate causes the eutrophication of rivers, also nitrate metabolites cause cancer.^{8,9} Furthermore, the environment is threatened by highly mobile pertechnetate that is produced by reprocessing nuclear fuel and is released into the ocean.¹⁰ It is clear that for the benefit of the environment and medical therapies, it is important to coordinate anions specifically.

Table 1.1: A comparison of the radii (r) of isoelectronic cations and anions in octahedral environments.¹¹

Cation	r [Å]	Anion	r [Å]
Na⁺	1.16	F⁻	1.19
K⁺	1.52	Cl⁻	1.67
Rb⁺	1.66	Br⁻	1.82
Cs⁺	1.81	I⁻	2.06

Due to anions being larger than isoelectronic cations (see Table 1) and their consequentially reduced charge to radius ratio, designing anion receptors is difficult.¹¹ Compared to the electrostatic binding interactions of smaller cations, those of anions are less effective. Also, anions may lose their negative charge at low pH, as they may become protonated. This means anion receptors can only operate within the confines of the pH that the anion remains negatively charged. The design of receptors is further challenged by the range of geometries adopted by anionic species (Figure 1.1), potentially restricting the scope of receptor-anion interactions.

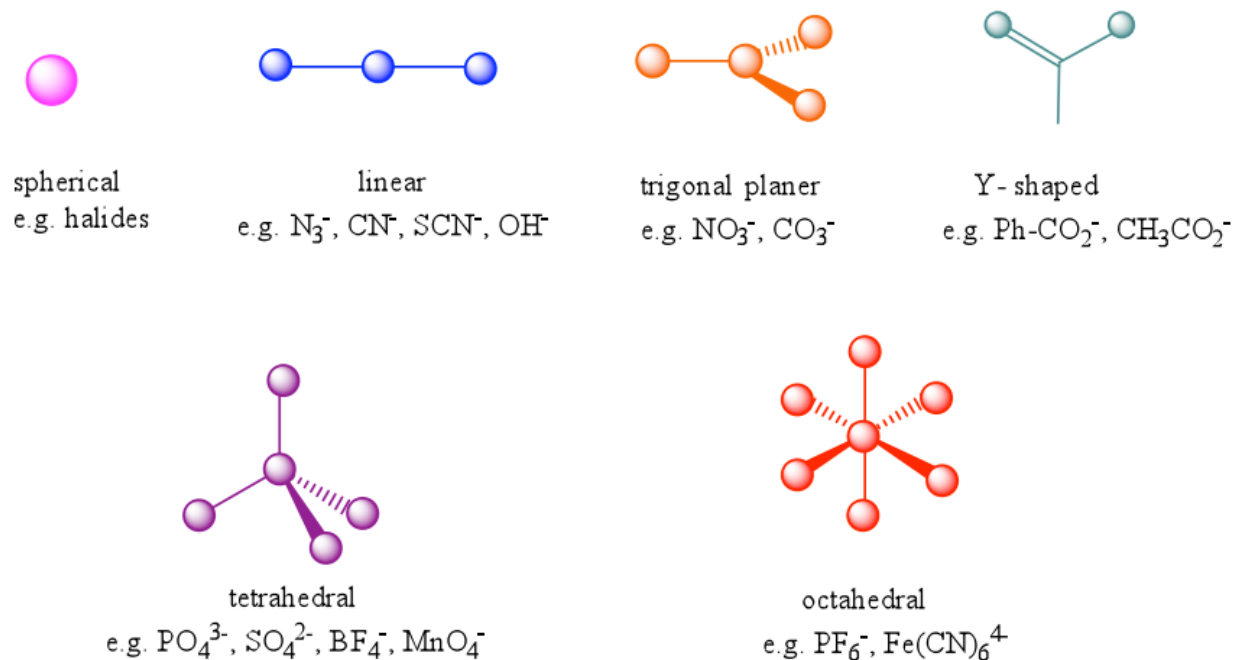


Figure 1.1: The variety of anion geometries.

The strength and selectivity of anion binding is also influenced significantly by solvents. The solvation of anions is primarily controlled by electrostatic interactions, and strong anion-hydrogen bonds form in particular with hydroxylic solvents. Therefore, for anions to be recognised by anion receptors, the receptors must overcome the attraction of the solvent environment. For example, charged receptors are able to bind highly solvated anions in protic solvent media; in contrast, neutral receptors that use ion-dipole interactions to bind anions will only be successful if the anions are in aprotic organic solvents. Biological anion receptor systems have evolved so that selectivity is determined by the difference between free energy lost by dehydrating the anion and the free energy gained by the anion interaction with the binding site.¹ This has facilitated receptors to develop high levels of specificity for particular environments. Receptor selectivity is also affected by hydrophobicity. In the Hofmeister series¹⁰ (Scheme 1.1), anions are ordered according to their hydrophobicity (ergo, the extent of their aqueous solvation). This series was determined by

researching the effect of salts upon the solubility of proteins. In general, hydrophobic anions bind most strongly to binding sites that are also hydrophobic.



Scheme 1.1: The Hofmeister series of anion salts.

The focus of this chapter is the key developments in research into anion binding motifs. Means of controlling and applying the hydrophobic effect is of particular interest; however, the hydrogen bonding and electrostatic interactions are also considered.

1.1.1 Anion Coordination Chemistry

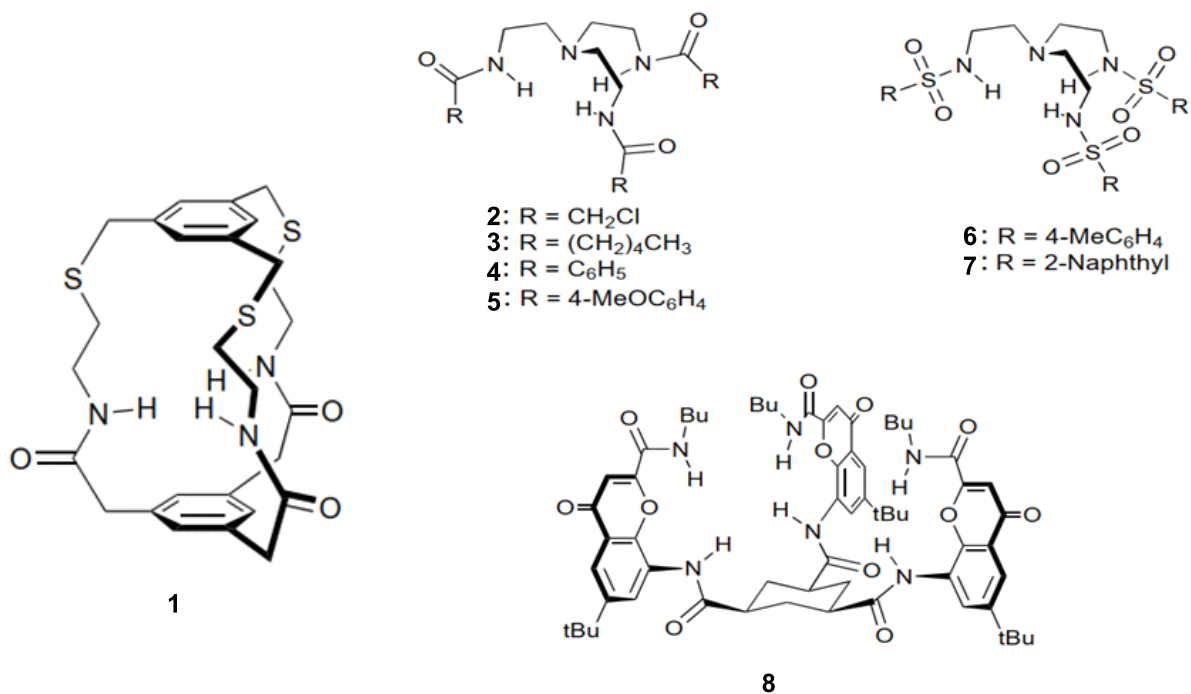
The solubility, basicity and geometry of the anion need to be factored into any design of selective anionic receptors. Selectivity is determined by the receptor and anion being able to form complexes. Consideration of the types of noncovalent interactions between the receptor and anionic guest is a helpful method of classifying anion receptors. Such interactions include electrostatic interactions, hydrogen bonds, hydrophobic interactions and combinations of these.

1.1.1.1 Hydrogen Bonds

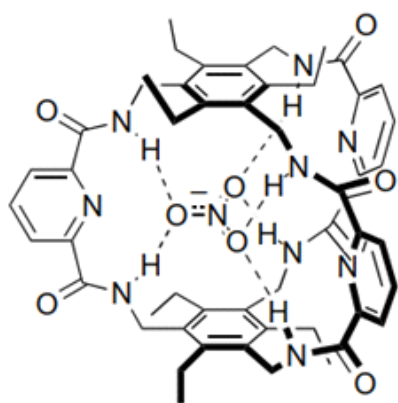
Receptors can be designed to exploit the directional quality of hydrogen bonds. Such receptors could be designed to adopt shapes that can distinguish between anionic guests in nonpolar solvents that have different geometries or hydrogen-bonding requirements.

The first anion receptor based exclusively upon amides was created by Pascal in 1986.¹² Receptor **1** showed evidence of binding fluoride ions in DMSO-d₆. A number of acyclic tripodal receptors bearing amide groups (**2-7**) were synthesised by Reinhoudt et al. in 1993.^{13,14} Meanwhile, pre-

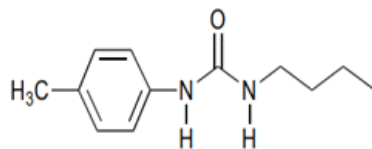
organised amide-modified cyclohexyl ring (**8**) was prepared by Raposo et al.¹⁵ Receptors **2-8** have C_3 symmetry; in all instances, their arrangement is intended to enable the binding of tetrahedral anions best.



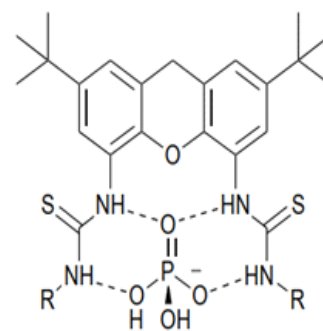
A trigonal box was synthesised by Anslyn et al. by condensing 1,3,5-tris(aminomethyl)-2,4,6-triethylbenzene with three equivalents of 2,6-pyridinedicarbonyl dichloride in dichloromethane in the presence of trimethylamine.¹⁶ The trigonal prismatic arrangement of the amide NH groups in **9** confers the ability to coordinate planar anions of p-electron systems, such as carboxylates and nitrate. The crystal structure of **9** shows the acetate anion is bound to the cavity of the box, forming an acetate complex. Because nitrate is planar and was also very strongly bound, Anslyn et al. postulated that it too had to bind within the box's cavity. In CD₃CN/CD₂Cl₂ (3/1 (v/v)) solution it is bound only 2.6 times less strongly than acetate even though it is 106 times less basic). The development of receptor **9** is significant as it coordinates nitrate, which typically, is a weak coordinating ion.



9 . NO₃⁻



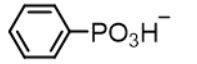
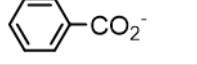
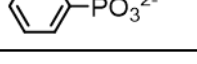
10



11: R = Bu
12: R = Ph

Urea and thiourea are excellent receptors for carboxylate and other Y-shaped anions because of their ability to donate hydrogens, forming two H-bonds. As demonstrated by receptor **10**, which is urea-based, highly charged bidentate anions that are more basic than the receptor, are able to form stable complexes (Table 1.2).¹⁷

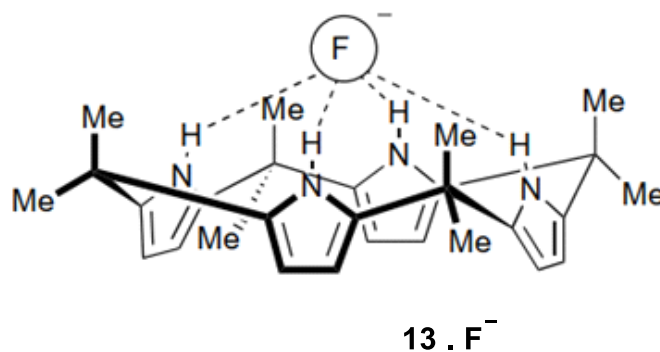
Table 1.2: The basicity and stability constant (in DMSO) of various bidentate anion receptor **10**

Guest	pK _b	K [M ⁻¹]
	13	30
	12	140
	10	150
	7	2500

A series of acyclic thiourea cleft molecules have been synthesised by Umezawa et al. Included among these molecules were some highly pre-organised systems, which incorporated a xanthene spacer.¹⁸ Receptors **11** and **12** bind anions very strongly; with **12** binding H₂PO₄⁻ ions with stability

constants of up to 195000 M^{-1} (in DMSO). This can largely be attributed to these receptors exhibiting a high level of pre-organisation. It is the hydrogen-bonding array capable of forming four hydrogen bonds present in the clefts that confers the selectivity for H_2PO_4^- ions.

Anions may also H-bond with pyrrole NH groups. According to Sessler et al. (1996) the calix[4]pyrroles (*meso*-octaalkylporphyrinogens) macrocycles were produced for the first time by Baeyer in the nineteenth century. These also coordinate to anions, as shown by *meso*-octamethylcalix[4]pyrrole **13**, which in CD_2Cl_2 , forms complexes with chloride, dihydrogen phosphate and fluoride with 350, 100 and $17200, \text{M}^{-1}$ respective stability constants.¹⁹ Upon anion complexation, the macrocycle's solid-state conformation undergoes a radical change as the free calixpyrrole adopts a 1,3-alternate conformation with neighbouring rings adopting opposite orientations. However, as shown by the crystal structure of **13**, when complexed with chloride, the macrocycle takes on a cone conformation, and the four pyrrole NH groups form H-bonds with the bound chloride ion.



Being readily able to generate high yields of calixpyrroles makes them attractive to use in industrial applications. For example, Gel M (Figure 1.2), synthesised by, Sessler et al., is a calixpyrrole-modified solid support used to separate anions by high-performance liquid chromatography.²⁰ As Figure 1.2 demonstrates, oligonucleotides that are 12–18 bases long can be separated by Gel M. Macrocycles have a number of other applications, such as being used in electrodes that are ion-

selective, and as isolated molecular hosts that are electrochemically active, to detect anionic guests, and incorporate into anionic optical sensors.^{21,22}

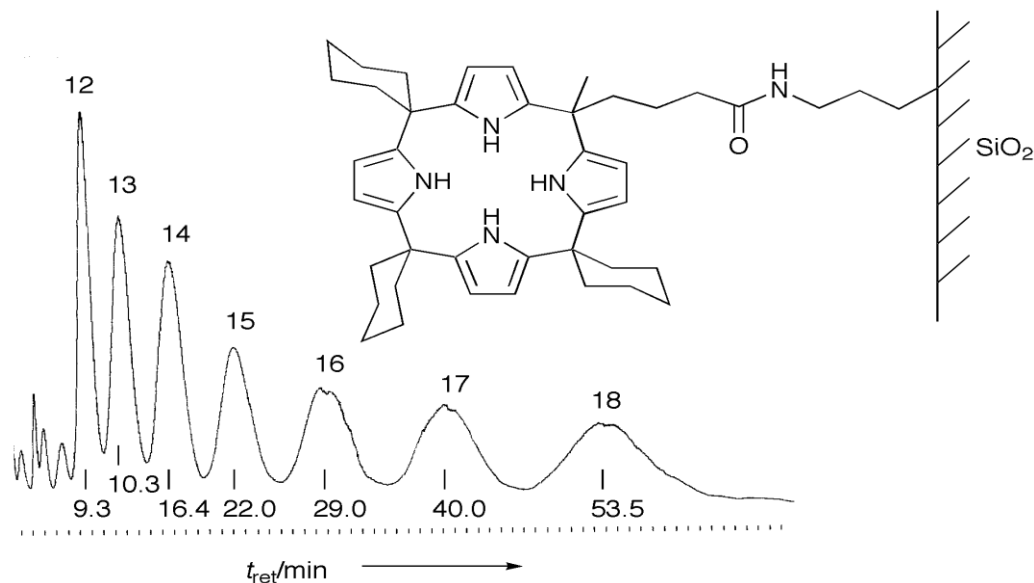


Figure 1.2: The separation of a mixture containing between 12 and 18 nucleotide subunits on calixpyrrole-modified silica gel.²⁰

A bipyrrrole-based [2]catenane **14** capable of forming highly stable anion complexes has been devised by Sessler, Vögtle et al. The very high stability of the ion binding of catenane was established using NMR titration techniques; stability constants of up to $10^7 M^{-1}$ with $H_2PO_4^-$ in $[D_2]1,1,2,2$ -tetrachloroethane were achieved.²³ The mechanism considered responsible for this stability is due to the tetrahedral cavity that forms between the rings; the coordination geometry of this structure is perfect for tetrahedral anion coordination (Figure 1.3).

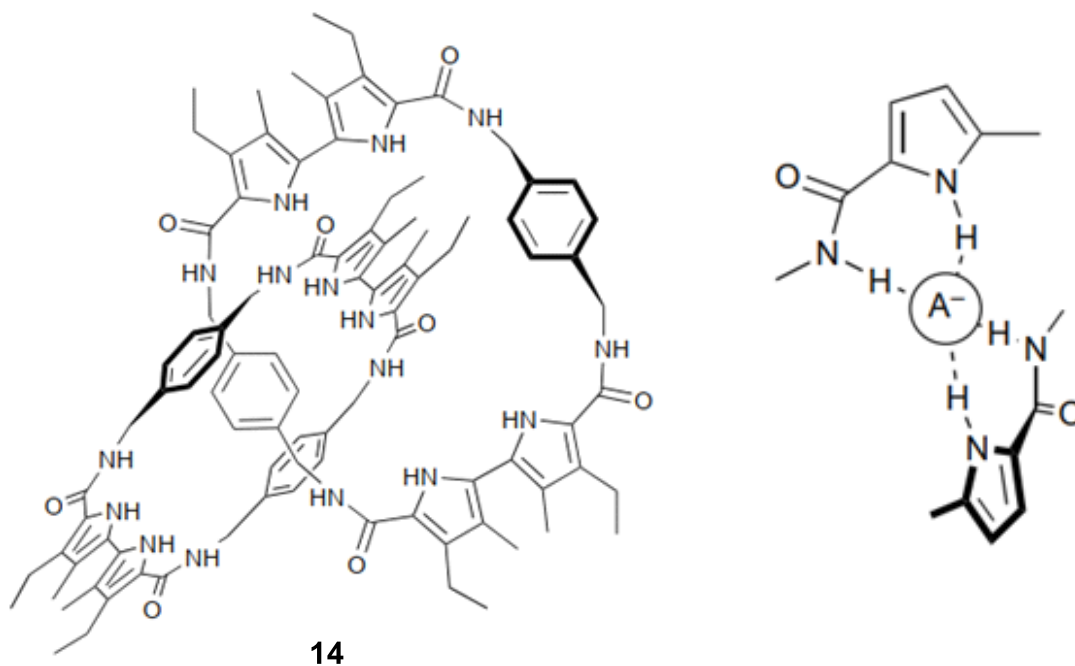
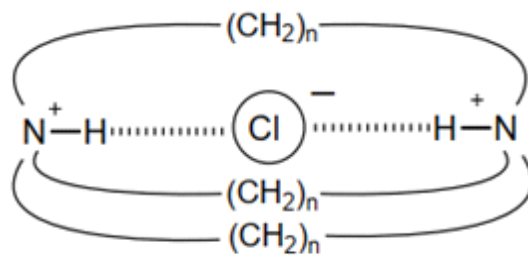


Figure 1.3: Catenane **14** provides an array of tetrahedral donor hydrogen bonds.²³

1.1.1.2 Hydrogen Bonds and Electrostatic Interactions

Anion receptors of high efficiency can be generated through joint use of hydrogen bonds and electrostatic interactions. In 1968, a mixture of such interactions was employed by a prototype of a macrocyclic synthetic anion receptor for anion binding. For halide ion coordination based on electrostatic interactions and hydrogen bonds, a number of macrobicyclic ammonium cages (e.g. **15**, **16**) were developed by Park and Simmons.²⁴ The binding of the halide ions in the cage between two protonated nitrogen atoms was revealed by NMR and crystallographic analysis.

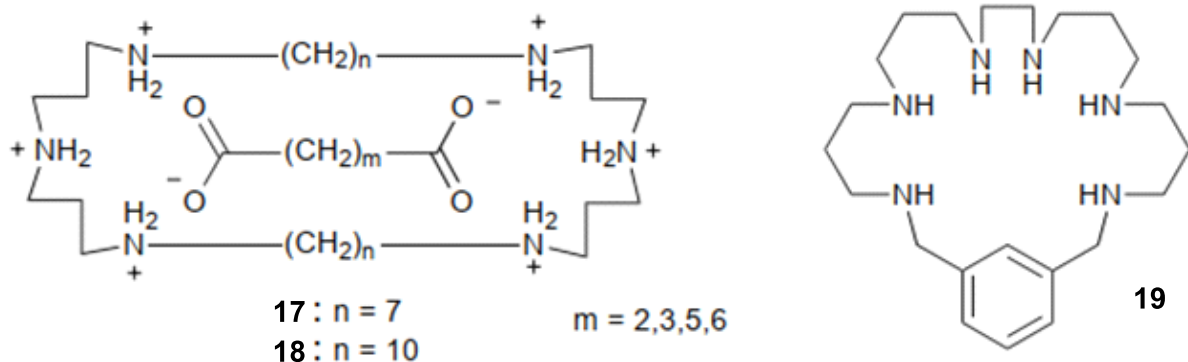


15: $n = 9$

16: $n = 10$

Protonated ammonium macrocycles **17** and **18** were demonstrated by Hosseini and Lehn to be capable of size-based differentiation of dicarboxylate ions.^{25,26} Stronger binding of shorter chain carboxylates ($m = 2, 3$) and preferential binding of longer alkyl chain carboxylates ($m = 5, 6$) are exhibited by receptor **17** and receptor **18**, respectively.

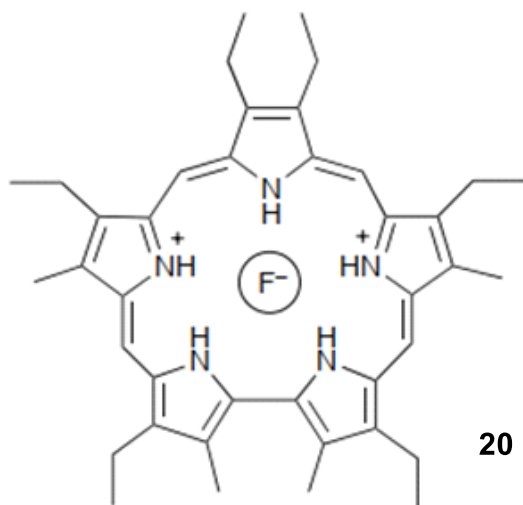
The protonated form of hexaazametacyclophane **19** has been shown to bind AMP, ADP, and ATP in aqueous solution.¹⁰ Nucleotide anion phosphate groups coordinate with the macrocycle through a combination of electrostatic and hydrogen-bonding interactions, while NMR studies have shown that the base nucleoside stacks with the benzene ring present in the macrocycle.



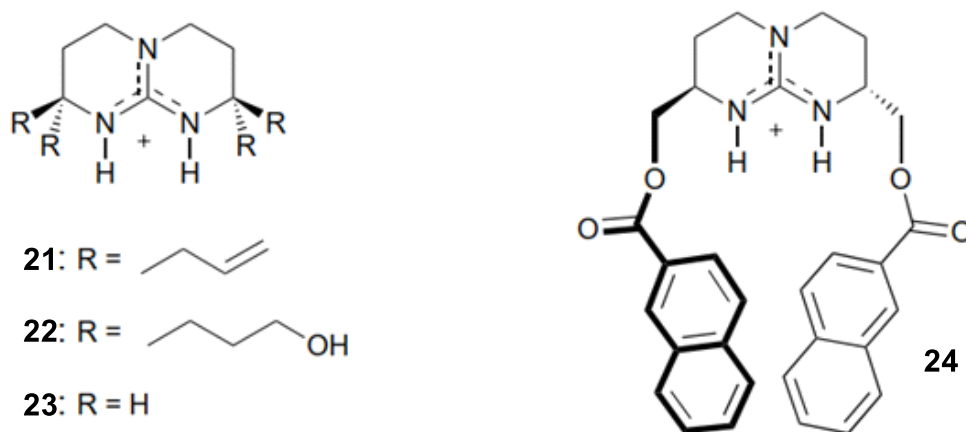
Protonated polyammonium receptors require a cautious approach to ensure that the acidity of the environment is high enough to prevent their de-protonation, but not excessively high to cause the

protonation of a potential anionic guest. Guanidinium ion results from guanidine protonation and its stabilisation is ensured by resonance and charge delocalisation. For instance, by comparison to protonated secondary amine with $pK_a = 10.5$, guanidinium cation with $pK_a = 13.6$ displays stability that is around three orders of magnitude higher. Consequently, guanidinium enables anion receptors to function over a wider pH spectrum because its protonation is maintained up to high alkaline levels.

Receptors that are heavily inclined towards anions are formed through the integration of pyrrolic NH groups and electrostatic interactions. Woodward and colleagues were the first to achieve the synthesis of pentapyrrolic expanded porphyrins known as sapphyrins.²⁷ These porphyrins were then shown by Sessler and colleagues to be able to coordinate to anions. Double protonation of the sapphyrin macrocycle **20** core can result in a positively charged receptor and a series of five groups with NH hydrogen binding. Compared to bromide or chloride ions, the binding of fluoride ions to deprotonated sapphyrin is more than 1000 times more robust, according to solution-phase experiments.^{28,29}



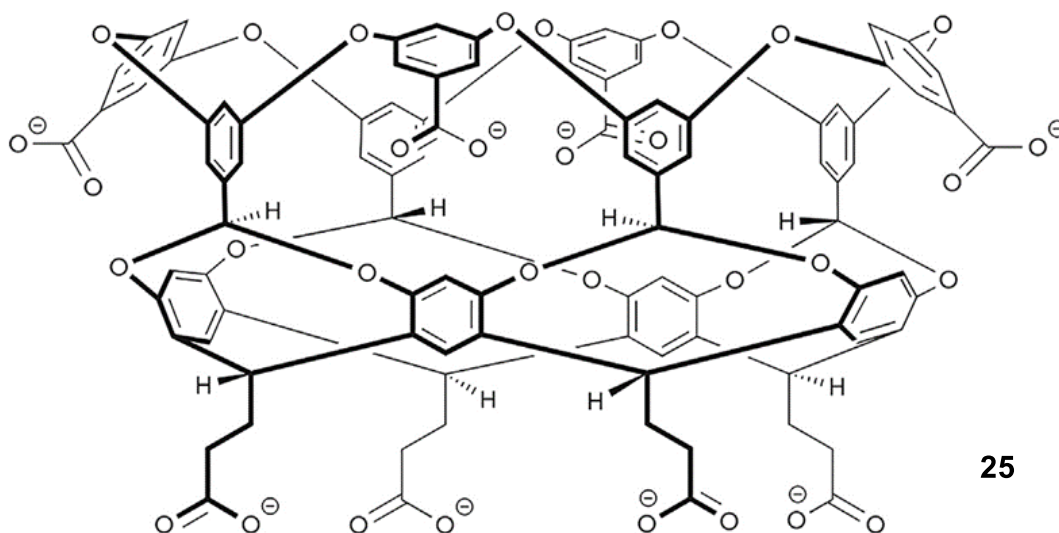
The guanidinium group was integrated into a bicyclic ring by Schmidtchen¹⁰ and colleagues to form **21-23**. Such receptors have identical clusters of hydrogen bonding to those present in ureas. This has resulted in extensive use of guanidinium-based receptors for binding guests with additional carboxylate or phosphate. For instance, affinity for extraction of tertbutoxycarbonyl (Boc)-protected L-tryptophan into chloroform from a racemic mixture in water is demonstrated by the chiral receptor **24**, with π - π stacking bolstering the interaction between guanidinium and carboxylate.³⁰



1.1.1.3 Hydrophobic Effect

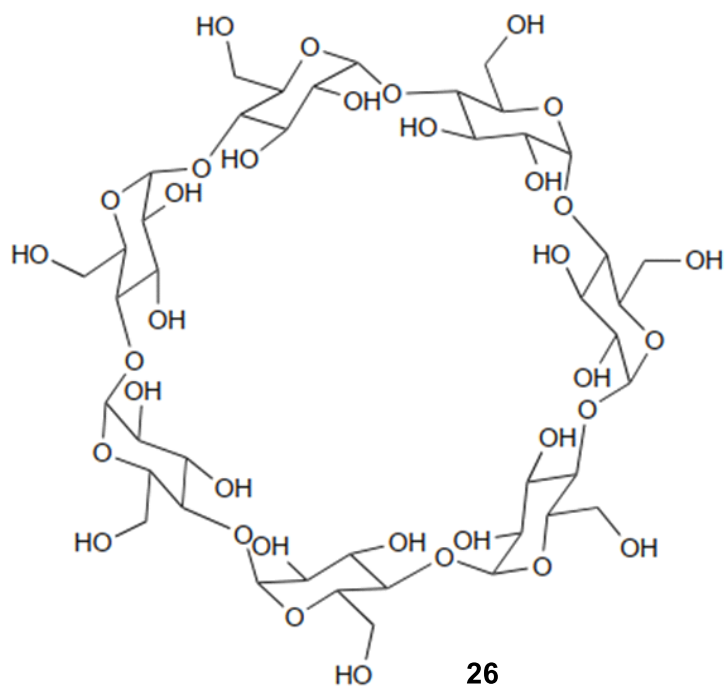
In addition to covalent, ion-dipole and ionic forms of binding, anion binding can also take the form of hydrophobic interactions. Carnegie et al. studied the Hofmeister effect, and explored what happened to coexisting salts when ClO_4^- was bound to **25**, an octa-anionic cavitand in water.¹⁰ The research highlighted that direct ion-solute interactions were important. The ionic strength of the solutions was adjusted by modifying Na^+ salts with a number of different anions. These included chaotropic (weakly hydrated) SCN^- to kosmotropic (strongly hydrated) F^- anion, were used; ¹HNMR titrations were used to determine the binding constants between of **25** and ClO_4^- . Hydrophobic interactions are increased by kosmotropes and decreased by chaotropes; thus, kosmotropic salts (e.g., NaF) were found to promote the binding of ClO_4^- , and chaotropic salts,

such as, NaSCN weakened the binding of ClO_4^- . However, the behaviour of intermediate salts, such as NaClO_3 that are not extreme chaotropes or kosmotropes, is more complicated. At low concentrations, the binding of ClO_4^- increases slightly, but at high concentrations, binding is reduced. The researchers applied the data to a model that considered both the co-anion binding competitively to the cavity of **25** and the improved binding of the anion provided by Na^+ /carboxylate complex of **25**. The researchers established that; (1) chaotropes provoked “salting-out”, where the hydrophobic anion bound competitively to the hydrophobic cavity, resulting in attenuated binding; and (2) kosmotropes led to “salting-in”, which promoted binding. This is primarily attributed to the reduced net charge arising from the cation binding to the anionic host. Intermediate salts exhibited complex behaviour, which for (1) was attributed to competitive anion binding at high concentrations of salt; and for (2) enhanced cation-induced binding at low concentrations of salt being the dominant mechanism.

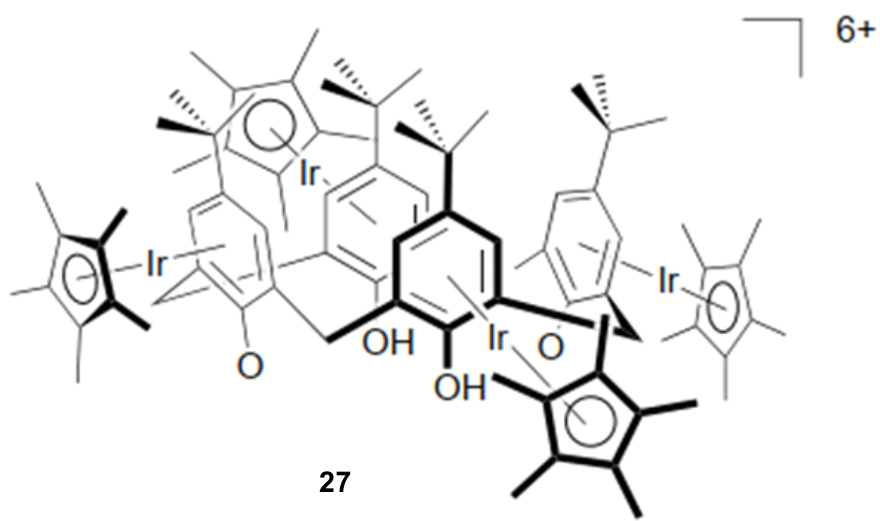


Experimental binding studies using **25** and calculations of its binding to a number of anions were undertaken by Sokkalingam et al.¹⁹ Their results revealed that in water, **25** weakly binds hydrated anions. The highest affinity, the anions evaluated by isothermal titration calorimetry (ITC), was $\text{Cl}_3\text{CCO}_2^-$, ($6,337 \text{ M}^{-1}$), with ClO_4^- exhibiting intermediate affinity (160 M^{-1}); the affinity of I^- was weak (17 M^{-1}), while Cl^- failed to demonstrate any measureable bonding at all. The ITC results point to anion binding being determined by enthalpy at the expense of entropy. The evidence provided by MD simulations indicates that compared with in the bulk, when bound in the cavity, ClO_4^- and I^- kept approximately half of their solvation shell water molecules. In contrast, when Cl^- was bound, it retained the majority of its solvation shell. These findings led to the proposition that organised solvated waters in the cavity attract a high cost in entropy, making the affinity of small and “hard” ions low or absent and totally inhibiting large ions inside the cavity from being solvated.

The incorporation of a series of naphthalenesulfonates into β -cyclodextrin (**26**) in water was the focus of work conducted by Inoue et al.³¹ The primary binding mechanism for these complexes arises from the hydrophobic effect of water molecules being displaced from the cyclodextrin’s internal cavity by the naphthalene residue. The naphthalene group is orientated within the cavity as a consequence of the anionic sulfonate group remaining in contact with the solvent external to the cavity.



To make the cavity more agreeable to hydrophobic anionic guests, Atwood et al. reduced the electron density present within the cavity by coordinating transition metals to the outside of calixarenes (**27**).³² The complexation of Cl^- in aqueous solution achieved stability constants of up to 550 M^{-1} .³³



1.1.2 Biological Anion Receptors

Anion detection in water depends greatly on biological systems, which use diverse and elaborate mechanisms of anion manipulation in water. The “nest” is a specific fold of great significance for anion-binding proteins.³⁴ As shown in Figure 1.4a, two neighbouring residues with such an arrangement create an atom-sized concave space encompassing the two main-chain NH groups alongside the subsequent amino acid point, which enables anionic or δ^- atom coordination. The NH groups are organised as crown ether oxygen atoms. This permitted generalisation of particular anion-binding motifs (e.g. alpha turn, paperclip/Schellman loop).³⁵

Longer residues with such dihedral angles make up compound nests, leading to wider spaces like the P-loop comprising a nest with four residues, which is the chief ATP or guanosine triphosphate (GTP)-binding motif in proteins (Figure 1.4b). Stabilisation of a tetrahedral oxyanion intermediate in serine protease is ensured by an additional nest with four residues and ion-sulphur clusters are frequently supported by nests with up to eight residues.³⁶

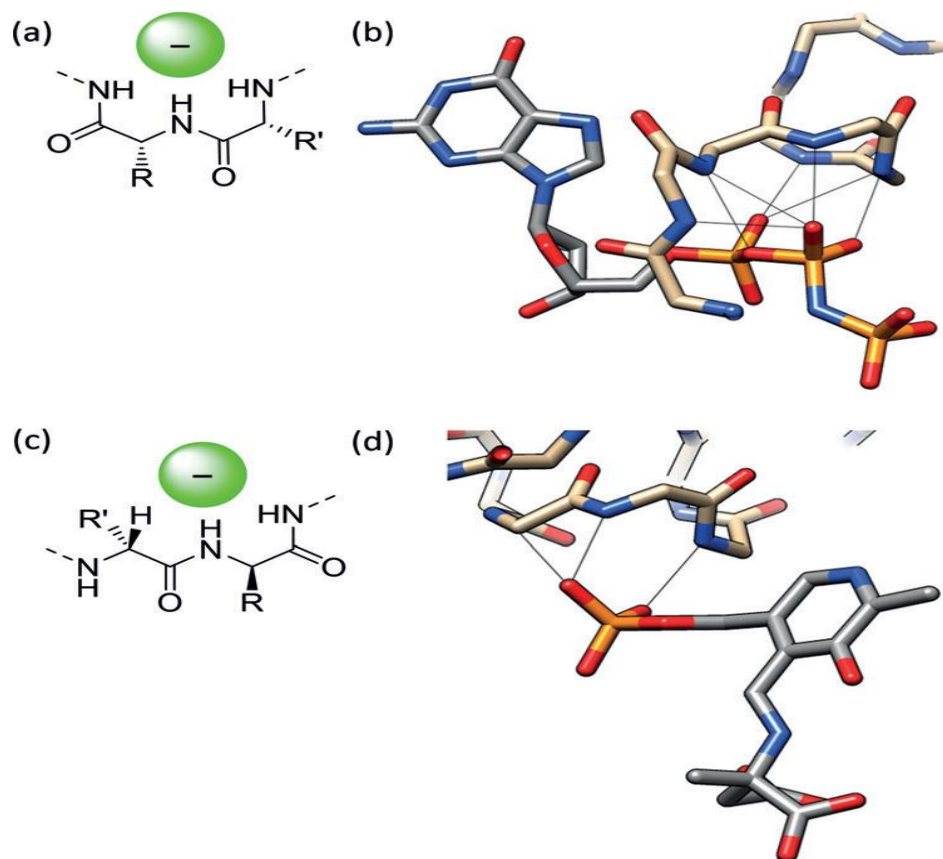


Figure 1.4: a) Simplified illustration of the most basic nest motif. b) GTP analogue bound by hydrogen bonds from five consecutive main-chain amides in a nest formation. c) Simplified illustration of the C^αNN motif. d) Binding of a phosphate group by a C^αNN motif located at the end of a helix. Image taken from Ref ¹⁰

A helical hairpin eicosapeptide is an anion host crystallising with an incorporated acetate anion in a nest spanning the two helices.³⁷ Furthermore, a minimal hexapeptide with a nest resembling a P-loop exhibited robust HPO₄²⁻ binding in water at neutral pH.³⁸ Similar to phosphate-binding proteins, a phosphate-derived hydrogen bond is accepted by a lysine side chain deprotonated amine.

Comprising two main-chain amide hydrogen bonds and a C-H hydrogen bond from the subsequent α -carbon atom, the C^αNN motif represents a comparable anion-detection moiety to the nest (Figure 1.4c).³⁹ Originally a phosphate-detection unit (Figure 1.4d), the binding of the C^αNN fragment Leu-Gly-Lys-Gln to the anchor helix N terminus allowed observation that the conformation

alteration displayed by sulphate detection in water resembled an “induced fit” system.⁴⁰ Conformation change from non-helical to helical structure was confirmed by computational analysis to be caused by both sulphate and phosphate binding.⁴¹

Insight into natural anion coordination mechanisms has been derived from new knowledge of oxoanion binding.⁴² Cyanobacteria rely on sophisticated capture systems for nitrate binding, thus affording nitrogen fixation for whole marine ecosystems. Asymmetrical nitrate binding occurs in the nitrate-binding protein NrtA affixed to the cyanobacterial membrane extracellular part within a transporter system.⁴³ In water, the three nitrate oxygen atoms are identical, but when bound, the charge centres on a single oxygen atom, which is surrounded by auxiliary groups with positive charge; the hydrogen bonding of the other oxygen atoms is less robust, with the protein hosting the nitrite anion as well, because one atom is in a strongly hydrophobic cleft. The asymmetrical coordination of this system may explain its high affinity to the cyanobacterial bicarbonate-binding protein CmpA.⁴⁴ During anaerobic respiration, oxoanion rather than oxygen can be decreased by bacteria based on a different nitrate receptor included within the staphylococcus nitrate regulatory element (Nre). Just four hydrogen bonds are offered by the mainly hydrophobic binding pocket, which can host iodide anions as well; remarkably, activation of the biological activity of the protein is also possible when iodide is present.⁴⁵

The discovery that anion alteration permitted bacteria to assimilate molybdate and tungstate was made in 2009. Previously, tetracoordinate metal centres were established in every known Mo- or W-containing metalloprotein structure, while transporter proteins displayed octahedral coordination, with additional coordination straight to the metal centres being supplied by two carboxylate groups and oxygen atoms being supplemented by hydrogen-bond donors.⁴⁶ This can serve as a basis for development of novel mechanisms of multiatomic anion binding. The redesign

of the molybdate-binding protein to make it selective for perrhenate as a model for pertechnetate (for ^{99m}Tc) and for ^{188}Re and ^{186}Re with beta emission was prompted by the opportunity of radionuclide non-covalent incorporation within nuclear medicine.⁴⁷

Although it may appear impractical to coordinate anions based on nucleic acids, which have a phosphate backbone with multiple negative charges, aptamers provide several noteworthy options. Oligonucleotides with single strands (aptamers) achieve binding of a particular substrate in liquid environments by folding in a specific manner.⁴⁸ Inorganic cations are added to enable charge screening necessary for folding and detection. Constituting antibody substitutes, aptamers are “raised” via straightforward *in vitro* selection against various targets, including monoatomic ions, small molecules and proteins and entire cells.^{49,50} However, in spite of the ample instances of metal-ion binding, aptamers have not been extensively investigated for anion detection.^{51,52} There is extensive knowledge about aptamers for nucleoside phosphates, and especially an ATP aptamer with high selectivity for longer rather than shorter oligophosphates, indicating that nucleic acids are capable of robust and selective polyanion binding when Mg^{2+} ions are present.^{53,54} A sensor with high selectivity was attained in one study by binding an AMP aptamer to fluorescent nanoparticles.⁵⁵ Furthermore, the potential of aptamers for detecting anions in water was reinforced by the discovery of their association with anion porphyrins of biological significance.⁵⁶

Recent research indicated that pattern-based identification of aqueous anion pollutants was possible based on DNA-like oligomers with nucleobase-substituting synthetic units.⁵⁷ Beads from six monomers were the basis for the formation of a library comprising 1296 tetrameric strands. Binding locations were created through addition of metals and 17 anions in aqueous buffer solution were employed to analyse the fluorescent reaction of the beads. Eight highly responsive systems were

eventually established and these were capable of anion differentiation and measurement of micromolar concentrations when used together.

1.1.3 Receptors for radioactive anions and decontamination

Sedimentary rocks contain radionuclides classified as “primordial” nuclides that have existed since the time these elements were formed. These nuclides are called “*normally occurring radioactive materials*” (NORM). Uranium and thorium are two radionuclides that represent natural resources existing in our environment. It is found that thorium’s compounds are solely transported with water while uranium’s compounds are transported in several ways such as water, gas and oil or sludge condensates. When oil is extracted NORM located in the sedimentary rocks is brought up to the surface along with the crude oil, gas and water, as a result, this might cause sludge accumulation, deposits and damage of the equipment that is used in monitoring changes at various conditions, such as; temperature pressure and pH. These changes increase the amount of radionuclides as ^{226}Ra and ^{228}Ra found when extracting crude oil from oil fields.^{58,59}

Deposits are formed when seawater experiences changes in temperature, pressure and acidity when extracted which causes radium to co-precipitate with barium, strontium and silicates of calcium that forms the radioactive deposits. Radium is found in sludge and scrapings as well, along with other radionuclides such as lead-210 and polonium-210. Natural gas is free of sludge and scrapes, however, NORMs such as Radon-222 find a way to the surface combined with gas. The decay products make a thin film inside the equipment used. These products can convert to hazardous material due to gamma radiation from bismuth-214 or lead-210. Seawater injection system which used to bring the oil to the surface, can increase the amount of uranium located in deposits, when large amounts of water are used. The radioactivity measured in the deposits is low and shows no hazard, unless its exposed to extreme amounts over a long period of time. Produced water is the

major part of the waste created by the oil and gas industry, the rate of water production is tremendously higher than oil production. Produced water contains elevated NORMs such as ^{226}Ra and ^{228}Ra that also exists in natural seawater, although with lower activity.⁶⁰

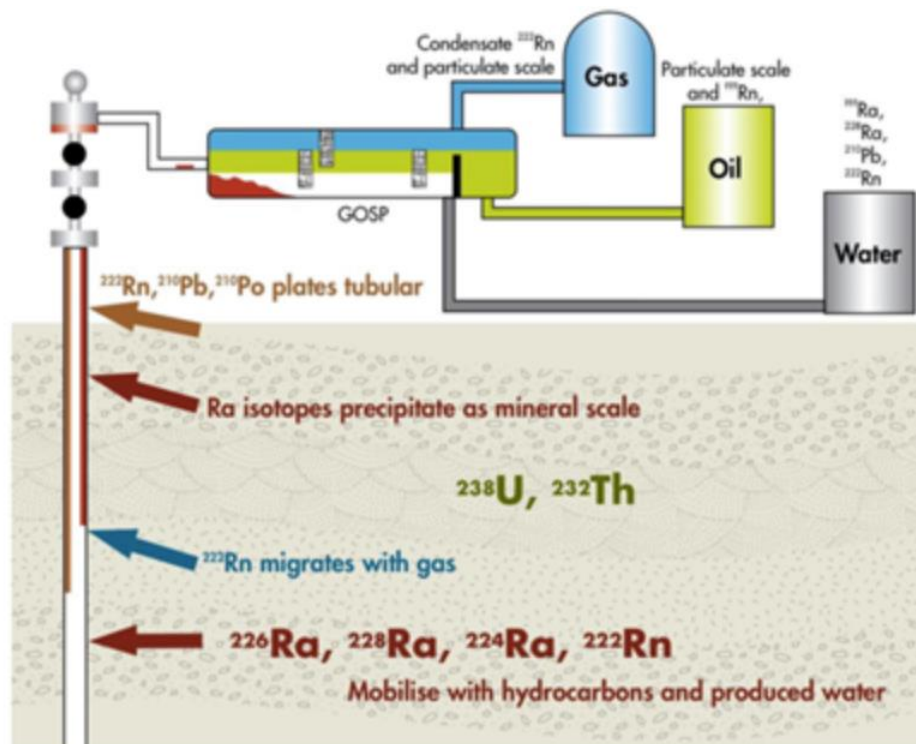


Figure 1.5: How radioactive waste behaves under extracting of oil. Image taken from Ref ⁶⁰

Additionally, the highly toxic and radioactive pertechnetate ($^{99}\text{TcO}_4^-$) anion is produced as a by-product of the nuclear fuel industry, and poses a significant environmental threat due to its long half-life, high water solubility and stability under aerobic conditions. However, direct study of this anion has been limited because of its radioactivity. Therefore, the perrhenate anion (ReO_4^-), which has an identical geometry, similar size and hydration energy, has often been used as a surrogate.^{61,62}

Cornes, Sambrook and Beer reported the preparation of two anion receptors of pyridinium donor motifs attached to diametrically opposed positions on the primary rim of a macrocyclic

oligosaccharide (α -cyclodextrin (α -CD)) by utilising either halogen bonding (XB) iodotriazole or hydrogen bonding (HB) prototriazole. This receptor is known to complex inorganic anions within its central hydrophobic cavity to provide selective recognition of perrhenate in neutral aqueous media (Figure 1.6).⁶³

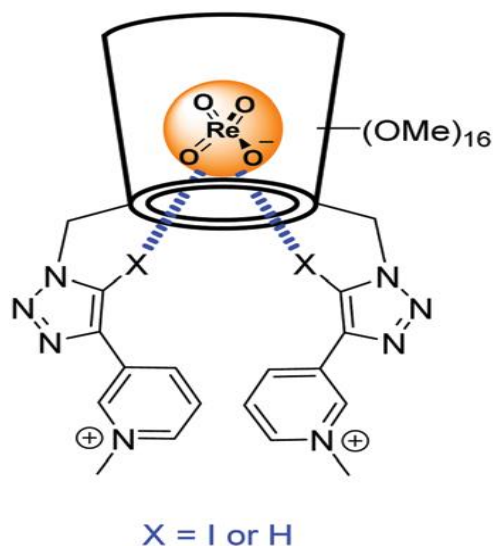


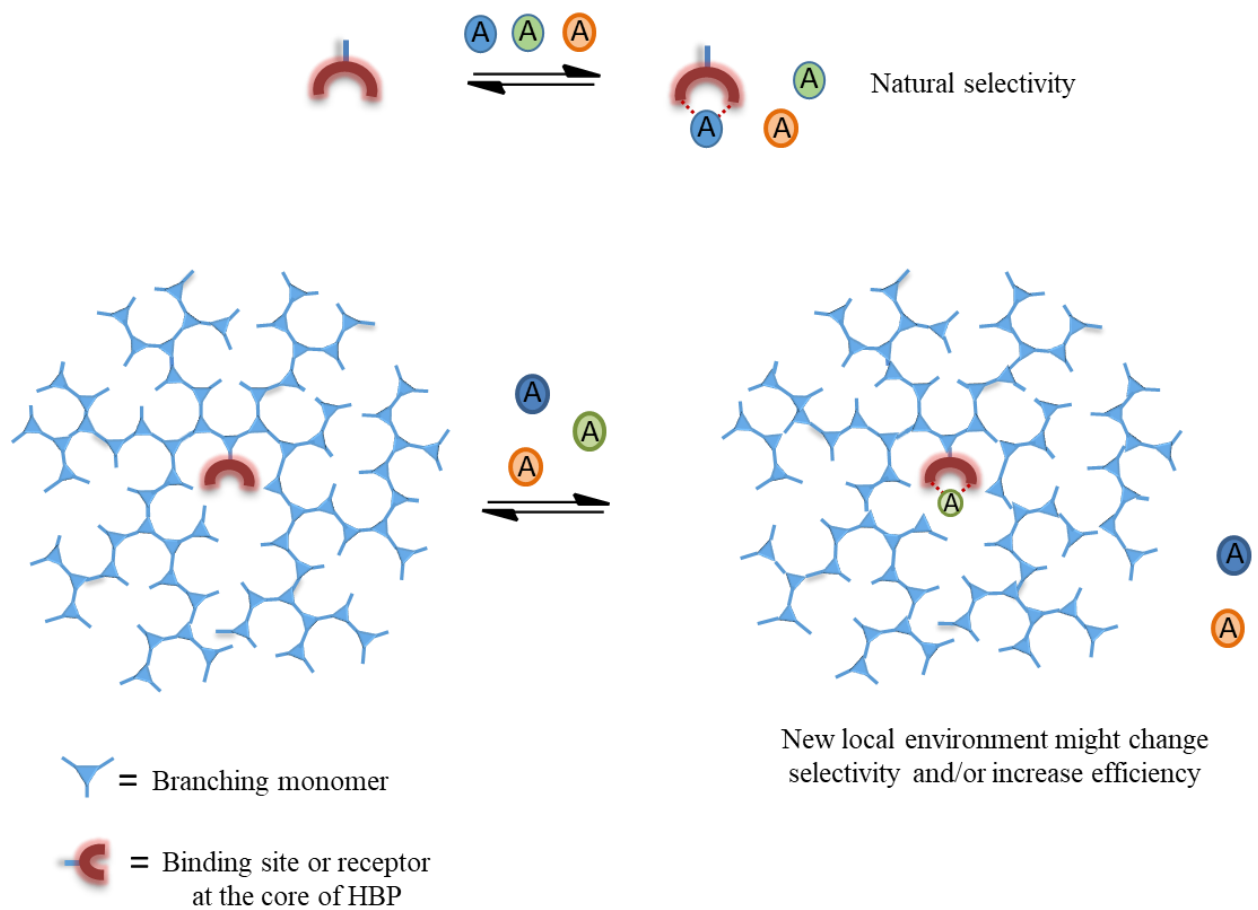
Figure 1.6: Schematic representation of the perrhenate binding mode of the XB and HB receptors ($X = I$ or H).Image taken from Ref ⁶³

An investigation was carried out by Ammir and co-workers to study the radioactivity contamination of water from and near oil fields in north of Iraq. It was found that the concentrations of ^{238}U and ^{232}Th vary between 0.20 and 3.50 ppm and from 0.03 to 1.83 ppm, respectively. The annual effective dose of U and Th were higher than the average water dose, which is recommended to be 0.1 mSv/y. Thus, most of the produced water from the studied oil fields is not useful for any direct purpose.⁶⁴

Despite their potential application in the medicine, biological and environmental fields, there are relatively rare examples of anion host system that function in pure water. This is mainly due to the inherent properties of anions, such as pH dependence and high energy hydration.⁶⁵ Moreover, the

preparation of water-soluble host system presents a significant synthetic challenge.⁶⁶ In this project, we aim to synthesise anion host systems that can be used for removal of radioactive anions. However, we will use a variety of non-radioactive anions, which have identical properties of the radioactive materials that might be found in a contaminated area.

Chapter Two: Functionalisation of HBP for Controlled Microenvironment of Isophthalamide Anion Receptor



2.1. Introduction

2.1.1 Hyperbranched polymers: Structures and properties

Hyperbranched polymers (HBPs) consist of macromolecules with a number of branches that make up three-dimensional dendritic structures. The branches associated with these macromolecules are irregular and typically arranged according to AB_n monomers with one-pot polymerization.⁶⁷⁻⁷⁰ The structure of HBPs was first introduced in 1952 by Flory, but at the time was only considered speculative.⁷¹

In 1982, Kircheldorf first introduced the concept of highly branched polyester, consisting of AB and AB_2 monomers that were copolymerized. Later, the realisation of hyperbranched polyphenylenes using homopolymerisation of AB_n type monomers was introduced by Kim and Webster.⁷² These two discoveries have resulted in greater attention being paid to hyperbranched polymers in recent decades. Hyperbranched polymers consist of both dendritic and terminal units. Specifically, terminal units can be found in all aspects of the polymeric volume, as shown in Figure 2.1.

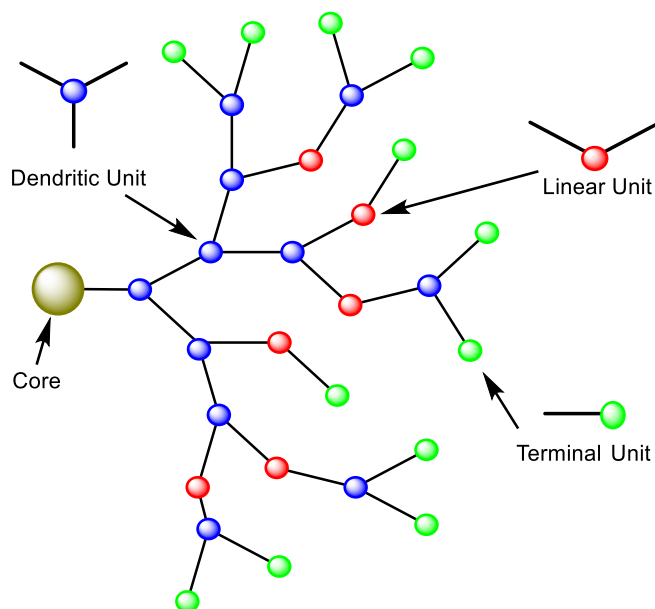


Figure 2.1: Unit types for AB_2 HBPs.

It is possible for partially reacted, or linear, units to occur in the polymeric structure during HBP synthesis, due to the random addition of monomers. This feature means that the degree of branching of HBPs is significantly different than that of their analogues. The term *degree of branching* (DB) was first introduced in 1991 by Fréchet to characterise and designate the ratio of non-linear units to the total number of units. This is demonstrated in the following equation.⁷³

$$DB = \frac{D + T}{D + L + T} \quad \dots \text{Equation 2.1}$$

Where D is the number of dendritic units, T the number of terminal units and L is the number of linear units.

The properties of the DB ratio are exemplified when comparing dendrimer and linear polymers and hyperbranched polymers. A structurally perfect dendrimer has a DB of 100%, and linear polymers introduce a DB of 0%, whereas HBPs synthesised from AB_2 monomers have a statistical DB of around 50%.

Although they have different DB ratios, HBPs and dendrimers have similar physical properties, including comparably low intrinsic viscosities. However, the interaction between HBPs molecular weight and their intrinsic viscosity is adherent to the Mark-Houwink equation for linear polymers.⁷⁴ This is due to the fact that steric inhibitions impact HBP growth, where the spherical design of the dendrimer prevents that structure from adhering to the same growth impacts. This means that a dendrimer structure is more closed than that of HBPs, which are elongated in design.

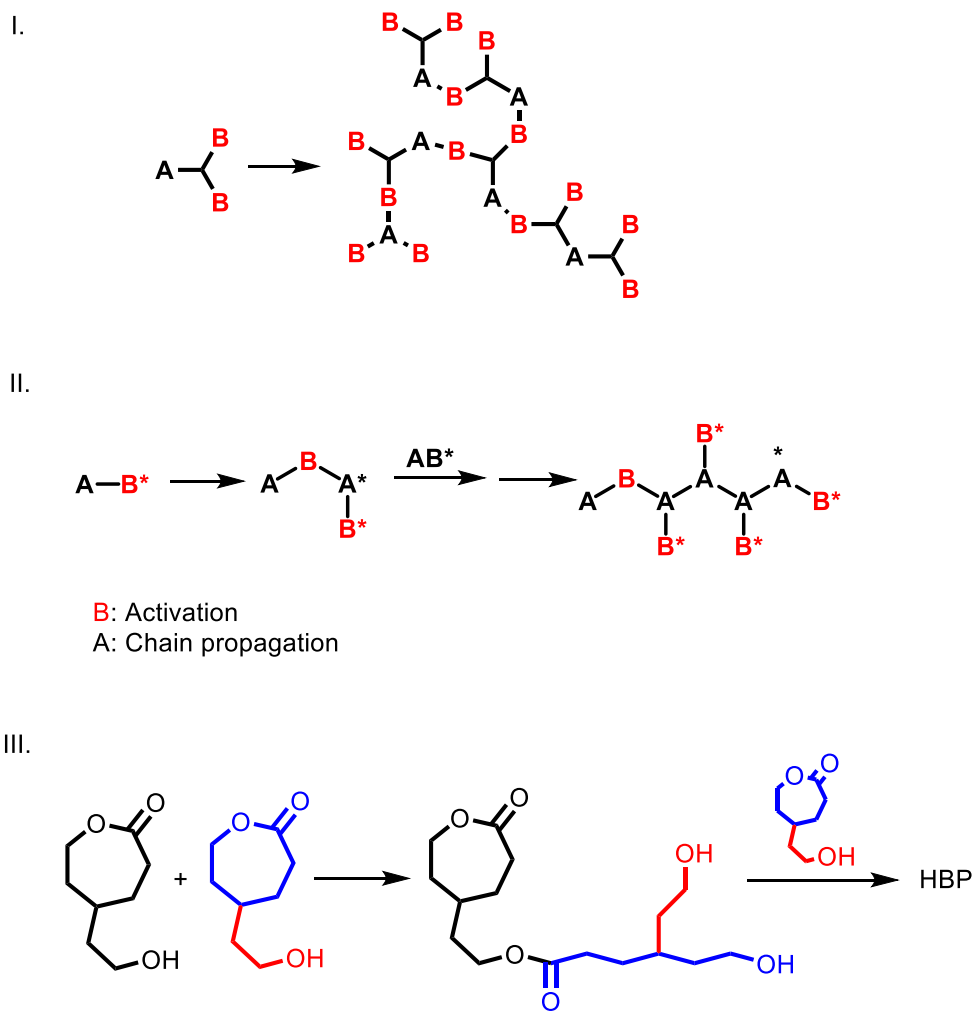
Because HBPs have a greater numbers of terminal groups than their linear analogues, they are more soluble. The DB positively correlates with solubility, which results in HBPs having an inferior solubility when compared with perfectly branched dendrimers.⁷⁵ However, HBPs can be utilised for a number of applications due to their customisable thermal, chemical, rheological and solution properties.⁷⁶

2.1.2. Synthesis of HBPs

HBPs can be easily synthesised through a one-step reaction, requiring significantly less effort than the synthetic process for a dendrimer. Scheme 2.1 shows the three main methodologies for preparing an HBP for synthesis. The most widespread methodology is polycondensation of AB_n monomers (where $n \geq 2$), as first documented by Kim and Webster in 1988.⁷⁷ There are two means of carrying out this style of polymerisation: slow addition of the branching AB_n monomer, or simultaneous inclusion. Both impact on the molecular weight distribution, as well as the branching density. HBPs synthesised through polycondensation include polyphenoles,⁷³ polyesters, polyamides, polyethers, and polyurethanes.^{72,78,79}

Another methodology is the self-condensing vinyl polymerisation (SCVP), first introduced by Frechet et al.^{80,81} SCVP produces HBPs using one initiating moiety (AB^* monomers) and one vinyl group. In this type of polymerisation, the activated species are a radical, carbanion, or cation. By using SCVP, it is possible to circumvent the gelation or cross-linking reactions that otherwise occur due to chain transfer or dimerization. The SCVP methodology is excellent for synthesising poly methacrylates and HB polystyrenes.

The final methodology for HBP synthesis is ring-opening polymerisation. Suzuki first developed this method in 1992. In ring-opening polymerisation, the reactive centre is made up of a terminal polymer function, which then links to a cyclic monomer chain formed through ionic propagation. With each additional monomer step, a new reactive centre is formed. Ring-opening polymerisation is used to synthesise polyesters, polyamines and polyethers.^{82,83}



Scheme 2.1: Examples of three different approaches to synthesis HBP (i. Step growth polycondensation; ii. Self-condensing Vinyl Polymerisation; and iii. Ring opening polymerisation)

2.1.3. Applications of HBPs

Due to their distinctive properties, HBPs are utilised for a number of purposes, as shown in Figure 2.2. These include biomimics, additives for surface modification, nanoreactors, multifunctional platforms, catalysts, gene/drug vectors, surface coatings, and nanocapsules. Additional applications continue to be researched.^{76,84} One potential application being considered is the use of HBPs in supramolecular chemistry. Intramolecular cavities in core-shell amphiphilic HBPs mean that such structures can be used to bind guest molecules in a supramolecular process. Another potential application being explored is the encapsulation of guests such as drugs, inorganic nanoparticles, metal-ion complexes and dyes within amphiphilic HBPs, such as

poly(sulfoneamine), poly(amidoamine), and poly(esteramide). Because HBPs can be used to encapsulate guests for later release, they are also being considered as a means for purification or separation of compounds, particularly in terms of environmental protection.^{85–89}

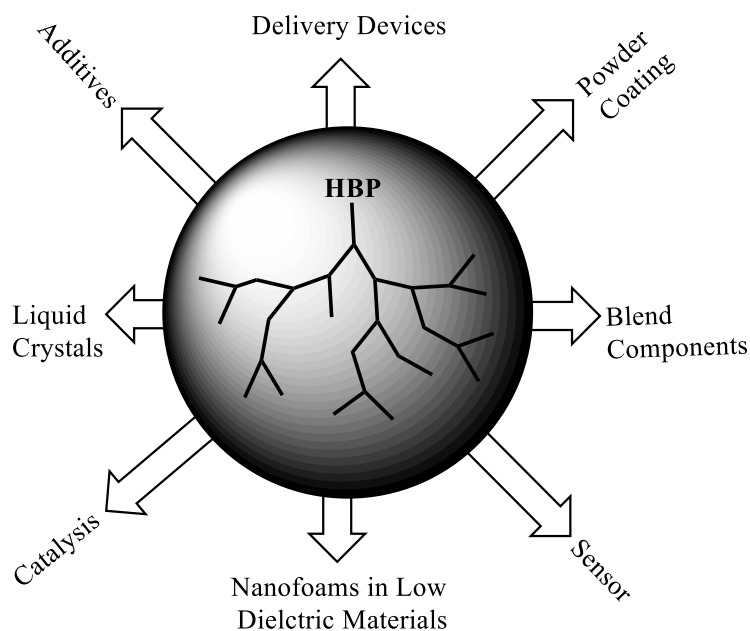


Figure 2.2: Representative figure of some HBPs' applications

2.1.4. Use of HBPs in anion recognition

The concept of a host-guest designer complex is often described using a lock and key analogy. The key is the guest molecule, whose grooves align with those in the lock, which is represented by the receptor molecule. Emil Fisher introduced this analogy in 1894 when describing the relationship between substrates (keys) and enzymes (locks). Fisher noted that the guest must be analogous in shape and size to the binding site of the host, and therefore the lock and key analogy was born.

The dimension, chemical properties, and structure of host-guest HBPs must also be considered. This includes aspects such as hardness, bonding and charge. Additional aspects to take into account in the binding process include rival molecules (and their exclusion), as well as the binding medium. The host should be modified to meet the design of the guest. Therefore, the properties of the guest must first be considered. The vital phenomena of anion recognition was described earlier, in the introduction chapter.

2.1.5. The optimum molecular weight of HBPs for anionic interaction

The effect of size on the interaction of a variety of pyridyl ligands using a zinc porphyrin cored hyperbranched polymer was reported by Ellis and Tywman.⁹⁰ The aim of this study was to probe the concept of a dense packed (or shell) theory for HBPs. Electronic and steric effects were identified as the two main driving forces that affect interaction. A core unit surrounded by polymer units may have a different electronic environment to that of bulk solvent and can provide a guest species with a more favourable environment. Steric effects also play a critical role, as binding will be hindered if there is a steric barrier between the core unit and the ligand. In this study, the interactions are optimal when the pyridyl ligands are coordinated perpendicular to the zinc porphyrin plane, thereby allowing maximum orbital overlap. Thus, sterics could restrict the optimal orbital overlap, and binding affinity would decrease. The study predicted that dense packing would take place as the molecular weight of HBP increased and the ligand would no longer be able to access the core unit at the point dense packing took place. The results of this work indicated an increase in binding due to positive electronic effects provided by the polymeric structure. This increase continued until the HBPs' molecular weight reached 8000 g/mol for each ligand. At this point there was a sharp decline in the association constant as the molecular weights increased (beyond 8000). These results confirm that any positive electronic impacts were overcome by steric effects, as the onset of dense packing took place. The graph below shows the effect of dense packing on pyridine ligand interaction (Figure 2.3).

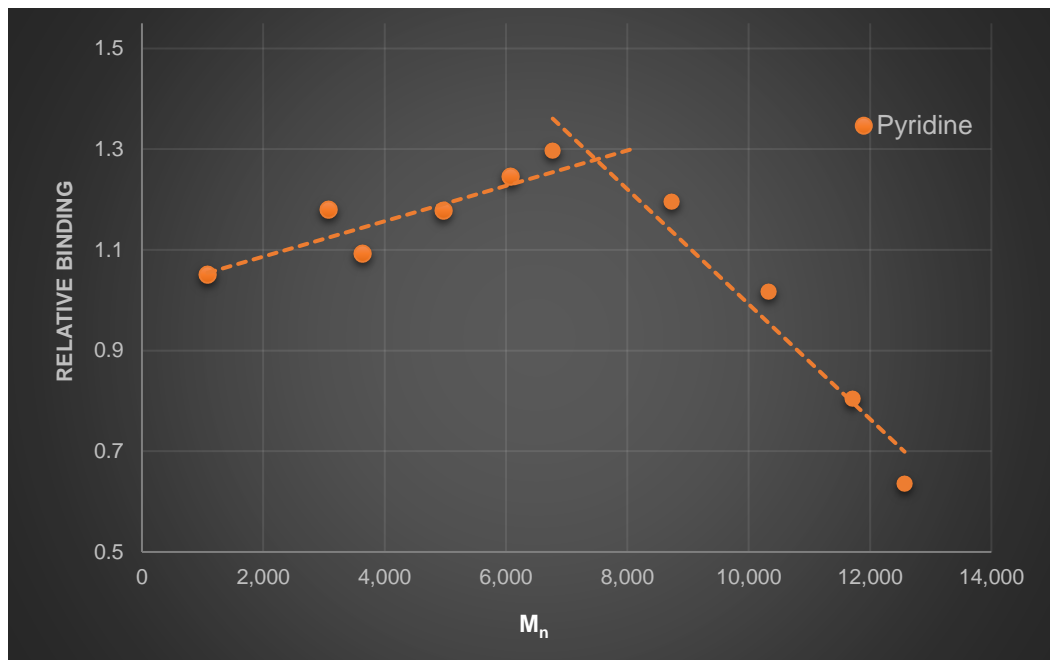


Figure 2.3: The binding data for interaction of varying molecular weight of zinc porphyrin cored hyperbranched poly 3,5-diacetoxybenzoic acid, with a pyridine ligand.⁹⁰⁻⁹²

2.1.6. Principles of anion binding receptor

Although an ionic bond generated by a positive charge receptors forms a strong interaction with anions, the non-directional nature decreases the selectivity of such charged receptors towards anion guests. Moreover, accompanying counter ions could compete with the anionic guest for the binding site, which further reduces selectivity and increases the possibility of steric hindrance. Therefore, neutral anion receptors are the most favourable options for this work, as they are not affected by these disadvantages. Neutral anion receptors are able to operate in water with hydrogen bonding interactions that forms dipole-dipole attraction between a hydrogen atom and a strongly electronegative atom with a lone pair of electrons allowing the formation of a strong bond. The strength of hydrogen bonding can be enhanced by increasing the hydrogen bond donors within the binding site. Generally, these types of bonds are stronger than ordinary dipole-dipole forces, but weaker than true covalent and ionic bonds. However, to synthesise an anion receptor that gives priority to hydrophobic species, the environment around the binding site needs to be hydrophobic

in nature. The aromatic structure of the receptor could also promote cooperative π - π stacking interactions and enhance the overall complex stability. On the other hand, the hydrogen bonding attractions require specific configuration or positioning of the concerned atoms. Thus, this type of interaction may cause a difficulty for design. The following section outline the aim and objectives that should be considered for the first part of this project.

2.2. Aim and Objectives

For many years, the use of small molecules as anion receptors has received more attention than macromolecules. In living systems, most encapsulation processes occur in aqueous media using the controlled environment within macromolecules. Therefore, biology is an important point of reference when designing molecules for anion binding in water. The primary aim of the research presented in this chapter is to create a system that has a specific local environment in which a hydrophobic macromolecule surrounds an anion binding site. This microenvironment should allow selectivity when binding anions in water (Figure 2.4). However, this system can only affect the electrostatic and steric environments, as it's more difficult to control or fix the precise geometry in the same way as in an enzyme.

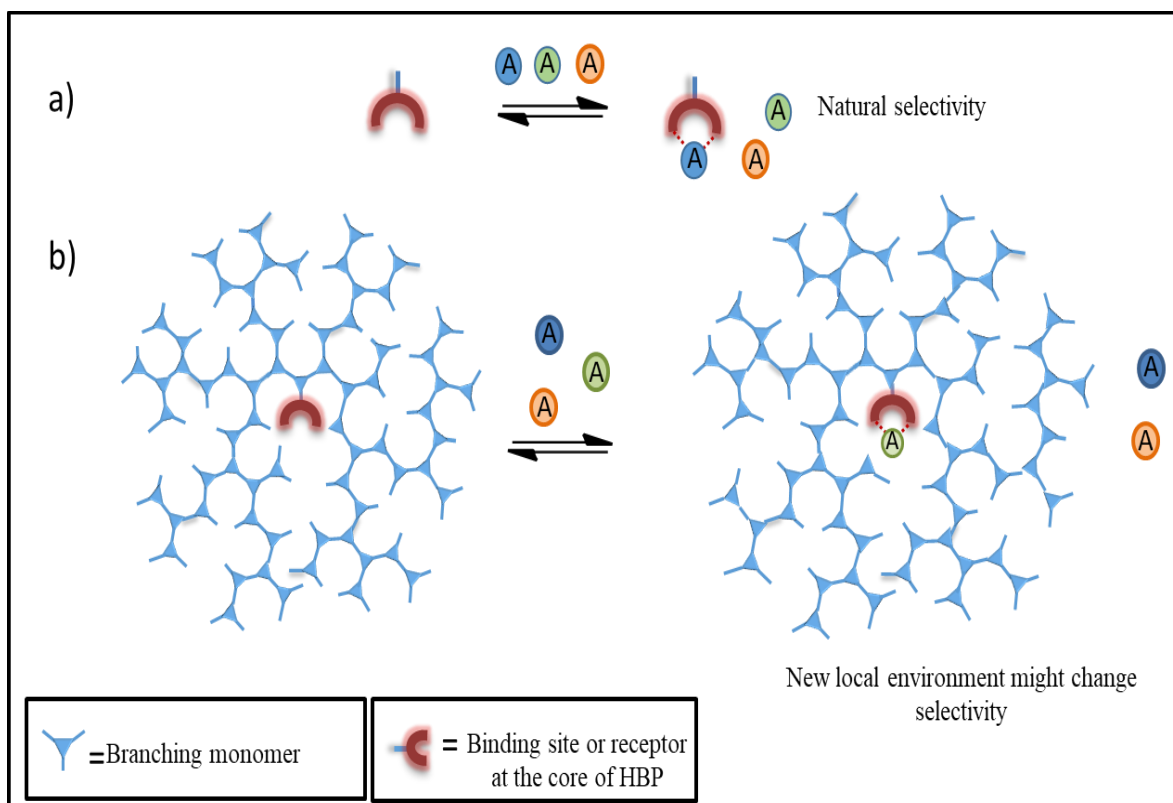


Figure 2.4: Changing of selectivity towards guests, (a) small molecule receptor, (b) hydrophobic macromolecule holding binding anion receptor.

2.2.1 Synthetic approach and consideration

The ultimate aim for this research project is to produce an anion binding system, where the anion receptor is incorporated within a water-soluble macromolecule. Therefore, the initial aim will be to investigate the covalent incorporation of a binding core within an organic soluble HBP. An organic soluble HBP is synthetically simpler to create than a water-soluble polymer. The system will be compared to the same receptor without the HBP shell. Our group has previously developed an effective HBP system where a core functionalised HBP was synthesised using 4-nitrophenyl acetate as the core and the simple AB₂ monomer 3,5- diacetoxybenzoic acid. Core incorporation was controlled precisely using a reversible polymerisation.⁹³ A similar process could be used to synthesise an anion binding system by using the binding site as a core. The monomer used has an aromatic ring, which could provide additional interactions for aromatic anions due to cooperative π - π stacking.

2.2.1.1 Design of an anion receptor molecule

When considering an appropriate anion receptor, there are specific criteria that need to be taken into account, the first of which is a stable core that can tolerate the reaction conditions required for the polymerization process. In addition, it should be compatible with the mechanism involved. Finally, the core should be analytically visible in the final product. There are two general types of receptor we could consider, a cyclic receptor or a cleft receptor (Figure 2.5A & B).⁹⁴ A cyclic receptor is a pre-organised system in which the anion receptor is fixed in the binding state. However, this type of receptor is synthetically challenging. On the other hand, a cleft receptor is not pre-organised and free rotation is allowed. As such, the receptor is not always in the binding configuration and can only be fixed when the anion is present. This requires a change in geometry, which can weaken binding. However, its preparation poses less of a challenge.

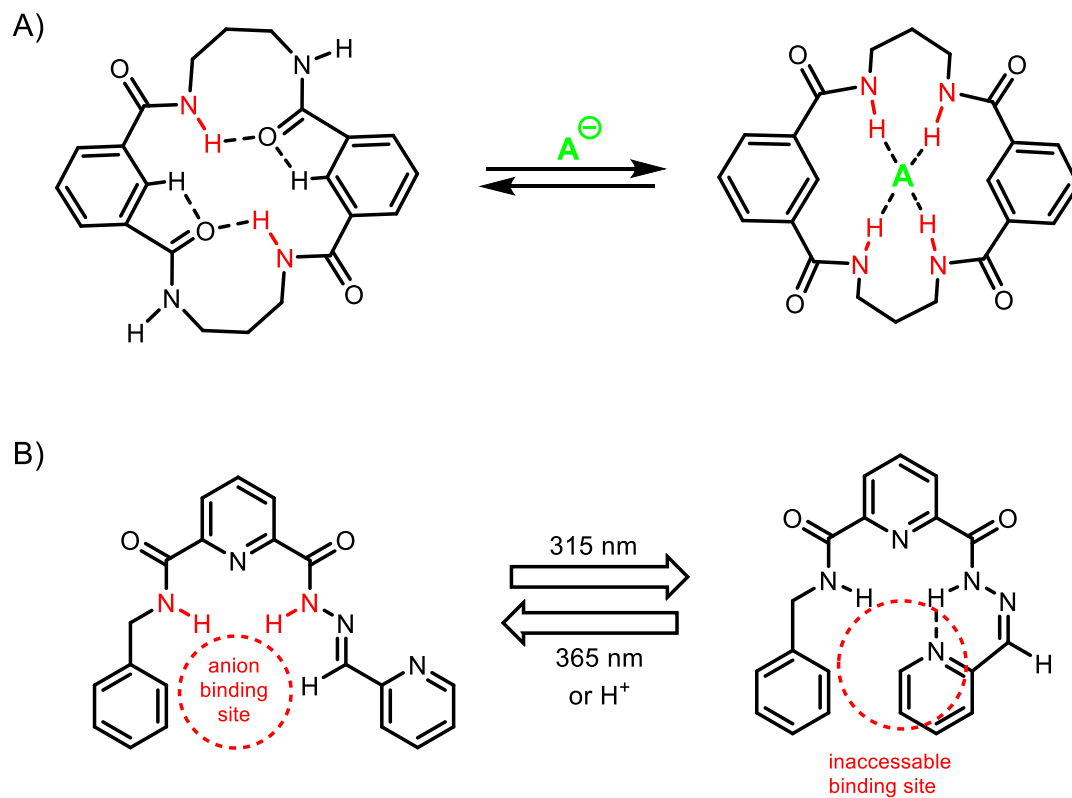
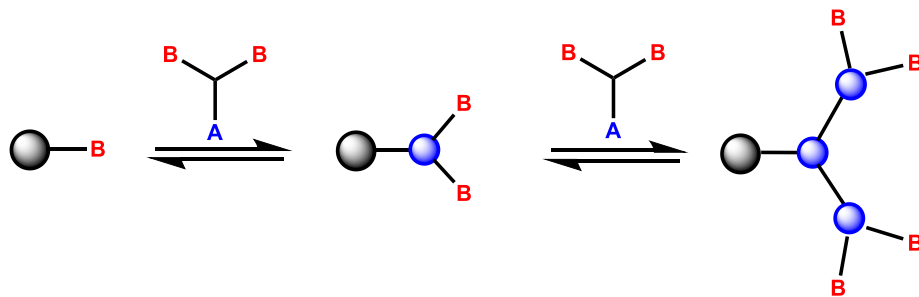


Figure 2.5: A) Crystallographic structure of preorganised cyclic receptor. B) Dynamic rotamers of cleft receptor.⁹⁴

Furthermore, synthesising a receptor with little preorganisation, allows the manufacture of receptors on a multi gram scale from economically priced starting materials. Therefore, a cleft receptor seemed a suitable choice to start with.

When considering the cleft structure, it was decided that a difunctionalized symmetrical molecule would allow simultaneous polymerisation to occur at both sites, which would ensure efficient incorporation within the hyperbranched polymer. The functionality would be solely dependent upon the monomer in question and the mechanism of polymerisation. We will use an AB₂ monomer, which means that it is a requirement for the core unit to have a two B functionality. The B group of the core unit interacts with the A group of a monomer unit, resulting in core functionalised B₂ unit. At this point, it is not possible to react with a second core unit (Scheme 2.2).



Scheme 2.2: The incorporation of a core and an AB₂ monomer.

Anion receptors that possess an isophthalamide moiety (Figure 2.6) have received a great deal of interest as anion receptors. Therefore, this functional group was chosen and would be used in our HBPs.

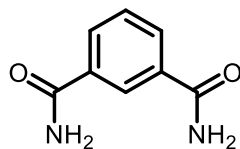
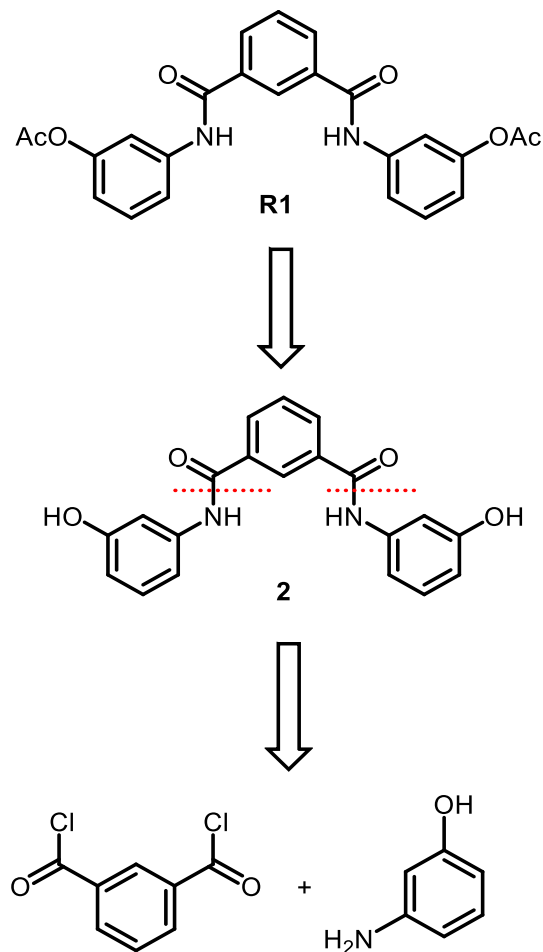


Figure 2.6: The chemical structure of isophthalamide.

The design of the receptor requires a di-functional, symmetrical, isophthalamide based receptor. The chemical structure of the desired receptor **R1** will have two acetoxy functional groups that can react with the acetoxy AB₂ monomers and propagate the polymerisation process. From the retrosynthetic analysis, the simplest route to the desired product would be the synthesis of N,N'-bis (3-hydroxyphenyl) isophthalamide **2**, followed by the acetylation of the terminal hydroxyl groups (Scheme 2.3).



Scheme 2.3: Retrosynthetic route of the target molecule N,N'-bis (3-acetoxyphenyl) isophthalamide into the corresponding synthons.

2.2.1.2. Design of an anion receptor based on HBPs

The overall aim is to encapsulate an anion receptor in an environment that is capable of being dissolved in water (i.e. a water-soluble system). However, it is initially worth ascertaining whether or not anion binding is affected by covalent incorporation of receptor molecules inside an HBP environment. Hence, to demonstrate the feasibility of the principle, it is necessary to test covalent incorporation inside an organic soluble polymer system. Critically, this attempt should take place before encapsulation inside a water-soluble system (which would be more difficult). The synthetic approach associated with an organic soluble system is characterised by substantially greater convenience. If a new electronic environment is added to the receptor's surroundings, one of the

following will take place: the normal pattern of anion interaction with the native receptor may be modified, which produces a difference in selectivity, due to the fact that the novel environment could be perfectly suited for a particular anions. Alternatively, relative binding trends may remain exactly the same compared to the native receptor. It is also worth noting that due to steric effects, the anionic guest's binding affinity could be lowered. With these considerations in mind, the first activity was to examine the impact of covalent incorporation within an organic HBP.

2.2.3. Transportation of anion within an organic soluble environment

The preliminary aim of the research discussed in this chapter is to formulate a host-guest system wherein a hyperbranched polymer can accommodate an organic soluble species at its core (receptor). To test the design of the system, we will use a 'U-tube' experiment, which has been widely-used to study the transportation of guests via carrier molecules (see Figure 2.7).⁹⁵ In a U-tube experiment, our guests are the anions, while the carrier molecules are the host receptors. The guests can be transported by the carrier molecules according to either facilitated or passive diffusion. In the case of passive diffusion, the guests are soluble in the organic solvent, and can diffuse through the medium in an unimpeded way without a host. Facilitated diffusion involves a carrier 'picking up' a guest from the aqueous layer (AqI) and moving it through the organic layer on the other side (AqII). Specificity and kinetic measurements are viable ways to differentiate between passive diffusion and facilitated diffusion. Velocity increases linearly with the concentration of diffusing guests in the context of simple diffusion.⁹⁶

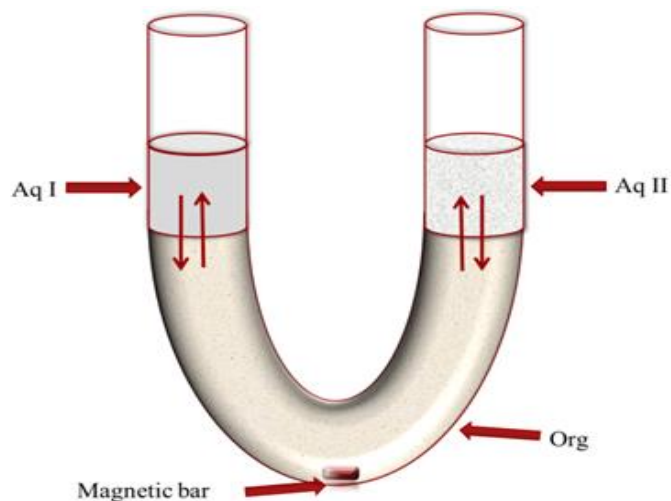


Figure 2.7: Schematic representation of the ‘U-tube’ model used to measure anion transport rates.

To ensure that the binding requirements are satisfied, close attention must be paid to the conditions. For example, organic anionic molecules must have compatibility with the receptor sites. These molecules should be characterised by a significant level of solubility in the aqueous phase. Additionally, the anions chosen should have low solubility, or not be soluble in the organic phase, since these conditions attenuate the passive diffusion effect. Another important condition is that the carrier (i.e. a cored HBP molecule) must be organic soluble with no aqueous solubility.

To investigate anions, effective analytical techniques, include Orion-Combined Fluoride Electrode, ultraviolet-visible (UV/Vis) spectroscopy, and nuclear magnetic resonance (NMR) spectroscopy, can be applied. In the present research, UV/Vis spectroscopy is employed. Furthermore, various molecular weights for HBP can be utilised to investigate quantitative aspects of the host system’s selectivity, while it is also possible to target various organic anion molecules.

2.3. Results and Discussion

2.3.1. Synthesis of N,N'-bis-(3-acetoxyphenyl) isophthalamide

The core must have functional groups that compatible with AB₂ monomer 3,5-diacetoxybenzoic acid. Consequently, the di-functional acetyl receptor based on isophthalamide **R1** was chosen.

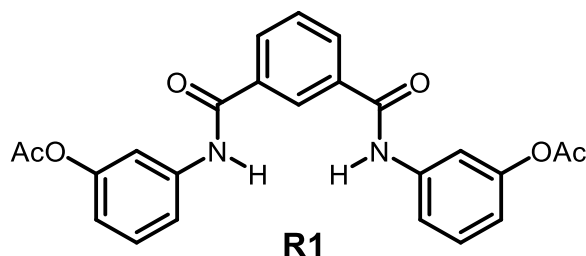
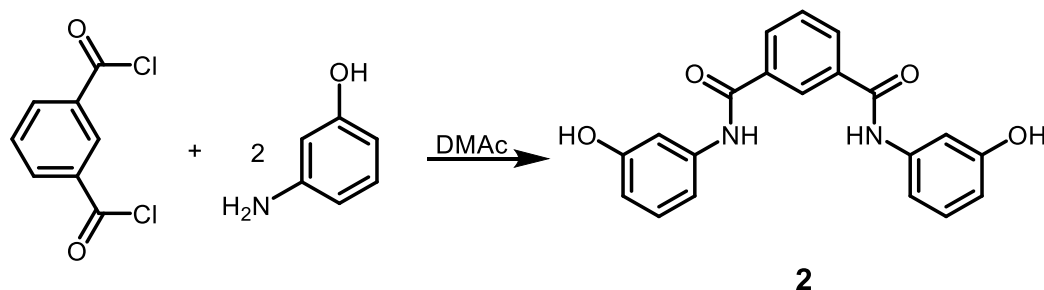


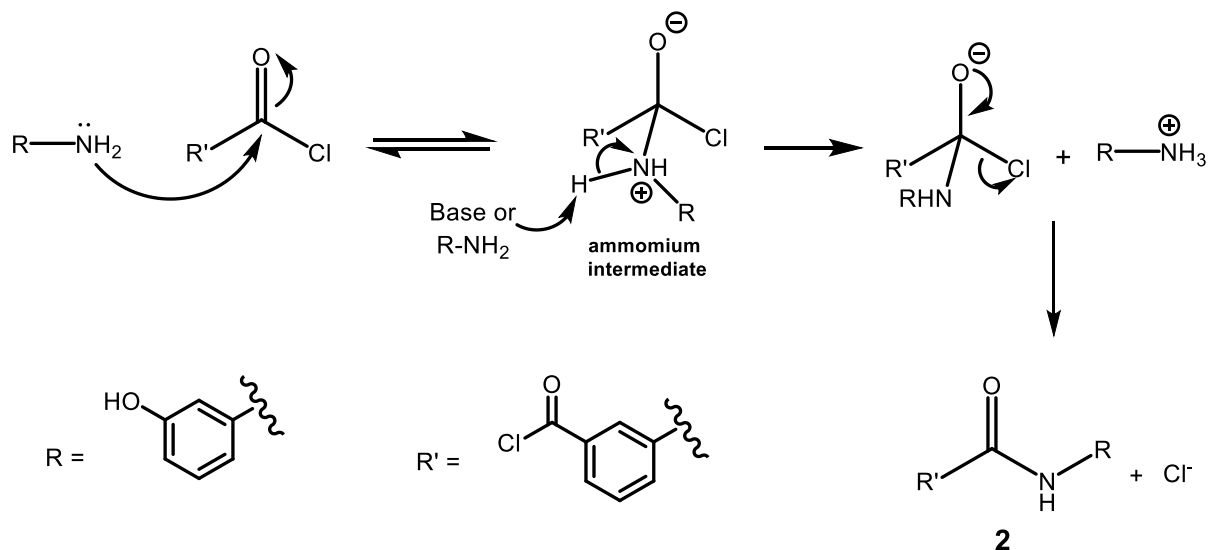
Figure 2.8: Chemical structure of free receptor/core (**R1**).

The first step in the process was the synthesis of N,N'-bis-(3-hydroxyphenyl) isophthalamide (**2**), which was achieved according to the modified procedure described by Malone et al.⁹⁷ The mixture of two equivalents of 3-aminophenol and anhydrous N,N'-dimethylacetamide (DMAc) were degassed and flushed with argon and the reactor cooled to 0 °C. One mole of isophthaloyl chloride was added slowly over 30 min and stirred for 6 hours at room temperature. The product was precipitated from cold distilled water to give product **3** as a white solid in a good yield of 75% (Scheme 2.4).



Scheme 2.4: Synthesis of N,N'-bis(3-hydroxyphenyl) isophthalamide.

The mechanism is comprised of three stages (Scheme 2.5). 3-aminophenol functions as a nucleophile and attacks the carbonyl group of isophthaloyl chloride compound to form a tetrahedral intermediate. The second stage involves deprotonation of the atom from the ammonium intermediate using another amine as base. This led to reintroduction of the carbonyl group with chloride as the leaving group.



Scheme 2.5: Mechanism of nucleophilic substitution reaction of carboxylic acid derivatives.

Analysis of the ^1H NMR spectrum's coupling and integration confirmed the structure of amide **2**. The peaks corresponding to the OH and NH protons were observed as two singlets, both with an integral of two at 10.28 ppm and 9.46 ppm respectively. A highly deshielded single peak at 8.48 ppm corresponding to one aromatic proton (H_a), attributed to the very strong effect of two carbonyl groups. Another singlet at 6.52 ppm corresponded to two aromatic protons (H_g) (Figure 2.9). The mass spectrum showed a signal at 347, indicative of the MH^- ion. The FT-IR spectrum of amide **2** shows a new peak at 1681 cm^{-1} that corresponds to the amide stretching vibration. The obtained N,N'-bis-(3-hydroxyphenyl) isophthalamide was pure enough to be carried forward to the next stage of synthesis.

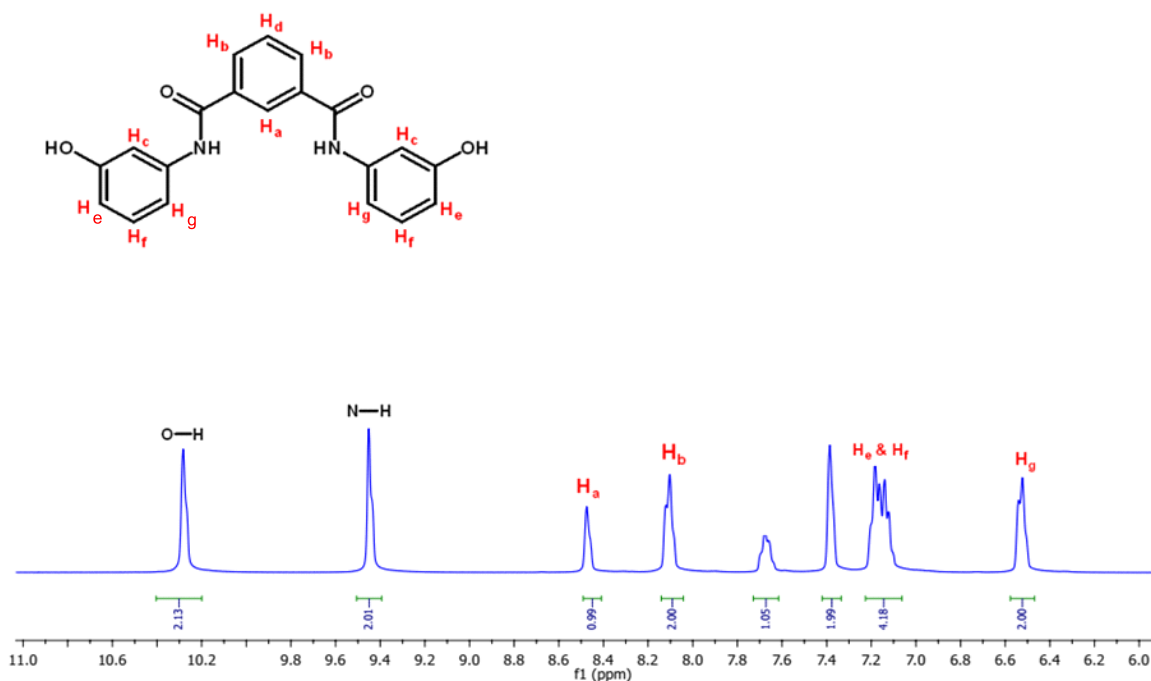
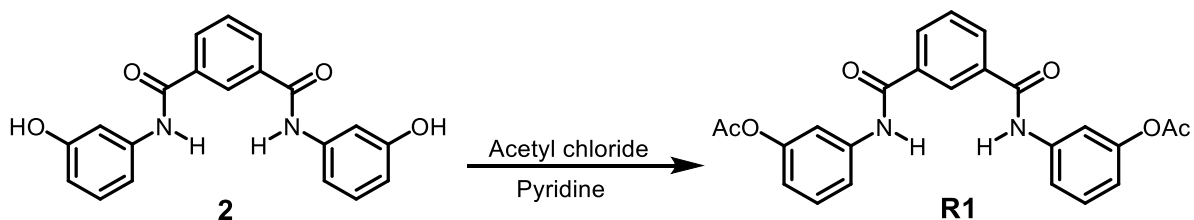


Figure 2.9: The ^1H NMR spectrum for N,N'-bis(3-hydroxyphenyl) isophthalamide (**2**).

The next stage of the synthetic procedure was to acetylate the hydroxyl terminal groups of amide **2** (Scheme 2.6).



Scheme 2.6: Synthesis of N,N'- bis(3-acetoxy-phenyl)-isophthalamide

The amide **2** was dissolved in anhydrous pyridine and cooled in an ice bath. Acetyl chloride was then added dropwise after degassing. The reaction was stirred at room temperature for 4 hours. The solvent was removed, and the crude product was dissolved in DCM and washed with saturated NaHCO_3 solution and distilled water to remove the by-product (acetic acid). The product was dissolved again in chloroform and filtered. The cream solid was then recrystallized in a minimum

of DCM and petroleum ether (40-60), yield obtained was 56%. Acetylation of a hydroxyl group was performed in the presence of pyridine, which played an important role in the synthesis while also acting as a solvent. It successfully neutralized the acid protons formed during the synthesis and also worked as a nucleophilic catalyst, helping to speed up the reaction.⁹⁸

The ¹HNMR spectrum shows that the acetylation process was successful as the –OH signal, present at 10.28 ppm in the spectrum for amide **2** was no longer visible. In addition, a singlet at 2.29, corresponding to six methyl protons of the acetate groups, was now visible (Figure 2.10). A mass spectrum gave a signal at 433 for the MH⁺ ion confirming the exact chemical formula

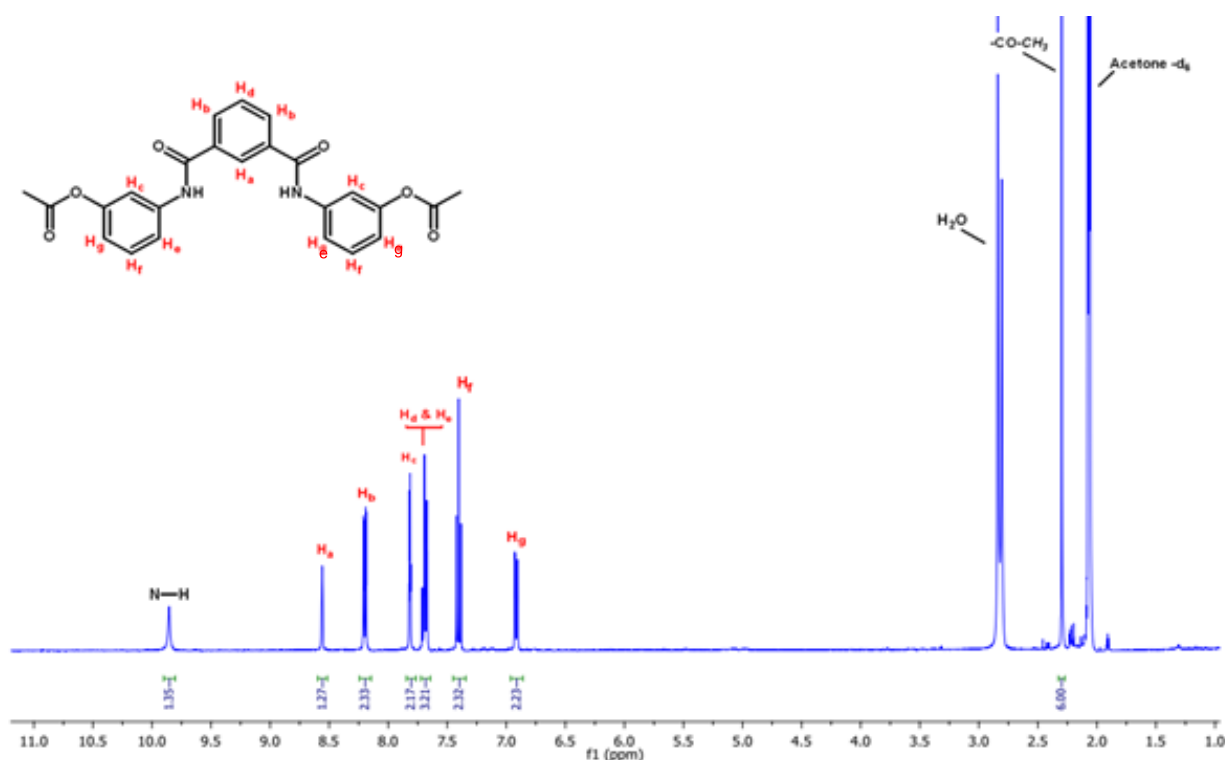


Figure 2.10: ¹HNMR spectrum for [N,N'-bis-(3-acetoxyphenyl)-isophthalamide] receptor.

As mentioned in the introduction of this chapter, cleft-like receptors have a variety of different conformations because of free rotation in solution – only syn-syn is optimised for binding (Figure 2.11).⁹⁹ However, in the absence of a guest, it is more likely that rotation of bonds will favour other conformations.

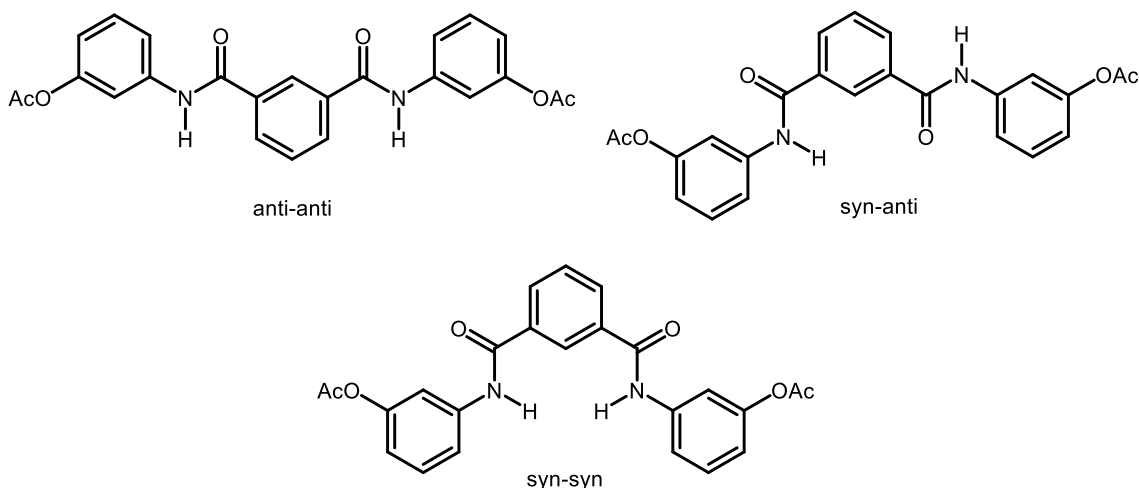


Figure 2.11: The different conformations of N, N'-bis (3-acetoxyphenyl) isophthalamide.¹⁸⁵

The crystals of the core **R1** were analysed by X-ray crystallography (Figure 2.12). Kavallieratos et al.⁹⁹ reported that isophthalamide-based receptors demonstrate *syn-anti* or *anti-anti* conformations in the absence of an anionic guest, as opposed to the *syn-syn* conformation, which is optimal for anion interaction. Usually, the binding *syn-syn* conformation is adopted when an anionic guest is included, which is driven by the two linear hydrogen bonds. In our case, it was pleasing to observe that the crystals were in the *syn-syn* conformation as the X-ray represents the lowest energy solid state.

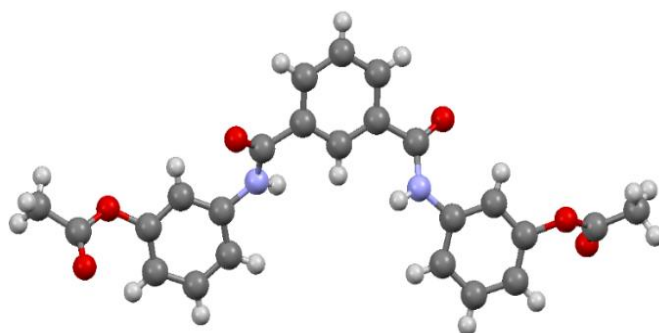
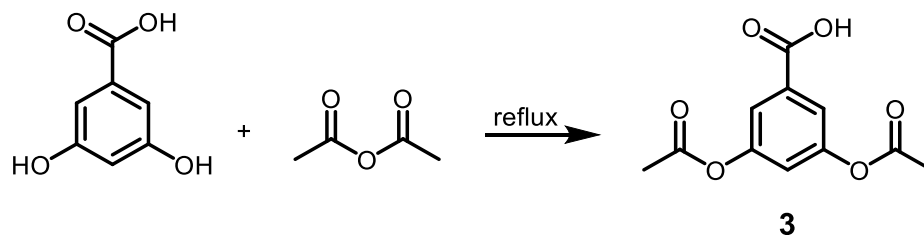


Figure 2.12: Shows the X-ray crystal structure of N,N'- bis (3-acetoxyphenyl) isophthalamide.

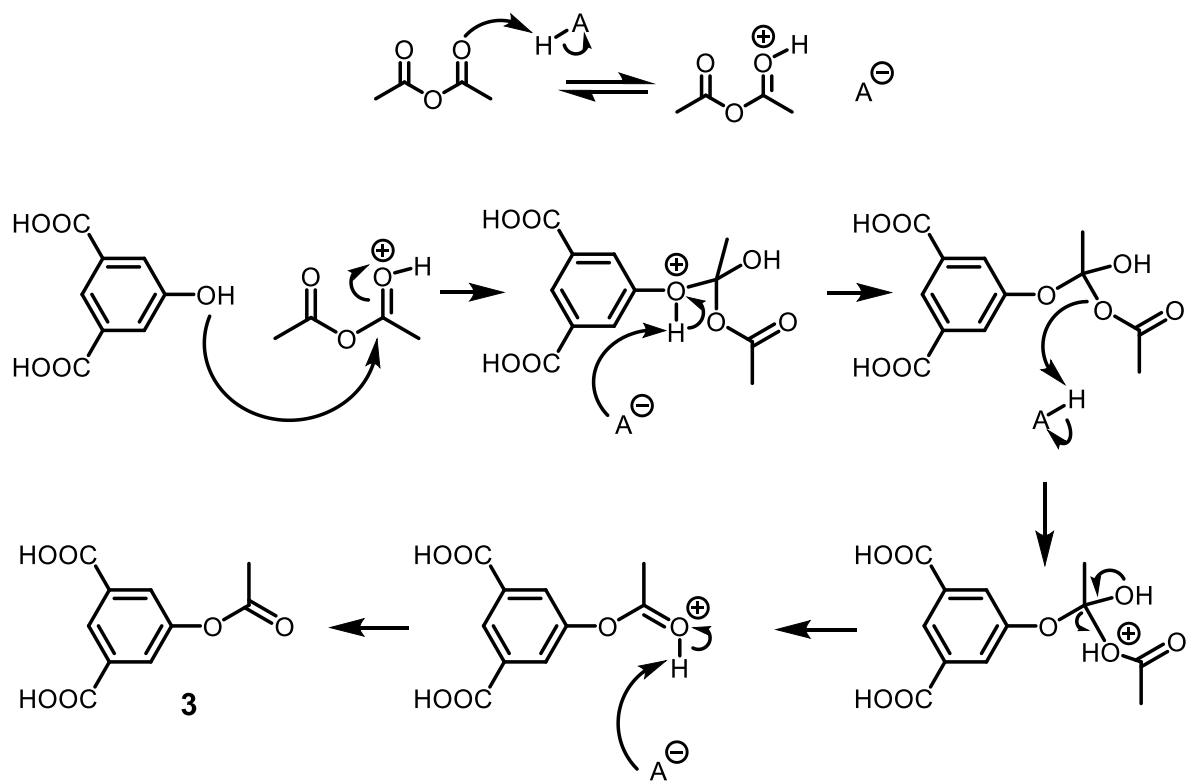
2.3.2. Synthesis of monomer unit 3,5-diacetoxybenzoic acid

The monomer 3,5-diacetoxybenzoic acid **3** is the AB₂ monomer used for the preparation of our target HBP. The AB₂ monomer **3** was produced by reacting commercially available 3,5-dihydroxybenzoic acid and acetic anhydride (Scheme 2.7).¹⁰⁰



Scheme 2.7: Synthesis of 3,5-diacetoxybenzoic acid (**3**).

The dihydroxy acid was acetylated at the 3,5-positions by refluxing with excess of acetic anhydride. The crude product was dissolved in hot chloroform and filtered, before precipitating in petroleum ether to give a white solid product in a yield of 44%. Extra care was taken to ensure that the temperature did not exceed 80°C, to avoid the risk of any self-polymerization. The mechanism of the acetylation reaction is shown in Scheme 2.8.



Scheme 2.8: The mechanism of acetylation reaction of 3,5-dihydroxy-benzoic acid in presence of acid (H-A).

The ^1H NMR spectrum displays a broad singlet at 9.84 ppm, indicative of the carboxylic acid proton. A doublet and triplet at 7.75 and 7.22 ppm corresponded to the three aromatic protons. An intense singlet peak was observed at 2.34 ppm, which integrated to six protons, confirming the presence of the acetoxy groups (Figure 2.13). The structure was further confirmed by mass spectrometry, which showed a molecular ion peak at 237 Daltons. The IR spectrum shows a new intense peak at 1691 cm^{-1} , corresponding to $\text{C}=\text{O}$ for the ester functional group, and an absence of a broad peak at 3198 cm^{-1} for the O-H functional group.

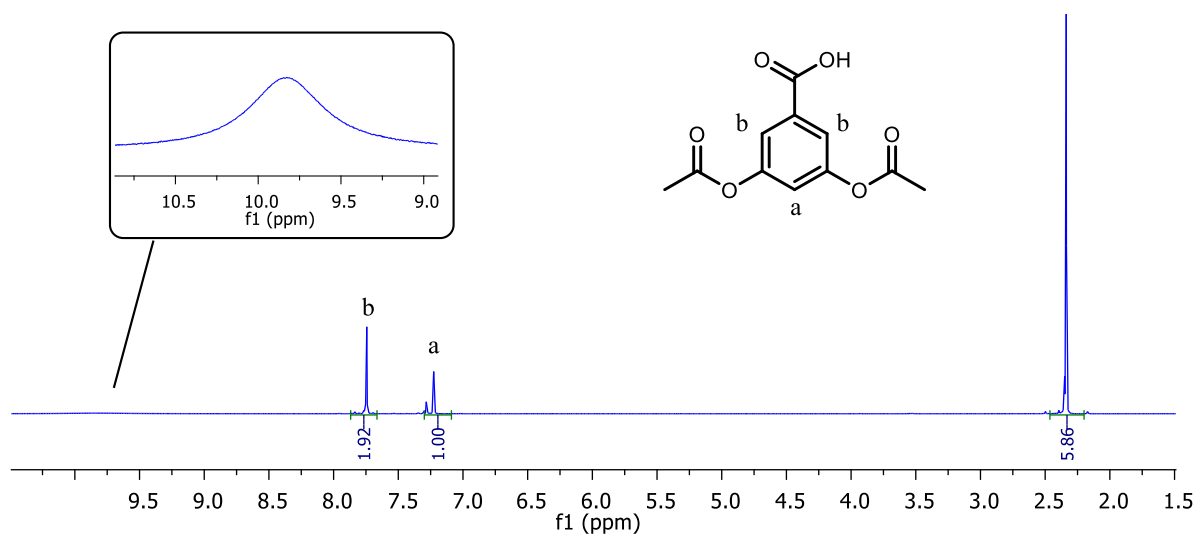
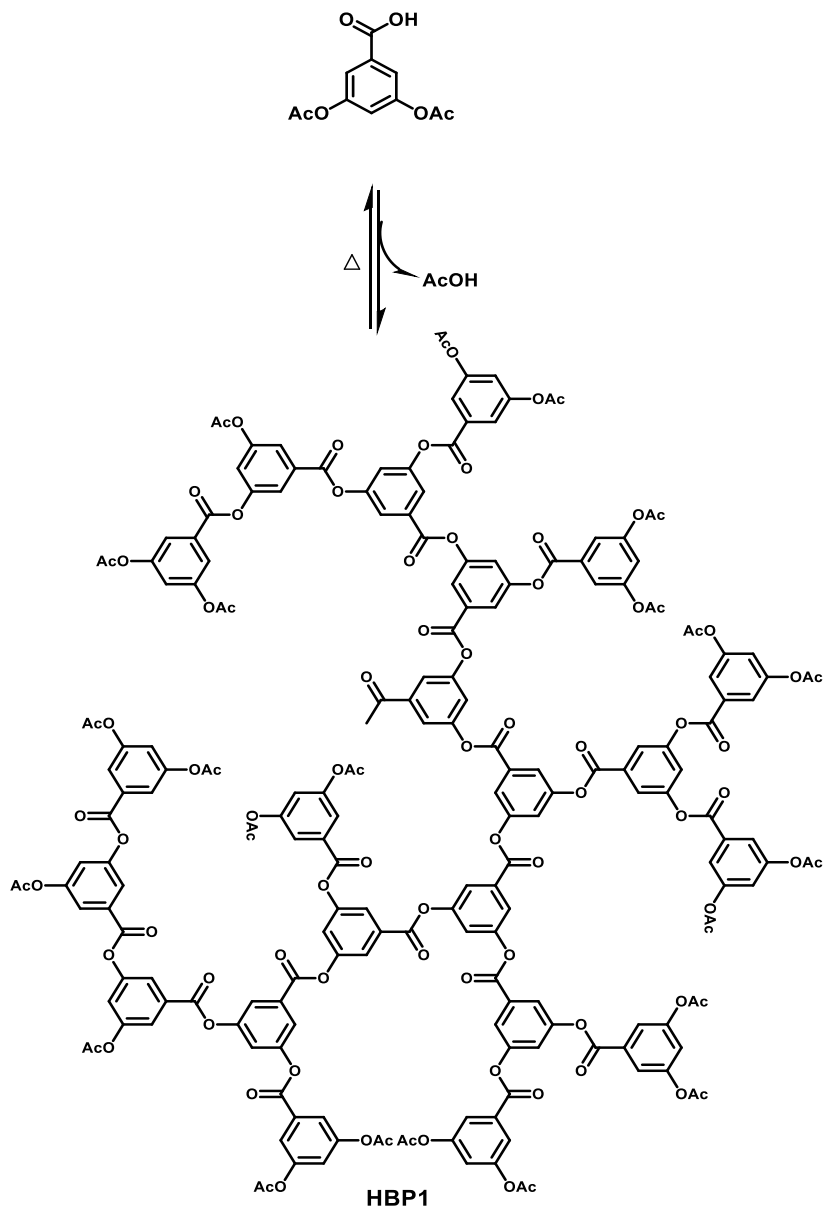


Figure 2.13: ¹H NMR spectrum for 3,5-diacetoxybenzoic acid.

2.3.3. Homo polymerisation of 3,5-diacetoxybenzoic acid

The polymerisation was initially performed without a core as a resulting polymer would be used as a reference in control experiment. The non-cored HBP was synthesised using diphenyl ether as a solvent. The procedure involves two different temperatures to execute through the reaction. Firstly, it was heated to 225°C for 45 minutes, whereby the solvent melts to ensure complete monomer dissolution and initial oligomers were formed. The temperature was then lowered to 180°C for 4 hours, and the system placed under vacuum to drive the polymerisation to equilibrium. This allowed the removal of the by-product (acetic acid) and led to the completion of the reaction (Scheme 2.9).



Scheme 2.9: The polymerisation of 3,5-diacetoxybenzoic acid.

The successful polymerisation was verified using ^1H NMR spectroscopy, which is confirmed by the absence of the carboxylic acid proton at 9.84 ppm. Also noteworthy was a decrease in the intensity of the peak for methyl protons at 2.32 ppm. As the polymerization occurs, the ratio of the terminal acetoxy peak to the aromatic peaks decreases, which is the cause of the decrease of methyl

peak. The HBP has three types of repeat unit, known as the dendritic unit (D), linear unit (L), and terminal unit (T) (Figure 2.14).

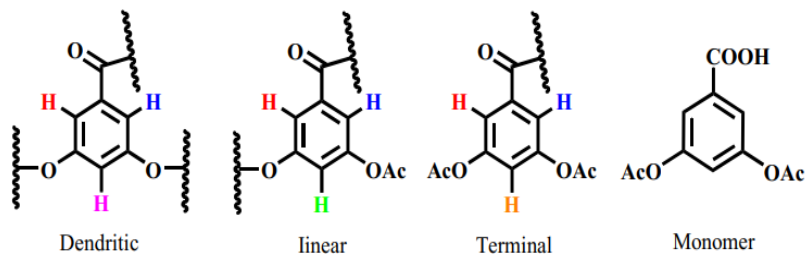


Figure 2.14: Structural units of *ortho*- and *para*-protons present in HBP.

After polymerisation, the *ortho*-protons to the carbonyl, which were equivalent in the monomer (at 8.21 ppm), are no longer equivalent. These protons can be a broad peak between 7.70 and 8.10 ppm (Figure 2.15).

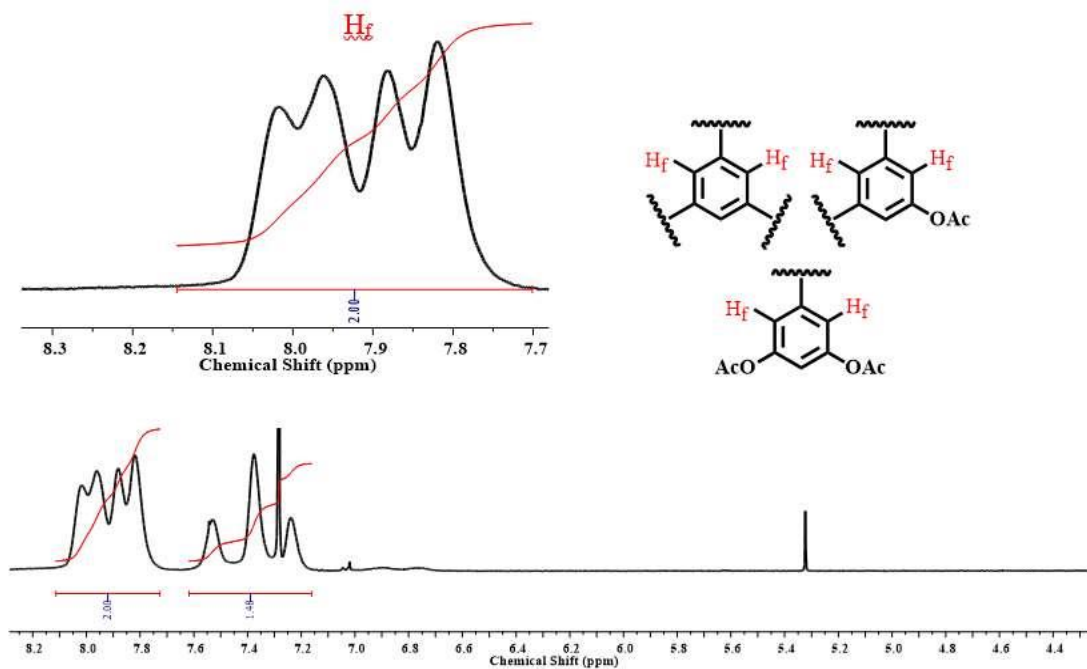


Figure 2.15: The ^1H NMR spectrum of aromatic protons of poly (3,5-diacetoxybenzoic acid).

In addition, three peaks attributed to the protons *para* to the carbonyl can be seen at 7.23 ppm, 7.38 ppm, and 7.55 ppm. These are the dendritic (D), linear (L), and terminal (T) protons, respectively (Figure 2.16). The relative integration ratios (from ^1H NMR) of these units can be used to calculate the degree of branching using Equation 2.1 (See section 2.1.1).

Assignments of D, L and T were made by understanding that the number of dendritic (D) units and terminal (T) units are almost equivalent. This makes it relatively straightforward to identify linear (L) units as the large peak at 7.38 ppm. The peaks at 7.23 ppm and 7.55 ppm are approximately equal and correspond to the terminal units or dendritic units. We can distinguish the D or T units based on chemical shift, as the D protons have strong electron withdrawing aromatic groups on each side. As such, we can assign the D peak on the signal at 7.55 ppm. This leaves the peak at 7.23 ppm, which must be the T unit. Applying the integration values of 0.24, 0.50, and 0.26 obtained from the polymer (see Figure 2.16) in Equation 2.1 provided a DB around 50%, which is consistent with this type of AB_2 polymerisation.¹⁰¹

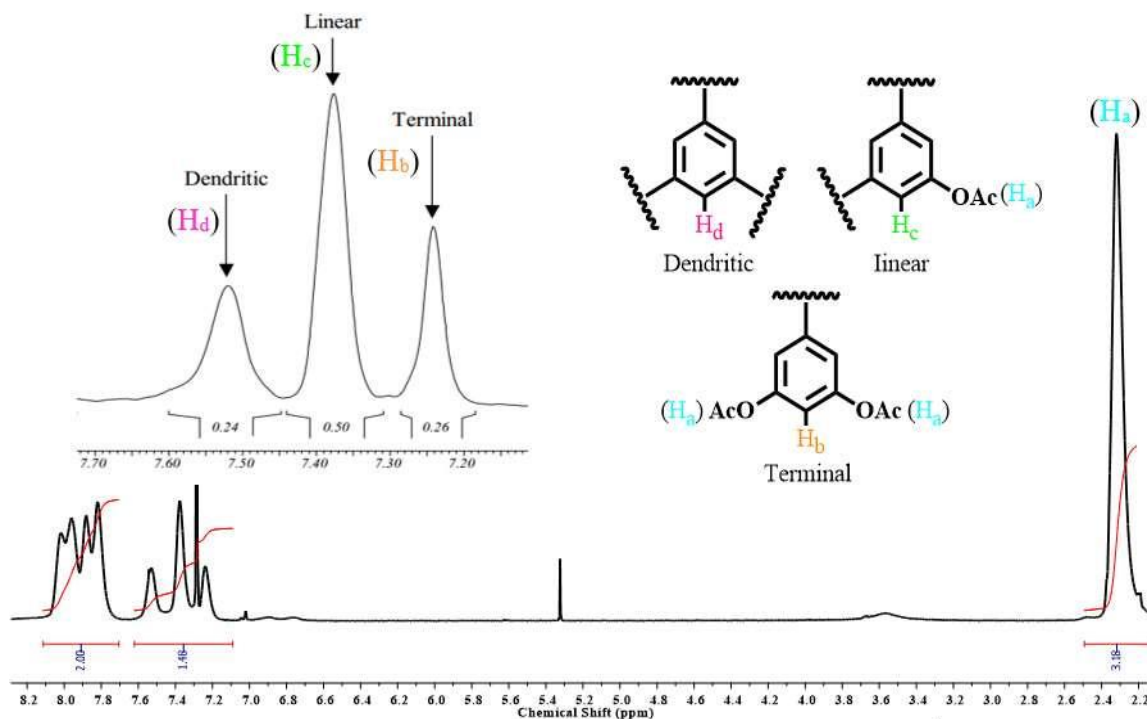


Figure 2.16: The ^1H NMR spectrum of *para*-proton of poly(3,5-diacetoxybenzoic acid); assigning the values of dendritic (D), linear (L), and terminal (T) units.

Gel permeation chromatography (GPC), calibrated against polystyrene standard, showed an $M_n = 4439$ Da and a $PD = 1.6$. Typically, HBPs that are synthesised without control have a high PD.¹¹⁸
¹¹⁹ The IR spectrum provided additional information regarding the successful preparation of the HBP, which no longer showed the carboxylic acid peaks at 1769 cm^{-1} and 3600 cm^{-1} .

2.3.4. Synthesis of core functionalised HBP 1:15

After successful synthesis and characterisation of the homo HBP, we next attempted to synthesise a variety of molecular HBPs with anion binding cores. The general polymerization procedure used for the homo polymerisation of 3,5-diacetoxybenzoic acid was followed, but a core was added. The ratio of core to monomer was 1:15 (mole ratio) and mixed with an equal mass of diphenyl ether as a solvent. The resulting polymer was isolated by precipitation and washed repeatedly with cold methanol to remove any trace amounts of unreacted core. The **R1** core unit reacts via the same mechanism described in section 2.3.3; the acetoxy groups react with the carboxylic acid groups on the monomer unit.

It should be noted that we decided to use DMSO- d_6 as NMR solvent instead of using $CDCl_3$ to avoid the solvent peak overlapping with the products aromatic region. Moreover, the calibration of the core's peaks with polymeric peaks would be more accurate and easier to calibrate. The ^1H NMR spectrum (Figure 2.17) indicated a new broad signal from the core at 6.90 ppm and to the right of the polymer signals, which corresponded to the protons **H_g** (in position *para* to the amide group in the core molecule). These are the most shielded core protons. At 8.73 ppm to the left of the polymer signal, a broad multiplet was seen corresponding to the **H_a** signal of the core. The broadness of the signals provides evidence that the core had been incorporated. A broad multiplet can be seen at 7.30-8.30 ppm, corresponding to the polymeric protons. It should be noted that there is considerable amount of overlap between the remaining core signals and polymer signals due to the similarity in chemical shifts. As a result, direct assignment of these particular signals is extremely difficult.

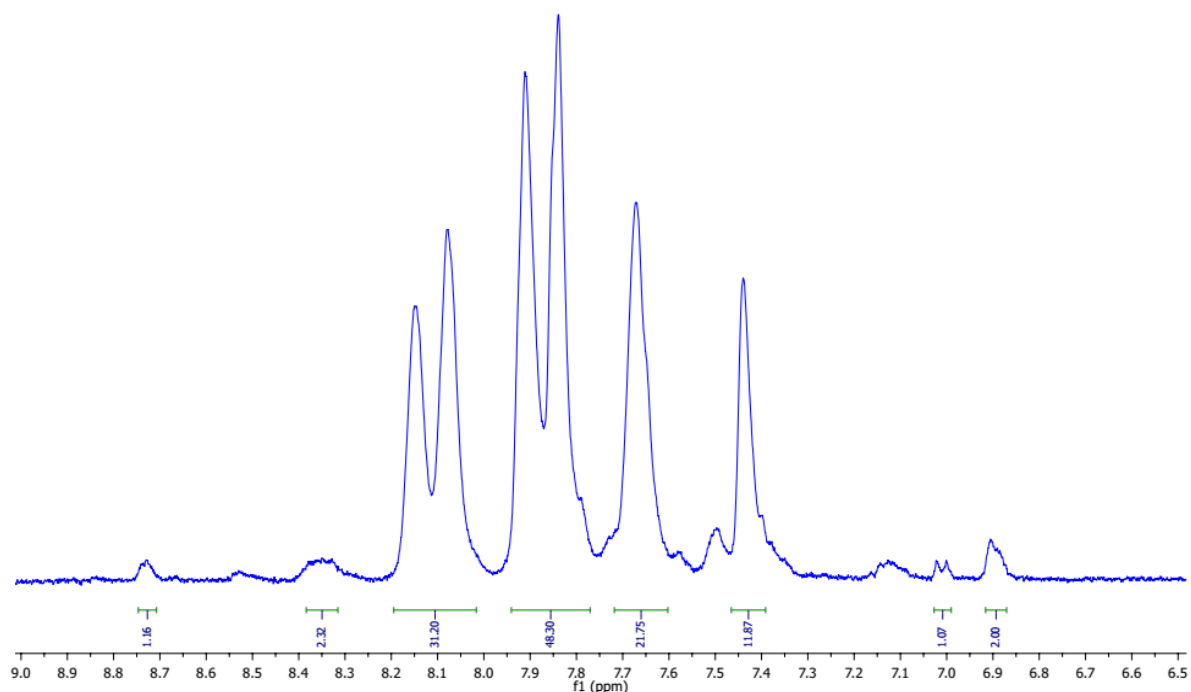


Figure 2.17: ^1H NMR expansion (6.5 to 9 ppm) of HBP 1:15. On the right, a monitored signal (\mathbf{H}_g) at 6.90 ppm corresponding to the incorporated core can be seen, using DMSO-d_6 .

Gel Permeation Chromatography (GPC) gave an approximate molecular weight of 6000 g/mol. It should be noted that GPC underestimates the molecular weight of HBPs since it is calibrated against linear polystyrene. HBPs adopt a globular conformation in solution, which are smaller in volume than an equivalent linear analogue. Another technique used to calculate M_n was ^1H NMR analysis, which overestimates molecular weight, giving an M_n of 8000 g/mol. This is calculated by integrating the peak at 6.89-6.91 ppm, corresponding to two protons \mathbf{H}_g (in position *para* to the amide group of the core). The AB_2 monomer 3,5-diacetoxybenzoic acid has two acetoxy groups and a single carboxylic acid, which is consumed after each monomer is added. However, two acetoxy group are subsequently introduced. The number of monomer units present can be estimated from ^1H NMR spectrum, by integrating the monitored peak (\mathbf{H}_g) of the core to the HBP's peaks, which allows us to calculate the number of polymeric protons (AB_2 monomer protons). Thus, an

approximate number of monomer units around the core could be estimated. The monomer units in **HBP6000** would be almost 40 units. In this case, we can estimate the structure shown (Figure 2.18). By increasing the globular structure of the HBP, we expect to see more discrepancy between M_n of GPC and NMR. This is because of using a linear polymer as standard in GPC device, which increases the error when compared with a non-linear polymer.

However, at the $6000 \text{ g}\cdot\text{mol}^{-1}$ (estimated by GPC), the **HBP6000** was just below the onset of dense packing. This means that the core in **HBP6000** should bind well to anions. The next step in this study was to synthesize HBP systems that were both higher and lower than the optimum dense packing limit ($6000\text{-}8000 \text{ g}\cdot\text{mol}^{-1}$). These would provide insight into whether steric effects, geometric limitations, and/or electronic effects play a significant role in anion binding studies.

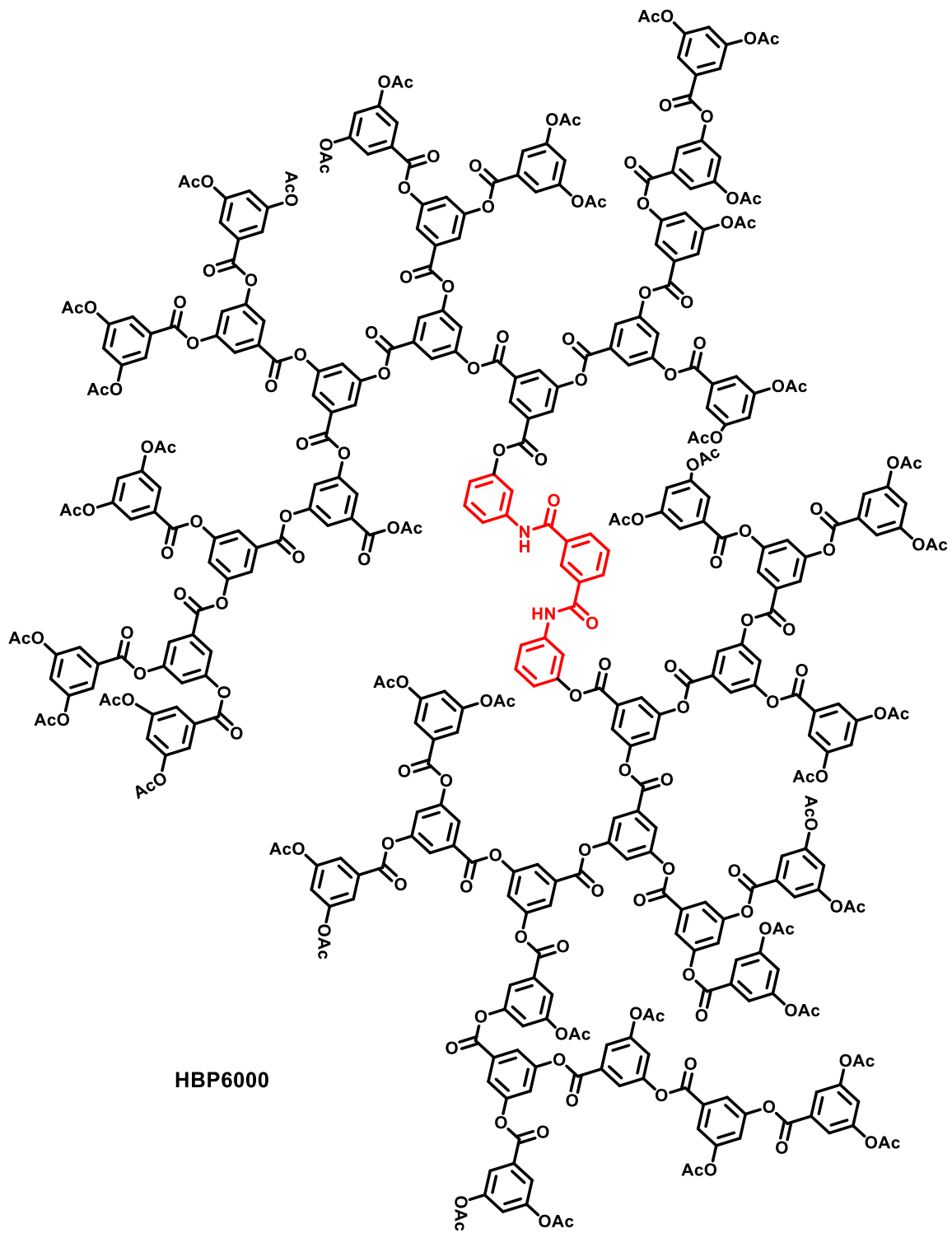


Figure 2.18: Representative structure of cored **HBP6000** (ratio 1:15).

2.3.5. Synthesis of core functionalised HBP 1:5

Although a HBP with an Mn 6000 g/mol would be an ideal polymer for optimum anion interactions. A 1:5 core to monomer ratio should give a HBP with small Mn and allow us to test the theory of dense packing using a smaller less well-defined HBP. We would predict weaker binding for this polymer. The general procedure of homo polymerisation of 3,5-diacetoxybenzoic acid, as discussed in section 2.3.3, was used. ^1H NMR would be used to determine the success of core incorporation; the spectrum can be seen in Figure 2.19. The polymer signals should become less dominant as the core peaks increase; this was observed for HBP with 1:5 ratio. The spectrum shows singlet at 6.89 ppm, which corresponds to the protons *para* to the amide group of the core, as these are the most shielded protons present. A multiplet can also be seen at 8.74 ppm, indicative of the H_a signal, which is the most deshielded peak. The remaining core signals are harder to see, as they were overlapped with the polymer signals between 7.30 and 8.30 ppm (Figure 2.19).

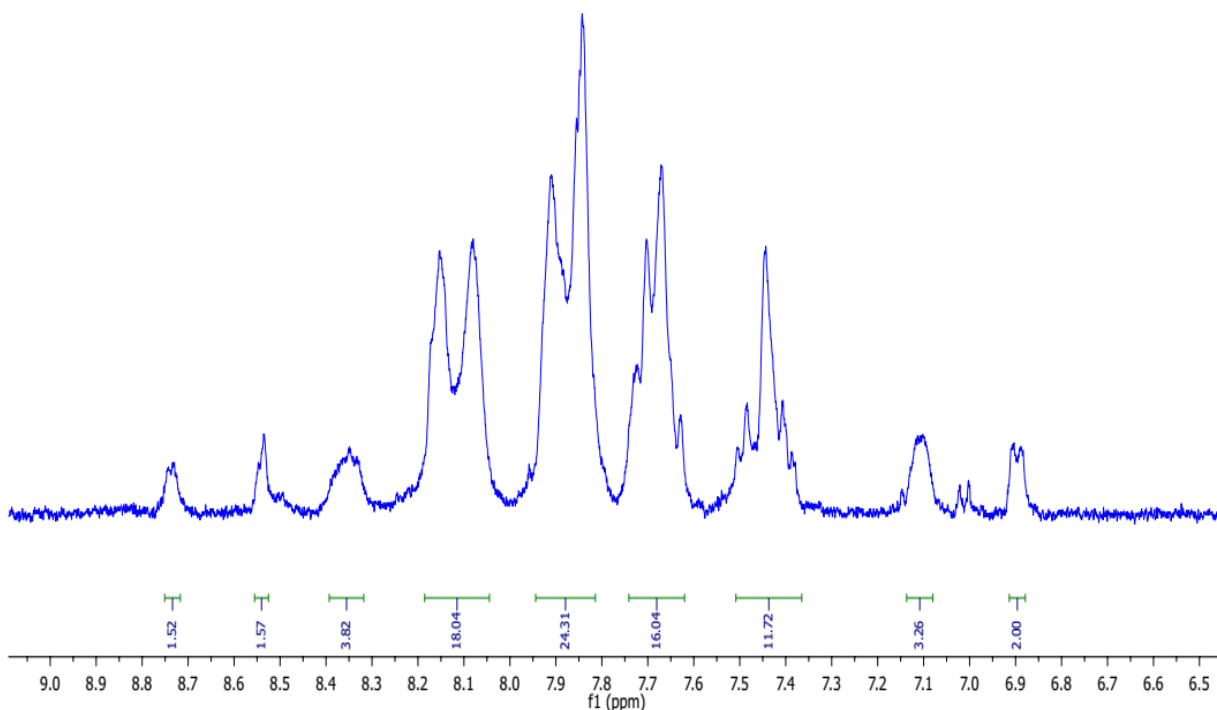


Figure 2.19: ^1H NMR expansion (6.5 to 9 ppm) of HBP 1:5. On the right, a monitored signal (H_g) corresponding to the incorporated core can be seen, using DMSO-d_6 .

The molecular weight of this HBP was 3000 g/mol, as determined by ^1H NMR, with GPC giving a value of 2800 g.mol $^{-1}$. The small margin between the estimated Mn values provide confidence in a high level of core incorporation. From the ^1H NMR, we estimated that almost 12 monomer units surrounded the core unit, creating a less globular or oligomeric structure system (Figure 2.20).

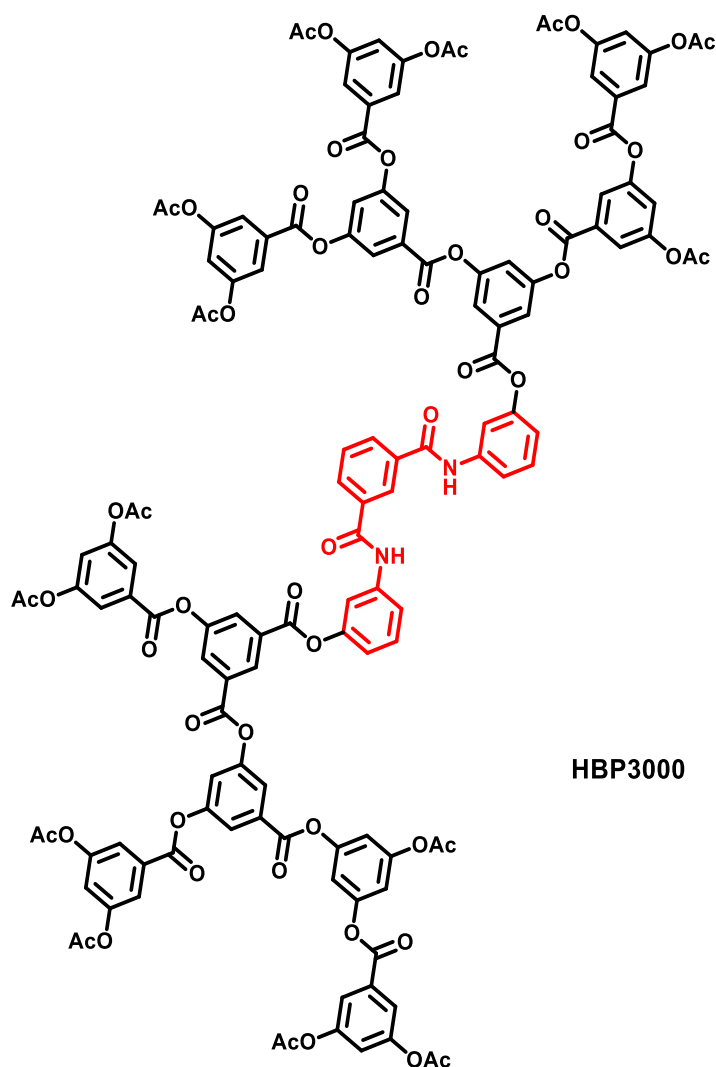


Figure 2.20: Representative structure of cored functionalised **HBP3000** (ratio 1:5).

2.3.6. Synthesis of core functionalised HBP 1:25

To further test the dense packed limit of the HBP, we wanted to synthesise a polymer with an Mn above the dense packed limit. Binding to this polymer would be difficult due to steric effect. We predict much weaker binding for this polymer. The general polymerisation procedure was used with an increased core-monomer ratio of 1:25. The ^1H NMR signals of the polymer become more

dominant, thereby reducing the sharpness of core signals (Figure 2.21). A broad doublet at 6.91 ppm is seen for the \mathbf{H}_g protons of incorporated receptor. For HBPs with high molecular weight, the determination of the incorporated core's peaks was difficult, as the core signals are weak relative to the monomer; this can therefore lead to high inaccuracy in any spectral interpretation or calculation based on the integration of these peaks.

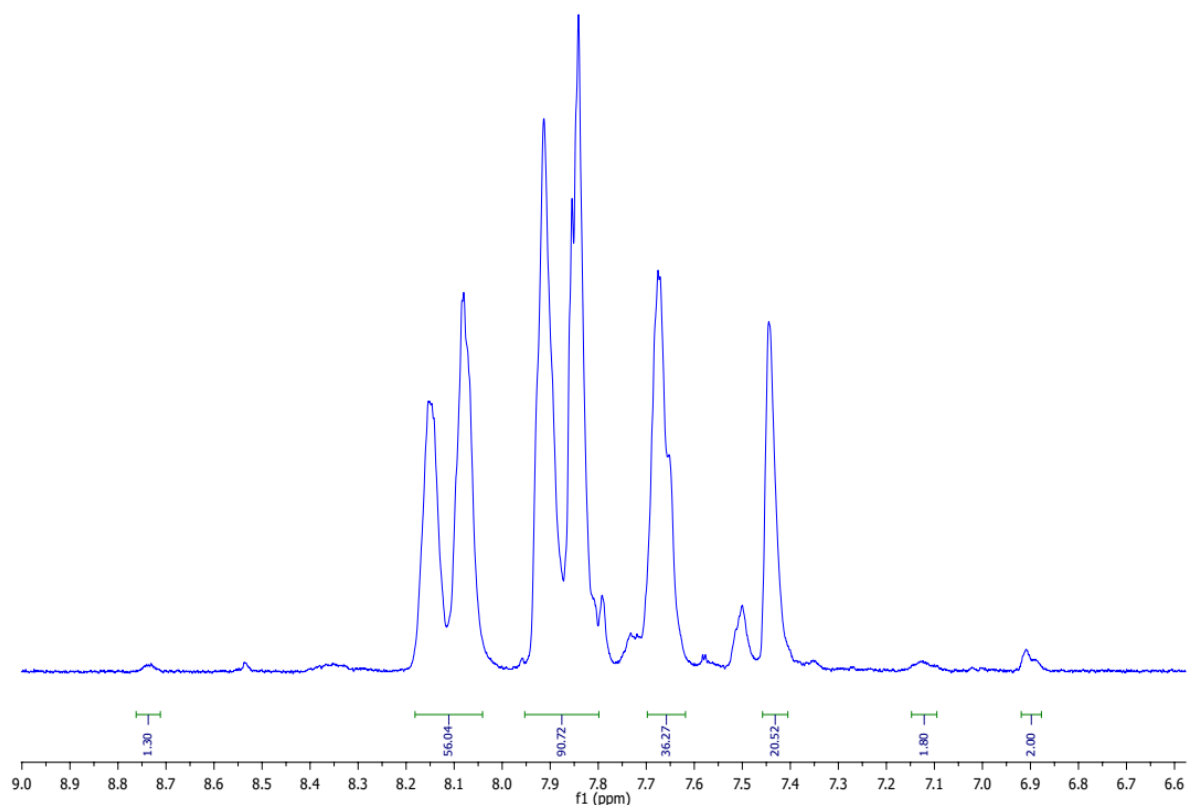
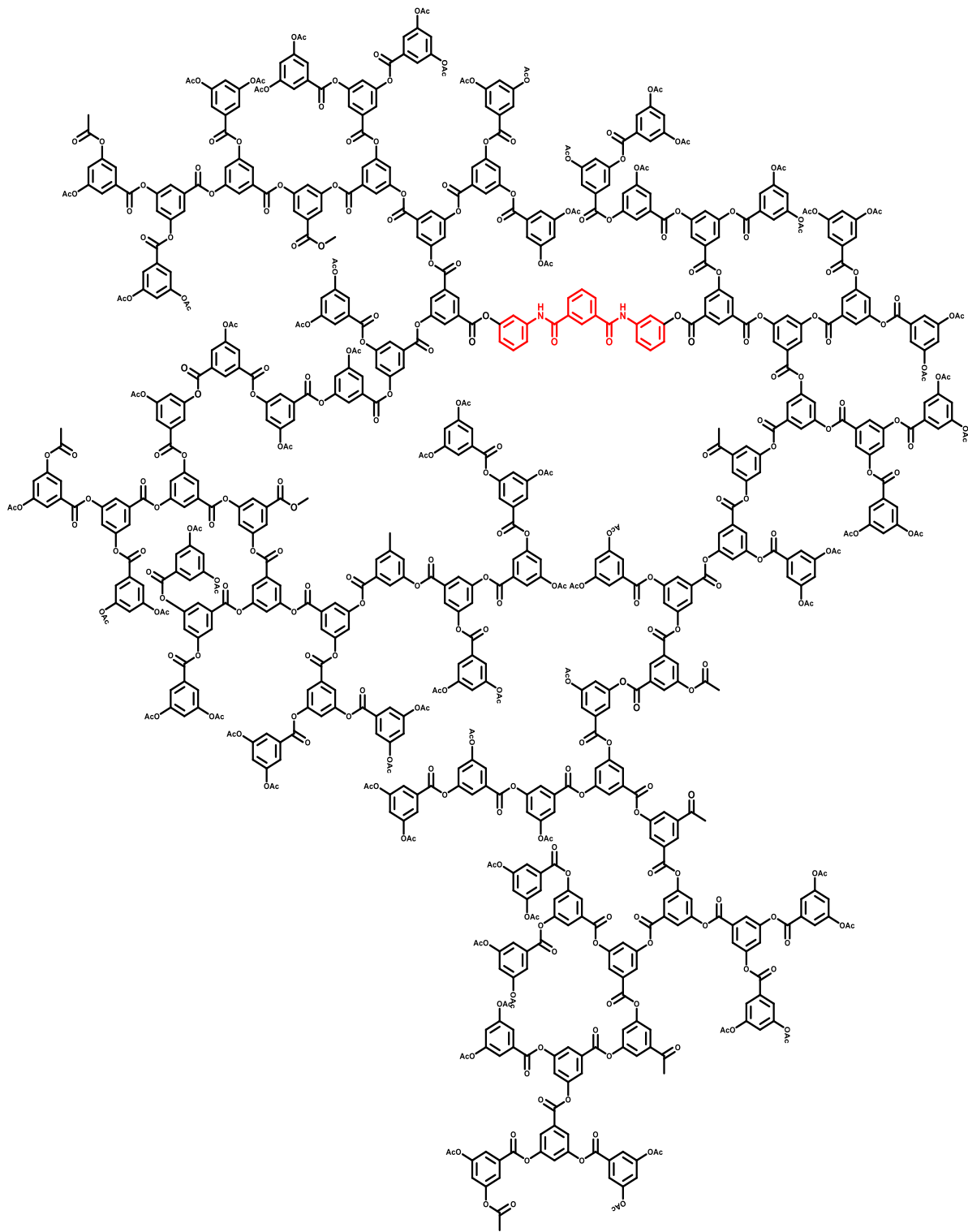


Figure 2.21: ^1H NMR expansion (6.5 to 9 ppm) of cored HBP 1:25. On the right, a monitored signal (\mathbf{H}_g) corresponding to the incorporated core can be seen, using DMSO- d_6 .

Analysis of the HBP with ratio 1:25 by GPC gave a molecular weight of $3,000 \text{ g}\cdot\text{mol}^{-1}$, and NMR gave an M_n of $22,000 \text{ g}\cdot\text{mol}^{-1}$. However, the discrepancy between estimated molecular weights of HBP 1:25 is much higher than observed for the **HBP6000** and **HBP3000** systems. GPC and NMR only provide an estimated molecular weight. In our case, we used a core group analysis but not

every HBP might have a core unit. In our case, it is likely that core incorporation within the polymeric structure is relatively low.

Accordingly, the reaction failed to give a large molecular weight. Therefore, it was decided to continue heating and to add more monomer (to increase the ratio of the incorporated core within the HBP). As a result, the molecular weight doubled to $6000 \text{ g}\cdot\text{mol}^{-1}$ as measured by GPC and ^1H NMR gave an M_n value of $14,000 \text{ g}\cdot\text{mol}^{-1}$. This means that the ratio of core within the HBP had increased. We subsequently repeated the reaction and in an attempt to drive the equilibrium, a high vacuum pump was used. The analysis of the molecular weight obtained from the second attempt was $14,000 \text{ g}\cdot\text{mol}^{-1}$ by GPC and NMR. Analysis also conducted around 80 monomer units surrounded the core to give the globular polymeric system shown in Figure 2.22. This means that the **HBP14000** was starting to become a much less open structure and the core was sterically hindered.



HBP14000

Figure 2.22: Representative structure of cored functionalised HBP 1:25.

2.3.7. Anion binding assay using ^1H NMR titration analysis

Following the successful synthesis of an anion receptor based on isophthalamide and its core incorporation within several HBPs, the next step was to evaluate the anion binding efficacy of free receptor, and the HBPs (**HBP1**, **HBP3000**, **HBP6000** and **HBP14000**). A ^1H NMR titration was used to assess anion binding. Anions have various properties that must be considered in the design of receptor molecules. The most critical properties are size and shape. It was decided that a contrasting range of anions would provide a more in-depth set of results regarding selectivity. The anions chosen were halides (Cl^- , Br^-), which are spherical and soluble in water, hydrophobic anions such as *p*-phenolate, benzoate (Y-shaped) and sulphate (tetrahedral). The NMR experiments were carried out using *d*-chloroform as solvent. The anions were used as their tetrabutyl ammonium salts.

The core unit and the core-functionalised HBP solutions were made up fresh and each was titrated against the various anionic guests. Each titration solution began with 0.5 mL of the host species at a concentration of 20 mg/mL in an NMR tube. The anionic guest, at the same concentration, was added in aliquots (20-30 μL) to the host solution. ^1H NMR spectra were analysed and the chemical shift (ppm) of the NH protons and the proton **H_a** (in position *para* to the carbonyl group) were monitored (Figure 2.23). After each addition of the anionic guest solution, signals from the monitored protons were observed to shift downfield. This shift downfield continues to the point where the solution was saturated, and no further changes in shift were observed. Moreover, the intensity of the peak was reduced with each addition, along with a broadening of the peak. Topspin 2.6 software was used to process the spectra obtained.

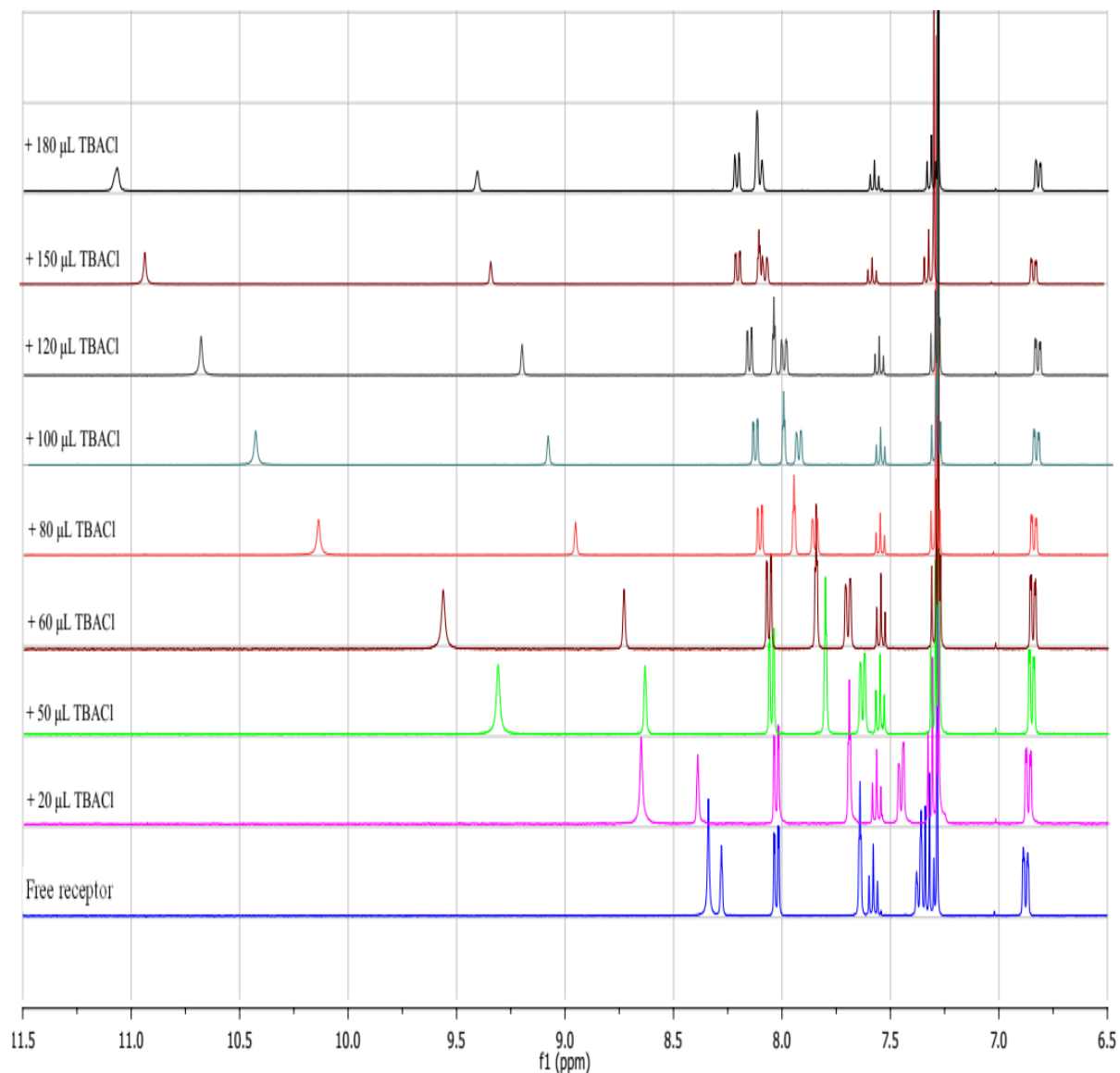
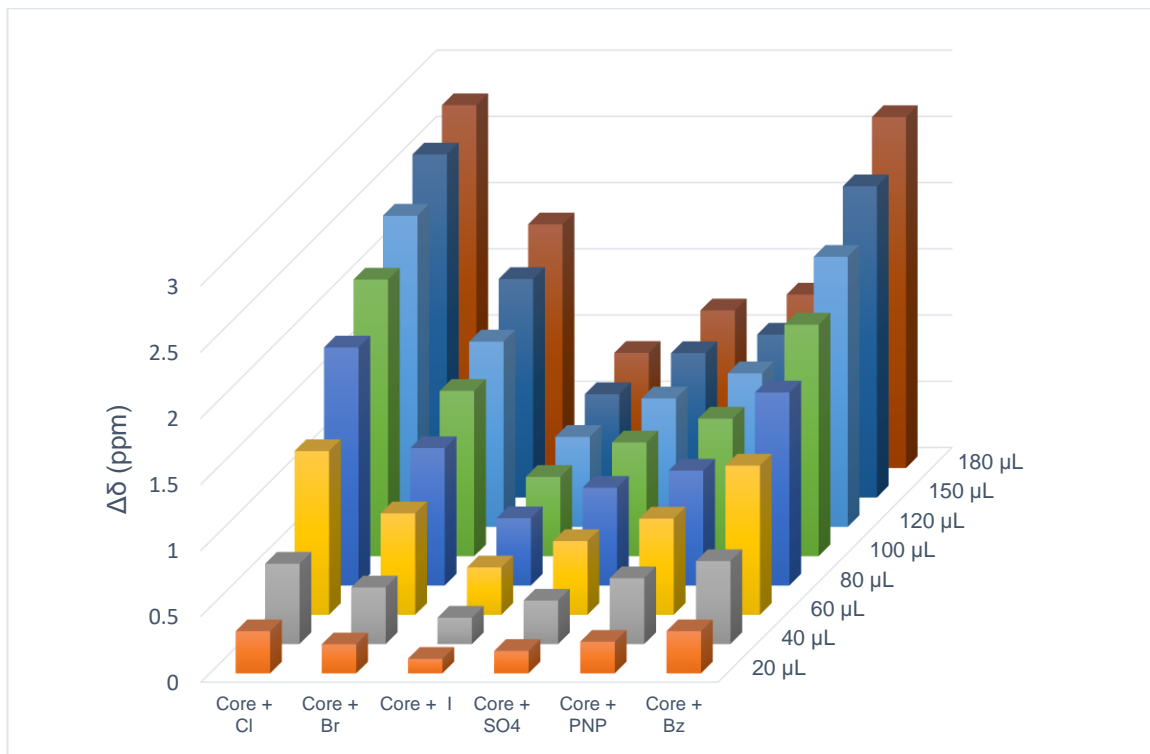


Figure 2.23: ^1H NMR spectra depicting the change in NH resonances in core when titrated against tetrabutylammonium chloride (using CDCl_3 as solvent).

The data for various anions binding to just the core unit is illustrated in Graph 2.1, which shows that increasing anion concentration leads to an increase in $\Delta\delta$, depending on the nature of the anion used. This indicates that hydrogen bonding between the isophthalamide receptor and anions has taken place. Thus, the ^1H NMR titration analysis confirmed that the synthesised core would bind anions.



Graph 2.1: ^1H NMR data obtained from titration of free receptor **R1** against variety of anions [chloride, bromide, iodide, sulphate, *p*-nitrophenolate, and benzoate].

However, when studying the polymers it was apparent from the spectra (Figure 2.24), that the polymer signals dominate, making it difficult to identify the core signals. Although, the strongest binding comes from chloride, it was extremely difficult to see any change in chemical shift. With a larger HBP, it becomes even more difficult. To overcome this problem, we had to do a large number of scans for each titration, however, it was still difficult to see any changes. Thus, we decided to look for a more practical and simpler method to estimate the level of encapsulation. A colourimetric method using UV-Vis was considered. A UV-Vis analysis requires that the anion be coloured. Therefore, the experiments focused on the coloured *p*-nitrophenolate anion.

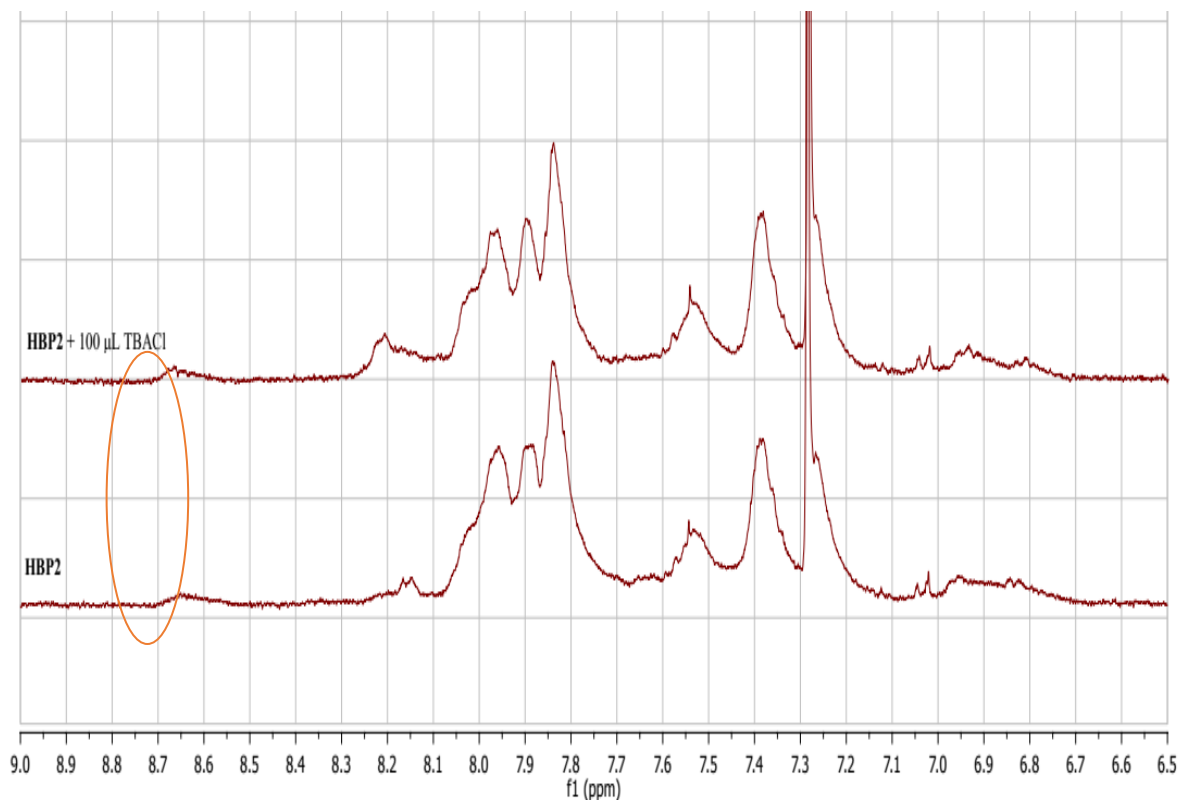
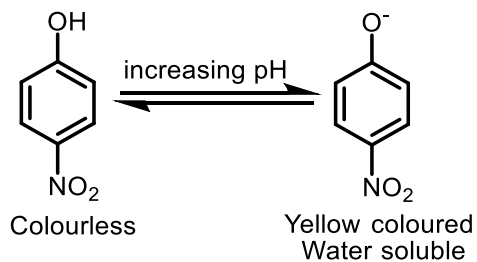


Figure 2.24: NMR data of **HBP3000** titrated against TBACl.

2.3.8. UV-Vis anion transportation study

To assess anion binding and the importance of the HBP, the ability to transport the water-soluble phenolate anion across a hydrophobic phase was used. As well as being coloured 4-nitrophenolate (PNP⁻) is water-soluble, which makes it suitable for use in a colourimetric method and detection using UV-Vis spectroscopy (Scheme 2.10). The transportation begins with the anion in the aqueous phase one (aq.I), which is carried to aqueous phase two (aq.II) through an intermediate organic phase.



Scheme 2.10: The equilibrium equation of 4-nitrophenol and 4-nitrophenolate anion.

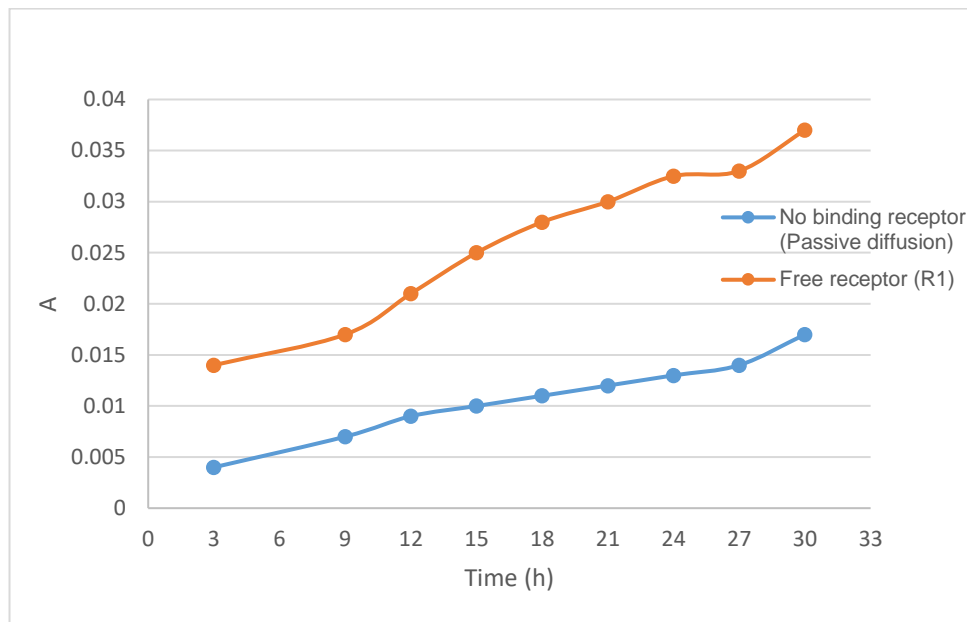
A tris buffer solution was used to prepare the solutions of *p*-nitrophenolate at different pH. 4-nitrophenolate has a pK_a of 7.16 at 22 °C, which means that it will be protonated at acidic pH. Dichloromethane was used as a solvent to prepare a range of organic solutions of **HBP3000**, **HBP6000** and **HBP14000** as well as the free receptor core **R1** at pH 8 (where the PNP will be mostly deprotonated). The concentration of the HBP solutions were prepared using the molecular weights estimated by GPC.

The next stage of study consisted of a comparison between core and functionalised HBPs. Different molecular weights of cored HBPs were chosen. According to the previous study,¹⁰² it was predicted that **HBP6000** (medium HBP) would have the best size for optimum binding, due to its open but ordered structure. On the other hand, the **HBP14000** (large HBP) would bind less well to anions, as a result of steric hindrance. Finally, the **HBP3000** has no steric hindrance, but the structure is 'too open', which will reduce the binding interactions from the HBP.

A U-tube was charged with an organic phase, with or without receptor, and a magnetic stirring bar was placed at the bottom. The coloured aqueous anion solution was carefully added in the first arm (Aq.I). The other arm (Aq.II) was charged with buffer solution only. The organic phase was continuously but gently stirred until the anion concentration gradient between Aq.I and Aq.II reached equilibration. Aliquots were analysed at specific times and it was observed that the colour decreased in Aq.I as it intensified in Aq.II, confirming that anions were transported from one arm to the other.

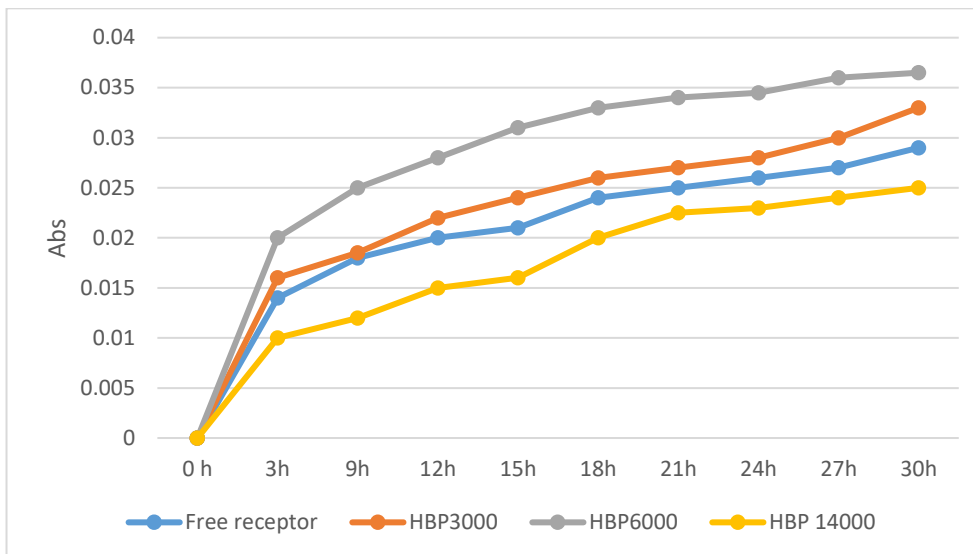
The anion efficacy of the carriers was measured by monitoring the transported *p*-nitrophenolate concentration using UV-Vis spectroscopy. The *p*-nitrophenolate anions absorbed at λ_{max} of 405 nm. Concentration of the transported anion was determined using a Beer - Lambert analysis: to give an extinction coefficient (ϵ) of $2.29 \times 10^5 \text{ mole}^{-1} \text{ L}^{-1} \text{ cm}^{-1}$. Thus, it was possible to determine the concentration of transported anions as a function of time. To compensate for passive diffusion, a control experimental using just DCM was carried out (Graph 2.2). This showed that the number

of anions transported by passive diffusion was relatively low. This amount was subtracted from the results obtained using the different anion receptors.



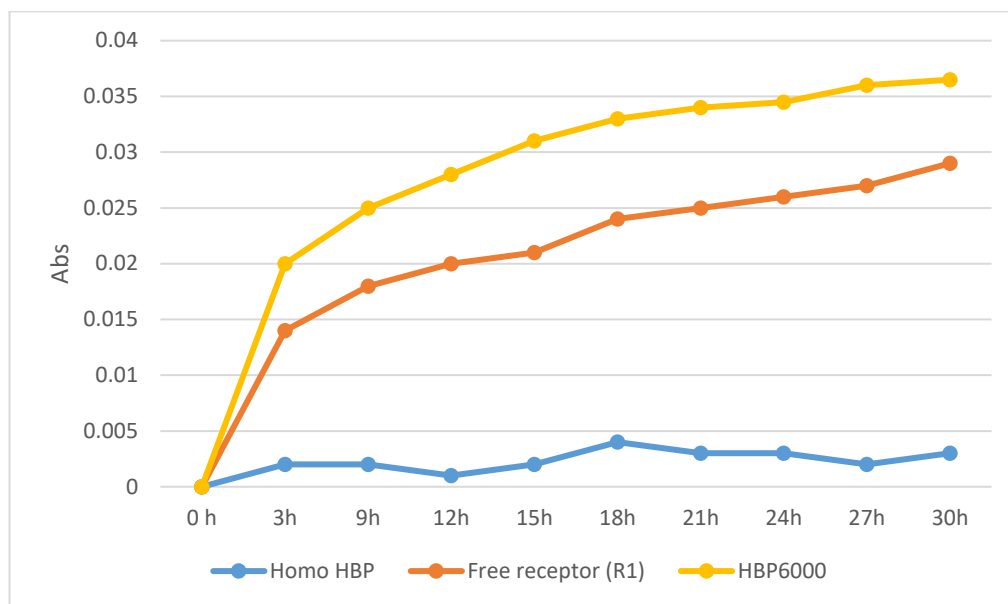
Graph 2.2: UV/Vis data for transported anion (*p*-nitrophenolate), using DCM (passive diffusion) and free receptor (**R1**) carrier.

The data obtained is shown in Graph 2.3. It is apparent **HBP6000**, the medium HBP showed the highest transport affinity for the phenolate. This result is supported by the dense packed theory.¹⁰² Interaction can also be supported by π - π and hydrophobic interactions, leading to optimum binding. However, within the free receptor, the hydrogen bond interaction is the only interaction that can be utilised for binding anions. Experiments were repeated at least three times and graph displays mean.



Graph 2.3: UV/Vis data for transported anion (*p*-nitrophenolate), using different carriers [Small HBP (3000 g.mol⁻¹), Medium HBP (6000 g.mol⁻¹), Large HBP (14000 g.mol⁻¹), and free receptor] (error was about ±5%). The molecular weight of the HBPs were calculated based on GPC data.

Moreover, although the small **HBP3000** has less affinity than the medium **HBP6000** to transport *p*-nitrophenolate anion, but it is still better than the receptor alone. However, the large **HBP14000** has less ability for anion transportation, because of the high steric hindrance. An additional control experiment was performed using uncured HBP (homo HBP 4000 and 9000 g.mol⁻¹). The data shows that the homo HBP did not have an effect on anion transportation. Experiments were repeated at least three times and graph displays mean (Graph 2.4).



Graph 2.4: UV/Vis data for transported anion (*p*-nitrophenolate), using different carriers [Medium HBP (6000 g.mol⁻¹), homo HBP (4000 g.mol⁻¹) and free receptor]. The molecular weight of the HBPs were calculated based on GPC data.

Consequently, π - π interactions are not sufficient alone for binding and transporting the aromatic phenolate. Furthermore, these experiments were repeated at pH 8.5 to try and optimize anion binding. The results were similar to those obtained at pH 8, with slightly faster transportation. This can be attributed to a higher concentration of the deprotonated *p*-nitrophenol molecules in AqI.

2.4. Conclusion

The initial target of this chapter was to synthesis an organic anion cleft receptor that would incorporated within a HBP system. An isophthalamide based anion receptor **R1** was selected, and synthesised via a two-step pathway. This receptor was incorporated within the HBP using a reversible transesterification reaction and 3,5- diacetoxybenzoic acid as a monomer. ¹HNMR and GPC techniques were used to confirm the structure, total core incorporation within the HBP and molecular weights

Three different cored functionalised HBPs were synthesised with core to monomer ratio of 1:5, 1:15 and 1:25 that gave different molecular weights, 3000, 6000 and 14000 g/mol (by GPC), respectively. After successful synthesis, the anion transport properties were performed in organic solvent. The purpose of this study was to determine whether the organic soluble cored hyperbranched polymers could encapsulate and transport a water soluble anion guests via its core, from an aqueous phase (aq. I), and through an organic phase to a second aqueous phase (aq.II). The anion transport study was performed using U-tube experiment, and UV/Vis spectrometry was chosen to calculate the concentration of transported anion species, and the anion solution was prepared at pH 8. The concentration of the different HBP systems were prepared based on the molecular weight, as determined by GPC analysis.

In order to compare the ability of binding anion species by different cored-HBP with the free receptor, it was concluded that the polymer system of 6000 g/mol (at the dense packing limit) accommodate and transport anion species better than free receptors. Non-covalent binding can be supported by π - π and hydrophobic interactions, leading to optimum binding. Within the free receptor, the hydrogen bond interaction is the only interaction that can be utilised for binding anions. Although the small **HBP3000** (below the dense packing limit) has less affinity than the

HBP6000 to transport *p*-nitrophenolate anion, it is still better than the receptor alone. However, the large **HBP14000** (over the dense packing limit) has less ability of anion transportation because of the high steric hindrance. It is noteworthy that, the non-cored HBP has no effect upon binding anion species.

2.5. Experimental

2.5.1 Chemicals and Instrumentation

Solvents and reagents

All chemicals and reagents were obtained from commercial supplier (primarily Sigma-Aldrich) and were used without further purification unless otherwise stated.

Nuclear magnetic resonance spectroscopy (NMR)

All NMR samples were prepared using deuterated solvents supplied by Sigma Aldrich. ^1H NMR and ^{13}C NMR spectra were recorded using a Bruker AV1400 MHz machine. The NMR spectra were analysed using Topspin 3.2 NMR software. Shifts are quoted as ppm and couplings quoted in Hertz.

Fourier transform infrared spectroscopy (FTIR)

FTIR spectroscopy was performed in the solid state (in reflectance mode) using Perkin Elmer Spectrum RX FT-IR System in the range of 700 to 4000 cm^{-1} .

UV-Vis spectroscopy

The ultraviolet absorbance was recorded on an Analytik Jena AG Specord s600 UV/Vis Spectrometer and analyzed using its attached Software (WinASPECT).

Fluorescence Spectroscopy

Fluorescence results were obtained using a HORIBA Scientific Fluoromax-4 spectrofluorometer using its attached software (FluorEssence V3).

Mass spectrometry

The form of ionisation used was dependent on the molecular weight of the sample in question. For samples with a low molecular weight, an Electrospray ionisation (ES) was used to record spectra. The instrument used was a WATERS LCT mass spectrometer. For samples with a high molecular weight, Matrix assisted laser desorption ionisation (MALDI) was required. The instrumentation used was a Bruker Reflex III MALDI -ToF mass spectrometer.

pH measurement

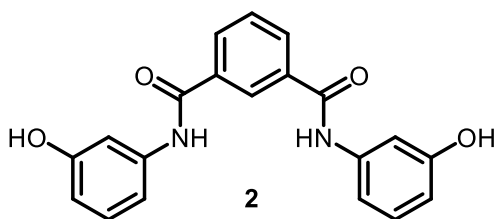
The pH of the buffer solutions prepared was substantiated using a pH 210 Microprocessor pH Meter from Hanna Instruments Ltd. (Leighton Buzzard, UK). The device was calibrated using pH 4.0 and pH 7.0 standard solutions, prepared with buffer tablets (Sigma-Aldrich, Poole, UK).

Gel Permeation Chromatography/ Size Exclusion Columns

Analytical THF GPC data was obtained at room temperature using either a high molecular weight column (3x300 mm PL gel 10 μm mixed-B), or a low molecular weight column (2x600 mm PL gel 5 μm (500 \AA) mixed-E). Calibration was achieved by using polystyrene standards (Mn 220-1, 1,000,000 Da) and molecular weights are thus reported relative to these specific standards used. The samples were run using Fisher GPC grade THF as a solvent stabilised with 0.025 % BHT (which was supplied to the columns by a Waters 515 HPLC Pump at 1.00 mLmin⁻¹). Toluene was added to the prepared sample as a flow marker, before injection through a 200 μL sample loop with a Gilson 234 Auto Injector. The concentration of a sample was studied using an Erma ERC-7512 refractive index detector and, where applicable, by UV using a Waters Millipore Lambda Max 481 LC Spectrophotometer. Aqueous GPC data was acquired using a Millipore Waters Lambda-Max 481 LC spectrometer with a LMW/HMW column. The eluent which was used was NaNO₃/NaH₂PO₄ (pH=7) buffer solution (unless stated otherwise). The data attained was then

analysed using GPC-online software. Samples were filtered using Whatman® GD/X syringe filters with a pore size of 0.45 μm prior to analysis.

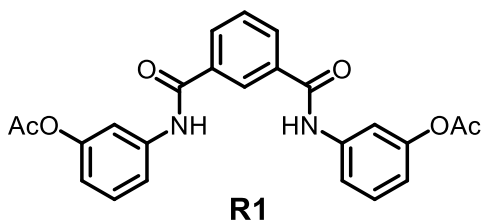
2.5.2. Synthesis of N,N'-bis-(3-hydroxyphenyl)-isophthalamide (2)



A 250 mL round bottom flask equipped with a stirrer was charged with 3-aminophenol (6.55 g, 60 mmol) and anhydrous N,N'-dimethylacetamide (20 mL). The mixture was degassed and flushed with argon. The reactor was cooled to 0 °C using ice-bath, then isophthaloyl chloride (6.09 g, 30 mmol) was added slowly over 30 min via syringe, stirring was then continued at room temperature for 6 h. The reaction mixture was then poured into cold distilled water and filtered followed by washing several time with distilled water. The crude product was purified by dissolving in a minimum amount of hot ethanol followed by hot filtration. The filtrate was then precipitated in distilled water and left overnight to crystallize. The product was dried in vacuum oven at 40 °C, yield 8.1 g (75 %).

^1H NMR (DMSO- d_6 , 400 MHz) δ : 10.28 (s, 2H), 9.46 (s, 2H), 8.48 (s, 1H,) 8.11 (dd, 2H, J=8.0, 2.0) 7.68 (t, 1H, J=8.0), 7.39 (m, 2H) 7.22-7.10 (bm, 4H), 6.52 (bm, 2H). ^{13}C NMR (DMSO- d_6 , 400 MHz) δ : 107.8, 111.7, 111.2, 127.3, 128.5, 129.7, 131.1, 135.4, 140.6, 158.2, and 165.3. FTIR (cm^{-1}): 3364 (N-H stretch) 3188, (O-H stretch) 1646, 1604 (amide C=O stretch), 1547, 1489, 1450, 1266, 683. ESI-MS (MH^-) = 347.0, and m.p. = 246-248 °C.

2.5.3. Acetylation of N, N'-bis-(3-actoxyphenyl)-isophthalamide (R1)

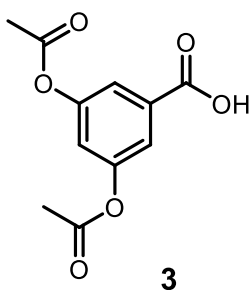


A dried round bottom flask was charged with N,N'-bis-(3-hydroxy-phenyl)-isophthalamide (2.50 g, 5.80 mmol) and dissolved in anhydrous pyridine (20 mL). The flask was degassed with nitrogen in ice bath for 10 min before

dropwise addition of acetyl chloride (2.44 mL, 34.40 mmol), resulting in the mixture colour gradually changed to deep red. The reaction mixture was then stirred at room temperature for a period of 4 h. Pyridine was then distilled off under vacuum distillation. The crude product was dissolved in DCM and followed by washing with saturated solution of sodium hydrogen carbonate and distilled water to remove any trace amount of acid. The organic layer was then separated using separating funnel and the solvent was evaporated under reduce pressure. The product was dissolved in chloroform and left to slowly evaporate overnight. The product was dissolved in 30 mL chloroform and filtered. The cream solid was recrystallized by dissolving in a minimum amount of hot DCM, followed by adding dropwise of petroleum ether (40-60) until the yellow solution remained cloudy. The solution was left to evaporate slowly, the cream coloured crystals were collected, yield 1.4 g (56%).

^1H NMR (acetone- d_6 , 400 MHz) δ : 9.86 (s, 2H), 8.56 (s, 1H), 8.21 (dd, 2H, $J=8.0, 2.0$), 7.81 (t, 1H, $J=2.0$), 7.72-7.65 (bm, 4H), 7.43-7.37 (bm, 2H), 6.92 (dd, 2H, $J=8.0, 1.0$), 2.29 (s, 6H). ^{13}C NMR (acetone- d_6 , 400 MHz) δ : 168.9, 164.7, 151.5, 140.3, 135.5, 130.4, 128.7, 126.5, 117.2, 117.2, 117.0, 113.6, and 20.0. FTIR (cm^{-1}): 3050-3100 (aromatic C-H, stretch), 1765 (acetate C=O, stretch), 1646 (amide C=O). ESI-MS (MH^+) = 433.1, and m.p. = 166-168 $^\circ\text{C}$.

2.5.4. Synthesis of 3,5-diacetoxybenzoic acid (3)



A 500-mL round-bottomed flask that was fitted with a reflux condenser and equipped with a magnetic stirrer bar was charged with 3,5-dihydroxybenzoic acid (160 mmol, 25.01 g) and acetic anhydride (75 mL). The reaction mixture was heated to reflux at 160 $^\circ\text{C}$, gradually the dihydroxybenzoic acid went into acetic anhydride giving a brown solution then the reaction was kept to reflux for 6h. The acetic acid by-product and the excess acetic anhydride were removed under high vacuum distillation. The remaining solid was dissolved in about 100 mL of refluxing

chloroform and filtered hot. A white solid compound was obtained by adding appropriate amount of petroleum ether to the mother liquor. The mixture was then left overnight to crystalize, was filtered and washed with cold petroleum ether. The collected white solid product was dried in vacuum oven (40 °C). Same procedure was repeated for further recrystallization, yield 11.0 g (44 %).

¹HNMR (CDCl₃, 400 MHz) δ: 9.48 (br s, 1H), 7.75 (d, 2H, J=2), 7.22 (t, 1H, J=2), 2.34 (s, 6H).

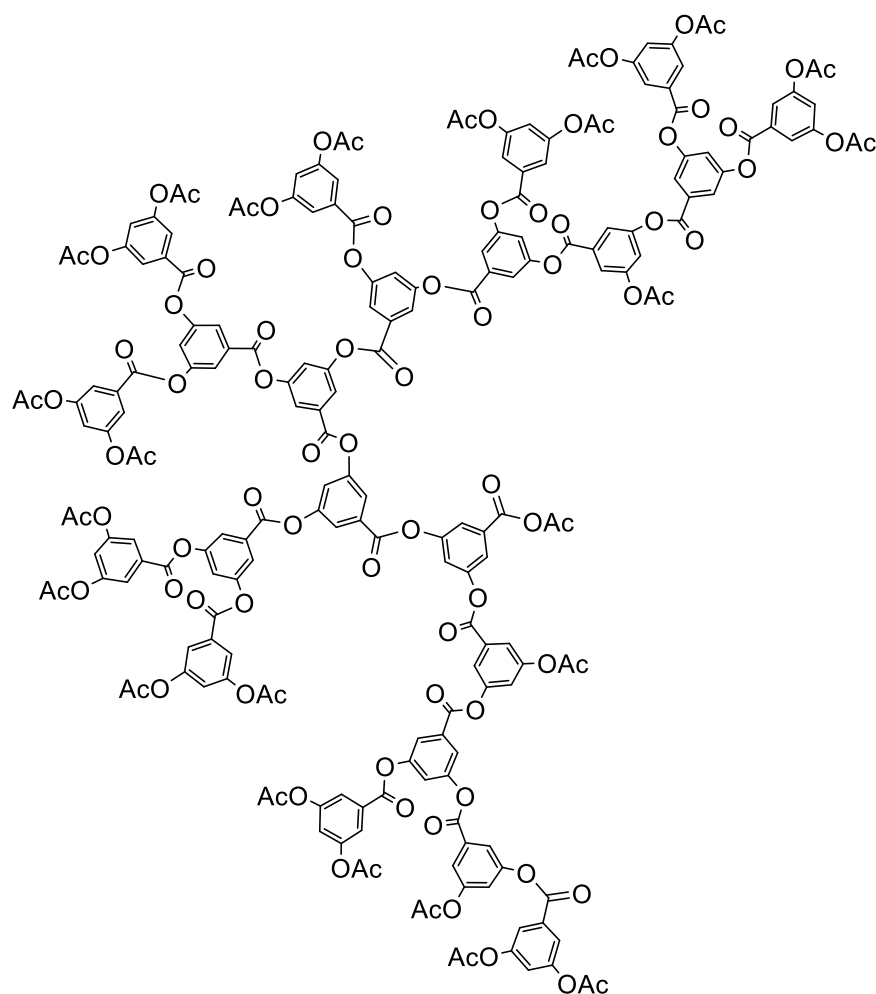
¹³CNMR (CDCl₃, 400 MHz) δ: 170.5, 168.5, 150.8, 130.8, 121.0, 120.6, and 20.62. FTIR (cm⁻¹)

3400-2400, 1765 (COOH), 1691(COOR). ES-MS (MH-) 237, and m.p. = 140-142 °C.

2.5.5. General procedure for polymerisation of 3,5-diacetoxybenzoic acid

3,5-Diacetoxy benzoic acid (various amounts) and diphenyl ether (various amounts) were dispensed into a 250 mL round bottom flask, which was then thoroughly degassed and flushed with nitrogen. The mixture was heated to 225 °C and stirred for a period of 45 minutes. The temperature was reduced to 180 °C and the reaction was subsequently placed under reduced pressure for 4 hours. The crude mixture was dissolved in refluxing THF and precipitated into cold methanol (800 mL) and placed in a freezer overnight to maximise precipitation. The resulting solid was filtered off and washed with cold methanol, yielding the polymer.

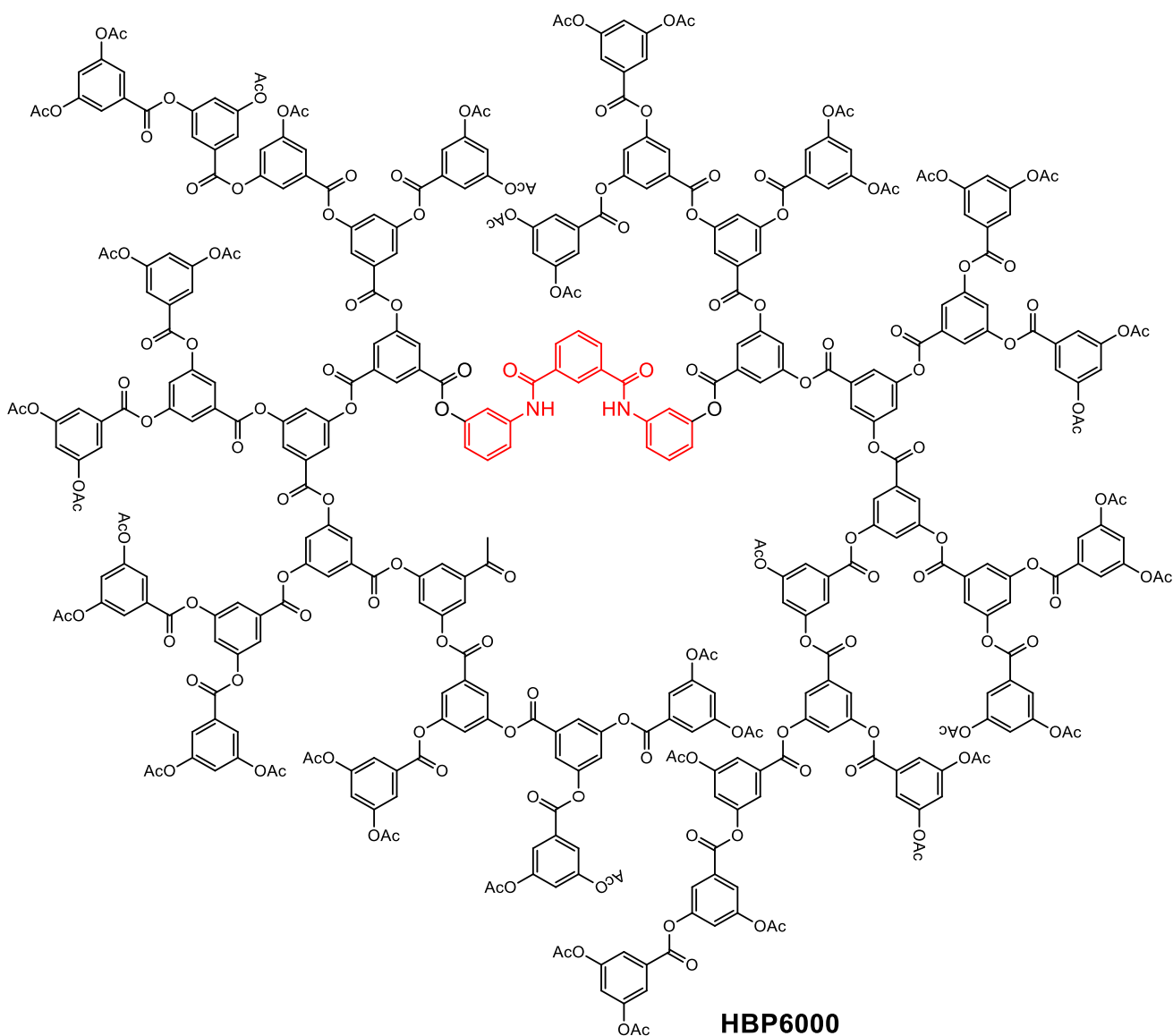
2.5.5.1 Polymerisation of 3,5-diacetoxybenzoic acid (non-cored HBP)



The general procedure was followed where 3, 5-diacetoxy-benzoic acid (3.95 g, 20 mmol) and diphenyl ether (3.95 g, 20 mmol) were reacted together, yielding 2.05 g (51%).

^1H NMR (CDCl_3 , 400 MHz) δ : 8.20-8.02 (br d, 1H), 7.96-7.79 (br d, 2H), 2.38 (br s, 3H). ^{13}C NMR (CDCl_3 , 400 MHz) δ : 169.7, 165.5, 150.1, 131.1, 130.7, 121.3, 120.9, and 21.0. FTIR (cm^{-1}) 2979, 2218, 2045 (aromatic C-H, stretch) 1744, (ester C=O, stretch) 1367, 1276. GPC: $M_n = 4000$, and PD = 1.89.

2.5.5.2 Polymerisation of 3,5-diacetoxybenzoic acid with N,N'-bis-(3-acetoxyphenyl)-isophthalamide core using a 1:15 ratio

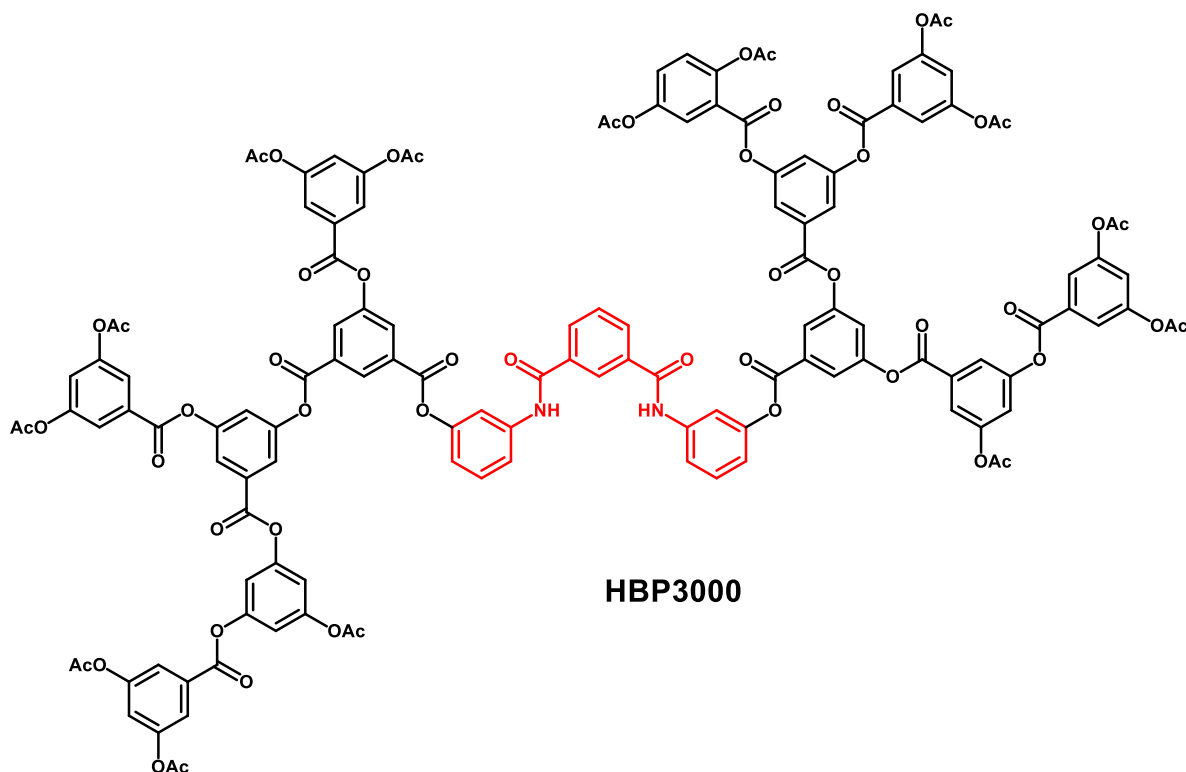


The general procedure was followed where 3,5-diacetoxy-benzoic acid (2.18 g, 9.15 mmol), 3-N,N'-bis-(3-acetoxyphenyl)-isophthalamide (0.25 g, 0.72 mmol) and diphenyl ether (2.5 g, 5.58

mmol) were reacted together, yielding the polymer, which was a light brown/grey solid powder in appearance, yield 369 mg (54 %).

^1H NMR (DMSO- d_6 , 400 MHz) δ : 8.55-8.67 (bm, 2H), 8.20-8.33 (bm, 1H), 7.65-8.08 (bm, 1H, 2H), 7.40-7.64 (bm, 4H), 7.19-7.39 (bm, 2H [core], 2H, [polymer]), 6.72-6.90 (bm, 2H [core]), 2.25 (bs, 3H, [polymer]). ^{13}C NMR (DMSO- d_6 , 400 MHz) δ : 168.8, 163.8, 162.8, 151.2, 139.1, 130.9, 130.7, 129.7, 121.3, 120.9, 117.5, 114.0, and 21.0. FTIR (cm^{-1}) 2009-2158 (aromatic C-H) 1741 (ester C=O, stretch) 1369, 1286, 757. GPC: $M_n = 6300$, $M_w = 12100$, PD = 1.39 and M_n (by NMR estimation) = 8000.

2.5.5.3 Polymerisation of 3,5-diacetoxybenzoic acid with N,N'-bis-(3-acetoxyphenyl)-isophthalamide core using a 1:5 ratio

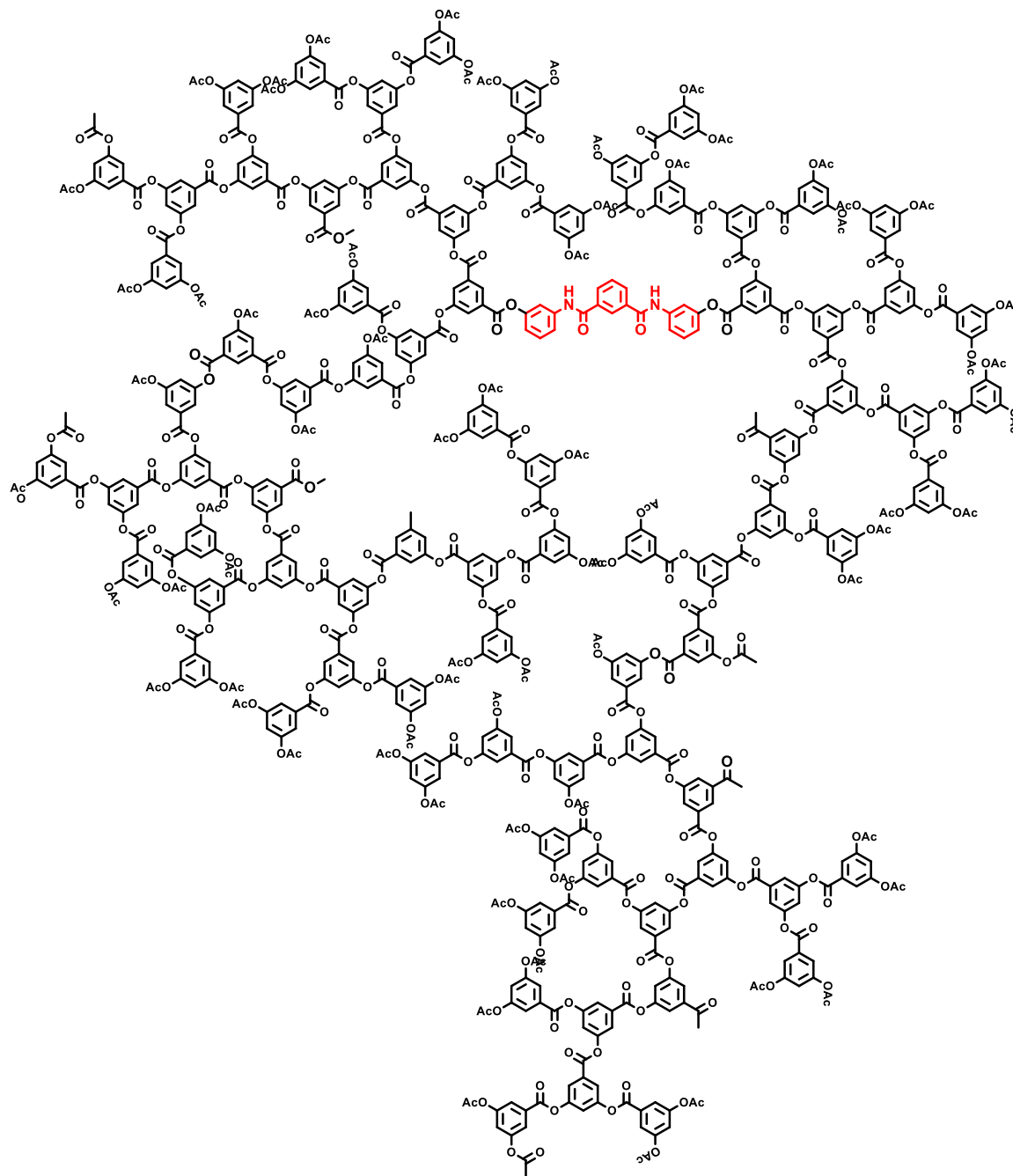


The general procedure was followed where 3,5-diacetoxy-benzoic acid (688 mg, 2.89 mmol), 3-N,N'-bis-(3-acetoxyphenyl)-isophthalamide (0.25 g, 0.72 mmol) and diphenyl ether (0.95 g, 5.58

mmol) were reacted together, yielding the polymer, which was a light brown/grey solid powder in appearance, yield 393 mg (57 %).

^1H NMR (DMSO- d_6 , 400 MHz) δ : 8.57-8.74 (bm, 2H, [Core] NH) 8.06-8.33 (bm, 1H [Core], 2H [Core]), 7.67-8.04 (bm, 1H [Core], 2H [Polymer]), 7.47-7.66 (bm, 4H, [Core]), 7.04-7.46 (bm, 2H [Core], 2H, [Polymer]) 6.71-6.94 (bm, 2H, [Core]) 2.34 (bs, 3H [Polymer]). ^{13}C NMR (DMSO- d_6 , 400 MHz) δ : 169.7, 168.8, 164.5, 163.8, 163.5, 162.8, 151.2, 139.0, 133.3, 131.3, 130.7, 129.5, 129.2, 128.3, 125.6, 121.3, 120.9, 117.5, 113.9, and 21.0. FTIR (cm^{-1}) 2000-2050 (aromatic C-H) 1740 (ester C=O stretch) 1370, 1287, 757 GPC: $M_n = 3800$, $M_w = 7300$, PD = 1.89 and M_n (by NMR estimation) = 2700.

2.5.5.4 Polymerisation of 3,5-diacetoxybenzoic acid with N,N'-bis-(3-acetoxyphenyl)-isophthalamide core using a 1:25 ratio

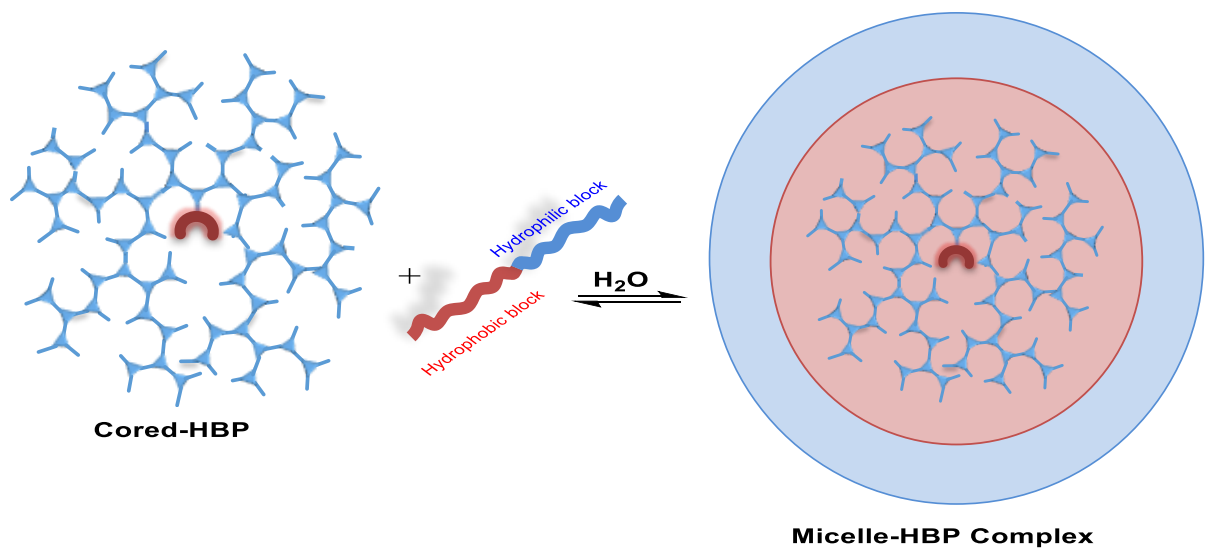


HBP14000

The general procedure was followed where 3,5-diacetoxy-benzoic acid (5.41 g, 22.7 mmol), 3-N,N'-bis-(3-acetoxyphenyl)-isophthalamide (0.25 g, 0.72 mmol) and diphenyl ether (3.01 g, 17.68 mmol) were reacted together, forming the white solid powder, yield 3.51 g (65%).

^1H NMR (DMSO- d_6 , 400 MHz) δ : 8.50-8.71 (bm, 2H [Core]), 8.22-8.43 (bm, 1H [Core]), 8.09-8.19 (bm, 2H [Core]), 7.75-8.11 (bm, 1H [Core], 2H [Polymer]), 7.19-7.62 (bm, 4H, [Core], [Core] 2H, [Polymer]), 6.72-6.89 (bm, 2H, [Core]), 2.31 (bs, 3H [Polymer]). ^{13}C NMR (DMSO- d_6 , 400 MHz) δ : 168.8, 162.8, 151.2, 130.9, 130.7, 129.7, 123.2, 121.3, 120.9, 118.9, and 21.0. FTIR (cm^{-1}) 2972, 2931, 2505 (aromatic C-H, stretch), 1742 (ester C=O, stretch), 1442, 1277, 754. GPC: M_n = 14000, M_w = 36000, PD = 2.48 and M_n (NMR estimation) = 22000.

Chapter Three: Incorporated Hydrophobic Anion Binding Receptors within Water-Soluble Diblock Polymers



3.1 Introduction

3.1.1 Diblock copolymers: Structures and properties

Copolymers that present qualities dictated by product composition are typically intermediate among the qualities of the parent homopolymers. Alternating copolymers are distinguished as those single monomers that may follow one another consistently in the polymeric chain within the limit. Meanwhile, there are two approaches for regularly combining monomers. One approach involves end-to-end addition to connect the extended linear sequences of one monomer to the linear sequences of another, resulting in block copolymers. The second approach involves fixing B chains at sites on the A backbone chain, resulting in the branched structure known as a graft copolymer. Figure 3.1 shows the potential structures that can be formed when these approaches are applied – it can be observed that the blocks are organised differently, and they may range in size from a few monomers to several thousand.¹⁰³

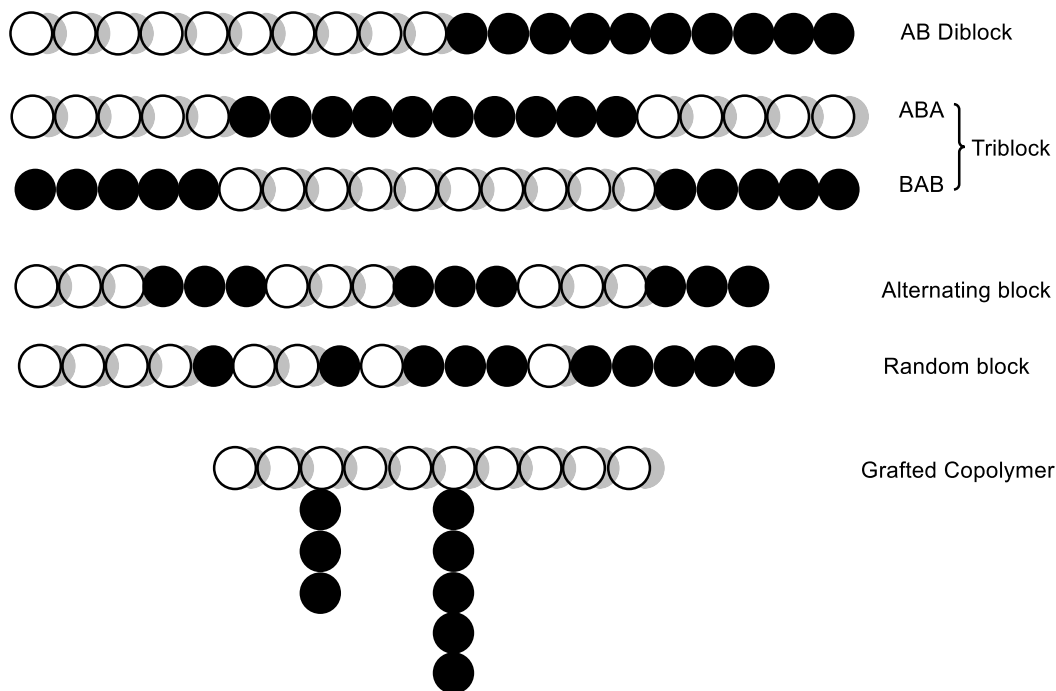


Figure 3.1: Block and graft copolymers

Block length and chemical composition dictate the properties of block copolymers. More specifically, the miscibility of two distinct block types is established by the chemical constitution of the blocks; miscibility is augmented by covalent bonding between two different blocks, yet a predisposition towards separation and development of heterogeneous systems is generally displayed by such structures. Various morphologies can thus arise, influenced by several factors, including the relative lengths of the blocks, whole-molecule molecular weight, the continuity of one phase by comparison to another, as well as sample preparation procedure.

3.1.2 Synthesis of diblock copolymers

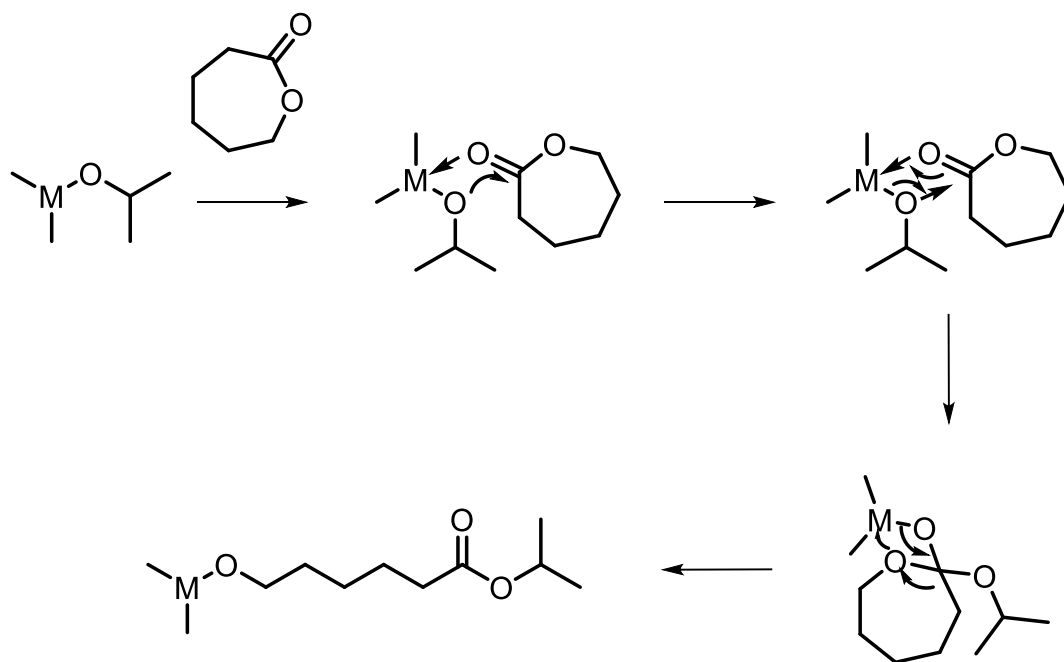
According to the architecture of the polymer of interest, a range of synthetic approaches can be employed. When synthesising polymers, an innate issue is that irreversible chain termination and transfer reactions hinder regulation of product molecular mass. Furthermore, it is challenging to control the aggregation of highly polydispersed polymers because of a lack of uniformity. However, the use of living polymerisation techniques can help to prevent this issue.¹⁰⁴ Living polymerisation reduces the possibility of the chain termination of a growing polymer occurring. Atomic transfer free radical polymerisation (ATRP) and ring opening polymerisation (ROP) are two examples of living polymerisation techniques that can facilitate the fabrication of diblock copolymers.¹⁰⁵

The formation of a carbon-carbon bond via a transition metal catalyst is enabled by ATRP. This technique is characterised by the balancing of a low concentration of active propagating species and a high number of dormant chains. The following chapter will address this polymerisation method in more detail.

A type of chain growth polymerisation, ROP is characterised by the fact that the polymer terminal end serves as a reactive centre, which is the site of joining of additional cyclic monomers, yielding

a polymer chain of greater length via ionic propagation. Anionic, cation and catalyst represent the existing forms of ROP mechanisms.^{106,107}

‘Monomer-activated’ and ‘coordination-insertion’ are the two types of catalyst-based ROP techniques. In monomer-activated ROP, a catalyst activates the monomer molecules and subsequently the polymer chain is attacked by the activated monomer. In the coordination-insertion ROP technique the mechanisms underpinning propagation are monomer-catalyst coordination and monomer insertion into a metal oxygen bond of the catalyst. As shown in Scheme 3.1, an alkoxide bond mediates the attachment of the growing chain to the metal in the propagation step.¹⁰⁸ Biodegradable and biocompatible polymers with a high molecular weight can be produced by catalysed coordination-insertion ROP.¹⁰⁹



Scheme 3.1: Mechanism of the initiation step for coordination–insertion ROP, adapted from M. Labet and W.

Thielemans.¹⁰⁸

3.1.3 Self-assembly of diblock copolymers

A chemical compound demonstrating hydrophilicity as well as hydrophobicity is classified as an amphiphile. The formation of an amphiphilic copolymer can be achieved through the use of hydrophilic and hydrophobic monomers or segments that have undergone polymerisation. Meticulous customisation of the two monomer units can enable the formation of diblock structures with particular properties. The properties of amphiphilic copolymers are similar to surfactants, which are also amphiphilic in nature (Figure 3.2).

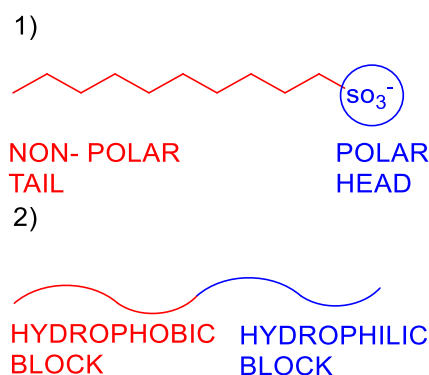


Figure 3.2: Similarity between two amphiphilic compounds 1) Surfactant (SDS) 2) Diblock copolymer

Figure 3.3 shows the various aggregated morphologies that can form from diblock copolymers. This is enabled by the fact that the two blocks interact differently with the surrounding environment, which results in self-assembled structures formed through hydrophobic interactions.¹¹⁰ Clustering of the hydrophobic portions of the molecule is induced by the preferential dissolution of the hydrophilic portion in water, being entropically better than the organisation of water around every individual hydrophobic portion of the polymer in solution. Compared to simple surfactant counterparts, these self-assembly polymer structures are significantly larger. The size, geometry, configuration and degree of architecture depends on the length of the hydrophobic and hydrophilic blocks, and the nature of the components, solvent system, temperature and concentration.

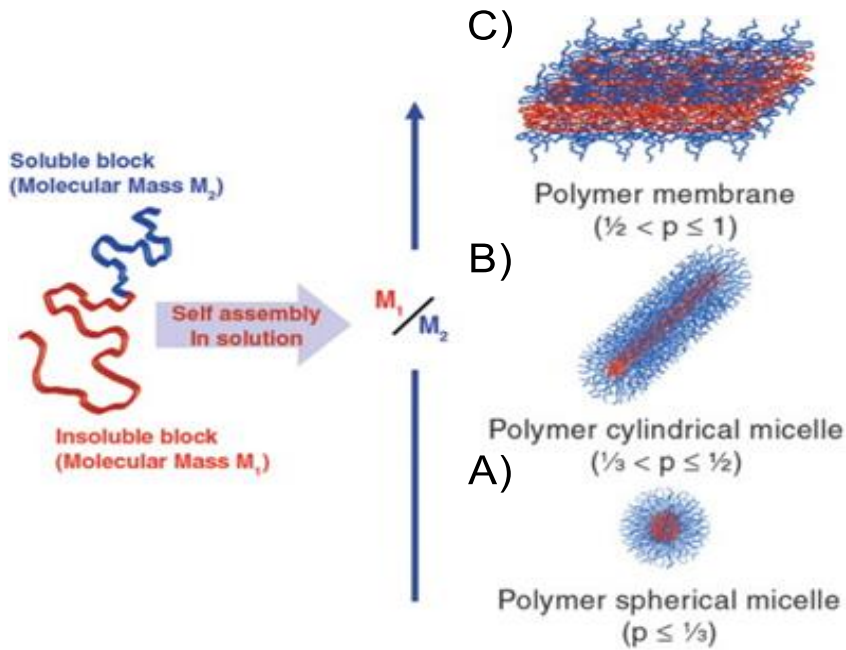


Figure 3.3: Different geometries formed by diblock copolymers in water taken from “Block copolymer nanostructures” Image taken from (T. Smarta, H. Lomasa, M. Massignania, M. V. Flores-Merino, L. R. Perez, and G. Battaglia).¹¹¹

- A) Spherical micelles. Interior formed of hydrophobic chain, with hydrophilic chains facing water. Characterised by low critical packing number and strong curvature. Radius is close to that of the length of the polymer chain.
- B) Cylindrical ‘rod like’ micelle. Cross section is similar to that of spherical micelles. Micelle length is highly variable so micelles are polydisperse.
- C) Membrane bilayer. Likely to form vesicle structures with two distinct water compartments, one forming the core and one in the external environment.

The critical micelle concentration (CMC) is a particular minimum concentration of unimers in solution necessary for amphiphiles to aggregate. At low concentration the soluble blocks are sufficient to maintain the solubility of the unimers, existing separately and demonstrating no aggregation. Self-assembly of block copolymers occurs as the concentrations exceed this minimum (the CMC), which reduces the free energy of the system. The relative sizes of the soluble and insoluble portions control curvature of the assembly and then dictate the type of structures that form (includes micelle and, vesicles).^{112,113}

The molecular shape of each amphiphile also influences the type of aggregated structures and is in turn dependent on the volume (V) of hydrophobic and hydrophilic blocks. As depicted in Figure 3.4, a small hydrophobic block gives a cone-shaped amphiphile, which forms micelles during self-

assembly. By contrast, structures resembling rods with an almost cylindrical amphiphile shape form vesicles at elevated volume.^{114–116} This dependence on the unimer shape is reformed to a ‘packing parameter’ (p), defined by Equation 3.1:

$$p = V/a \cdot l \quad \dots (3.1)$$

(V) the volume of hydrophobic block, (a) the area of the hydrophilic block, (l) length of the hydrophobic part.

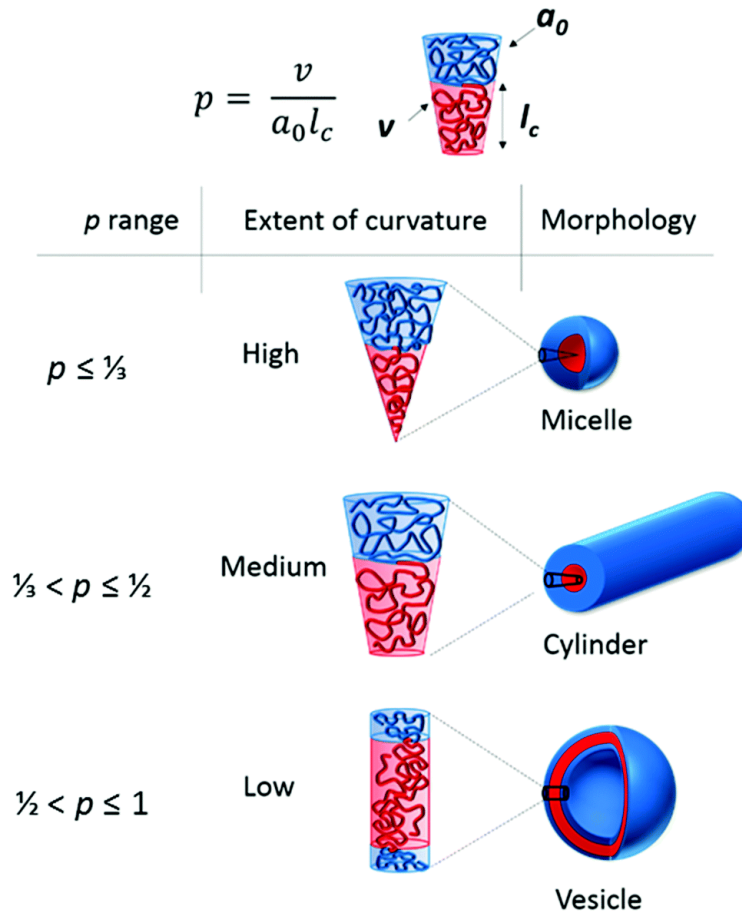


Figure 3.4: The different morphologies obtained by targeting different packing parameters, p . Image taken from Reference.¹¹⁷

To ensure the production of micelles, a low concentration and short hydrophobic segment are then required.

3.1.4 Exploiting the encapsulation properties of polymeric micelles

Amphiphilic block copolymers represent a wide range of materials, from the simple linear diblock structures that contain two hydrophilic and hydrophobic blocks, to far more complex systems. An extensive study of polymeric micelles has shown its potential for use in several applications, including nano-bioreactors, viral gene vectors and drug delivery agents.¹¹⁸ This interest in diblock copolymers has grown because of their ability to self-assemble in both bulk and solution. The spontaneous self-assembly of diblock copolymers can create supramolecular nanoparticles possessing a hydrophobic core shielded by a hydrophilic periphery. The hydrophobic interior of the micelle can be used to encapsulate hydrophobic materials, such as drugs. There are many other examples of utilising these micelles for specific applications.⁹⁸

Micelles based on the amphiphilic copolymer poly (ethylene oxide) and poly (ϵ -caprolactone), with both linear and star architectures, have been studied by Quaglia et al. The study showed that these types of polymeric micelles exhibit low toxicity towards red blood cells, thus they can be utilised as drug delivery agents for lipophilic drug molecules.⁹⁸

Zhang et al. synthesised a series of monomethoxy poly (ethylene glycol)- poly (lactide) (mPEG-PLA) diblock copolymers. These were used to investigate the encapsulation of Cyclosporin, which is a highly lipophilic immunosuppressant drug used in post-allogeneic organ transplant and severe cases of ulcerative colitis. The drug was encapsulated effectively by these nanocarriers and resulted in improved intestinal absorption, which promises improved oral absorption of weakly absorbed drugs.¹¹⁹

More recently, Wang et al.¹²⁰ examined the capability of polyethylene glycol-phosphatidylethanolamine (PEG-PE) micelles as drug carriers for doxorubicin hydrochloride and vinorelbine tartrate. The results showed that the loaded micelles reduced drug hydrolysis, in addition to sustained release.

Hongfan et al.¹²¹ synthesised star-shaped block copolymers based on poly(D,L-lactide-*co*-glycolide) (PLGA) and poly(ethylene glycol) (PEG) with different numbers of arms (3s/4s/6s-PLGA-PEG) in order to investigate their micelle properties and their loading capacity towards Doxorubicin (DOX) (Figure 3.5). The DOX-loaded 4s-PLGA-PEG micelles possessed the highest efficiency of cellular uptake and lowest cytotoxicity, probably because of the difference in micelles size and PEG distribution on the surface of the micelles.

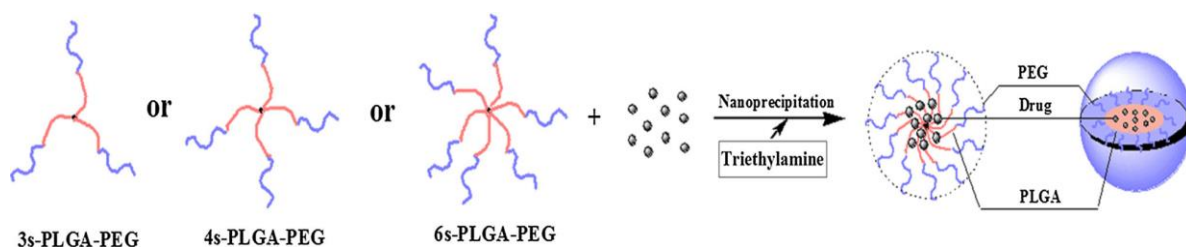


Figure 3.5: Structural tailoring of arm numbers from star shaped-PLGA-PEG copolymers (3-arm/4-arm/6-arm-PLGA-PEG) could provide a new strategy for designing drug carriers of high efficiency. Image taken from reference.¹²¹

3.2 Aim and Objectives

Our initial organic binding system was developed to serve as proof of principle and specifically to demonstrate that an anion receptor molecule can be covalently incorporated within a HBP and retain the ability to bind an anion. The ultimate goal was to develop a host system that can selectively bind and transport hydrophobic guests in water. We have an effective organic HBP binding system, but it requires functionalisation for its aqueous solubilisation. We can solubilize this organic HBP or synthesise a new water soluble HBP. It would be synthetically challenging to synthesise a new HBP or to convert the terminal groups of the organic HBP system.¹¹⁴ In addition, the interior of a water soluble HBP may not be sufficiently hydrophobic, as their architectures may allow water within their cavity. Therefore, we decided to encapsulate **HBP6000** within a water-soluble macromolecular aggregation.

For the purpose of this research, a linear amphiphilic diblock polymer could be used to encapsulate the anion binding **HBP6000** in aqueous medium. This self-assembled structure must be water-soluble, while maintaining sufficient internal hydrophobicity for the HBP to reside in. It was also important that the receptors have been retained within the micelle during any extraction process. Here, we decided to encapsulate the free receptor (**R1**) and the cored-**HBP6000** within the interiors of polymeric micelles system using an amphiphilic diblock copolymer of type AB (Figure 3.6).

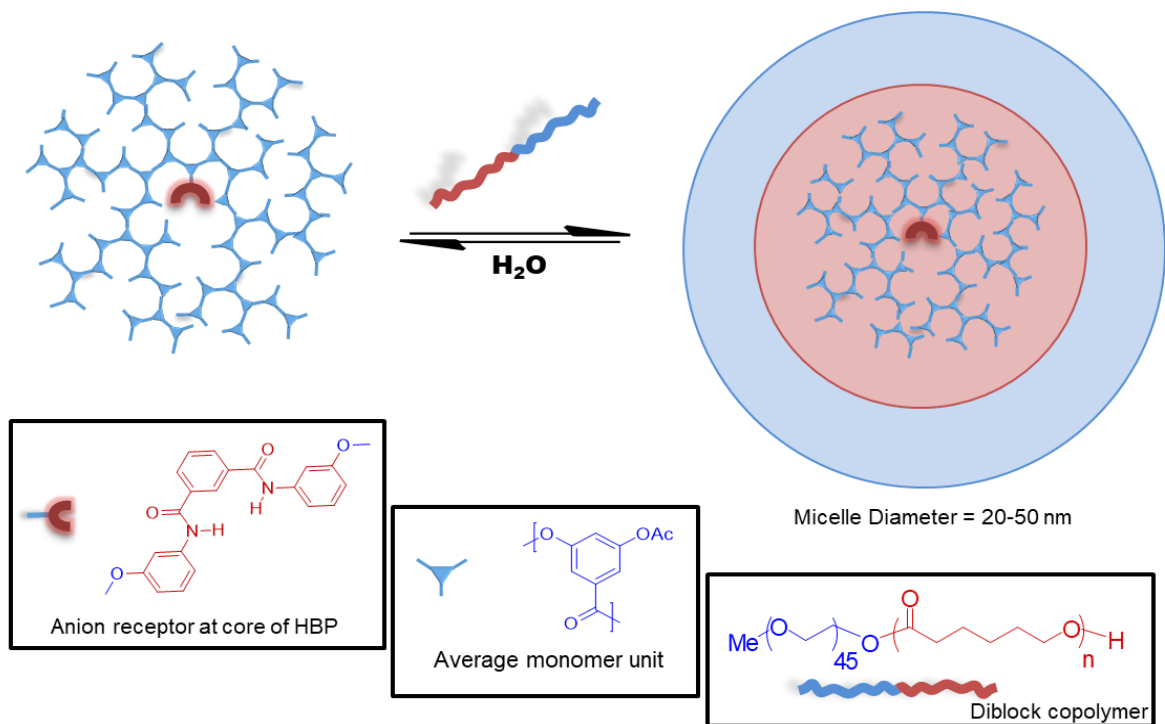


Figure 3.6: Representative of cored-HBP encapsulation within micelle in aqueous environment

mPEG is a common polymer; and is a popular choice for the hydrophilic block of a micelle system. Meanwhile, the hydrophobic block is crucial for creating a ‘dry’ micellar region. The compound initially considered for the synthesis of the hydrophobic block was polycaprolactone (PCL). This polymer is a widely studied biocompatible and non-toxic polymer.¹²² Hence, the diblock copolymer chosen was poly(ethyleneglycol) methylether-*block*-poly(ϵ -caprolactone) (mPEG₄₅-*b*-PCL_n). These are relatively easy to synthesise with control via a ring opening polymerisation (ROP) technique, as control is important.

The proposed hyperbranched polymer must reside within the hydrophobic pocket of the polymeric micelle. Therefore, it is crucial to determine the diameter of the hyperbranched polymer as well as the size of the hydrophobic interior of the micelle. It is therefore, important to make sure that the HBP system has adequate space within the hydrophobic region. The size capacity of micelles can be estimated by assuming the distance between three atoms in the chain (between a C1 and C3) is

around 1.5 Å. The length of one hydrophobic segment with 7 bonds will be around 6 Å (Figure 3.7).

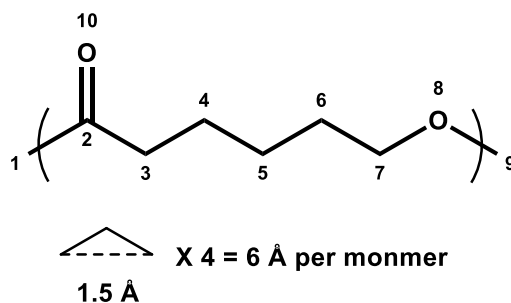


Figure 3.7: Calculation of the size of one ϵ -caprolactone monomer

Thus, for a micelle molecule consisting of 10 monomer units of PCL, the hydrophobic block of the diblock copolymer will have a maximum length of 60 Å, giving a micelle diameter of 120 Å (or 12 nm) when fully extended. The average molecular weight (M_n) of **HBP6000** has almost 40 monomer units. This HBP system contains approximately 20 bonds across its diameter. Consequently, the maximum diameter of the HBP will be 60 Å, making it possible to fit into the hydrophobic cavity of the micelle (Figure 3.8).

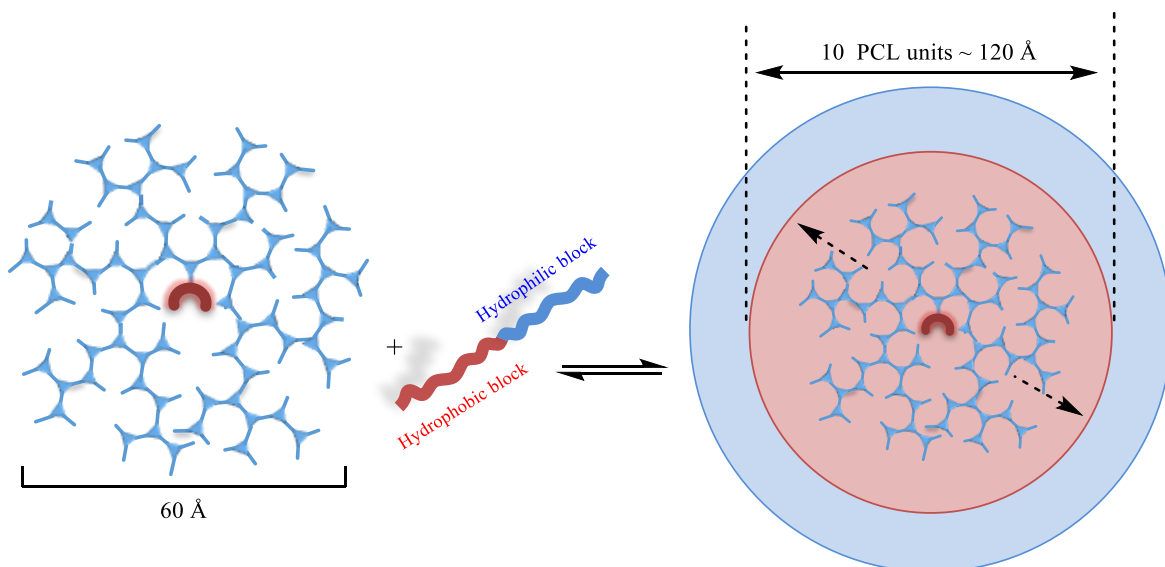
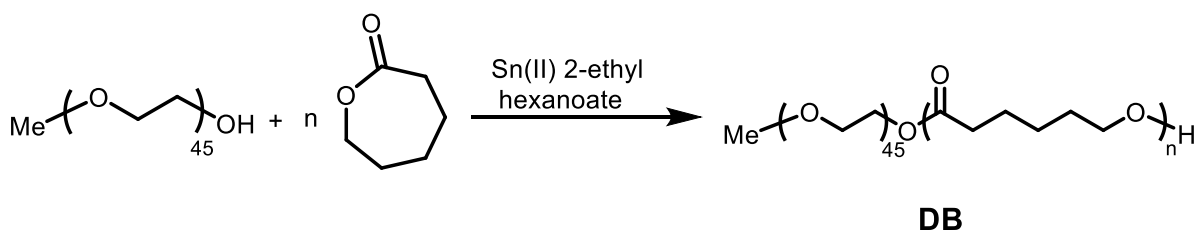


Figure 3.8: The fitting of HBP within micelle at equilibrium (figure shown is representative)

3.3 Results and Discussion

3.3.1 Synthesis of mPEG₄₅-*b*-PCL_n diblock copolymers

A series of amphiphilic diblock copolymers of poly (ethylene glycol) methyl ether-*block*- poly (ϵ -caprolactone) (mPEG-*b*-PCL_n) (**DB**), with varying mPEG/PCL molar ratios, were synthesised for comparison. This synthesis proceeded via the tin (II) catalysed ring opening polymerisation of ϵ -caprolactone, initiated by mPEG (Scheme 3.2). The first stage of synthesis involved drying the mPEG for 1 hour at 130°C under vacuum. The apparatus was then degassed and ϵ -caprolactone added. This was followed by the addition of tin catalyst and the reaction was stirred for 24 hours at 130°C. The white solid obtained was dissolved in dichloromethane and precipitated into petroleum ether 40-60 to yield the diblock copolymer.



Scheme 3.2: Synthesis of mPEG₄₅-*b*-PCL_n (**DB**)

The ¹HNMR spectra of the polymers (in deuterated chloroform) had singlets at 3.38 and 3.65 ppm, corresponding to the terminal methyl and methylene protons of PEG section, respectively. The five methylene units of the PCL block were observed at 2.32, 1.66, 1.39 and 4.07 ppm, corresponding to the α , $\beta+\delta$, γ and ϵ positions respectively (Figure 3.9). In addition, the IR spectrum had a peak at 1721 cm⁻¹, corresponding to the ester carbonyl instead of 1748 cm⁻¹ for the carbonyl in the ϵ -caprolactone monomer.

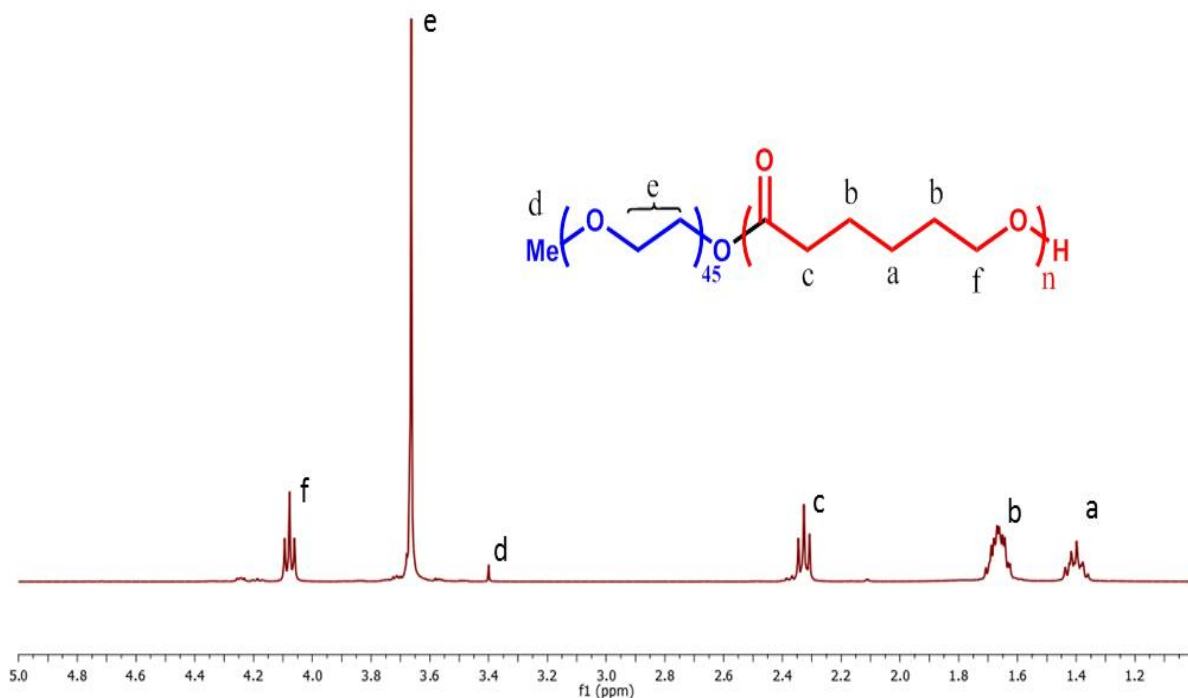
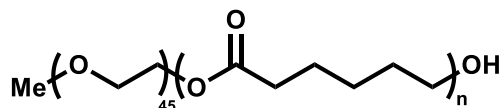


Figure 3.9: The ¹H NMR spectrum of mPEG₄₅:PCL₂₀ (**DB20**)

¹H NMR and GPC analysis were utilized to determine the PCL chain lengths (n), which were compared to the theoretical for the four polymers **DB10**, **DB20**, **DB40** and **DB60**. The number of protons in PEG was constant at 180 and set as standard for integration. Comparing the ratio of this standard peak to that of the PCL peaks at 1.39 ppm, 1.66 ppm and 2.33 ppm, the number of hydrogen atoms in the hydrophobic PCL region were determined, along with the number of repeat units and Mn. The molecular weights determined by GPC and NMR, and the theoretical and experimental chain lengths of the hydrophobic segment, along with the PDI are shown in Table 3.1.

Table 3.1: Summary of the molecular weights, polydispersity, and PCL units of mPEG₄₅-*b*-PCL_n determined by ¹H NMR spectroscopy and GPC



DB10: n=10 DB40: n=40

DB20: n=20 DB60: n=60

Number	Target	Actual	M _n /g mol ⁻¹			PD
	DP	DP ^a	Theoretical ^b	¹ H NMR ^c	GPC ^d	
DB10	10	15	3141	3700	3400	1.4
DB20	20	30	4282	5400	4400	1.8
DB40	40	70	6564	10,000	9900	1.4
DB60	60	100	8848	13,500	12,000	1.3

DP- Represents the number of repeat units per polymer chain of the hydrophobic segment.

a- PCL units calculated from methylene proton signal at 2.33 ppm, with the terminal methyl group of PEG unit set as the standard.

b- Calculation based on feed ratio of the monomer units to mPEG unit.

c- As determined by integration of ¹H NMR in CDCl₃.

d- As determined by LMW THF GPC (reported as polystyrene-PSTY equivalents).

The two complexes consist of fixed molecular weight.

The data shows that the M_n values via GPC are lower than those obtained by NMR, due to the calibration method. Overall, the data shows that the polymers were synthesised with some degree of control relative to the mPEG to monomer ratio. The next step is preparation of polymer micelles from the synthesised diblock copolymers for intended encapsulation.

3.3.2 Aggregation of Diblock Copolymers into Micelle Structures

Before further steps were taken, we examined the water solubility of the prepared diblock copolymers and their formation into micelle structures. The formation of micelles and their size

rely on their hydrophobic length and size, therefore, any chain elongation may result in the formation of alternative aggregates.¹²³ In addition, the degree of control over reaction conditions, such as the concentration of molecules, gives control over the hydrophobic chain lengths, which enables perfect spherical polymeric micelles to be formed. However, the results have shown that the 1:40 and 1:60 mPEG:PCL_n ratios were insoluble in aqueous solution. Previous results within the group have shown similar results using various chain lengths of the hydrophobic CL segment.¹²³ Therefore, it was decided to work with hydrophobic chain lengths that were readily studied, specifically the diblock mPEG-*b*-PCL 1:10 (**DB10**) and mPEG-*b*-PCL 1:20 (**DB20**). The resulting micelles were expected to have sufficient internal space to encapsulate the proposed **HBP6000** system.

The aggregation properties of the selected diblock copolymers were analysed using a variety of methods. ¹HNMR spectra were obtained in CDCl₃ and D₂O to acquire a spectrum of the non-aggregated and micellar system respectively. In D₂O the hydrophobic part of diblock copolymers is essentially hidden from the solvent as it forms the internal environment within the aggregated structure. This results in a significant decrease of the peaks of the hydrophobic PCL units. The ¹HNMR experiments were carried out at relatively high concentration (>20 mg/mL) (Figure 3.10).

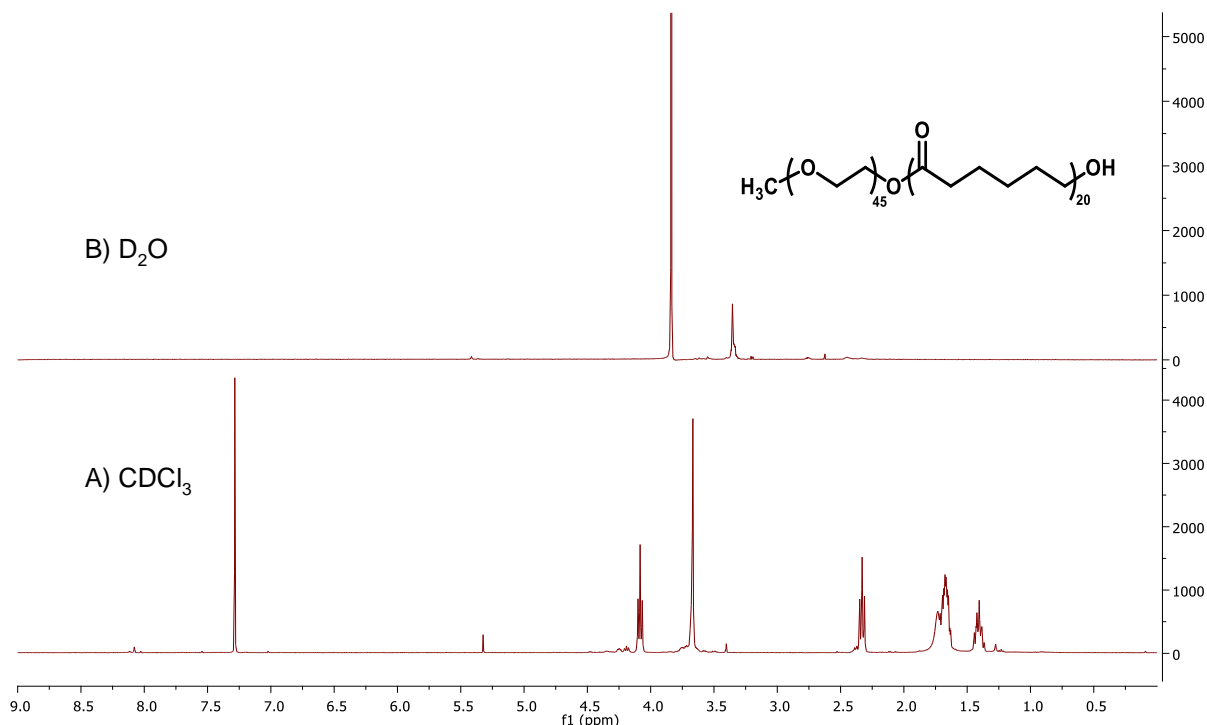


Figure 3.10: The ¹H NMR spectra of mPEG-*b*-PCL₂₀ in (A) CDCl₃ and (B) D₂O

3.3.3 Determination of critical micelle concentration (CMC)

Prior to any encapsulation studies, the appropriate concentration required to form micelles must be determined. In order to form the micelles, the concentration of polymer must be above the critical micelle concentration (CMC). This information is important: if the concentration is too low, then micelles will not form. If the concentration is too high, larger morphological species may form. The CMC could be used to describe the thermodynamic stability of the micelles.¹²⁴

Pyrene was used as a fluorescence probe to determine the CMC. This technique is based on the fact that a fluorescence dye (pyrene) displays different fluorescence properties according to its surroundings. That is, pyrene will exhibit different fluorescence behaviour inside or outside the micelle,¹²⁵ and this change in behaviour is used to determine the CMC.

Careful interpretation is required as the concentration of pyrene should be low (10^{-7} M) so that any changes can be precisely measured as micellization occurs. Also, changes in fluorescence can

sometimes be attributed to the presence of hydrophobic impurities, or association of the pyrene probe with individual polymer chains or pre-micellar aggregates.¹²⁶

The fluorescence spectrum of pyrene in water exhibits five predominant peaks. It has been shown that the ratio of the first (I_1 at 421 nm) and third peaks (I_3 at 439 nm) is a sensitive parameter affected by pyrene's environment. Thus, CMC was ascertained using the I_3/I_1 ratio.^{127,128} The I_3/I_1 pyrene ratio is monitored with respect to the concentration of diblock copolymer and is measured at constant excitation wavelength and variable emission wavelengths corresponding to I_1 and I_3 . The intensity of the I_3/I_1 of pyrene from the emission spectra were plotted against diblock copolymer concentration in Figure 3.11 and 3.12. The I_3/I_1 remains constant up to a certain diblock concentration and increases sharply as micelles form. The break point in the fluorescence behaviour of pyrene occurs around 5×10^{-6} mg/mL of **DB10** and 2×10^{-6} of **DB20**.

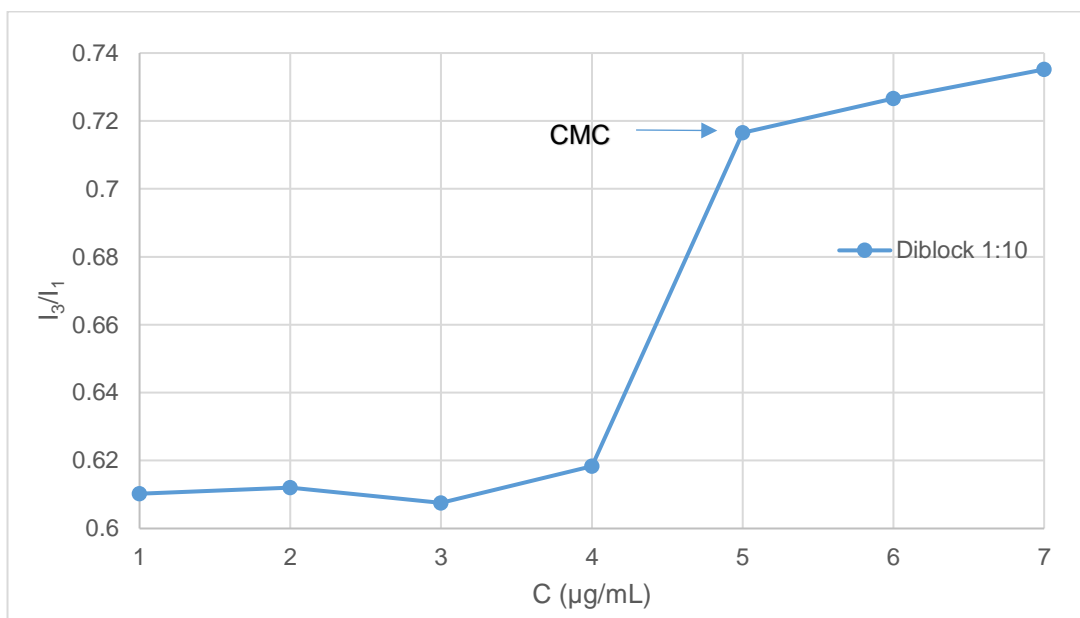


Figure 3.11: Plot of the total intensity ratio from pyrene emission spectra versus concentration of mPEG-*b*-PCL₁₀ (**DB10**).

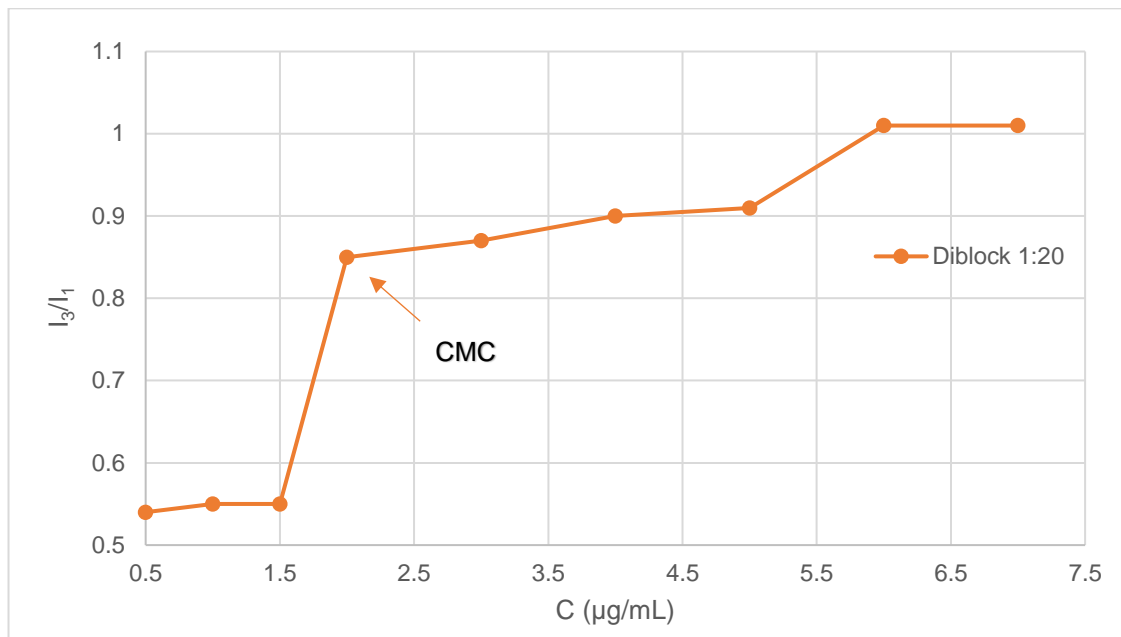


Figure 3.11: Plot of the total intensity ratio from pyrene emission spectra versus concentration of mPEG-*b*-PCL₂₀ (**DB20**).

At low concentration of copolymer, the I_3/I_1 remained unchanged. As the concentration of the diblock increased, the I_3/I_1 started to increase, as it entered a more hydrophobic environment. This therefore provides information on the location of the pyrene probe in the system confirming the formation of micelles.¹²⁹ The **DB20** has more hydrophobic content, and a lower CMC than **DB10**. The specific CMC for micelle formation of the polymers **DB10** and **DB20** were 5×10^{-6} and 2×10^{-6} mg/mL respectively.

A CMC can also be determined using Dynamic Light Scattering (DLS), which monitors the size of various morphological structures (micelle, vesicles and tubes) as they increase with increased concentration.^{130,131} A number of diblock copolymer solutions were prepared in aqueous solution with the concentrations ranging from 1×10^{-6} to 2×10^{-3} mg/mL. The data obtained with respect to concentration was plotted and the graphs for **DB10** and **DB20** are shown in Figure 3.12.

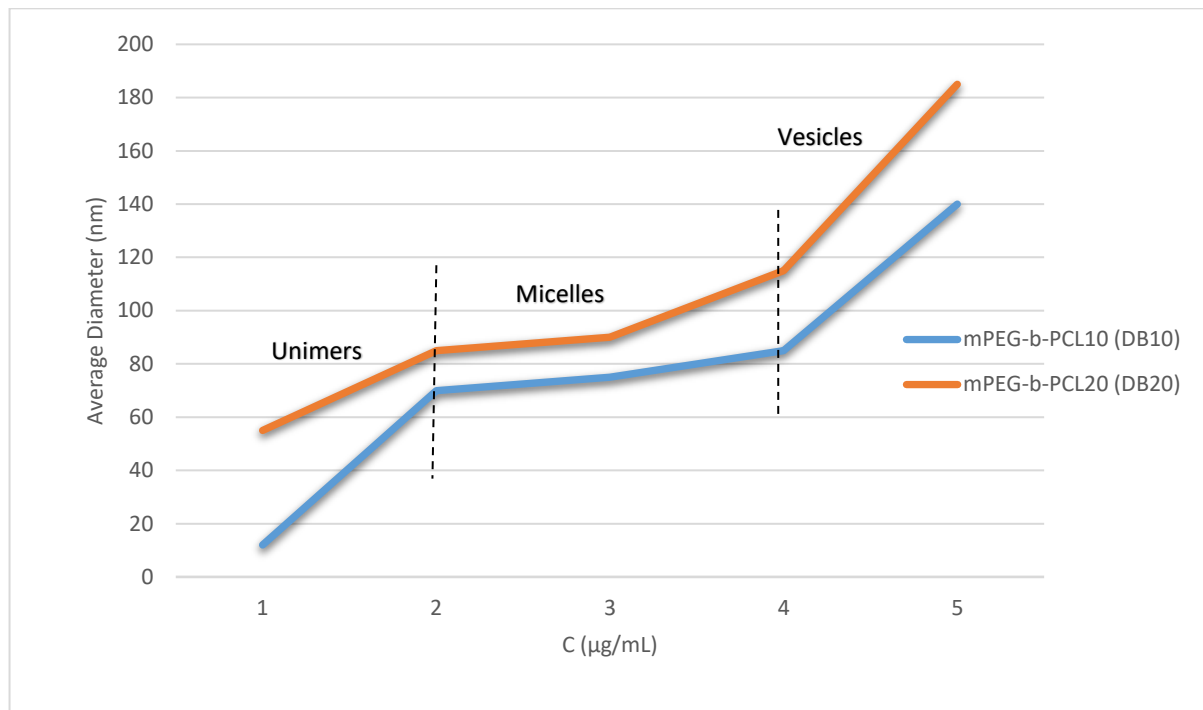


Figure 3.12: Effective hydrophobic diameter of mPEG-*b*-PCL₁₀ (**DB10**) and mPEG-*b*-PCL₂₀ (**DB20**) at changing concentrations.

The graph in Figure 3.12 shows three distinctive areas, indicating three possible aggregated structures (unimers, micelles and vesicles). The average diameter at concentrations between 1-5 µg/mL were between 75-85 nm and 85-115 nm for the solvated micelles of **DB10** and **DB20**, respectively. The formation of micelles was examined within the CMC values measured using pyrene and fluorescence.¹³²

The DLS values were considerably larger than expected for a standard micelle. This is because it is a measurement of the micelles plus the associated solvent, which in this case is water.^{110,133} As a result, the diameter measurements by DLS are an overestimation of the actual particle sizes. Table 3.2 highlights the CMCs of DB10 and DB20 were measured by fluorescence (using pyrene) and DLS.

Table 3.2: CMC of **DB10** and **DB20** measured by fluorescence (using pyrene) and DLS (at concentration 1×10^{-6} – 4×10^{-6} mg/mL).

	DB10	DB20
CMC/pyr [$\mu\text{g/mL}$]	4-5	1.5-2
CMC/DLS [$\mu\text{g/mL}$]	2-4	2-4

3.3.4 Non-covalent encapsulation of anion receptor

Polymeric micelles play an important role in the transportation, incorporation and release of active substances, particular for water-insoluble molecules.¹³⁴ For example, it has been reported that the encapsulation of an insoluble porphyrin within a poly methyloxazoline-*block*-poly phenyloxazoline (PMO-*b*-PPO) micelle improved its water solubility, making the porphyrin more suitable for pharmaceutical and medical applications.¹³⁵ Hence, the utilisation of a polymeric micelle could also solubilise our receptors (**R1** and **HBP6000**) in aqueous medium.

Before starting the anion binding study, it was important to examine two important variables. First, if the simple anion receptor **R1** could be encapsulated inside the micellar core to form a micelle complex. Second, whether or not this complex would be stable during extraction study. That is, the receptor would stay inside the micelle when organic solvent was added. We selected the free receptor **R1** for our encapsulation study as it was simple to synthesise and was insoluble in water. As such, a successful encapsulation inside the micelles could offer a controlled binding site within bulk water, with the possibility of providing a different binding behaviour towards anions.

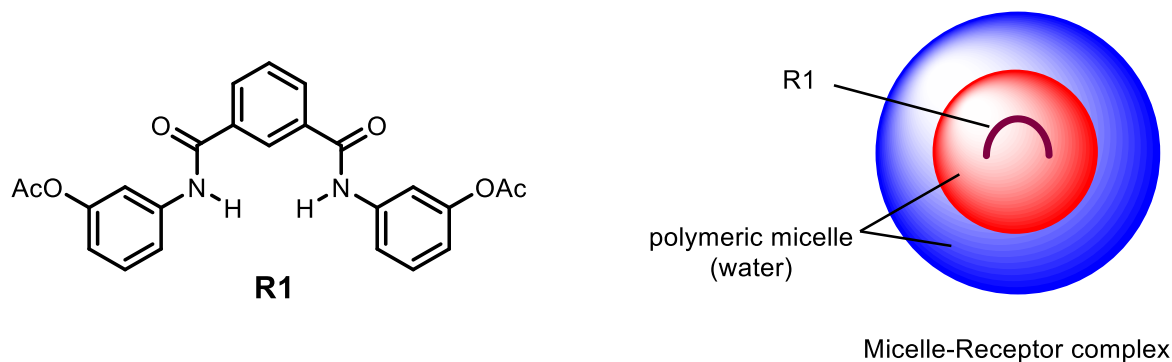


Figure 3.13: Chemical structure of free receptor **R1** (left), and encapsulation of **R1** within polymeric micelle **DB10** in water, cartoon representative (right).

The encapsulation of free receptor (**R1**) into polymeric micelles (**DB10**) was carried out by an ‘oil-dispersion’ technique. The micelles were firstly prepared in buffer solutions (pH 7.04, 0.02M) at 7×10^{-4} M. Next, a 4×10^{-5} M DCM solution of the receptor **R1** was added drop-wise to the micelle solution. The mixture was continuously stirred until the DCM had evaporated, yielding a micelle free receptor complex. Initial encapsulation was assessed using UV-Vis spectroscopy. The analysis revealed that **R1** was completely insoluble in water, but was soluble in the presence of micelle with an intense band at 270 nm, confirming successful encapsulation of **R1** within the micelles. The receptor **R1** had an extinction coefficient of $42604 \text{ M}^{-1}\text{cm}^{-1}$, as determined via Beer-Lambert plot.

After encapsulation of the receptor within the micelles was confirmed, the stability of the complex in water was investigated (would the free receptor stay inside the micelle phase when organic solvent was added). 2 mL of DCM was added to a solution of the micelle-receptor complex and shaken for 30 min. The aqueous layer was then collected and measured by UV-Vis spectroscopy. The result is shown graphically in Figure 3.15. Unfortunately, the data revealed that the micelle-receptor complex has very weak stability in water and the receptor could be easily removed from the micelle.

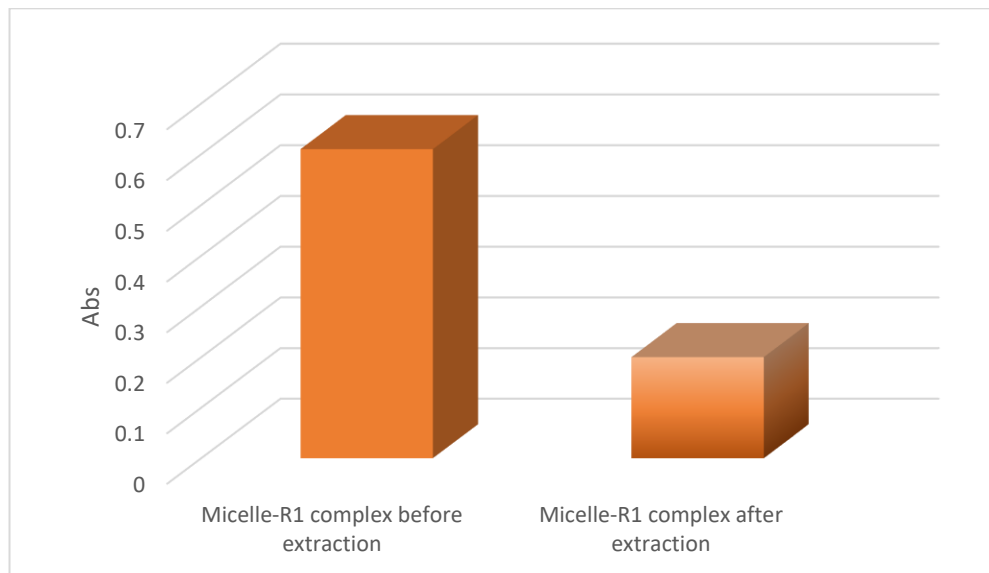


Figure 3.15: Uv-Vis measurement of micelle-**R1** complex before and after extraction showing poor stability of the receptor (**R1**) in the micelle during extraction conditions using DCM and shaken for 30 min.

This indicates that the micelle does not provide strong enough interactions to support or hold the receptor. Although the micelle can provide a hydrophobic environment to bind the receptor in water, it is relatively weak. There are also no additional interactions that could help provide a strong cooperative interaction to prevent the receptor being extracted with organic solvents.

We hoped that the **HBP6000** might have improved stability within the micelle. That is the large hydrophobic hyperbranched polyester could provide additional interactions via electrostatic interactions between the PCL and hyperbranched polyester. In addition, these interactions may enable the HBP to work as a non-covalent crosslinker that could stabilise the micelle and help prevent extraction by organic solvent. The solubility of the HBP was higher in ethyl acetate than DCM (Figure 3.16). As such, the micelle PCL structure is similar to ethyl acetate and may provide a better solvating environment than the external DCM (the organic solvent used for extraction).

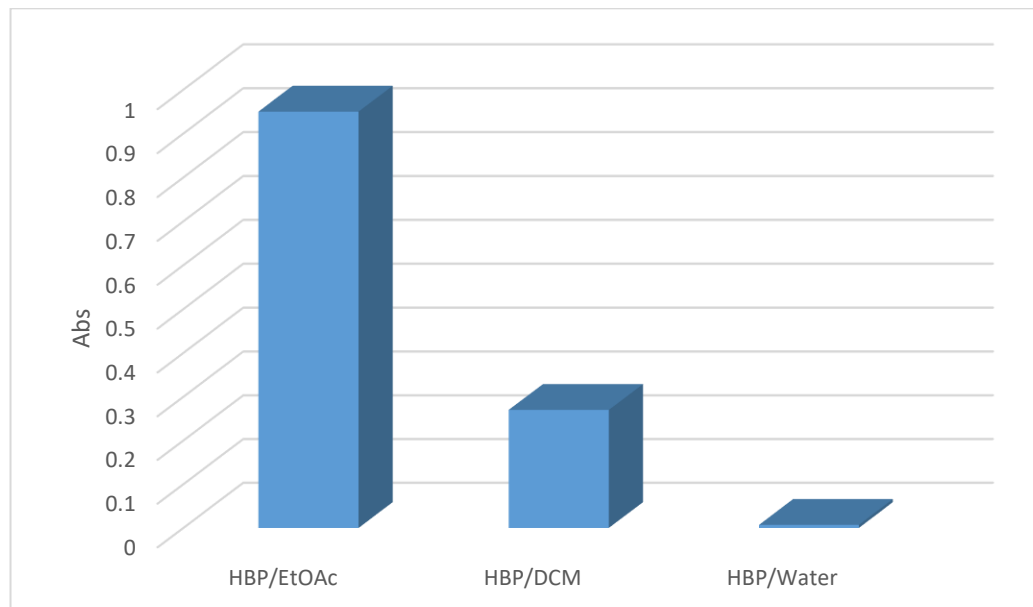


Figure 3.16: Effect of solvent on the solubility of HBP (1×10^{-5} M).

As such, we predicted that the proposed micelle-HBP complex would have a higher stability than the micelle-receptor complex. We examined the encapsulation of **HBP6000** and the stability of the resulting micelle- **HBP6000** complex using the same procedure described above (Figures 3.18).

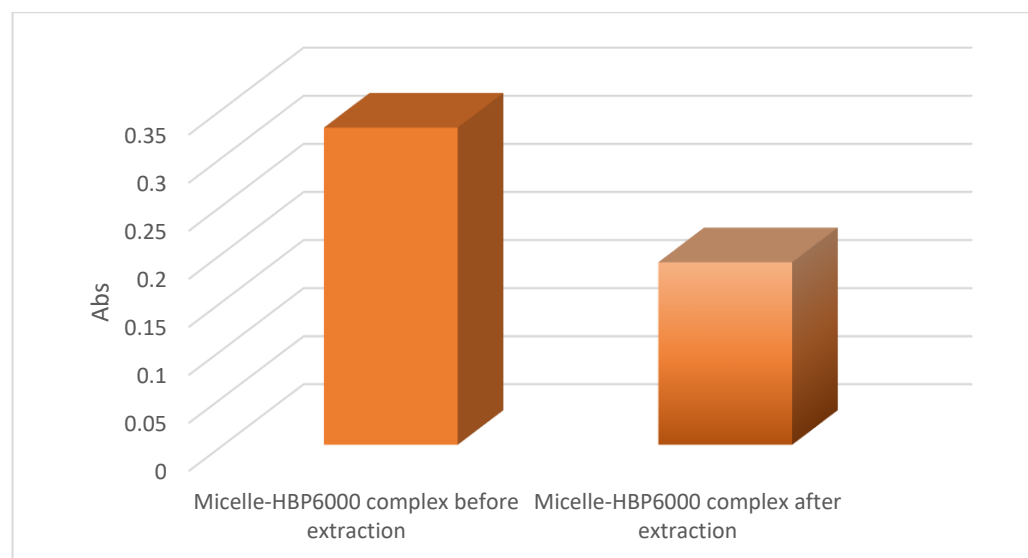


Figure 3.18: Uv-Vis measurement of micelle-**HBP6000** complex before and after extraction using DCM showing more stability of the receptor (**HBP6000**) in the micelle during extraction conditions using DCM and shaken for 30

Although the extraction results showed that the micelle-**HBP6000** complex was more stable than the micelle-**R1** complex, the amount of HBP extracted from the micelle was still too high. Therefore, this method cannot be applied for anion extraction experiments, as a significant amount of the binding site would be removed from the micelle. Therefore, we need to find another method that could increase the stability of the anion receptor within the polymeric micelle.

3.4 Conclusion

Developing an organic system was to serve as proofs of principle, demonstrating that an anion receptor can be covalently incorporated and still maintain the ability to bind anionic species. The main goal of this chapter was to develop a core functionalised water soluble system. An effective organic binding system has been realised; therefore, the next stage was development of a core functionalised water soluble polymeric system. Here, we decided to encapsulate the free receptor and the cored-HBP within the interiors of polymeric micelles system using an amphiphilic diblock copolymer of $m\text{PEG}_{45}\text{-}b\text{-PCL}_n$. We examined the CMC of the prepared diblock copolymers $m\text{PEG}_{45}\text{-}b\text{-PCL}_{10}$ and $m\text{PEG}_{45}\text{-}b\text{-PCL}_{20}$ in water using fluorescence technique and pyrene as probe. The specific CMC for micelle formation of the polymers $m\text{PEG}_{45}\text{-}b\text{-PCL}_{10}$ and $m\text{PEG}_{45}\text{-}b\text{-PCL}_{20}$ were 5×10^{-6} and 2×10^{-6} mg/mL respectively. Another technique such as DLS was also utilised for determining the CMC.

The encapsulation of free receptor **R1** and **HBP6000** into polymeric micelles $m\text{PEG}_{45}\text{-}b\text{-PCL}_{10}$ was conducted using Uv-Vis spectroscopy. The extraction results showed that the micelle-HBP complex (**MH**) was more stable than the micelle-free receptor complex (**MR**). However, the amount of HBP extracted from the micelle was still too high for the transportation method to be applied for anion extraction, as a significant amount of the binding site would be removed from the micelle complex.

3.5 Experimental

3.5.1 Chemicals and Instrumentation

Solvents and reagents

All chemicals and reagents were obtained from commercial supplier (primarily Sigma-Aldrich) and were used without further purification unless otherwise stated.

Nuclear magnetic resonance spectroscopy (NMR)

All NMR samples were prepared using deuterated solvents supplied by Sigma Aldrich. ^1H NMR and ^{13}C NMR spectra were recorded using a Bruker AV1400 MHz machine. The NMR spectra were analysed using Topspin 3.2 NMR software. Shifts are quoted as ppm and couplings quoted in Hertz.

Fourier transform infrared spectroscopy (FTIR)

FTIR spectroscopy was performed in the solid state (in reflectance mode) using Perkin Elmer Spectrum RX FT-IR System in the range of 700 to 4000 cm^{-1} .

UV-Vis spectroscopy

The ultraviolet absorbance was recorded on an Analytik Jena AG Specord s600 UV/Vis Spectrometer and analyzed using its attached Software (WinASPECT).

Fluorescence Spectroscopy

Fluorescence results were obtained using a HORIBA Scientific Fluoromax-4 spectrofluorometer using its attached software (FluorEssence V3).

pH measurement

The pH of the buffer solutions prepared was substantiated using a pH 210 Microprocessor pH Meter from Hanna Instruments Ltd. (Leighton Buzzard, UK). The device was calibrated using pH 4.0 and pH 7.0 standard solutions, prepared with buffer tablets (Sigma-Aldrich, Poole, UK).

Dynamic light scattering (DLS)

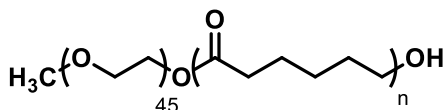
DLS results were obtained using the Brookhaven instrument 90 Plus Particle Size Analyser (Holtsville, NY, USA) 35 mW solid state standard laser. This instrumentation was used to determine the hydrodynamic diameter of nanoparticles. Particle sizing software 9kpsdw32.exe.ver.3.80 was used for characterisation. Light was scattered at an angle of 90 ° with each run lasting 2 minutes at a temperature of 37.5 °C. Samples were filtered using Whatman[®] GD/X syringe filters with a pore size of 0.45 µm, prior to analysis. Results reported are based upon volume distribution.

Gel Permeation Chromatography/ Size Exclusion Columns

Analytical THF GPC data was obtained at room temperature using either a high molecular weight column (3x300 mm PL gel 10 µm mixed-B), or a low molecular weight column (2x600 mm PL gel 5µm (500 Å) mixed-E). Calibration was achieved by using polystyrene standards (Mn 220-1, 1,000,000 Da) and molecular weights are thus reported relative to these specific standards used. The samples were run using Fisher GPC grade THF as a solvent stabilised with 0.025 % BHT (which was supplied to the columns by a Waters 515 HPLC Pump at 1.00 mLmin⁻¹). Toluene was added to prepared sample as a flow marker, before injection through a 200 µL sample loop with a Gilson 234 Auto Injector. The concentration of a sample was studied using an Erma ERC-7512 refractive index detector and, where applicable, by UV using a Waters Millipore Lambda Max 481 LC Spectrophotometer. Aqueous GPC data was acquired using a Millipore Waters Lambda-Max

481 LC spectrometer with a LMW/HMW column. The eluent which was used was NaNO₃/NaH₂PO₄ (pH=7) buffer solution (unless stated otherwise). The data attained was then analysed using GPC-online software. Samples were filtered using Whatman® GD/X syringe filters with a pore size of 0.45 μm prior to analysis.

3.5.2. General procedure for the synthesis of di-block copolymers



DB10: n= 10 DB40: n=40
DB20: n= 20 DB60: n=60

A dried two-neck round bottom flask was filled with dry mPEG₂₀₀₀ and stirred under vacuum at 130 °C for 2h. The reaction system was refilled with nitrogen gas and ε-caprolactone (varied in ratio to the mPEG monomer units) was added by using syringe through the rubber septum followed by stannous octoate (few drops). The solution was stirred overnight at 130 °C. The resulting white solid at room temperature dissolved in DCM and precipitate into petroleum ether 40-60 °C to yield methyl polyethylene glycol-*block*-polycaprolactone.

3.5.2.1 Synthesis of mPEG-*b*-PCL₁₀ di-block copolymers (DB10):

ε-Caprolactone (1.83 mL, 16.5 mmol) was reacted with mPEG₂₀₀₀ (3.00 g, 1.5 mmol) to yield 3.75 g of mPEG-*block*-PCL₁₀.

¹HNMR (CDCl₃, 400MHz) δ: 1.39 (p, 2H, γ-CH₂), 1.64 (p, 4H, β and δ-CH₂), 2.31 (t, 2H, α-CH₂), 3.48 (s, 3H, CH₃O-), 3.64 (s, 180H, OCH₂CH₂O), 4.05 (t, 2H -CH₂OH). ¹³CNMR (CDCl₃, 400MHz,) δ: 24.8, 25.5, 28.9, 34.1, 64.0, 70.8, and 173.5. FTIR (cm⁻¹): 2987 and 2865 (CH₂), 1719 (COOR), 1991 (C-O-C). GPC: M_n = 3400, M_w = 4700, PD = 1.41. M_n (estimation NMR) = 3700.

3.5.2.2. Synthesis of mPEG-*b*-PCL₂₀ di-block copolymers (DB20):

ε-Caprolactone (3.66 mL, 33 mmol) was reacted with mPEG₂₀₀₀ (3.00 g, 1.5 mmol) to yield 7.4 g of mPEG-*block*-PCL₂₀.

¹HNMR (CDCl₃, 400 MHz) δ: 1.39 (p, 2H, γ-CH₂), 1.67 (m, 4H, β and δ-CH₂), 2.32 (t, 2H, α-CH₂), 3.40 (s, 3H, CH₃O-), 3.66 (s, 180H, OCH₂CH₂O), 4.07 (t, 2H -CH₂OH). ¹³CNMR (CDCl₃, 400 MHz) δ: 24.3, 25.9, 28.3, 34.5, 64.2, 70.5, and 173.8. FTIR (cm⁻¹): 2987 and 2868 (aliphatic CH₂), 1720 (COOR), 1189 (C-O-C). GPC: M_n= 4400, M_w= 8000, PD = 1.84, and M_n (by NMR estimation) = 5400.

3.5.2.3. Synthesis of mPEG-*b*-PCL₄₀ di-block copolymers (DB40):

ε-Caprolactone (6.85 mL, 60 mmol) was reacted with mPEG₂₀₀₀ (3.00 g, 1.5 mmol) to yield 7.4 g of mPEG-*block*-PCL₄₀.

¹HNMR (CDCl₃, 400 MHz) δ: 1.4 (p, 2H, γ-CH₂), 1.67 (m, 4H, β and δ-CH₂), 2.33 (t, 2H, α-CH₂), 3.39 (s, 3H, CH₃O-), 3.65 (s, 180H, OCH₂CH₂O), 4.08 (t, 2H -CH₂OH). ¹³CNMR (CDCl₃, 400MHz) δ: 24.9, 25.5, 28.1, 34.7, 64.2, 70.5, and 173.5. FTIR (cm⁻¹): 2987 and 2868 (CH₂), 1720 (COOR), 1185 (C-O-C). GPC: M_n= 9900, M_w= 13900, PD = 1.40. M_n (estimation NMR) = 10000.

3.5.2.4. Synthesis of mPEG-*b*-PCL₆₀ di-block copolymers (DB60):

ε-Caprolactone (11.30mL, 102mmol) was reacted with mPEG₂₀₀₀ (3.00 g, 1.5 mmol) to yield 12.93 g of mPEG-*block*-PCL₆₀.

¹HNMR (CDCl₃, 400 MHz) δ: 1.41 (p, 2H, γ-CH₂), 1.65 (m, 4H, β and δ-CH₂), 2.34 (t, 2H, α-CH₂), 3.41(s, 3H, CH₃O-), 3.65 (s, 180H, OCH₂CH₂O), 4.08 (t, 2H -CH₂OH); ¹³CNMR (CDCl₃, 400MHz) δ: 24.7, 25.6, 28.1, 34.1, 64.1, 70.7, and 173.5. FTIR (cm⁻¹): 2944 and 2864 (CH₂), 1719 (COOR), 1974 (C-O-C). GPC: M_n = 12000, M_w = 16300, PD = 1.35. M_n (estimation NMR) = 13500.

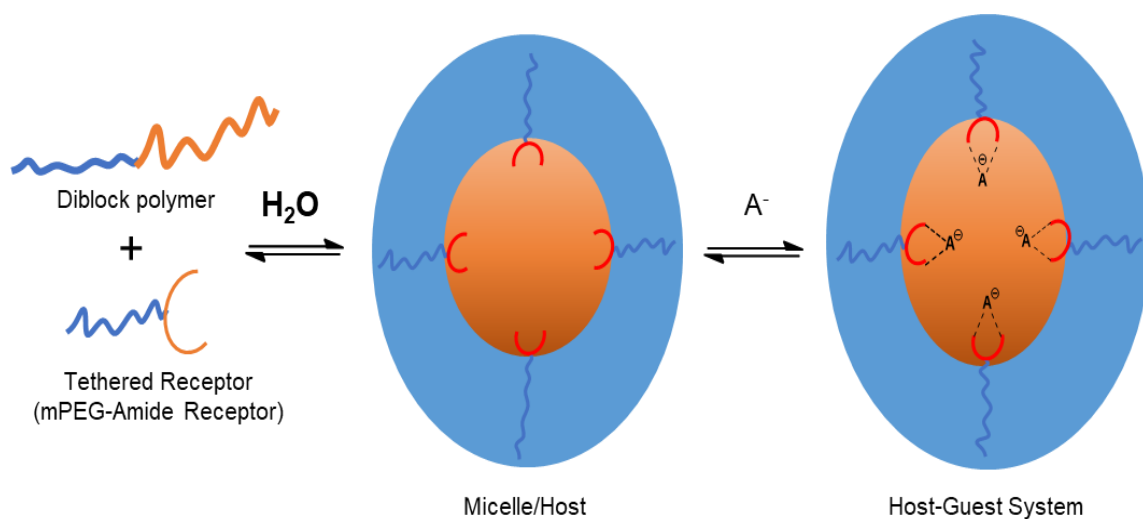
3.5.3 Micelle formation

Micelle samples of di-block copolymers were prepared by direct dissolution method in which an aqueous solution of polymer (1 mg mL^{-1}) was vigorously stirred for 2h, sometimes heating was required.

3.5.4 Encapsulation of HBP within polymeric micelles

HBP loaded/encapsulated polymeric micelles were prepared by an oil-in-water emulsion method for the slightly water soluble mPEG-*b*-PCL di-block copolymer. This method involved dropwise addition of HBP dissolved in a suitable organic solvent to the preformed micelle solution. The mixture was stirred for 1 to 2 hours to remove the organic solvent by evaporation.

Chapter Four: Co-micellization of mPEG-Amide Anion Binding Receptor with Water-Soluble Diblock Polymers



4.1 Introduction

According to the findings from the previous chapter, it was hypothesised that using a controlled microenvironment for a macromolecular anion binding receptor could trigger less “leaching” into the organic medium if the binding site was bound to a hydrophilic molecule. This was hypothesised to increase the stability of the anion receptor within the micellar structure during extraction studies, and the use of PEG to tether the receptor and hold it within the micelle was proposed for this purpose. Another reason for using tethered receptors is to isolate the binding sites from each other and prevent dimerization, as this phenomenon could inhibit anion binding by reducing the number of binding sites available, decreasing the efficiency of the receptor.

PEG is used in various chemical, biomedical and pharmaceutical applications, due to being non-toxic, non-immunogenic, biocompatible, and water-soluble.¹³⁶ However, one obvious disadvantage of PEG is a lack of reactive groups in its polymeric ether chains, which means that synthesis of PEG derivatives with active and functional terminated groups is of great interest.

An excellent example of a modification of PEG is PEGylation. PEGylation of a biomolecule can cause changes in its physicochemical properties such as hydrophilicity, size, and molecular weight, as well as adjustments in conformation and steric hindrance.¹³⁷ Arginine deiminase (ADI) has been studied as an anti-cancer enzyme in this context. However, ADI has a short circulating half-life, and it has thus been formulated with PEG to overcome this problem and increase its therapeutic activity (Figure 4.1). ADI-PEG retains half of its enzyme activity after forming an amide bond between the PEG and the protein, along with an obvious increase in the pharmacokinetic and pharmacodynamic properties of the formulation after PEGylation.¹³⁸

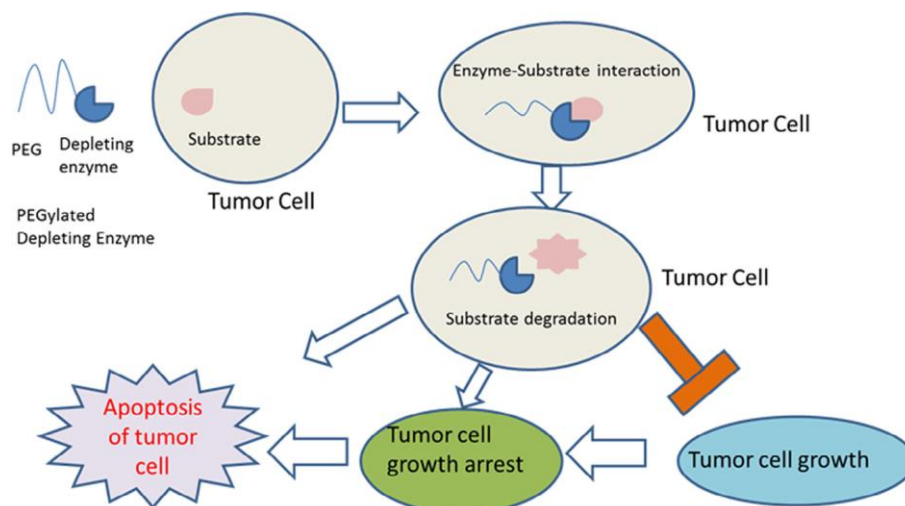
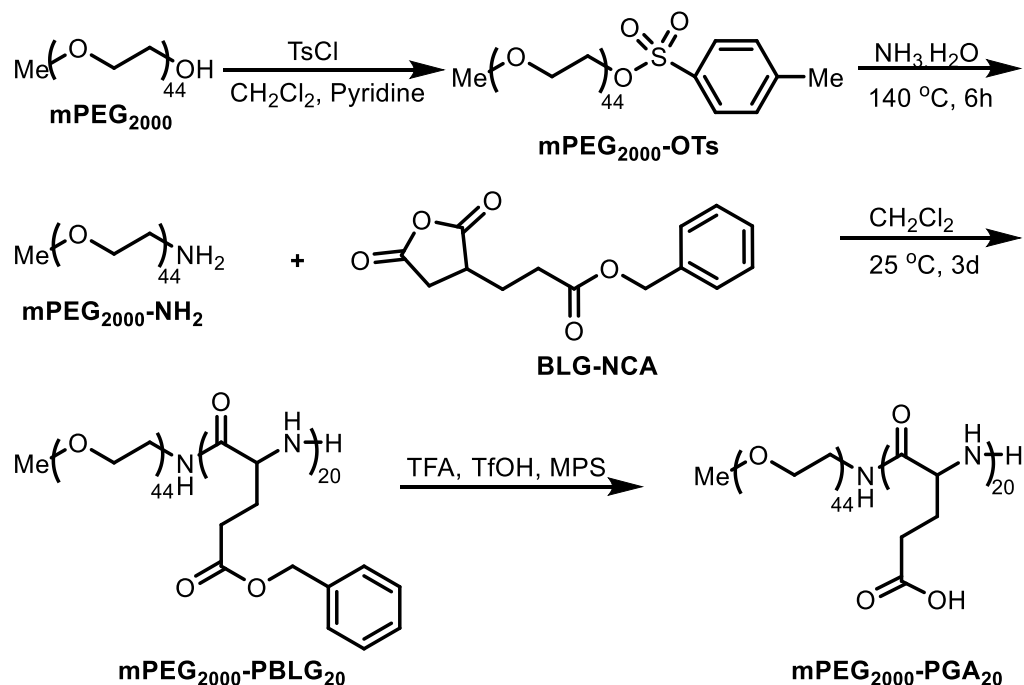


Figure 4.1: PEGylated ADI enzymes as used in anticancer therapy.¹³⁸

In recent decades, a large number of PEG derivatives have been synthesized;^{139–141} among these, amino terminated PEG is one of the most important. Several PEG preparation procedures with primary amino groups have been undertaken,^{142–144} but one of the most straightforward methods for the synthesis of PEG-NH₂ is through the conversion of the terminate hydroxyl group to a “good” leaving group (a halide or sulfonyl compound), followed by an amination reaction using the excess of ammonia.

Luan et al.¹⁴⁵ synthesised and evaluated methoxypolyethylene glycol–poly (glutamic acid) (mPEG–PGA) to act as a drug carrier. This synthesis was begun by substituting the terminal hydroxyl group of mPEG with an amino group, followed by ring opening polymerisation with BLG-NCA (Scheme 4.1).



Scheme 4.1: Synthesis of diblock polypeptide mPEG-PGA.

4.1.1 Amide based receptors

Amide NH groups have been used to generate a wide range of anion binding receptors, which can act as hydrogen bond donor groups. In 1986, Pascal et al.¹² discovered one of the first amide based receptors, deriving it from the protein salmonella typhimurium. The X-ray of its crystal structure shows that the sulphate interacts via seven hydrogen bonds, five of which contain amide N-H protons that form a polypeptide backbone. This discovery led to increased attention being paid to the design of neutral organic macrocycles encompassing several inwardly-facing N-H groups, in the hope that these might sufficiently enhance the binding of hydrophobic anions. The reported macrocycle compound is shown in Figure 4.2.

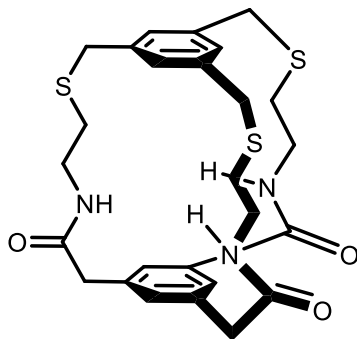


Figure 4.2: Chemical structure of 2, 15, 28-trioxo-3, 16, 29-triaza-6, 19, 32-trithial [7.7.7] (1, 3, 5- cyclophane).¹²

The tetra amide macrocyclic anion receptor (Figure 4.3) shows the highest level of affinity towards F^- from among a mixture of F^- , Cl^- , Br^- , AcO^- , and $H_2PO_4^-$ ions, according to UV/Vis and 1H NMR studies. The selectivity trend of amide-based receptors toward these anions is most probably triggered by size complementarity between the guest and the cavity. Moreover, the formation of hydrogen bonds between the receptor and the fluoride anion results in a visible colour change, offering the potential for use as a colourimetric sensor.¹⁴⁶

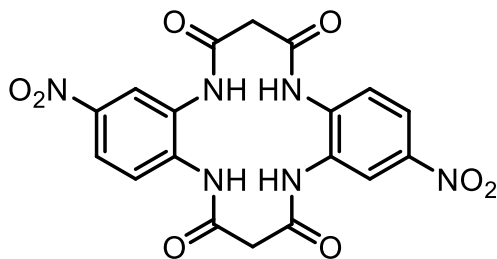


Figure 4.3: Chemical structure of Macrocylic tetra amide (3'-nitrobenzo)[2,3-d]-(3''-nitrobenzo)[9,10-d]-1,4,8,11-tetraazacyclotetradecane-5,7,12,14-tetraone.

The selectivity trend of anion binding in the carbazole receptor (Figure 4.4) was determined by Jurczak,¹⁴⁷ who showed that $H_2PO_4^- > PhCOO^- > Cl^-$. The selectivity towards $H_2PO_4^-$ is due to anion interaction with cavity size, though, in addition, the four oxygen atoms in the $H_2PO_4^-$ moiety increase the number of hydrogen bonding interactions and form a more stable complex. While the

chloride anions are also basic, the chloride volume is smaller than that of phosphate and the cleft is too wide for the chloride anions.

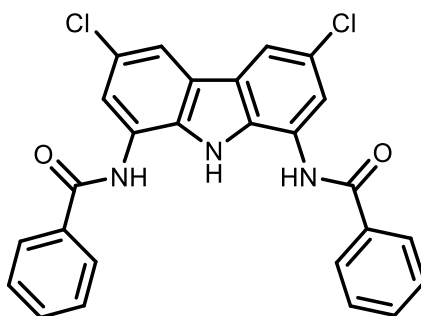


Figure 4.4: Carbazole receptor

Robina et al.¹⁴⁸ reported the use of amide bonds within a furyl-cyclopeptide receptor (Figure 4.5). According to ¹HNMR titration and ESI-MS studies, the developed cyclopeptide receptor produces 1:1 complexes with three different anions, though it shows high selectivity towards chloride.

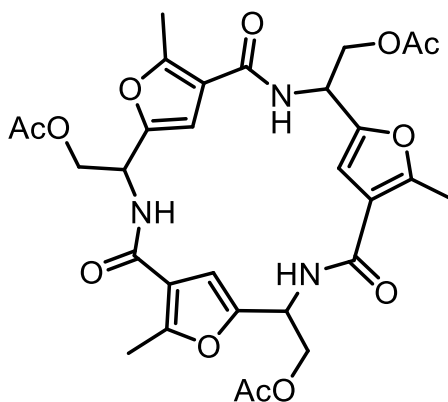


Figure 4.5: Chemical structure of C3-symmetric furyl-cyclopeptide receptor as developed by Robina et al.

4.2 Aim and Objectives

Based on the previous findings, which suggest that the use of a controlled microenvironment for anion binding in water could be achieved if the binding site was encapsulated within the hydrophobic interior of a polymer micelle, the simplest method would involve micelle encapsulated binding sites. However, if the methodology is used for extraction from organic media, there is a high chance of removing the binding site, as shown in Figure 4.6 A (and reported in the previous chapter). Thus, this study attempted to tether the receptor with a water-soluble PEG, on the grounds that this would form part of the micelle and reduce the possibility of leaching (Figure 4.6 B).

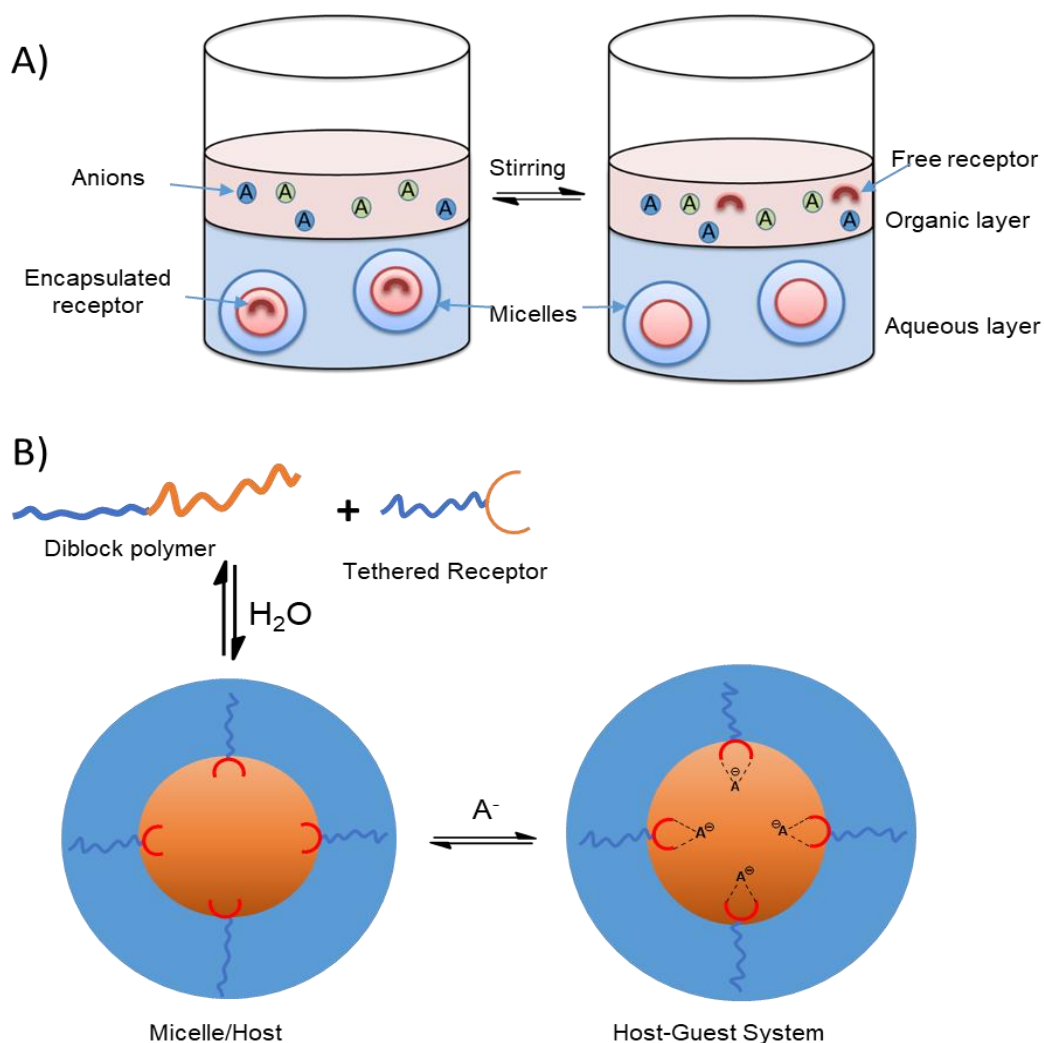


Figure 4.6: Graphical representation of Host-Guest system formed using diblock and functionalised mPEG.

This work thus represents a proof of principle. It is not an attempt to make the best ligand possible, but rather to prove the validity of using a PEG-tethered receptor within a polymer micelle. Hence, the initial stage of this project involved the selection of an anion binding cleft that could be tethered or co-micellized within the polymeric micellar structure, and the next stage thus became demonstrating increased selectivity towards hydrophobic species as compared to a free receptor in water.

This chapter focuses on using functionalised mPEG with an anion receptor, that can be co-micellized with an amphiphilic polymer to generate a stable encapsulated system to prevent the binding site from diffusing out of the micelle during the extraction process. Another advantage of using a functionalized mPEG is to prevent the receptor dimerizing, as shown in Figure 4.7, which is a known phenomenon that inhibits anion binding.

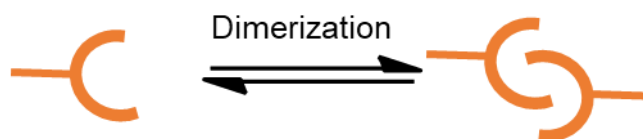


Figure 4.7: Representative structures showing the dimerization phenomenon.

The synthesis of the target molecules and their characterisation is presented in the next section, followed by an examination of the aggregation behaviour of the amphiphilic polymers. Finally, the anion binding efficiency of the host system, along with control experiments, is studied.

4.3 Results and Discussion

4.3.1. Synthetic strategies for designing a functionalised mPEG

The synthetic approach to developing receptor **R2** (Figure 4.8) included two main synthetic steps. The anion receptor 3,5-bis(benzoyl amino)-benzoic acid was chosen as a binding site, requiring preparation of an mPEG that was more reactive than mPEG-OH and which could produce a more stable compound. Thus, mPEG-NH₂ was chosen.

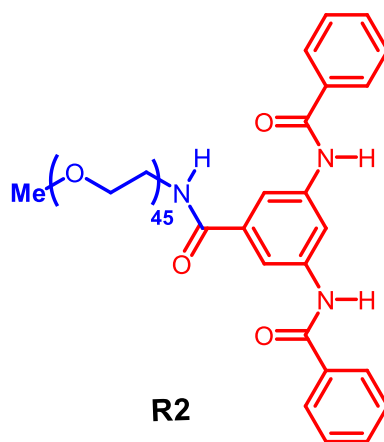
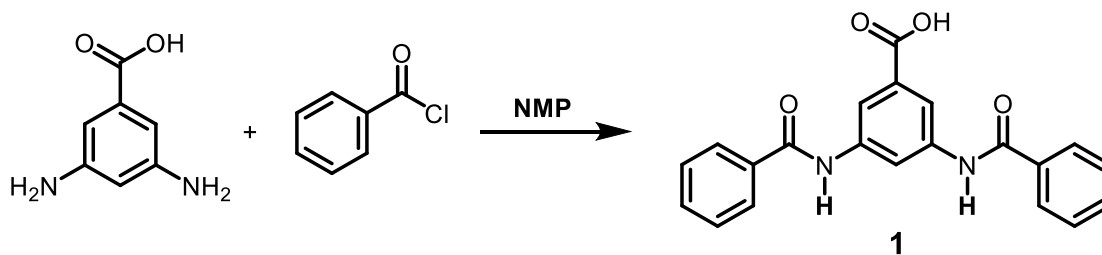


Figure 4.8: Structure of methoxy polyethylene glycol functionalised with amide based receptor.

4.3.1.1. Synthesis of 3,5-bis(benzoyl amino) benzoic acid (**1**)

The first step in synthesising receptor **R2** was the production of 3,5-bis(benzoyl amino)-benzoic acid **1**. This was achieved by activation of a carboxylic acid as the corresponding acid chloride, followed by an amine reaction. The high reactivity of acid chlorides with amines generally leads to fast coupling, which can be particularly useful for sterically hindered materials.¹⁴⁹ Anion receptor 3,5-bis(benzoyl amino) benzoic acid was thus synthesised in a single step using 3,5-diaminobenzoic acid and benzoyl chloride (Scheme 4.2). This synthetic procedure was based upon the methodology outlined in the work by Yunmei et al.¹⁵⁰



Scheme 4.2: Synthesis of 3,5-bis(benzoyl amino) benzoic acid.

The synthesis of amide **1** was carried out by stirring benzoyl chloride in solution with 3,5-diaminobenzoic acid into N-methyl-2-pyrrolidone (NMP). The reaction mixture was then precipitated into HCl/water, and the solid product washed with methanol to give amide **1**, which is a greyish product.

The ^1H NMR spectrum of amide **1** was in accordance with the literature (Figure 4.9), with singlet peaks at 13.10 ppm and 10.52 ppm, corresponding to the OH and NH protons, respectively. The most intense peaks, at 8.01 ppm and 7.49 ppm (c and d), were assigned as the 10 new aromatic protons (Figure 4.9). The mass spectrum showed an MH^+ signal at 361. IR spectroscopy was used for further characterisation, with peaks corresponding to the C=O (carboxylic acid) and N-H of the amide groups were seen at 1703 and 1666 cm^{-1} , respectively.

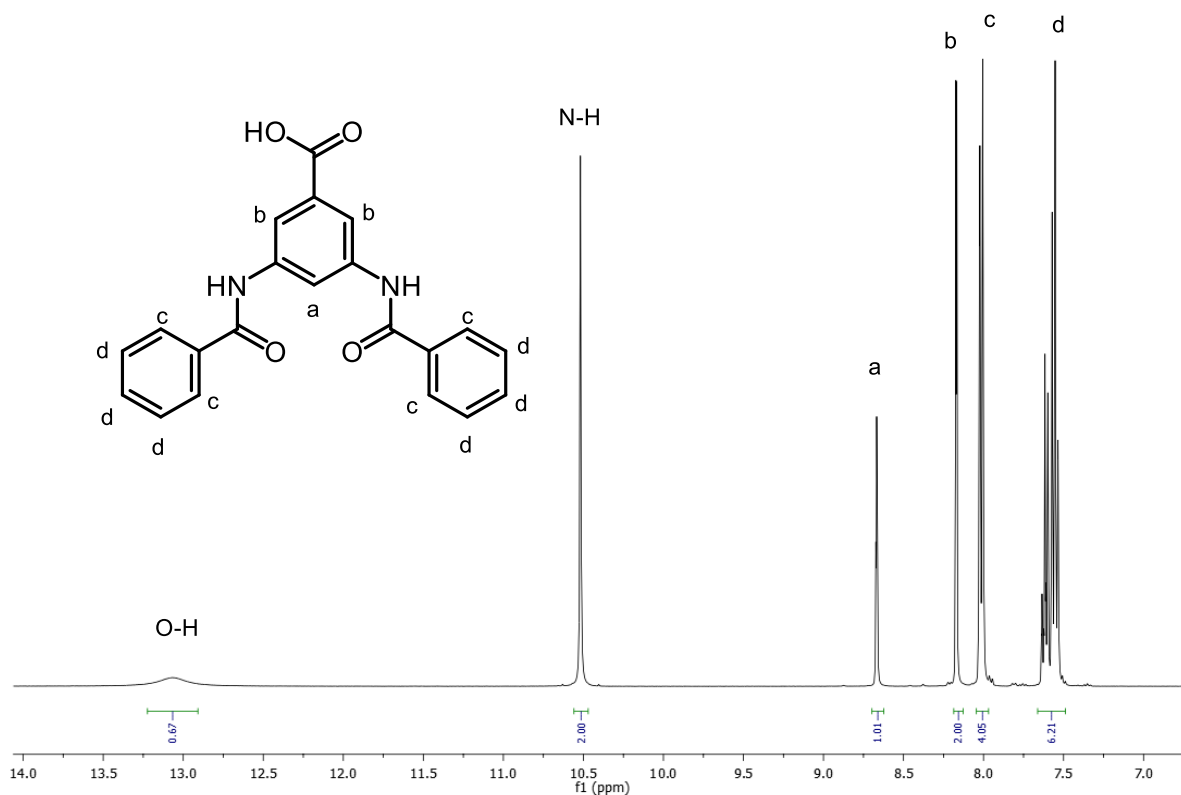
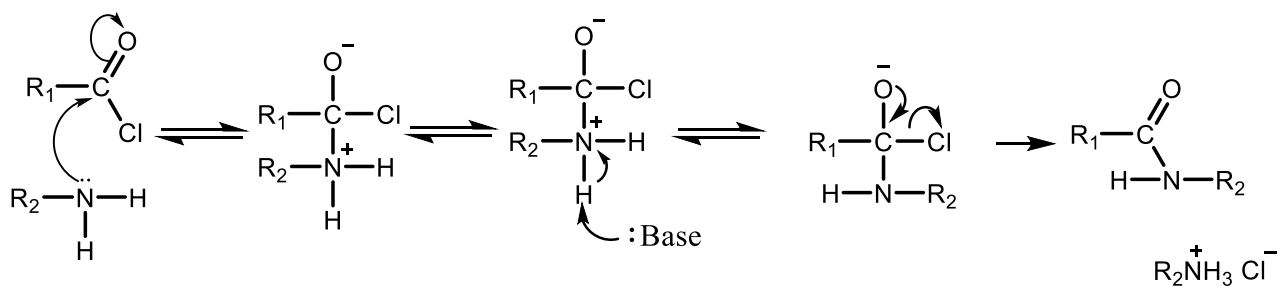


Figure 4.9: The ¹H NMR spectrum of 3,5-bis(benzoyl amino) benzoic acid.

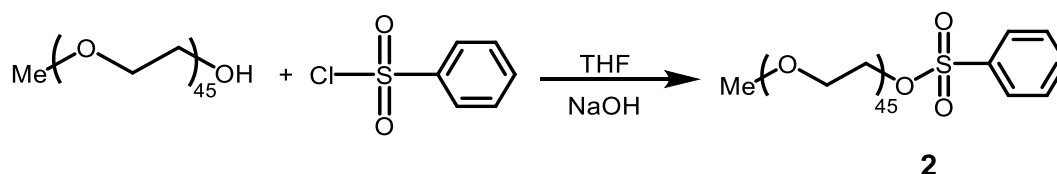
The mechanism for this involves two stages. The first is a nucleophilic attack by the lone pair on the nitrogen with the partially positive carbon of the carbonyl and followed by a proton being removed by a base. The second is removal of chloride as the double bond between the carbon and oxygen forms, and gives ammonium hydrochloride as a by-product (Scheme 4.3).



Scheme 4.3: Nucleophilic addition-elimination mechanism

4.3.1.2. Synthesis of mPEG-NH₂

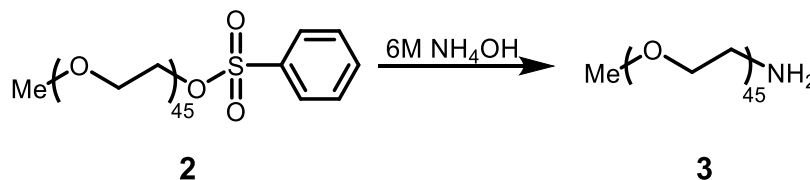
The mPEG-NH₂ for this study was prepared in two steps, creation of the tosylate derivative, followed by an amination reaction. Methoxy polyethylene glycol tosylate **2** (Scheme 4.4) was produced according to the method reported by Zhang,¹⁴⁵ in which NaOH solution was reacted with mPEG-OH, before the addition of tosyl chloride. The product obtained after work up offered an 88% yield as a white solid.



Scheme 4.4: Synthesis of mPEG-tosylate (**2**)

The success of the reaction was confirmed by the appearance of a new singlet at 2.48 ppm in the ¹HNMR spectrum. This corresponds to the methyl protons of the tosylate group. In addition, the new aromatic protons were seen at 7.32 to 7.80 ppm. The ¹³CNMR data also showed peaks at 126, 128, 139, and 144 ppm, confirming the presence of an aromatic ring, and the broad peak at 3300 cm⁻¹ for the O-H functional group was no longer visible in the IR, confirming the successful addition of the tosylate group.

Amination was achieved by dissolving tosylate **2** in a solution of 6 M ammonium hydroxide and stirring for 3 days at 60°C. The product was obtained after work up and purification by precipitation from petroleum ether (40-60) (Scheme 4.5).



Scheme 4.5: Synthesis of mPEG-NH₂ (**3**) by reacting tosyl **2** with ammonium solution for 3 days.

Confirmation that the tosyl group was removed was achieved by analysis of the proton NMR spectrum (Figure 4.10), with the aromatic protons signals no longer visible. Moreover, a triplet was seen in the upper field at 3.14 ppm, corresponding to the terminal methylene group adjacent to NH, rather than the signal 3.83 ppm, which is typical of PEG-OH.

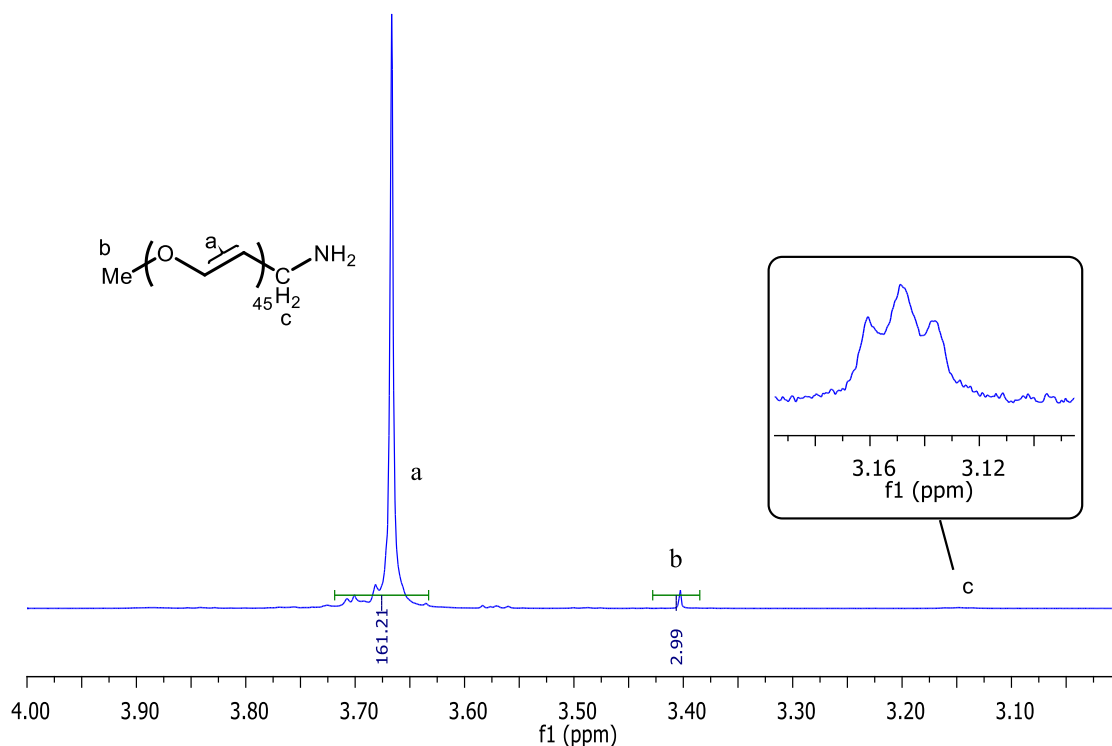
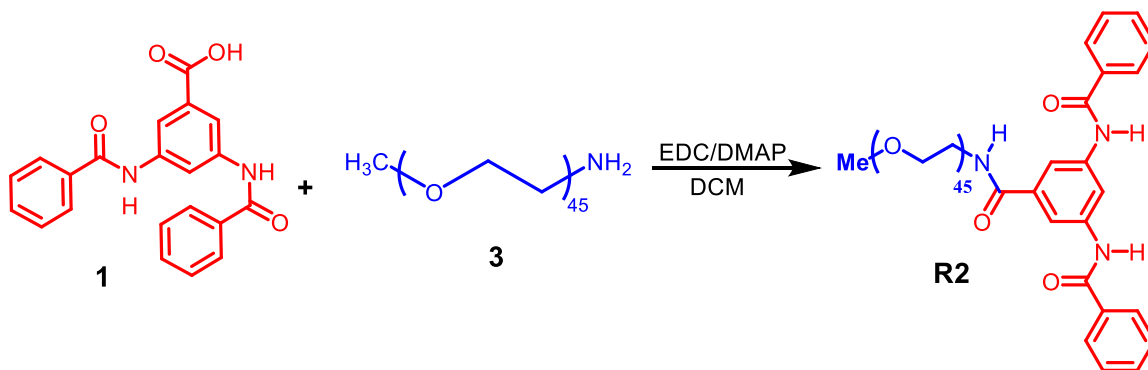


Figure 4.10: The ¹H NMR spectrum of mPEG-NH₂ in CDCl₃.

4.3.1.3. Synthesis of mPEG-R (R2)

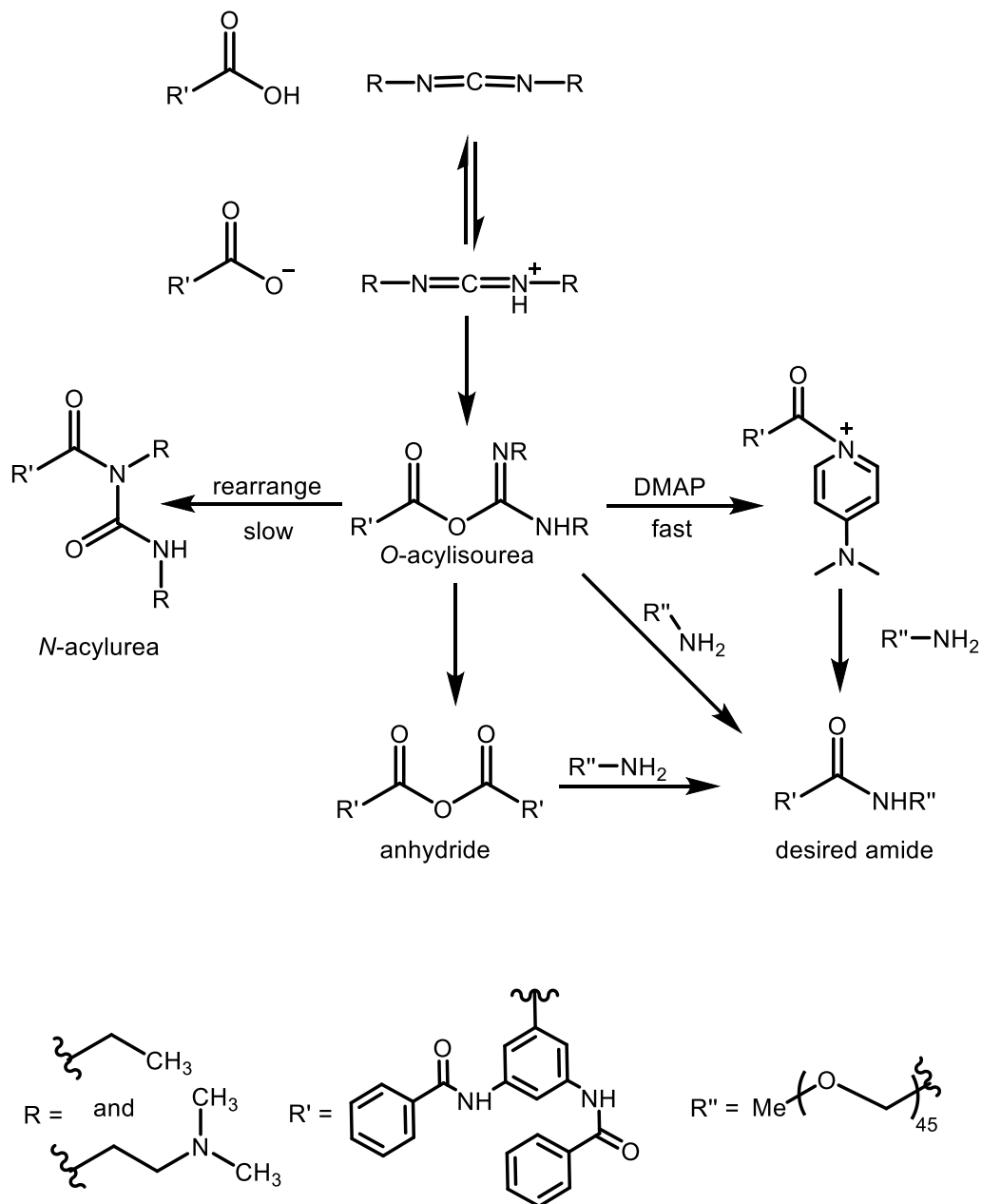
Amide cleft (**1**) can be added to the mPEG-NH₂ (**3**) through the formation of an amide bond (Scheme 4.6).



Scheme 4.6: Synthesis of functionalised mPEG with anion binding site.

This was achieved using carbodiimides reagents. Carbodiimides are popular coupling reagents, applied since 1955, they include N-(3-dimethylaminopropyl)-N'-ethylcarbodiimide.HCl (EDC.HCl), which offers the advantage that the urea by-product is readily soluble in water or most organic solvents and can be easily removed.^{151,152} The reaction is shown in Scheme 4.7. The first step is conversion of carboxylic acid to an O-acylurea, and this intermediate is then used to produce the amide via direct coupling. However, it is also possible to form other side products such as an N-acylurea or carboxylic acid anhydride, which can also yield amide after reaction with the amine, as shown in Scheme 4.7.¹⁵¹

This reaction was initially attempted using DMAP, which gave the desired product, albeit with a low yield. Adding a few drops of triethylamine to neutralize the HCl salt significantly increased the yield in subsequent attempts.



Scheme 4.7: The coupling of carboxylic acid and primary amines using EDC.HCl.

Examining the ^1H NMR spectrum showed that the coupling reaction was successful, as the $-\text{COOH}$ signal at 13.10 ppm (seen in the spectrum for **1**) was no longer visible. A singlet at 8.87 ppm, corresponding to the new amide protons of the binding site were also visible and were no longer observed after the addition of D_2O . In addition, two singlet at 3.67 and 3.39 ppm, corresponding to the methylene protons of the PEG and terminal methoxy group were visible (Figure 4.11). The IR

spectrum showed an absence of peaks at 1703 and 3500 cm^{-1} seen for the carboxylic acid group of amide **1**.

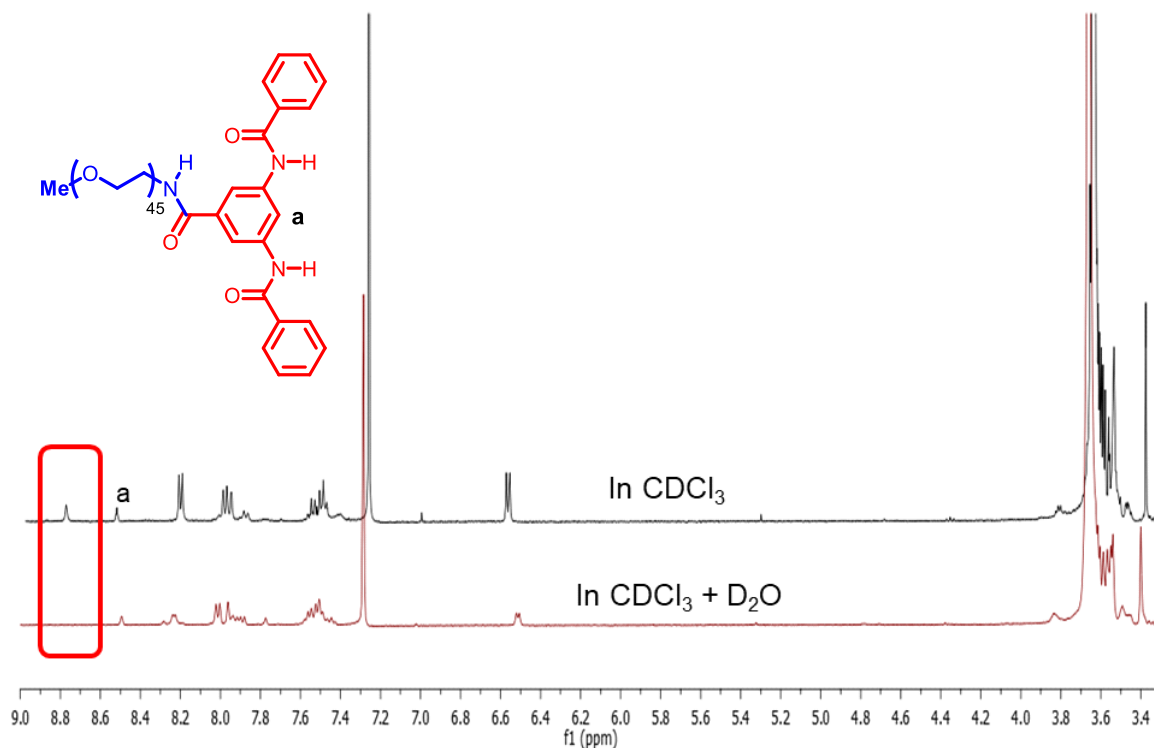


Figure 4.11: NMR of receptor **6** in CDCl_3 and receptor **R2** in CDCl_3 and D_2O .

4.3.2. Anion binding assay using NMR titration

The preliminary binding properties of receptor **R2** were examined using a ^1H NMR titration in which receptor **R2** (20 mg/mL) was titrated against tetrabutylammonium chloride (20 mg/mL) in CDCl_3 . The ^1H NMR data showed the NH peaks of the receptor moving slightly downfield (Figure 4.12). An increase in the anion concentration led to a further increase in $\Delta\delta$, indicating hydrogen bonding between the amide receptor and the anions. Although these shifts were small, this experiment confirmed that the receptor could indeed bind the anions. The next step was the formation of a host system by means of the co-micellization of receptor **R2** with a diblock polymer mPEG-*b*-PCL.

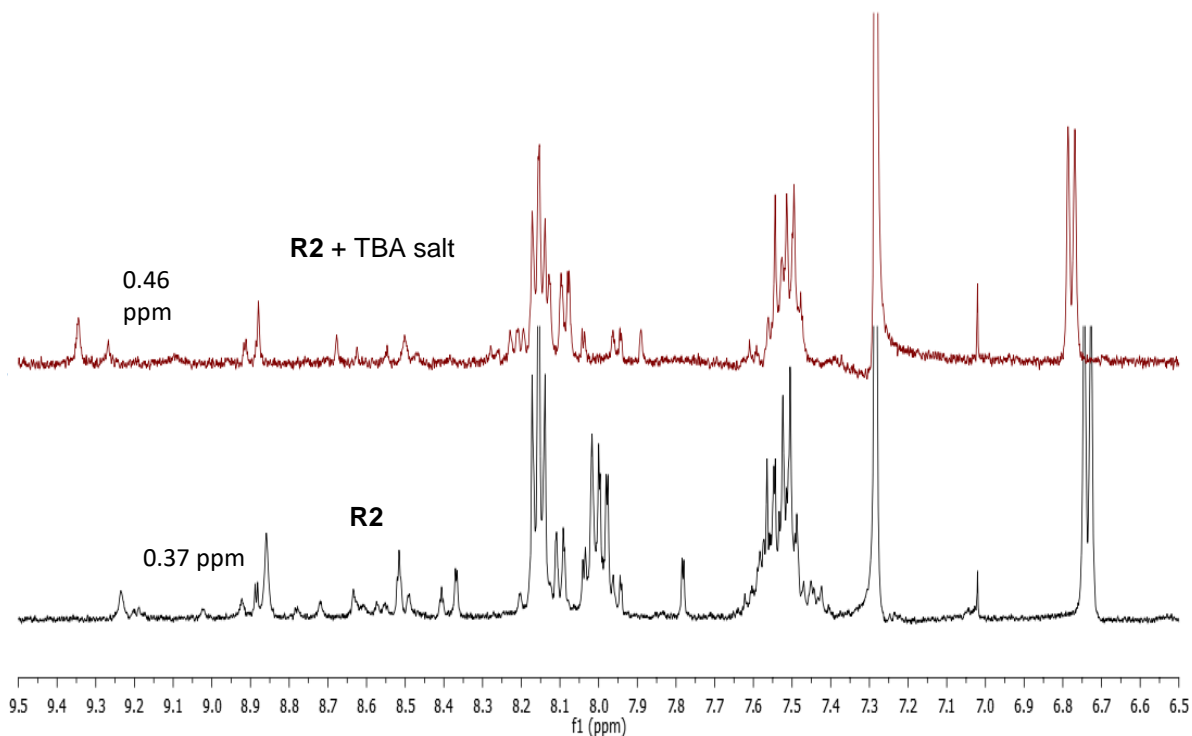


Figure 4.12: ^1H NMR spectra depicting the change in resonances of receptor **R2** when titrated against TBA salts at concentrations 20 mg/mL.

4.3.3. Co-micellization of receptor **R2** within micelles (Host formation)

After the successful synthesis and binding assessment of receptor **R2**, the next stage was preparation of the host complex by mixing receptor **R2** with diblocks mPEG-*b*-PCL **10** and **20** to form co-micelles in aqueous solution. Before doing this an experiment, the aggregation behaviour of receptor **R2** in water was examined for comparison. The intensity of the fluorescence peak at 502 nm was monitored with respect to the concentration of receptor **R2**, and the results showed that receptor **R2** followed the Beer-Lambert law, with no aggregation taking place at the concentrations used (Figure 4.13). The experiment was repeated in the presence of pyrene, following its I_3/I_1 ratio, over the concentration range covered by the CMC of diblock **10** (5 $\mu\text{g/mL}$) and diblock **20** (2 $\mu\text{g/mL}$), which did not change, confirming that receptor **R2** did not aggregate at the concentrations studied. Although receptor **R2** possess a hydrophobic head group (the binding

site), it is inherently less hydrophobic than the mPEG-*b*-PCL diblock, and thus less likely to self-assemble and form morphological structures in water at low concentrations.

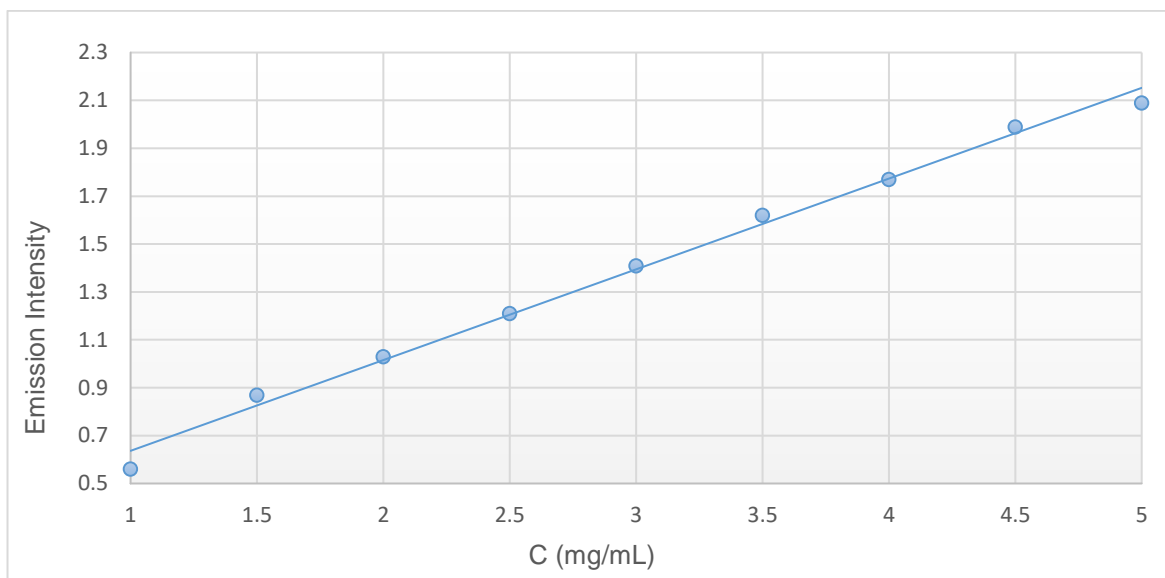


Figure 4.13: Plot of emission intensity versus concentration, confirming that receptor **R2** follows Beer-Lambert over a large concentration range and within the CMC range.

The binding site at the head of receptor **R2** is not soluble in water; thus, it orients itself so that the head is within the hydrophobic core and co-assembles with the diblock polymer. However, the co-micelle formed might self-assemble with a different CMC with respect to the diblock. Thus, the CMC was re-assessed using receptor **R2** and mPEG-*b*-PCL diblock at a mass ratio of 1:1 for a range of concentrations of **R2** and diblock **10** 1×10^{-6} to 1×10^{-3} mg/mL. The data obtained (Figure 4.14) indicated that co-micellisation then took place at a higher concentration than for the CMC of diblock **10** alone. Specifically, the CMC of the co-micelle was $\approx 50 \mu\text{g/mL}$ ($\pm 10 \mu\text{g/mL}$) as compared to a CMC at $5 \mu\text{g/mL}$ for diblock **10** alone.

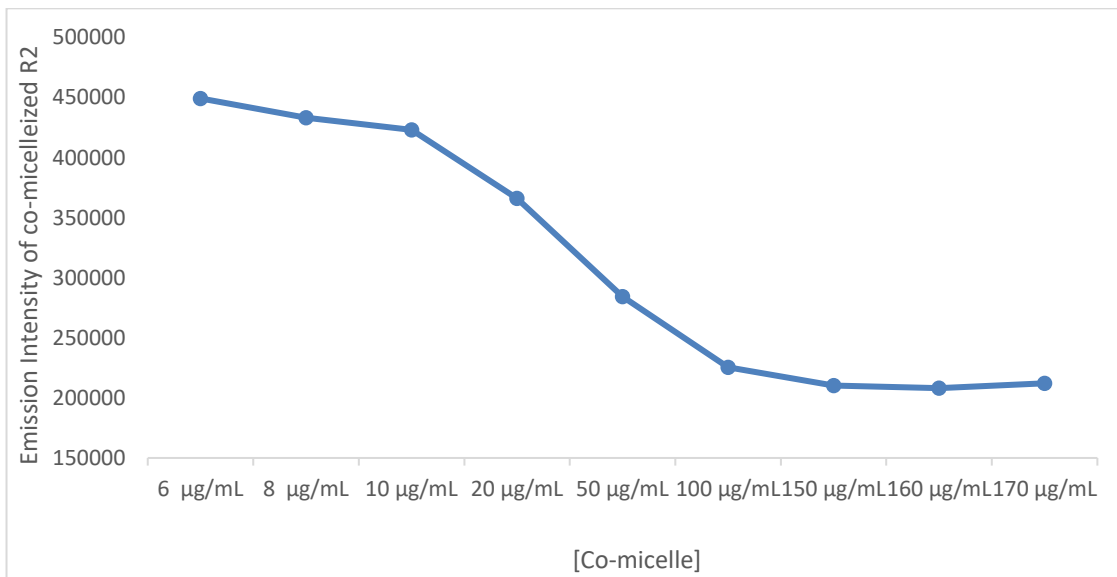


Figure 4.14: Characterisation of the CMC of co-micelles (**R2** and diblock 10) at different concentrations using a 1:1 ratio in water.

The next experiment was designed to study the co-micellisation of receptor **R2** with the diblock polymer. Co-micellisation was carried out using a mixture of **R2** and diblock **10** or **20**. The concentration of diblock used was 10 µg/mL for all measurements and the concentration of **R2** was also 10 µg/mL. In the absence of the diblock polymer, the intensity of the fluorescence peak from **R2** was low due to quenching from the solvent. This intensity increased in the presence of 10 µg/mL diblock, confirming that the **R2** molecules were in a new microenvironment (the co-micelle). Subsequently, experiments using a fixed concentration of 10 µg/mL of diblock and 10, 5, 2.5, or 1.25 µg/mL of **R2** were carried out, as shown in Figure 4.15. Interestingly, as the receptor concentration was diluted, the intensity initially increased. This was due to a reduction in self-quenching as the concentration of receptor **R2** within the micelle went down. This continued until a reduction in the intensity occurred due to simple dilution. These experiments confirmed that the receptor had been co-micellized with the diblock **10** micelle, as shown in Figure 4.16. The optimum concentration of receptor **R2** in 10 µg/mL mPEG-*b*-PCL₁₀ was 2.5-3.0 µg/mL.

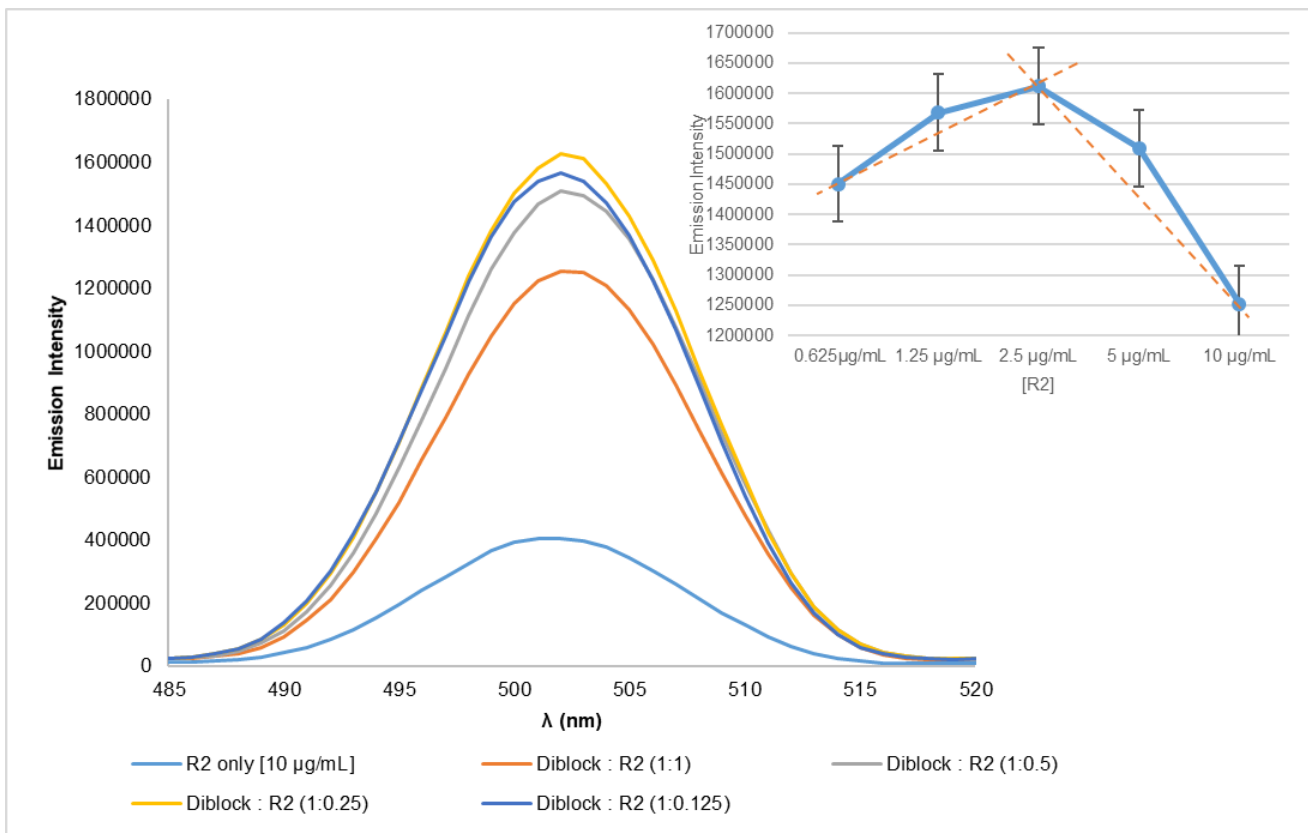


Figure 4.15: Emission intensity measurements versus different concentrations of mPEG-R (**R2**) [0.625 to 10 µg/mL] and constant concentration of mPEG-*b*-PCL₁₀ [10 µg/mL], exciting at 345 nm and emission recorded between 360-600 nm.

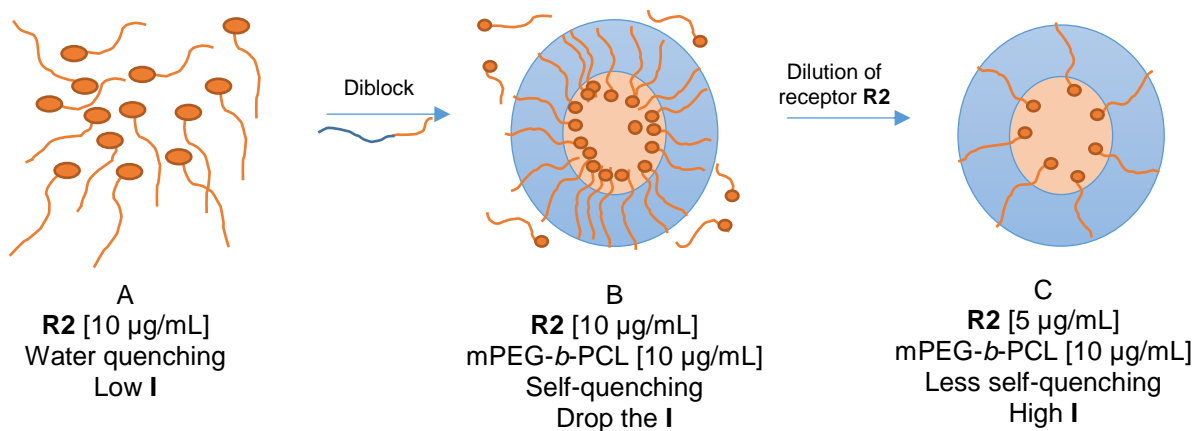


Figure 4.16: Co-micelle (host formation) stages; A) represent receptor **R2** molecules, B) and C) represent co-micelle at different concentrations of receptor **R2** and constant concentration of diblock (representative structures).

It is possible that the diameter of diblock copolymers could have an effect on the relative amount of receptor **R2** molecules that can be encapsulated. The hydrophobic diameter of diblock **10** is smaller than that of diblock **20**, and the receptor molecules within the diblock **10** micelle are thus closer together at the same ratio and may thus quench at lower ratios. The experiments were therefore repeated using receptor **R2** and diblock **20**; the results are shown in Figure 4.17.

On this occasion the expected behaviour was observed, such that the intensity was proportional to the concentration of receptor **R2**. Thus, at the highest concentration studied, there was no quenching. This confirms that diblock **20**, being bigger, can produce more space for the receptor.

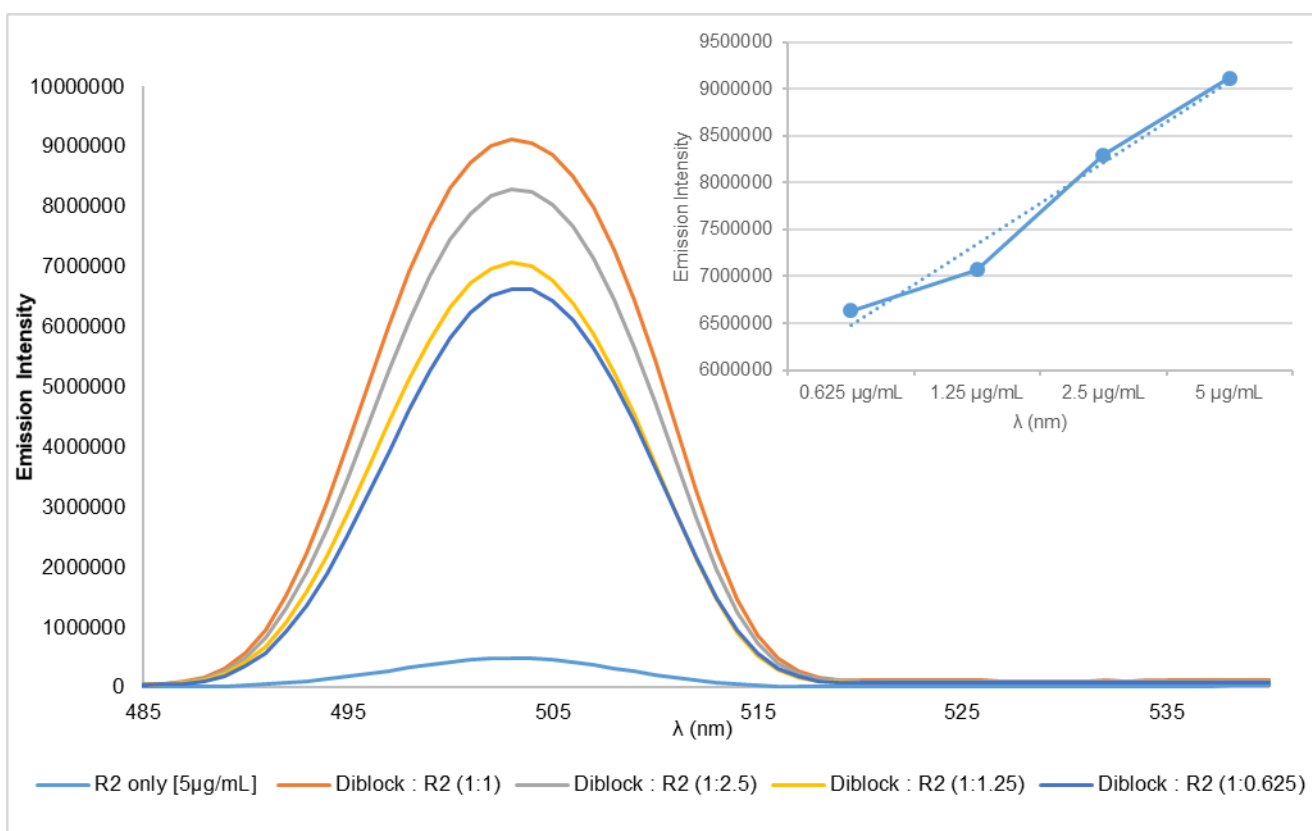
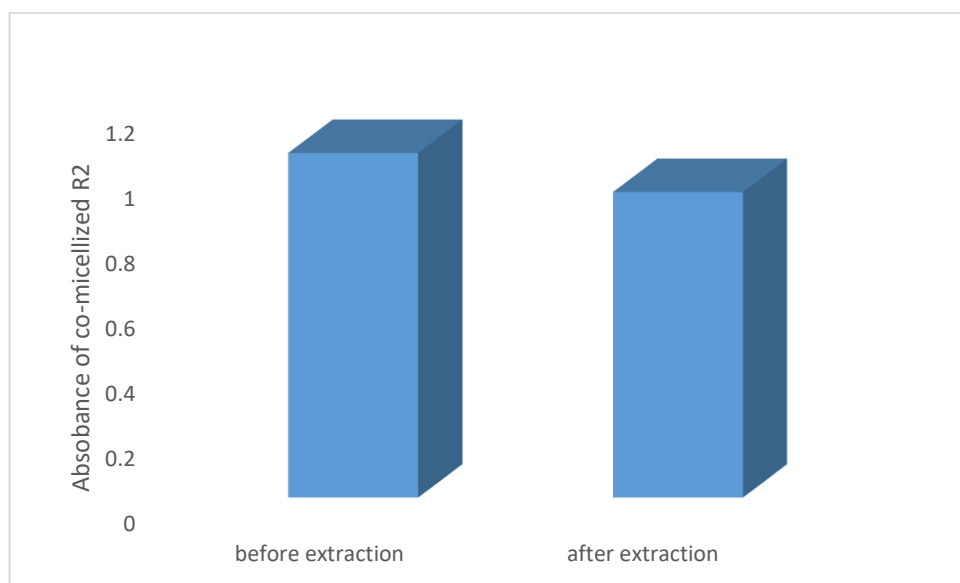


Figure 4.17: Emission intensity measurements versus different concentrations of receptor **R2** [0.625 to 5 μg/mL] and constant concentration of mPEG-*b*-PCL₂₀ [5 μg/mL].

4.3.4. Stability of co-micelle system during extraction

After co-micellisation of receptor **R2** was confirmed, the stability of the co-micelle in water under extraction condition was investigated. Initially, 2 mL of DCM was added to 2 mL of a solution of co-micelle **10** at concentration 1×10^{-3} M and shaken for 30 min. The aqueous layer was then collected and observed using UV-Vis spectroscopy. The results before and after extraction are shown in Graph 4.1. The data revealed that the co-micelle has a high stability in water and that the receptor could not be easily removed from the micelle, indicating that the PEG provides strong interactions with mPEG-*b*-PCL that help stabilise the co-micelle system.



Graph 4.1: Uv-Vis measurements of co-micellized **R2** highlighting co-micelle concentrations before and after extraction process.

4.3.5. Anion binding studies of the co-micelle host system

Anion binding was initially assessed using the hydrophobic anion PNP. The protonated and deprotonated forms of PNP have different λ_{\max} values, and spectrophotometric titration was used

to estimate the pKa of the PNP. The titration curve obtained allowed estimation of a pKa of 7.15 (± 0.15) (Figure 4.18).

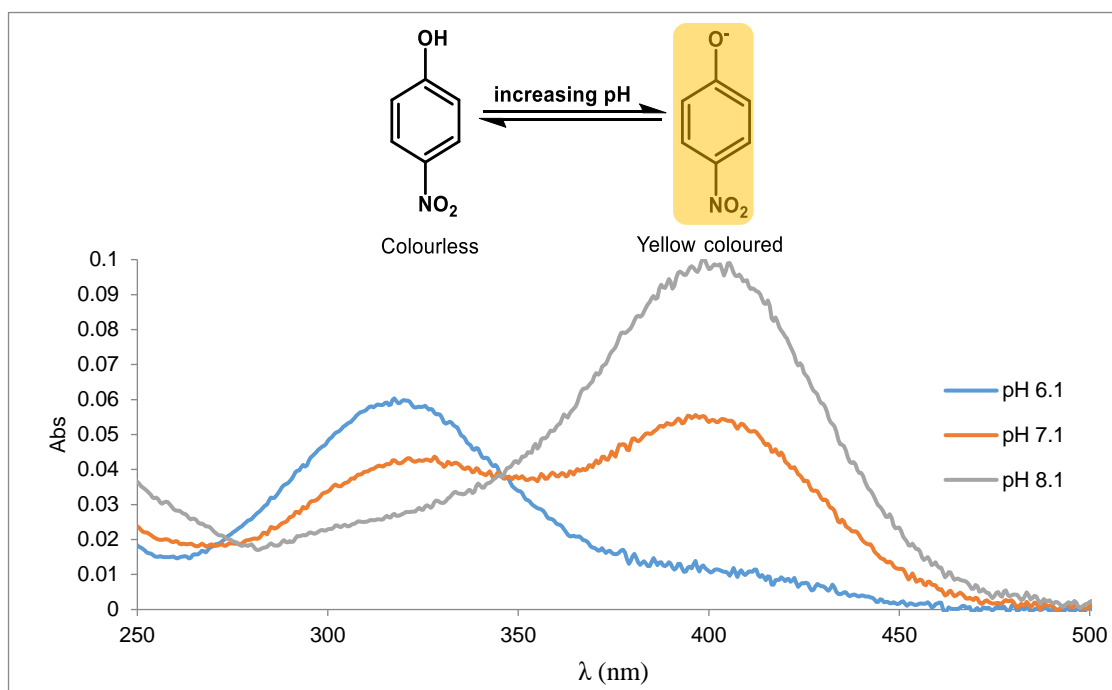
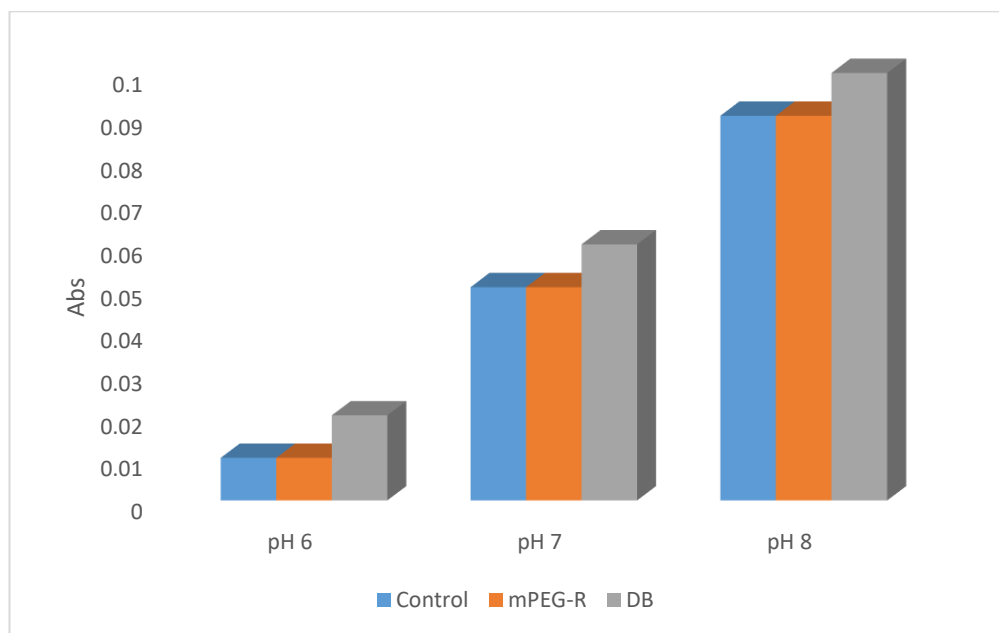


Figure 4.18: Spectrophotometric determination of the pKa of PNP.

The next stage was assessment of the phenolate binding at 0.01 mM with 10 mg/mL diblock 10 and 2.5 mg/mL receptor **R2**. Control experiments using just diblock (Homo diblock) and with no diblock or receptor were also carried out. It was predicted that adding the diblock polymer alone to a phenolate would not affect the absorbance, while adding **R2** to phenolate might reduce the colour intensity as a result of binding. On the other hand, using the co-micelle host system was predicted to reduce the absorbance the most, due to the hydrogen bonding interaction in combination with hydrophobic effects.

Initially, the homo co-micelle and receptor **R2** were studied separately as control systems. These experiments thus offered comparisons for whole host system, and the results are shown in Graph (4.2). For the homo micelle/diblock **10** (grey bar), the absorption was higher than for water alone

(blue bar) for all pH studied. This was not expected, and it suggests that the diblock increases deprotonation. However, when receptor **R2** (red bar) was used, there was no significant change with respect to water, confirming that the receptor **R2** alone does not bind. This was in contrast to expectations. The same results were obtained using diblock **20**.



Graph 4.2: Binding properties of receptor **R2** and homo-micelle (diblock **10**) as assessed using phenolate in buffer solution (control).

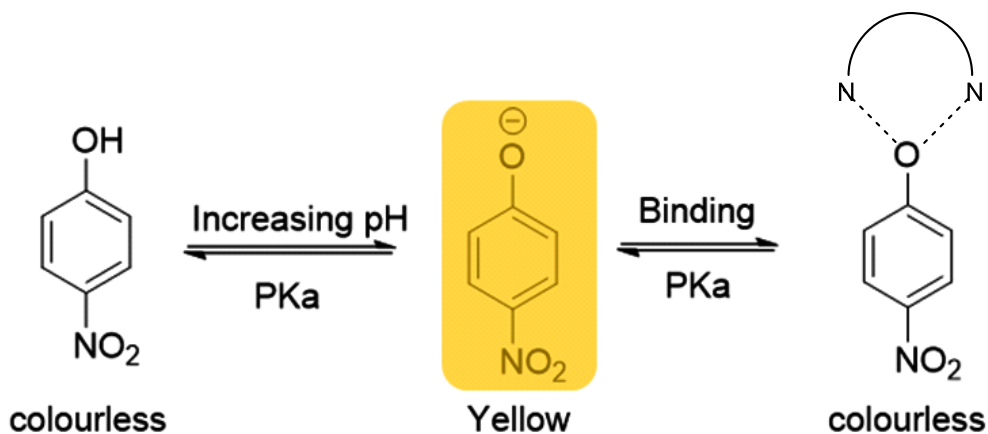
The next step involved forming the co-micelle using diblock **20**. It was expected that diblock **20** would enhance binding more compared to diblock **10**, due to its larger hydrophobic core.

Experiments were carried out using the co-micelles, and the data normalised for absorbance in water. The results are shown in Graph 4.3; these indicate that the co-micelles appear to decrease absorption, which is consistent with binding of phenolate. However, both polymers behaved similarly, this was due to identical concentrations of receptor **R2** being used for both systems.



Graph 4.3: Binding properties of co-micelles **10** and **20** as assessed in respect to homo-micelles using phenolate after subtracting the buffer (control).

The sheer multitude of equilibrium processes make it hard to explain the binding observed. Simple acid-base reactions as well as binding interactions may affect the protonation and deprotonation of phenolate in the bulk-solution differently to those inside the polymeric micelle (Scheme 4.8). However, more work needs to be done to discover the underlying mechanism of binding.



Scheme 4.8: Multi-equilibrium equations of protonation and deprotonation of PNP, both bulk-solution and local environment.

4.4 Conclusion

It was decided to tether an anion receptor with a water-soluble molecule and make it as part of the micellar system by co-micellisation. This is to reduce the probability of losing the receptor through the extraction process and to isolate the binding site from each other and so prevent dimerization of the receptor from taken place. For this purpose, we used mPEG₂₀₀₀ with amine spacer (mPEG-NH₂). Amide (**1**) and mPEG-R (**R2**) were successfully synthesised and its aggregation behaviour was examined. Co-micellisation of receptor **R2** and diblock polymer was monitored using fluorescence technique and the receptor itself as probe. The co-micelle system has a high stability in water and the receptor could not be easily removed from the micelle, indicating that the PEG provides strong interactions with mPEG-*b*-PCL that help stabilise the co-micelle system. The binding properties of the host complex was examined based on colour changing of 4-nitrophenolate solution and UV/Vis spectrometry was chosen to calculate the concentration of bonded anion.

The findings of this study was shown that creating the right microenvironment can help with binding hydrophobic anions in water. The system designed can thus be used for short extraction processes; however, the host system is not perfect for long extraction studies as some leaching remains. Thus, a new bulk method is required.

4.5 Experimental

4.5.1. Chemicals and Instrumentation

Solvents and reagents

All chemicals and reagents were obtained from commercial supplier (primarily Sigma-Aldrich) and were used without further purification unless otherwise stated.

Nuclear magnetic resonance spectroscopy (NMR)

All NMR samples were prepared using deuterated solvents supplied by Sigma Aldrich. ^1H NMR and ^{13}C NMR spectra were recorded using a Bruker AV1400 MHz machine. The NMR spectra were analysed using Topspin 3.2 NMR software. Shifts are quoted as ppm and couplings quoted in Hertz.

Fourier transform infrared spectroscopy (FTIR)

FTIR spectroscopy was performed in the solid state (in reflectance mode) using Perkin Elmer Spectrum RX FT-IR System in the range of 700 to 4000 cm^{-1} .

UV-Vis spectroscopy

The ultraviolet absorbance was recorded on an Analytik Jena AG Specord s600 UV/Vis Spectrometer and analyzed using its attached Software (WinASPECT).

Fluorescence Spectroscopy

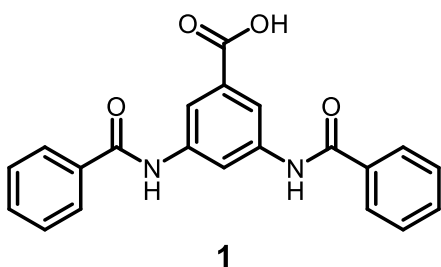
Fluorescence results were obtained using a HORIBA Scientific Fluoromax-4 spectrofluorometer using its attached software (FluorEssence V3).

Mass spectrometry

The form of ionisation used was dependent on the molecular weight of the sample in question. For samples with a low molecular weight, an Electrospray ionisation (ES) was used to record spectra. The instrument used was a WATERS LCT mass spectrometer. For samples with a high molecular weight, Matrix assisted laser desorption ionisation (MALDI) was required. The instrumentation used was a Bruker Reflex III MALDI-ToF mass spectrometer.

pH measurement

The pH of the buffer solutions prepared was substantiated using a pH 210 Microprocessor pH Meter from Hanna Instruments Ltd. (Leighton Buzzard, UK). The device was calibrated using pH 4.0 and pH 7.0 standard solutions, prepared with buffer tablets (Sigma-Aldrich, Poole, UK).



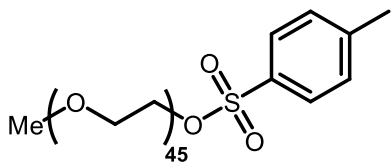
4.5.2 Synthesis of 3,5-bis(benzoylamino) benzoic acid (1)

At 0 °C benzoyl chloride (3.05 g, 58.6 mmol) was added to a solution of 3,5-diaminobenzoic acid (6.8 ml, 20 mmol) in N-methyl-2-pyrrolidone (40 mL) and was stirred for 3 hours.

The reaction mixture was poured into HCl/water (v/v = 1/20) to precipitate the product and then was collected by filtration. The precipitate was washed with methanol three times and dried to give 3.15 g as a greyish solid.

¹H NMR (DMSO-d₆, 400MHz) δ: 13.10 (br s, 1H), 10.52 (s, 2H), 8.65 (s, 1H), 8.16 (s, 2H), 8.01-7.94 (m, 4H), 7.64-7.49 (m, 6H). ¹³C NMR (DMSO-d₆, 400 MHz) δ: 116.3, 116.6, 127.7, 128.3, 130.2, 131.6, 134.5, 139.5, 165.6, and 167.1. FTIR (cm⁻¹): 1703 (s, C=O acid), 1666 (s, C=O amide). Mass spec: MH⁺ = 361, and m.p. = 293-296 °C.

4.5.3 Synthesis of methoxy polyethylene glycol tosylate (2)

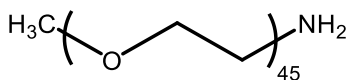


2

To a solution of mPEG₂₀₀₀ (12.5 g, 6.2 mmol) in THF (40 mL) was added a solution of 6M NaOH. After the mixture cooled to 0 °C, a tosyl chloride (25 g, 131 mmol) in THF (40 mL) was drop wise to the stirring mixture, then after one hour of stirring the reactor was warmed to ambient temperature, and was stirred another one hour. The resulting mixture was concentrated under vacuum. The residue was dissolved in acidic water and extracted with DCM in separation funnel. The organic layer was dried over anhydrous MgSO₄ and concentrated by the rotary evaporator to give tosylate as light yellow solid (14 g, 56%).

¹H NMR (CDCl₃, 400MHz) δ: 7.80-7.32- (d, 4H), 3.67 (s, 180H), 3.46 (s, 3H), 2.48 (s, 3H). ¹³C NMR (CDCl₃, 400 MHz) δ: 70.9, 116.6, 126.7, 128.3, 139.2, and 144.6. FTIR (cm⁻¹): 2876 (aliphatic CH₂, stretch), 1466, 1105 (C-O, asymmetrical stretch).

4.5.3.1 Synthesis of methoxypolyethylene glycol amine (3)

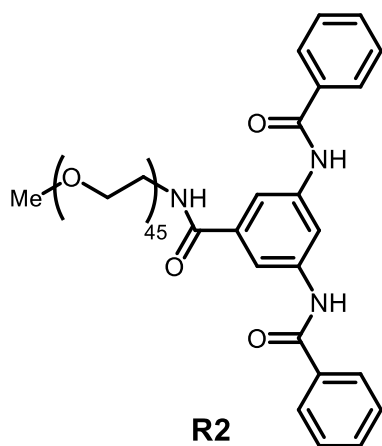


3

A 250 mL one-neck round-bottom flask was charged with mPEG-TS (5g, 2.23mmol) and ammonia solution (75%v/v). The reaction mixture was stirred at room temperature for 3 days. The resulting mixture was extracted with DCM to separate the ammonium toluene sulfonate salt from the aminated polymer, then the organic layer was washed with NaOH solution to produce the free amino polymer. The product was concentrated under vacuum and precipitated over petroleum ether then was stored in the freezer for a night. To this end, the product was decanted from the cold petroleum ether and dried to give light brown solid, yield 1.5g (32%).

¹H NMR (CDCl₃, 400 MHz) δ: 3.68 (s, 180 H), 3.37 (s, 3H), 3.14 (t, 3H). FTIR (cm⁻¹): 2877 (b, NH₂), 2153 (s, N-H), 1466 (C-O). Mass spec (MALDI): 2000.

4.5.3.2 Synthesis of mPEG-R (R2)



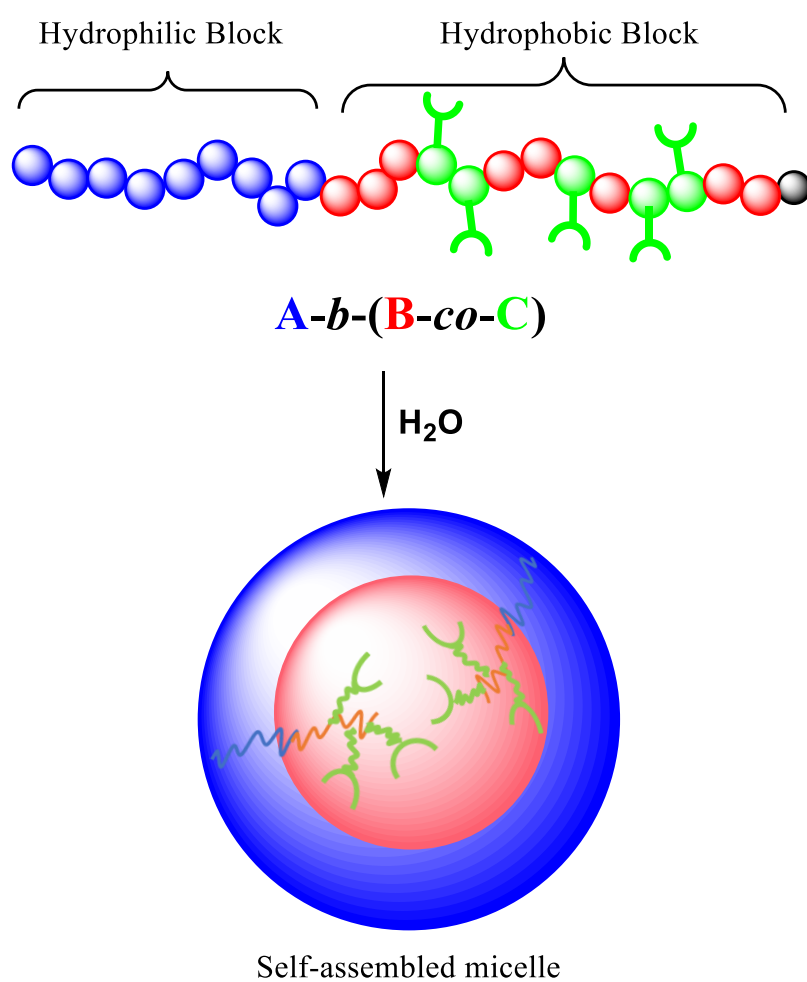
R2

A Schlenk flask equipped with a septum and a nitrogen inlet was charged with mPEG-NH₂ (2 g, 1 mmol), 3,5-bis(benzoylamino) benzoic acid **4** (0.364 g, 1 mmol), EDC (2 equiv) and DMAP (2 equiv) in 30 mL THF. A few drops of triethylamine was then added and the reaction mixture was stirred overnight. After the reaction, the solvent was evaporated under vacuum and the residual product dissolved in DCM, filtered out and the filtrate was then

precipitated in ether. The product was air dried to give 1.2 g as a light yellow solid.

¹H NMR (CDCl₃, 400 MHz) δ: 8.87 (s, 2H), 8.62 (s, 1H), 8.25 (s, 2H) 8.05 (m, 4H), 7.56(m, 6H), 3.67 (s, 178H), 3.39 (s, 3H), 3.14 (t, 2H). FTIR (cm⁻¹): 2854 (s, aliphatic C-H), 1630 (s, C=O amide), 1464 (C-O). Mass spec (MALDI): 2202.

Chapter Five: Synthesis of Amphiphilic Anion Sensors Using ATRP



5.1 Introduction

To prepare a high density of anion binding substances, covalently bonded to an amphiphilic polymer, a control polymerisation technique was used, as this offered further opportunities to prepare amphiphilic polymers for water based anion receptors in a controllable microenvironment and avoid the possibility of receptor leaching. In order to examine the anion binding and recognition, a displacement colourimetric method was used.

5.1.1. Anion sensors

Several anion sensors have been reported, almost all of which rely upon a functional moiety linked to the signal moiety (e.g. chromogene, electrochemical group, fluorescent group).^{153–158} Recent research has focused on the development of specific sensors with the capability to recognise particular anions or families of anions in a competitive media, such as water, which are commonly used in environmental, biological or medical applications.^{159–166} For practical applications, such sensors also need to satisfy strict photophysical criteria such as being able to absorb and emit at long wavelengths to facilitate the use of naked eye detection.¹⁶⁷ Such photoactive or redox sensors coordinate to anions and report their presence via changes in physical properties such as redox potential, fluorescence, or phosphorescence.^{168,169} In 1989, Beer reported the synthesis of the first redox-responsive anion receptors based on the cobaltocenium moiety (Figure 5.1).¹⁷⁰

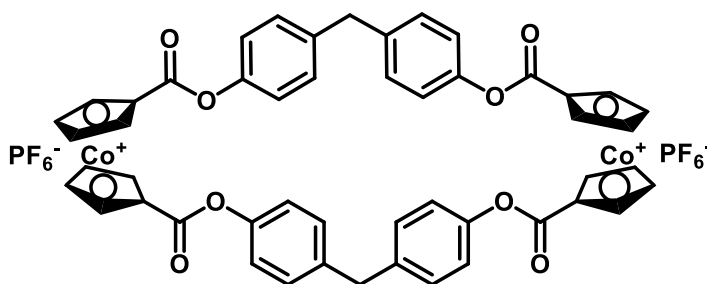
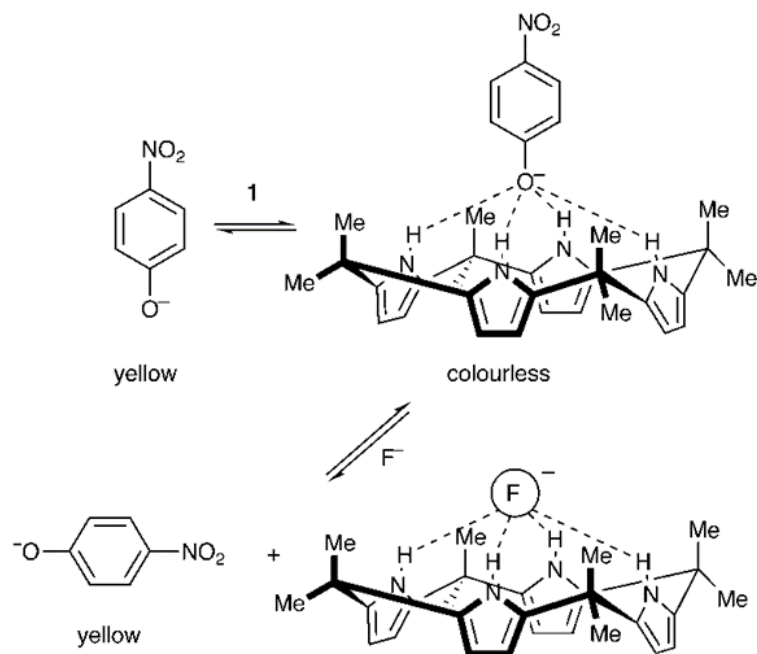


Figure 5.1: Anion sensor based cobaltocenium moiety.

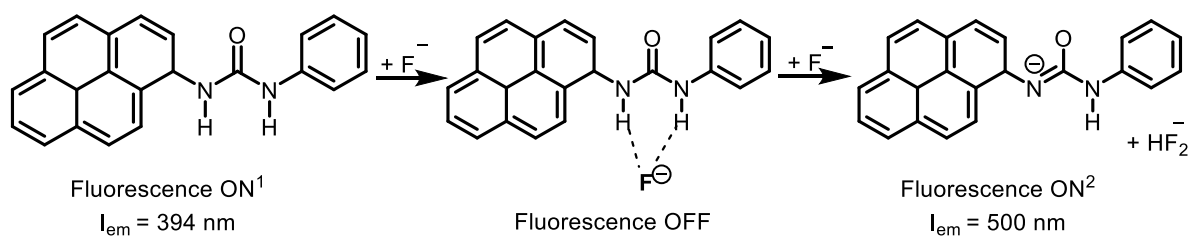
This ester-linked cobaltocenium macrocyclic receptor detected bromide guest anions in acetonitrile. However, poor solubility of these types of macrocyclic ligands coupled with the arduous synthesis process and lability to ester hydrolysis, led to research into new synthetic strategies.

Another approach to anion detection, pioneered by Anslyn et al., is the displacement assay, which requires the creation of a host–anion complex that dissociates in the presence of other anions, triggering a change in the properties of the system as a whole.¹⁷¹ Chemical systems that respond to the presence of anions by means of a colour change detectable by eye are extremely rare,¹⁷² yet colourimetric sensors do not require the use of a potentiostat or spectrometer to detect redox or optical perturbations and thus still have considerable advantages over other molecular sensors.¹⁷³ Formation of a calixpyrrole–anion complex with a coloured species such as 4-nitrophenolate anion (PNP) was investigated by Twyman et al. Their work showed that calixpyrrole (Scheme 5.1) could be used to produce anion sensors that could report the presence of anions by means of a colour change.¹⁷⁴ The addition of anions to solutions of calixpyrrole-PNP complex causes the yellow colour of 4-nitrophenolate anions to return as these are displaced from the calix[4]pyrrole anion binding site, supporting the displacement approach.



Scheme 5.1: Calixpyrrole–PNP complex and calixpyrrole–F complex structures using displacement approach.¹⁷⁴

Amendola et al.¹⁷⁵ reported that a urea derivative (Scheme 5.2) offered a fluorometric response from binding to different anions in CH₃CN and DMSO. Interestingly, this urea derivative exhibits a three-mode ON¹-OFF-ON² response to fluoride in CH₃CN, which corresponds to fluorescence quenching when the urea compound forms a hydrogen-bond complex with fluoride, followed by emission of a yellow fluorescence once the complex is deprotonated by an excess of fluoride.



Scheme 5.2: Hydrogen-bonding and proton-transfer interactions between urea derivative and fluoride anion.

5.1.2. Polymer based anion receptors

Polymers have been poorly researched, despite their benefits for detection purposes, including multivalent effects, microdomain development, solubility and physical property adjustment, and processability for material development. The discovery of binding as the cause of NMR line widening of the ^{127}I signal in water when polymers were present, was the basis of anion-polyolefin interaction (Figure 1.5).¹⁷⁶ For the PVP polymer, a correlation was established between binding strength and the Hofmeister series, with particularly robust interaction between more chaotropic anions.¹⁷⁷

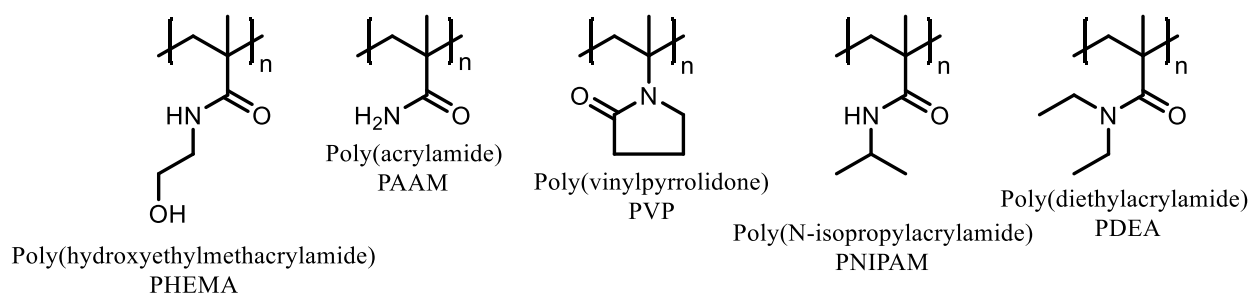


Figure 1.5: Polyolefins used in aqueous anion recognition.

In the past decade, new research on the PNIPAM polymer with lower critical solution temperature (LCST) (i.e. soluble in water only to a particular temperature) revealed that kosmotropic anions reduced the transition temperature, which was proportional to the hydration entropy.¹⁷⁸ By contrast, the transition temperature was increased by anions with poorer hydration ($\text{ClO}_4^- > \text{SCN}^- > \text{Br}^- > \text{NO}_3^-$), which salted in the polymer at diminished concentration. These anions salted out at high concentration due to heightened surface tension. Concentration/LCST curve examination indicated that the enhanced solubility was due to an element of direct anion binding and believed to be achieved via the amide group as a donor of hydrogen bonds. The LCST polymer PDEA with a tertiary amide (i.e. no obvious anion-binding location) was employed for in-depth analysis of the

salting-in structural foundation.¹⁷⁹ Interaction between identical chaotropic anions and the α -CH proton on the polymer backbone was revealed by joint NMR and IR spectroscopic investigations. Surprising as it may initially appear, this agrees with α -CH peptide proton participation in anion binding (e.g. C $^{\alpha}$ NN motif in Section 1.3, Chapter One).

For sensing purposes, the photophysical properties of conjugated system have been exploited, mainly by triggering desolvation, as the basis of polymer use for detection of anions in water.¹⁸⁰ For instance, pyrophosphate sensing via a detection-triggered aggregation mechanism yielding a ratiometric fluorescent reaction was achieved by adding cationic primary ammonium side chains to poly(phenylene-ethynylene) (Figure 1.6a).¹⁸¹ By contrast, when iodide and sulfonate-based surfactants are present, poly(thiophene) supplemented with pendant quaternary ammonium groups (Figure 1.6b) disintegrates in water, altering colour from red to yellow and reducing sensitivity to nanomolar level.¹⁸² Furthermore, tertiary ammonium groups on the thiophene block were used for functionalisation of poly(fluorene- β -thiophene) (Figure 1.6c), with halides in water ($\text{Cl}^- > \text{Br}^- > \text{I}^-$) quenching the fluorescence of that portion, without aggregation state alteration.¹⁸³ Measurement of sub-micromolar DNA concentrations was facilitated by the use of unchanging poly(fluorene) block fluorescence.

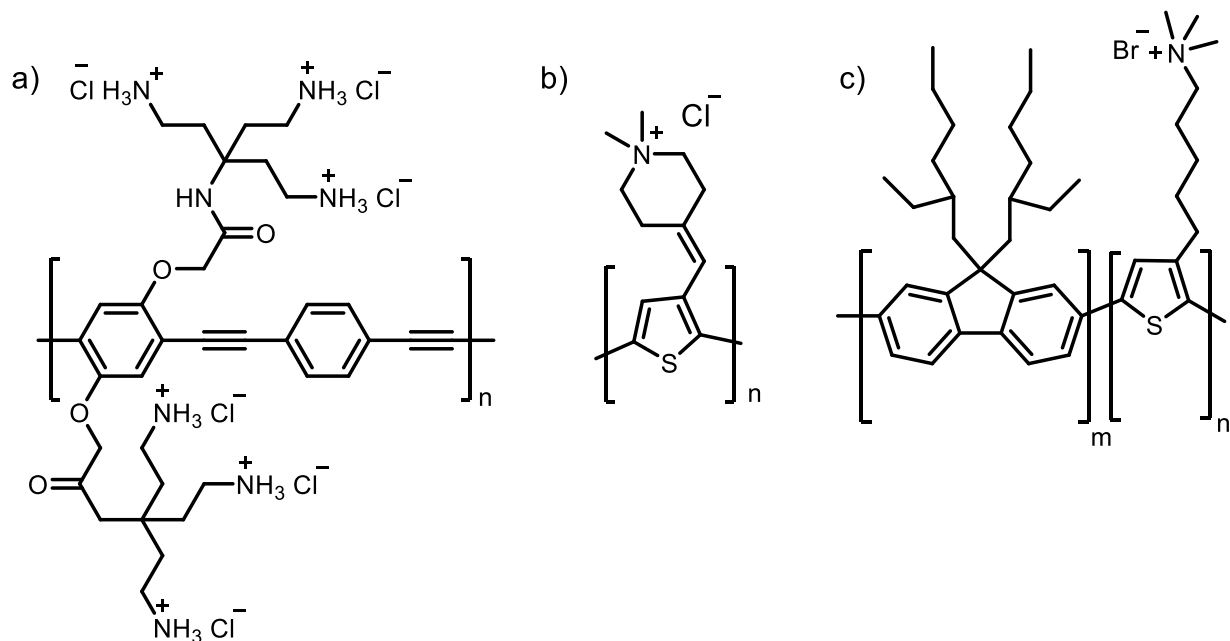


Figure 1.6: Polymers used in aqueous anion recognition. a) Ammonium-appended poly(phenyleneethynylene). b) Ammonium-appended polythiophene. c) Ammonium-appended poly(fluorene-*b*-thiophene).

The need for receptors within an aqueous media prompted a search for a polymerisation method that allowed formation of well-defined amphiphilic polymers that could be used as water-soluble anion sensors.

5.1.3 Controlled polymerisation

For the work described in this chapter, we proposed to use a polymeric micelle. In order to control the assembly of the micelle, we must control the synthesis of the polymers. If we do not do this, then broad polydispersities will occur, which leads to polydisperse aggregations.

The synthesis of polymers with well-defined compositions, architectures, and functionalities has long been a major concern of polymer chemistry. Using conventional radical polymerisation for the synthesis of amphiphilic copolymers may produce undefined structures with high polydispersity and large quantities of homopolymers.¹⁸⁴ Much of the current academic and

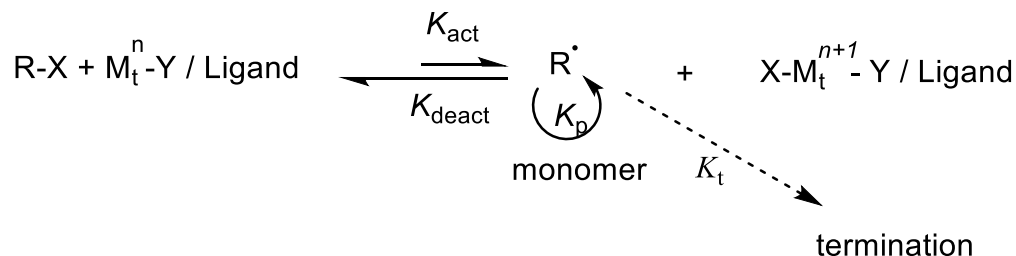
industrial research thus focuses on the development and understanding of new, more controlled polymerisation methods.¹⁸⁵ Generally, controlled polymerisation methods are based on establishing a rapid dynamic equilibration between a minute quantity of growing free radicals and a large majority of the dormant species. The dormant chains may be alkyl halides, as in atom transfer radical polymerisation (ATRP); thioesters, as in reversible addition fragmentation chain transfer processes (RAFT); or alkoxyamines, as in nitroxide mediated polymerisation (NMP).¹⁸⁶

This work focuses on utilising transition metal catalysed atom transfer radical polymerisation (ATRP). This method has many advantages over conventional living polymerisation, including the versatility of monomer types, tolerance of functional groups, and mild reaction conditions.^{187–189} This polymerisation technique has thus been found useful in the synthesis of well-defined structure polymers with low polydispersity.^{190,191}

ATRP is a multicomponent system consisting of a selected monomer, an initiator with a transferable halogen, and a metal catalyst (Scheme 5.4). Other factors such as solvent, ligand and temperature must also be considered for successful ATRP, however. Several typical monomers, such as styrenes, acrylates, acrylamides, and acrylonitrile, have been effectively polymerised using ATRP.¹⁹² Alkyl halides (RX) are typically used as the initiator in ATRP, and in terms of the concentration of RX, the rate of polymerisation is first order, and best control over molecular weight is found where the X is either bromine or chlorine.¹⁸⁶ The catalyst is possibly the most significant factor in ATRP, as it determines the equilibrium between the dormant and active species.

Scheme 5.4 illustrates the general mechanism for ATRP. The active species (radicals) are generated through a reversible redox process catalysed by a transition metal complex (the M_t^n -Y/Ligand,

where Y may be either another ligand or the counterion), which itself undergoes a one electron oxidation with concomitant abstraction of a pseudo-halogen atom (X) from the dormant species (R-X).



Scheme 5.4: Transition Metal-Catalysed ATRP.¹⁸⁶

This process occurs at a constant rate of activation (k_{act}) and deactivation (k_{deact}). The polymer chains grow in a comparable way to that seen in conventional radical polymerisation, based on the addition of the intermediate radicals to monomers at a constant rate of propagation k_p . In a well-controlled ATRP, no more than a few percent of the polymer chains undergo termination (k_t), which occurs mainly through radical coupling and disproportionation. However, other side reactions can restrict the molecular weights achieved.

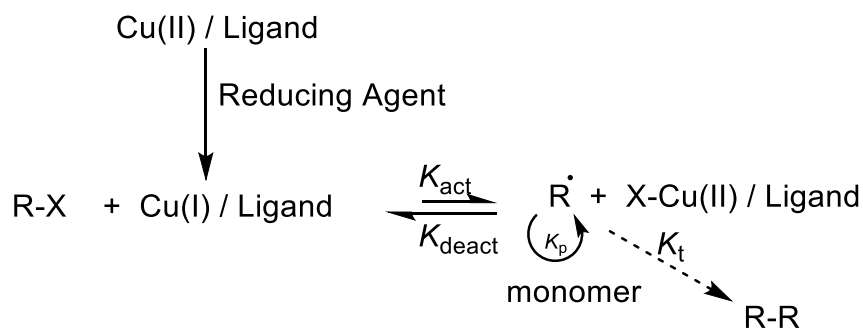
The oxygen sensitivity of ATRP is the biggest factor in terms of quenching the polymerisation. The use of an oxidatively stable catalyst in ATRP overcomes this air-sensitivity problem, which is associated with lower oxidation state metals. Thus, a reducing agent is added to reduce the catalyst system and keep the polymerisation going without losing control over the polymerisation.

5.1.4. AGET ATRP

Activators that can be generated by electron transfer (AGET) or activators regenerated by electron transfer (ARGET) have recently been reported as potential new initiation processes for ATRP.¹⁹³⁻

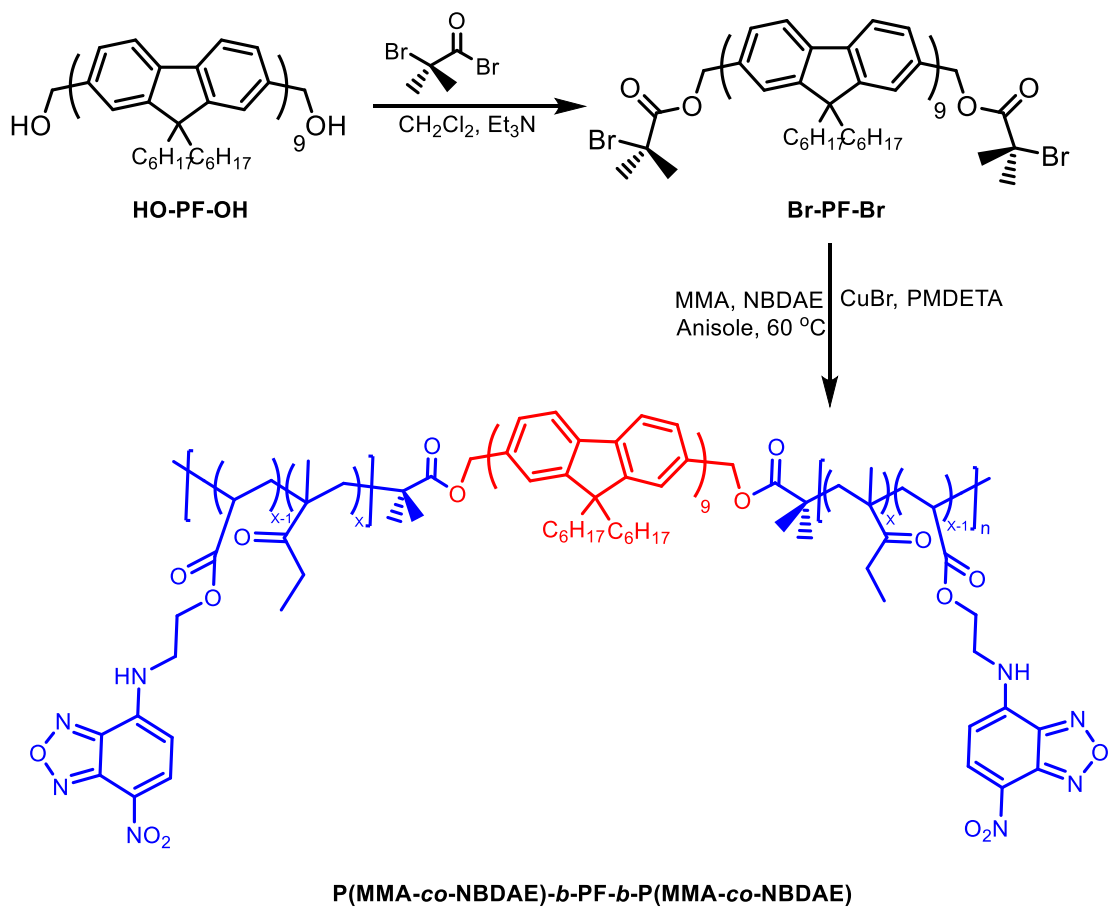
¹⁹⁵ These methods allow ATRP processes to be conducted with significantly lower concentrations

of catalyst (10 ppm or less) in the presence of excess reducing agents such as ascorbic acid, tin(II) 2-ethylhexanoate, or glucose. In one example of an AGET ATRP, the excess Cu(II) deactivator (formed in the termination reaction) was continuously regenerated to its original active Cu(I) state by the addition of an excess of reducing agent (Scheme 5.5).¹⁹⁶ It has also been demonstrated that the small amount of copper catalyst required not only leads to an environmentally benign polymerisation process but also drastically suppresses side-reactions between the chain end and the catalyst, enabling improved chain-end functionality and high molecular-weight polymers with low polydispersity.¹⁹⁷ Moreover, AGET ATRP of 2-(dimethylamino)ethyl methacrylate (DMAEMA) can be successfully carried out without the addition of external reducing agents as DMAEMA serves as both the monomer and internal reducing agent due to its tertiary amine group.¹⁸⁶



Scheme 5.5. Proposed mechanism of AGET ATRP.¹⁸⁶

ATRP was used to synthesise a coil-rod-coil triblock copolymer of P(MMA-*co*-NBDAE)-*b*-PF-*b*-P- (MMA-*co*-NBDAE, where MMA, NBDAE, and PF refer to methyl methacrylate, 4-(2-acryloyloxyethylamino)- 7-nitro-2,1,3-benzoxadiazole, and polyfluorene, respectively. These polymeric micelles serve as optical fluoride sensors, offering visual detection capability in several effective solvents such as THF and acetone (Scheme 5.3).¹⁹⁸



Scheme 5.3: Synthesis of triblock copolymer based fluoride sensor using ATRP technique.

5.2 Aim and Objectives

The main aim of this study is to produce anion sensors that report by means of colour change. To this end, 4-nitrophenol (PNP), a yellow water-soluble molecule when deprotonated that becomes colourless and organic soluble when protonated or bound to a receptor, is used. This colour change offers a practicable indicator for use as a colourimetric sensor, and the intensity of the colour can also be used to measure how strongly the anion (A^-) binds to the PNP-receptor complex by using a displacement approach. Colourimetric sensors are, after all, simply host-anion complexes that dissociate in the presence of other anions, triggering changes in the physical properties of the system.¹⁷¹

This chapter examines the preparation of a host-anion complex using phenolate anions bound to isophthalamide-based receptors incorporated within water soluble macromolecules to produce discrete molecular hosts capable of reporting anion binding through colour changes. It also investigates whether the local environment around the binding site provided by the macromolecule may disturb any anion binding properties, allowing further measurement of change in colour intensity to act as an indicator of binding affinity. A schematic representation of this is shown in Figure 5.2, where the phenolate anion is displaced by another anion with a stronger binding affinity, resulting in a return to a yellow colour visible to the naked eye.

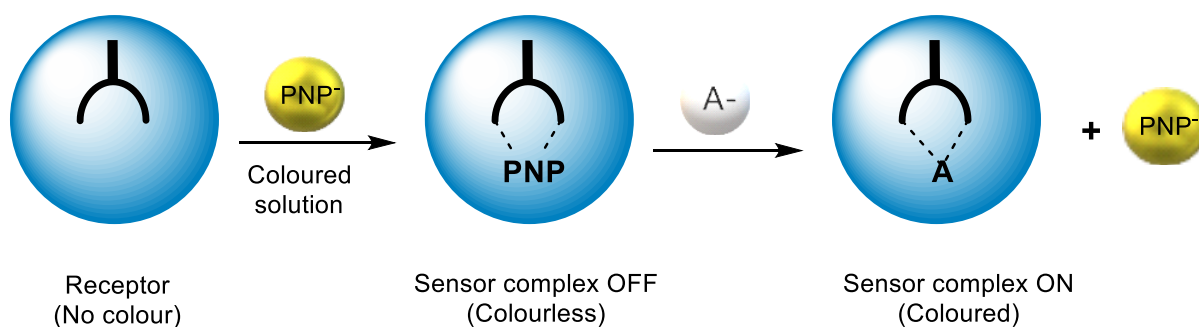


Figure 5.2: Hydrogen-bonding interactions between indicator complex based anion sensor; the A^- (anion) will eliminate the phenolate anion (PNP) from the binding site if it binds more strongly (schematic illustration).

For this purpose, an amphiphilic polymer involving a hydrophilic part (block A) and a hydrophobic part (block B-co-C) copolymerised with anion binding sites and hydrophobic units (Figure 5.3) is proposed.

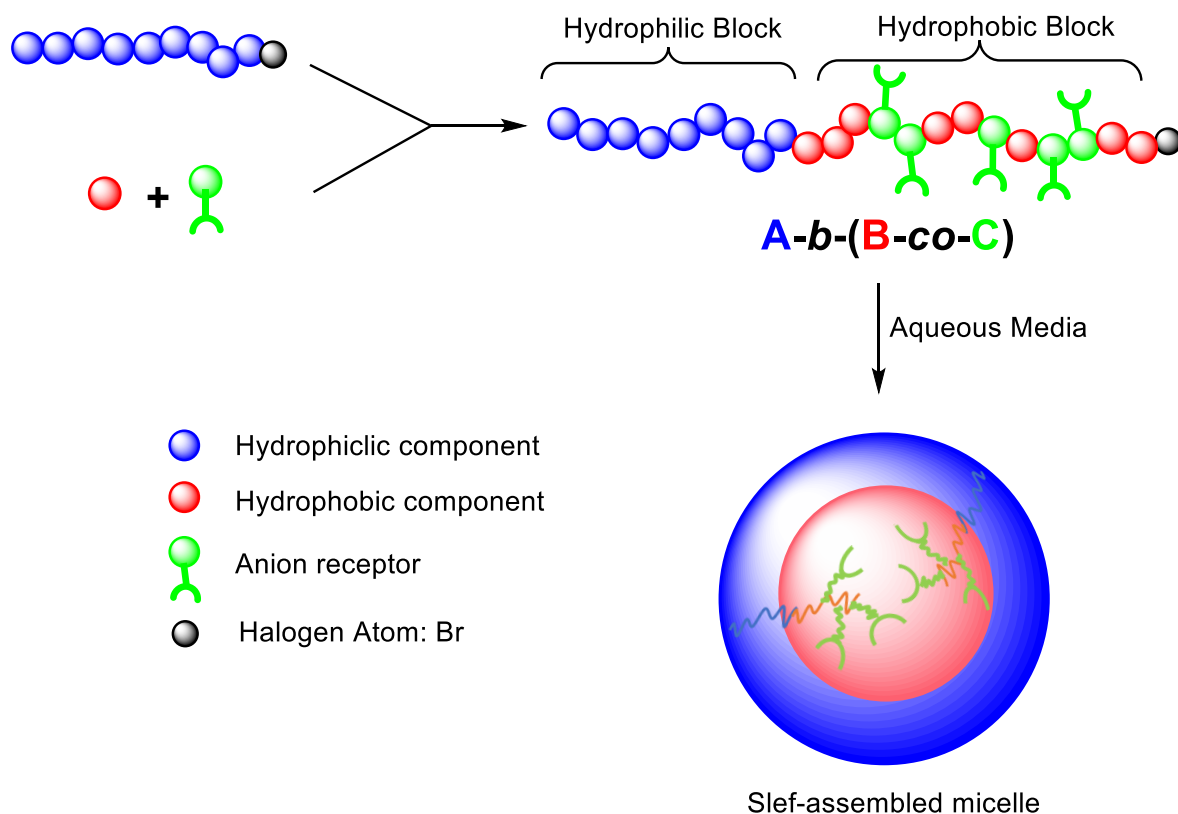
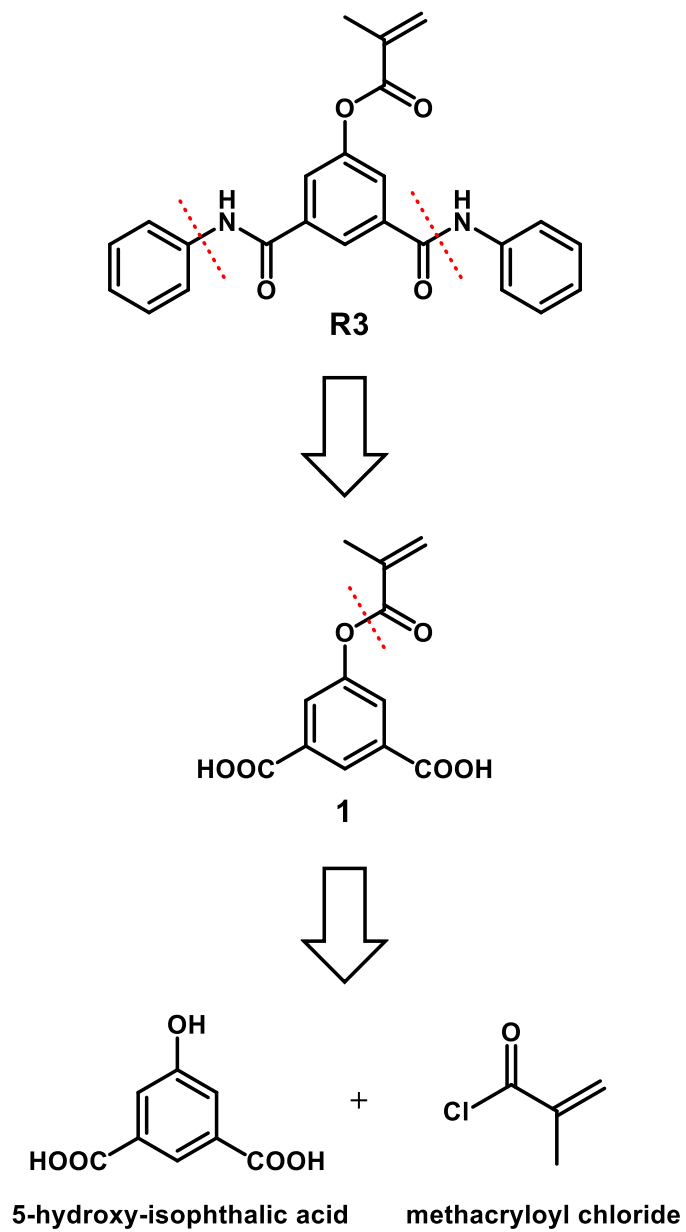


Figure 5.3: Macromolecular topology of mPEG-*b*-P(MMA-co-Rec) (Schematic representation).

The design of the anion binding monomer requires a polymerisable group such as the methacryloyl group, and an isophthalamide based receptor. This monomer can be polymerised with MMA in the presence of a mPEG macroinitiator. From the retrosynthetic perspective, the simplest route to the desired product, **10**, is the synthesis of 5-acryloyloxy isophthalic acid **9**, which is made by the acetylation of 3,5-diacetoxy phenol (Scheme 5.8).



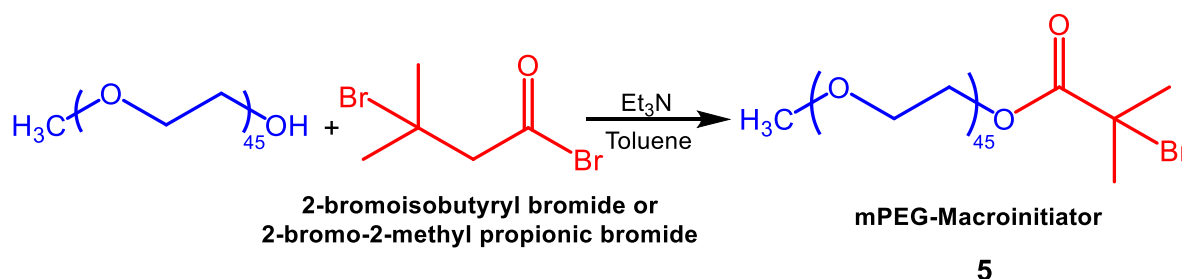
Scheme 5.6: Retrosynthetic route to the target molecule, changing 5-methacryloyloxy-N,N'-diphenyl isophthalamide into the corresponding synthons.

5.3 Results and Discussion

5.3.1 Synthesis of mPEG macroinitiator

PEG has a broad range of applications and is often seen in covalent attachments to other materials.¹⁹⁹ Several mPEG-based graft copolymers have been synthesised by employing methoxy polyethyleneglycol with 2-bromo- or 2-chloro-2-methylpropionate as the macroinitiator.^{200,201}

A preparation of mPEG-macroinitiator **5** was done following Dehgani,²⁰² reacting mPEG₂₀₀₀ with 2-bromoisobutyryl bromide and triethyl amine in anhydrous toluene. The product was obtained in a 60% yield after purification (Scheme 5.7).



Scheme 5.7: Synthesis of mPEG macroinitiator using triethyl amine as a catalyst.

The ¹HNMR spectrum in CDCl₃ showed that the reaction was successful, with a new signal, corresponding to the six protons of the two methyl groups becoming visible at 1.95 ppm. In addition, a peak at 3.64, corresponding to the 178 methylene protons of PEG, and another at 3.39 ppm, corresponding to the three protons of the methoxy in mPEG, also appeared (Figure 5.4). A carbonyl peak at 1741 cm⁻¹ was observed in the IR spectrum, indicating the formation of the α-bromocarbonyl ester. GPC indicated that the Mn was around 2000, comparable to the starting material, thus confirming the absence of polymer degradation. The mass spectrum results were similar to those from the mPEG, except that peaks were further separated by two mass units, due to the isotope of bromine, as seen in Figure 5.5.

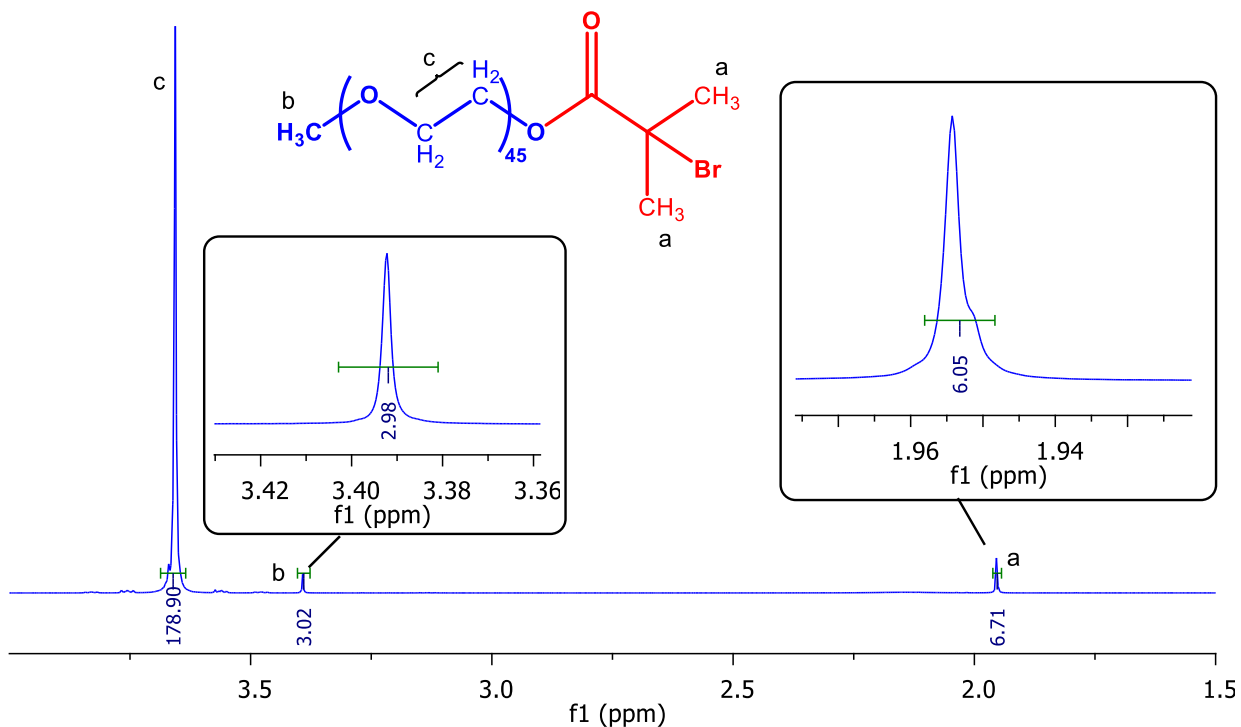


Figure 5.4: The ^1H NMR spectrum of the mPEG-macroinitiator using CDCl_3 .

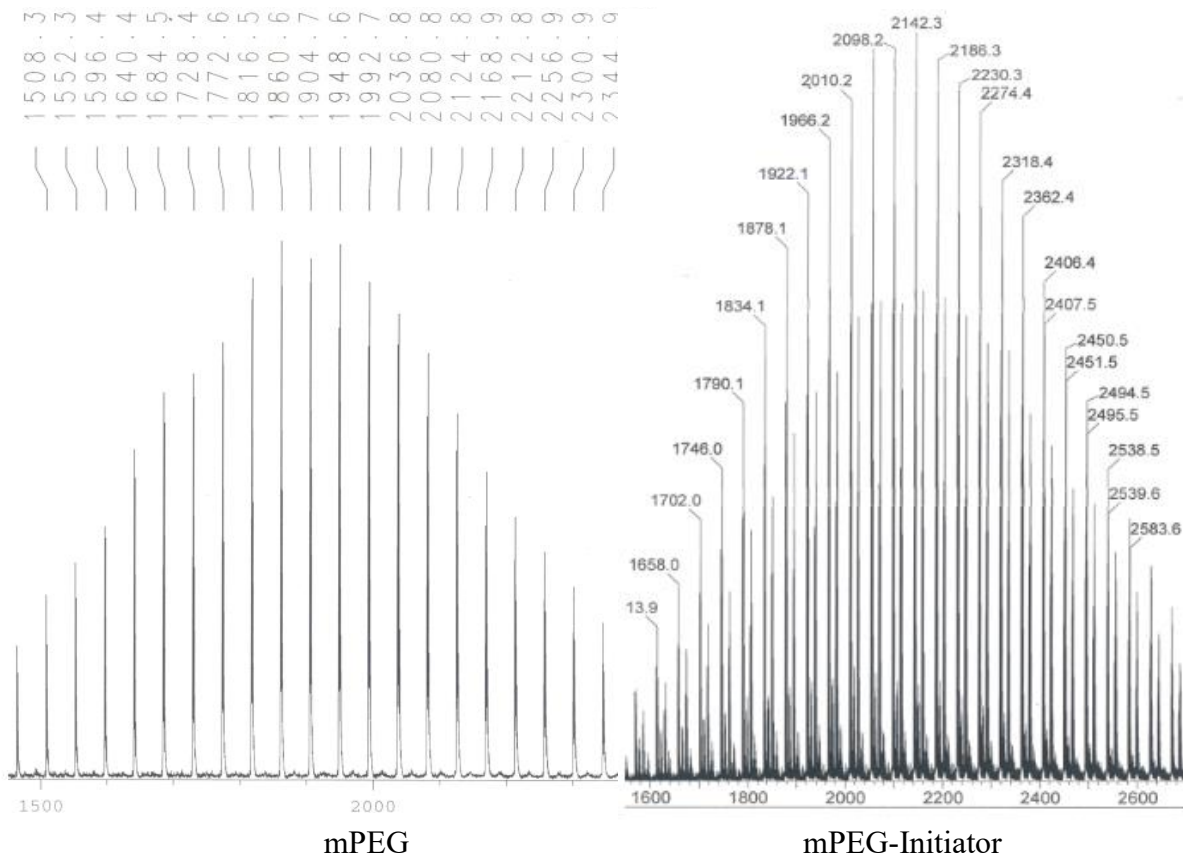
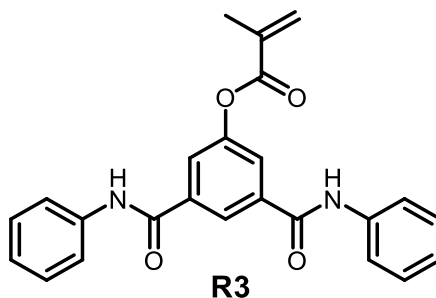


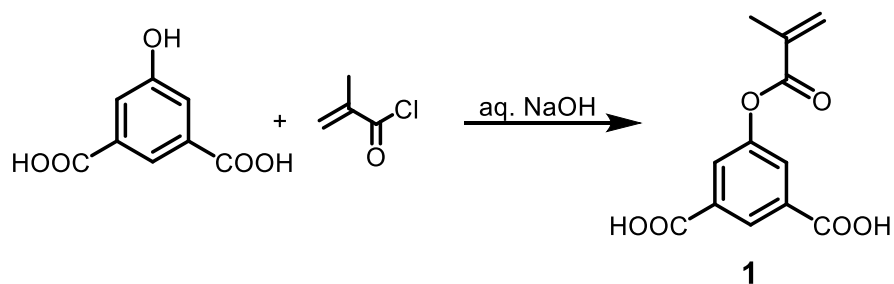
Figure 5.5: Mass spectrum of mPEG (left) and mPEG macroinitiator (right).

5.3.2 Synthesis of acryloyloxy-based isophthalamide monomers

As mentioned in the aims section of this chapter, acryloyl-based isophthalamide **R3** was chosen as the anion receptor, as it contains a suitable anion binding site and a polymerizable group.



The first step of the synthetic route was the synthesis of 5-methacryloyloxy-isophthalic acid **1** by means of the acylation/acrylation reaction of 5-hydroxy isophthalic acid. The acylation was carried out in mixture of water and ether in the presence of alkali (Schotten-Baumann conditions), 5-hydroxy-isophthalic acid was reacted with methacryloyl chloride in diethyl ether and NaOH. After the reaction, the organic phase was separated, and the crude product precipitated out of the aqueous phase by adding diluted HCl. A white solid product **1** was obtained in a very good yield of 87% after filtration and washing with water (Scheme 5.8).



Scheme 5.8: Synthesis of 5-methacryloyloxy isophthalic acid

Examining the ^1H NMR spectrum in DMSO-d_6 showed that the acrylation process was successful, as the $-\text{OH}$ signal, present at 10.28 ppm in the spectrum for the starting material, was no longer visible, while a singlet at 2.02 ppm, corresponding to three protons of the methyl group, and singlets at 6.33 and 5.91 ppm corresponding to the two protons of the methylene group, were visible. Peaks corresponding to the COOH protons were observed at 13.52 ppm as one broad singlet, with an integral of two protons. A singlet also appeared at 8.36 ppm, corresponding to one aromatic proton (H_a), with another at 7.97 ppm corresponding to the two remaining aromatic protons (H_b) (Figure 5.6). A peak at 18.8 ppm in the ^{13}C NMR spectrum corresponded to the carbon of the methyl group, and the carbon of the carbonyl group was seen at 167.5. The mass spectrum showed a signal for MH^+ at 251, and the product had a melting point of 254 to 256 $^\circ\text{C}$. These data together indicated that the 5-methacryloyloxy-isophthalic acid was pure enough to carry out the next stage of synthesis.

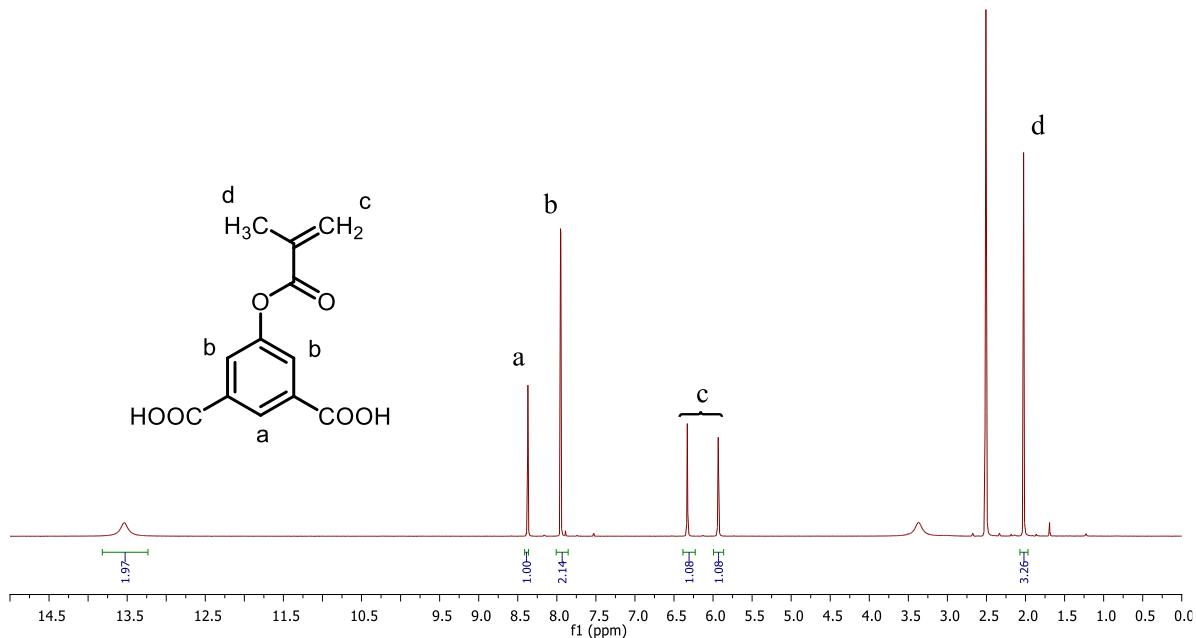
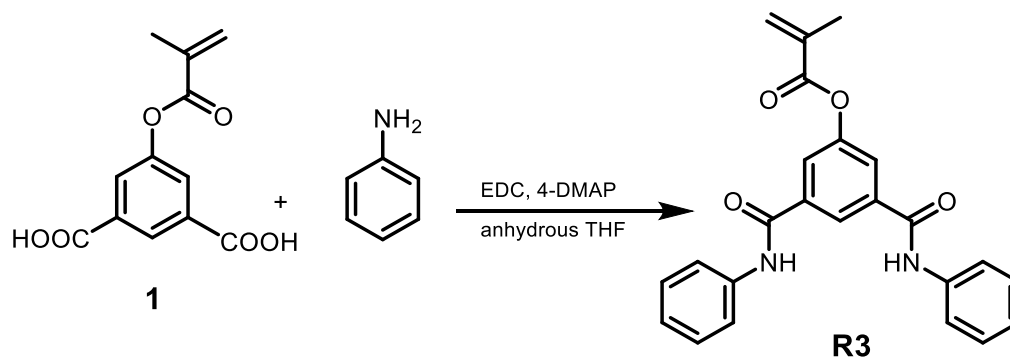


Figure 5.6: ^1H NMR spectrum for 5-acryloyloxy isophthalic acid.

The next stage of the synthetic procedure was the formation of the isophthalamide utilising the amide coupling reaction (Scheme 5.9), described by Azrah Abdul Aziz was followed.²⁰³



Scheme 5.9: Synthesis of 5-acryloyloxy-1,3-diphenyl isophthalamide

Freshly distilled aniline and 4-DMAP were dissolved in anhydrous THF, and a THF solution of 5-methacryloyloxy-isophthalic acid and EDC added. After work up, the resulting product was purified by flash chromatography to give a white solid with an 80% yield.

The ¹HNMR spectrum in DMSO-d₆ showed that the coupling reaction was successful, with the –COOH signal, present in the spectrum for **1**, being no longer visible at 13.10 ppm. A singlet at 10.50 ppm, corresponding to the two new amide protons, became visible, while a doublet peak at 7.80 ppm and two triplets at 7.40 and 7.13, corresponding to the 10 aromatic protons of the two new phenyl groups, were also visible (Figure 5.7). The mass spectrum had a signal for MH⁺ at 401.

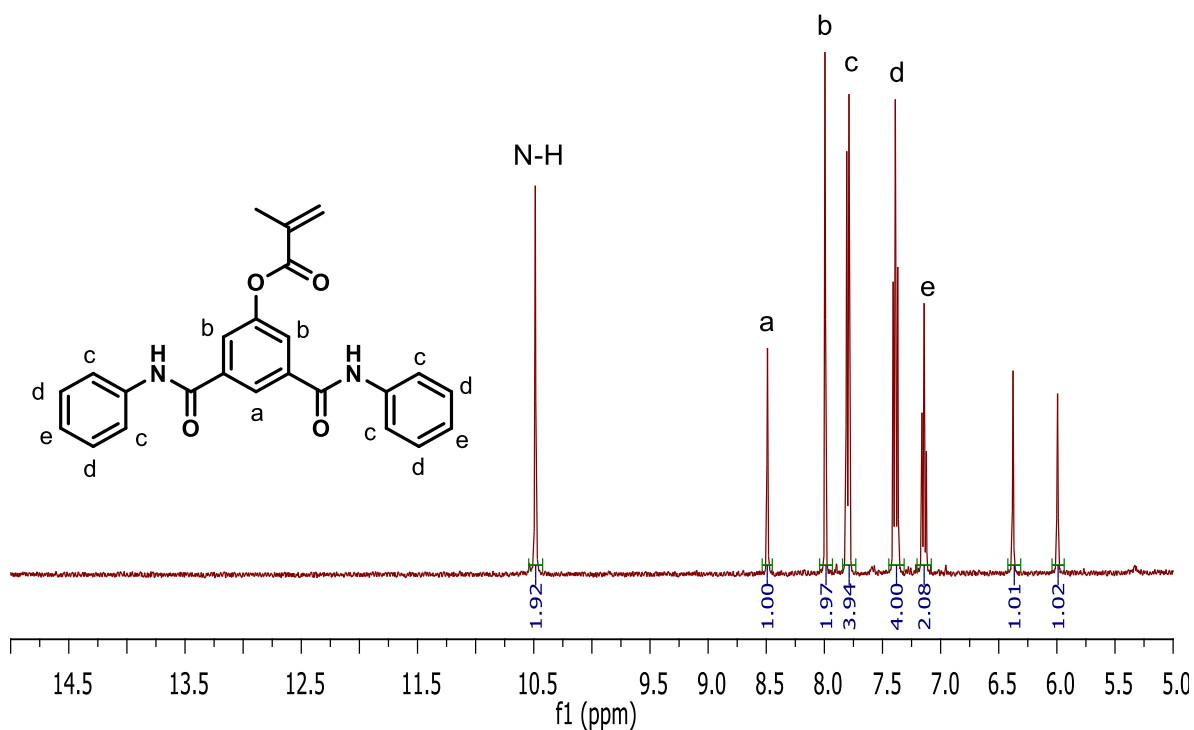
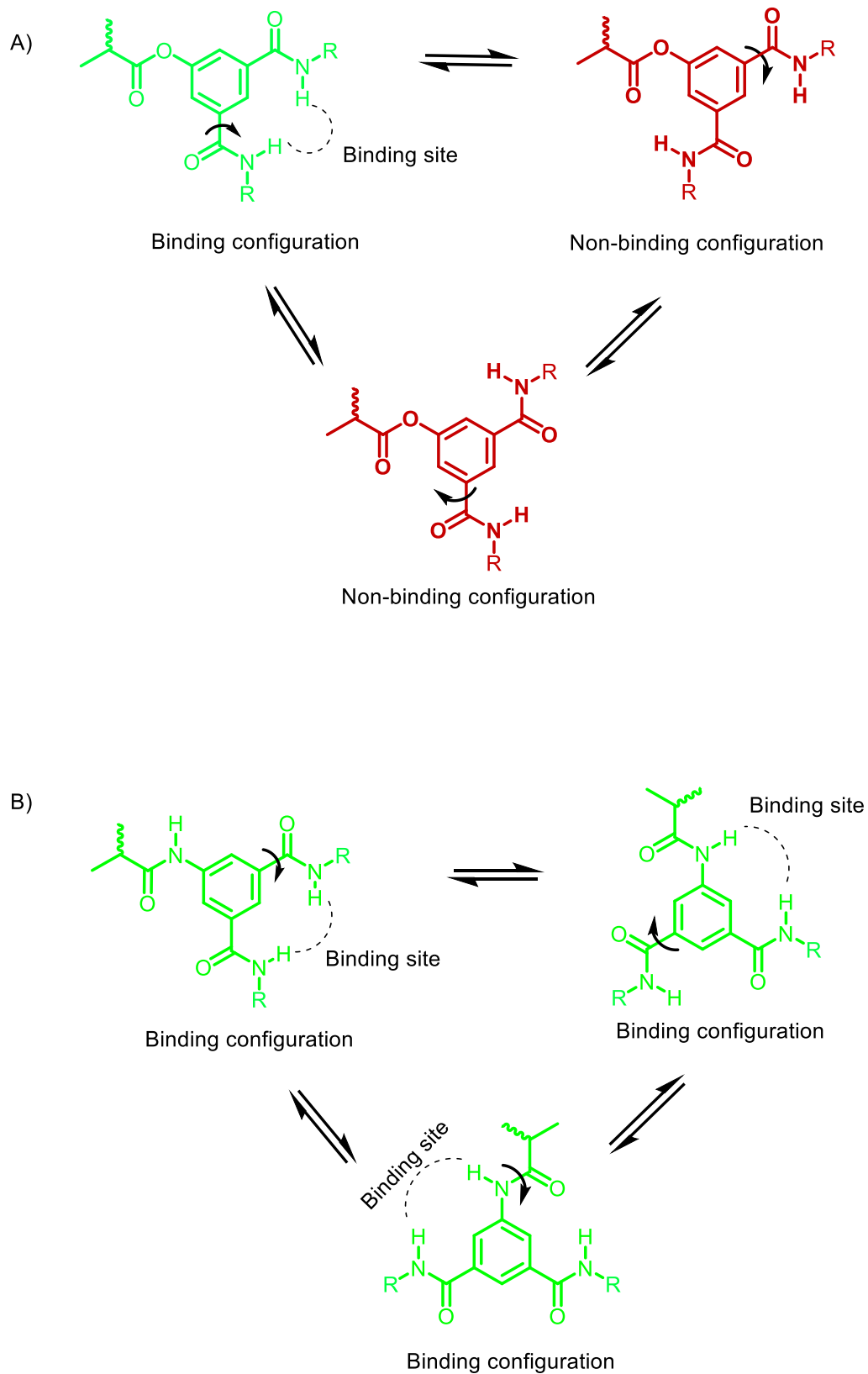


Figure 5.7: ¹H NMR spectrum using DMSO-d₆ for 5-acryloyloxy-N,N'-diphenyl isophthalamide receptor (**10**).

Isophthalamide receptor **R3** was only soluble in DMSO, which is a coordinating solvent. Unfortunately, this competes for H-bonding and thus prevents NMR binding studies. This lack of solubility was due to the aromatic molecules stacking together in π - π face-to-face. This was addressed by replacing the aromatic amine with an alkyl amine to reduce π stacking and improve solubility.

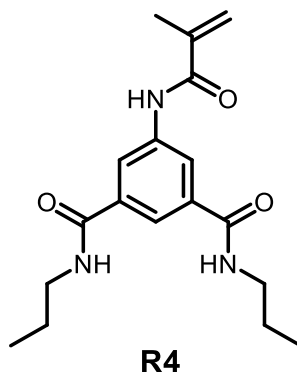
At this stage, the opportunity to modify the receptor, so that binding was maximised was also taken. For receptor **R3**, the ester linkage cannot become involved in binding, due to amide rotamers there is only one conformation that has the correct geometry to bind anions (Scheme 5.10A). However, replacing the ester with an amide allows all three conformations to provide suitable binding sites, as seen in Scheme 5.10B.



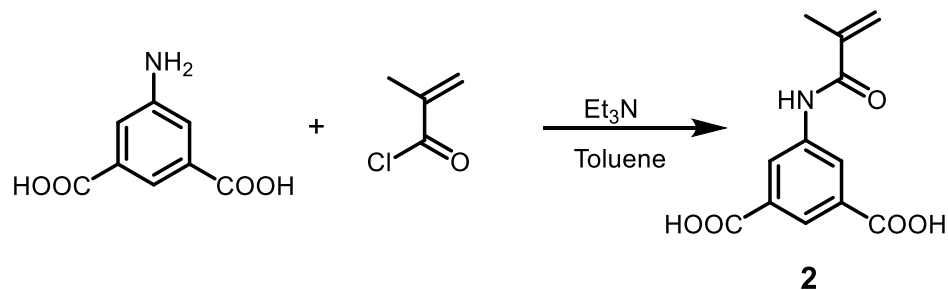
Scheme 5.10: A) Binding and non-binding configurations of ester-linkage receptor. B) Binding and non-binding configurations of amide-linkage receptor.

5.3.3 Acylation of 5-amino isophthalic acid with methacryloyl chloride

Isophthalamide **R4** was therefore selected as the target monomer, as this has more amides suitable for anion binding possess alkyl-solubilizing group. This was obtained by acylating 5-amino isophthalic acid to give amide **2**.



A solution of 5-amino-isophthalic acid and triethylamine in toluene, was reacted with methacryloyl chloride. After work up and purification, product **2** was obtained in an 80% yield (Scheme 5.11).



Scheme 5.11: Acylation reaction of 5-amino isophthalic acid with methacryloyl chloride in nonpolar organic solvent using triethylamine as a catalyst to produce 5-methacrylamide isophthalic acid (**2**).

The ^1H NMR spectrum of **2** showed that the NH_2 signal was no longer visible at 5.62 ppm. A new peak, visible at 10.80 ppm, was assigned to the N-H. This was no longer visible when CD_3OD used as the NMR solvent. A singlet at 1.98 ppm, corresponding to the three methyl protons, and two singlets at 5.79 and 5.45 ppm, corresponding to the two protons of the methylene group, were also observed in the spectrum. The peaks corresponding to the OH protons were observed as a broad singlet, with an integral of two protons at 13.10 ppm, though this was again no longer visible when CD_3OD was used as the NMR solvent (Figure 5.8). The mass spectrum showed an MH^+ at 250. 5-

methacrylamide isophthalic acid was deemed to be sufficiently pure to be carried forward to the next stage of synthesis.

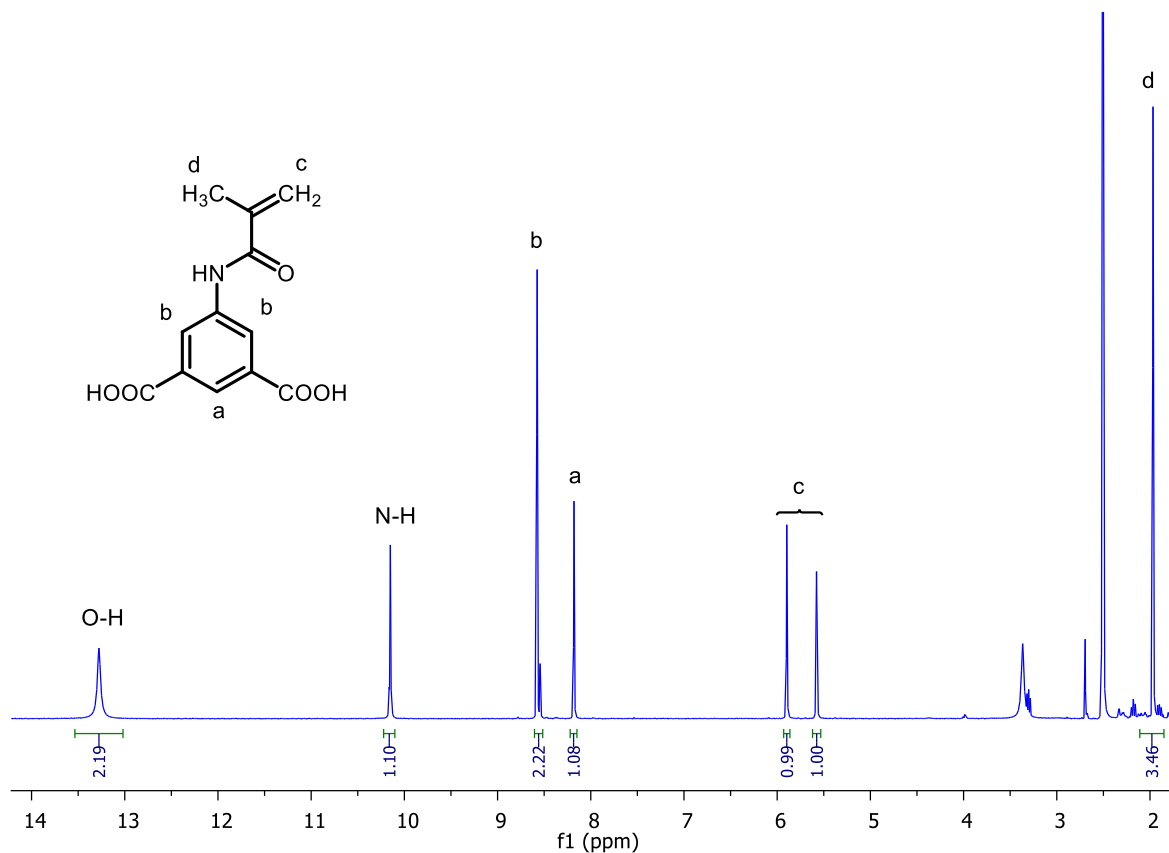


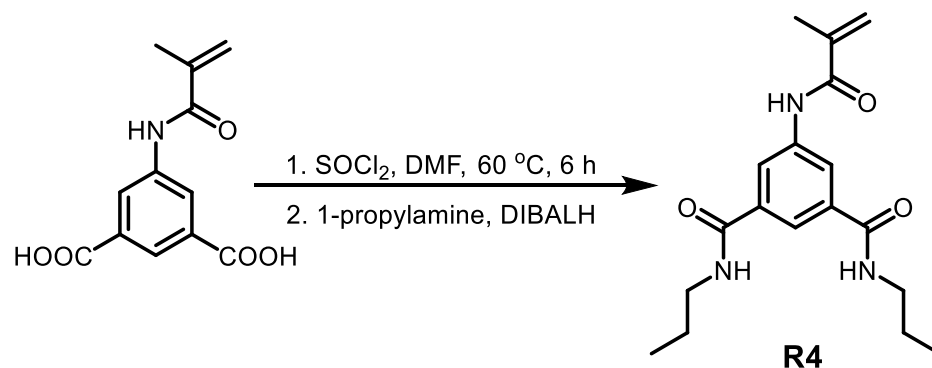
Figure 5.8: ¹H NMR spectrum of 5-methacrylamide isophthalic acid (**2**) in DMSO-d₆.

5.3.4 Synthesis of 5-methacrylamide-N,N'-dipropyl isophthalamide or N-(3,5-dipropylamine isophthaloyl)-2-methylprop-2-enamide (**R4**)

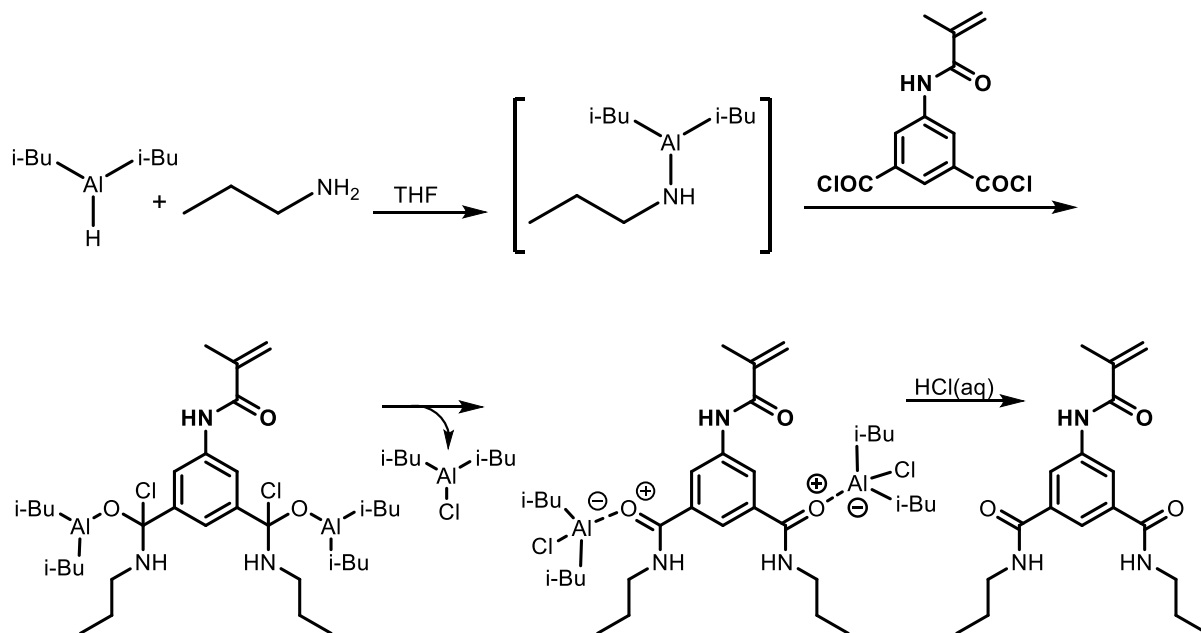
The first attempt to synthesise compound **R4** followed the previously determined amide coupling procedure outlined in section 3.2. However, this reaction was unsuccessful. A second attempt was made using the diacid chloride of **2** followed by reaction with amine. The isophthalic acid **2** was reacted with freshly distilled thionyl chloride in DMF, and the organic solvent and excess thionyl chloride were evaporated, with the resulting residue dissolved in a solution of chloroform and pyridine. Propylamine (2 eq.) was then added and the mixture stirred at 0 °C for five hours. The solvent was then removed, and the residue washed with distilled water to remove any unreacted

amine hydrochloride. The product was recrystallized from ethyl acetate, yielding isophthalamide **R4** as a white solid in 21% yield.

To improve the yield, it was decided to synthesise the amide using acid chloride and diisobutyl(amino)aluminium (DIBALH), as described by Park.²⁰⁴ DIBALH (1.1 M in hexane) was added dropwise to a solution of 1-propylamine and the mixture stirred for three hours at 0 °C. The 5-acrylamide-isophthalic chloride in DMF was then added slowly to the reaction mixture, and stirred for a further 10 minutes. The reaction was quenched with HCl and the product extracted using diethyl ether. The crude product was obtained by removing the ether, and purification using flash column chromatography to give isophthalamide **R4** as a white solid in a yield of 91% (Scheme 5.12). The mechanism suggested by Park²²⁴ is shown in Scheme 5.13.



Scheme 5.12: Synthesis of amide **R4** in two steps: forming diacid chloride, followed by amide formation using DIBALH.



Scheme 5.13: Steps involved in using DIBALH for amide formation.

The ^1H NMR spectrum showed that isophthalamide had been obtained, as the $-\text{COOH}$ signal present at 13.10 ppm was no longer visible, while a singlet at 8.49 ppm, corresponding to the two amide protons, was visible. Furthermore, a singlet at 10.47, corresponding to the N-H directly connected to the aromatic ring, two triplets at 3.23 ppm and 0.97 ppm, and a multiplet at 1.54 ppm, corresponding to the 14 protons of the two propyl chains (Figure 5.9). The mass spectrum showed a signal for the MH^+ at 332.

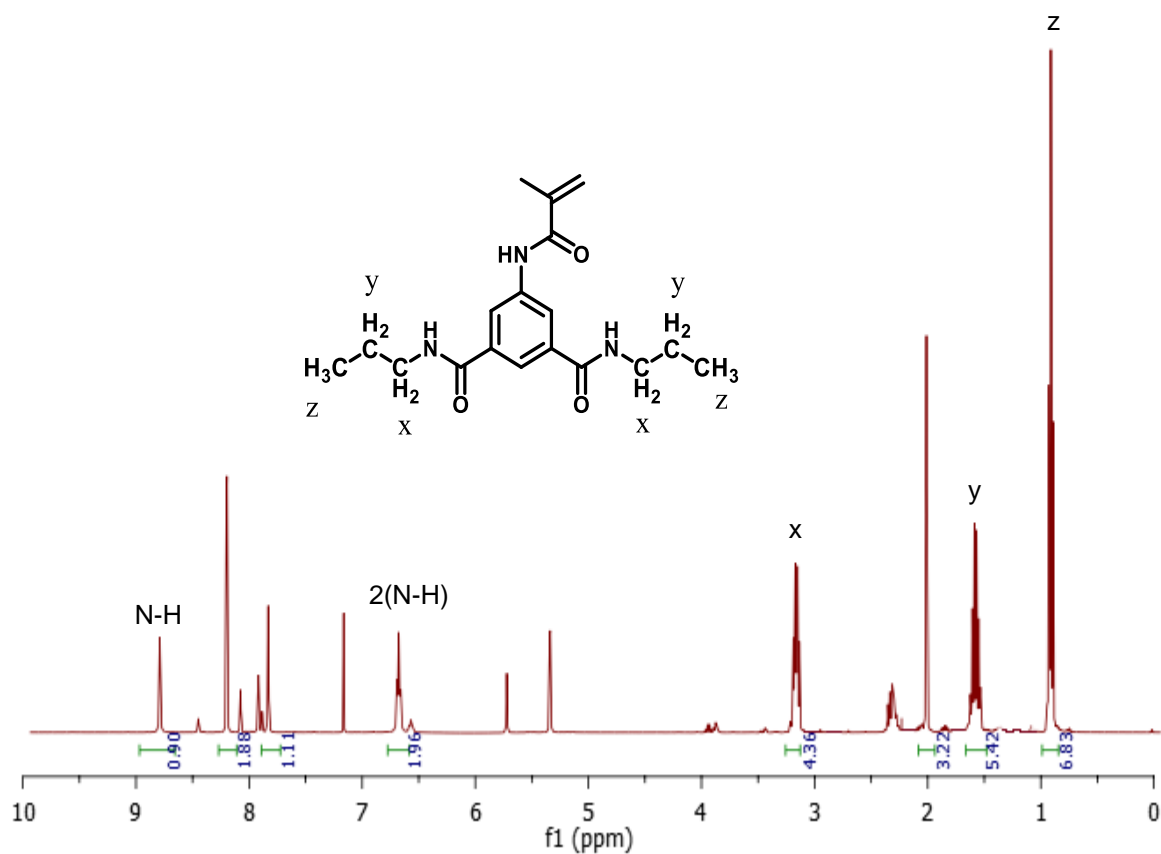


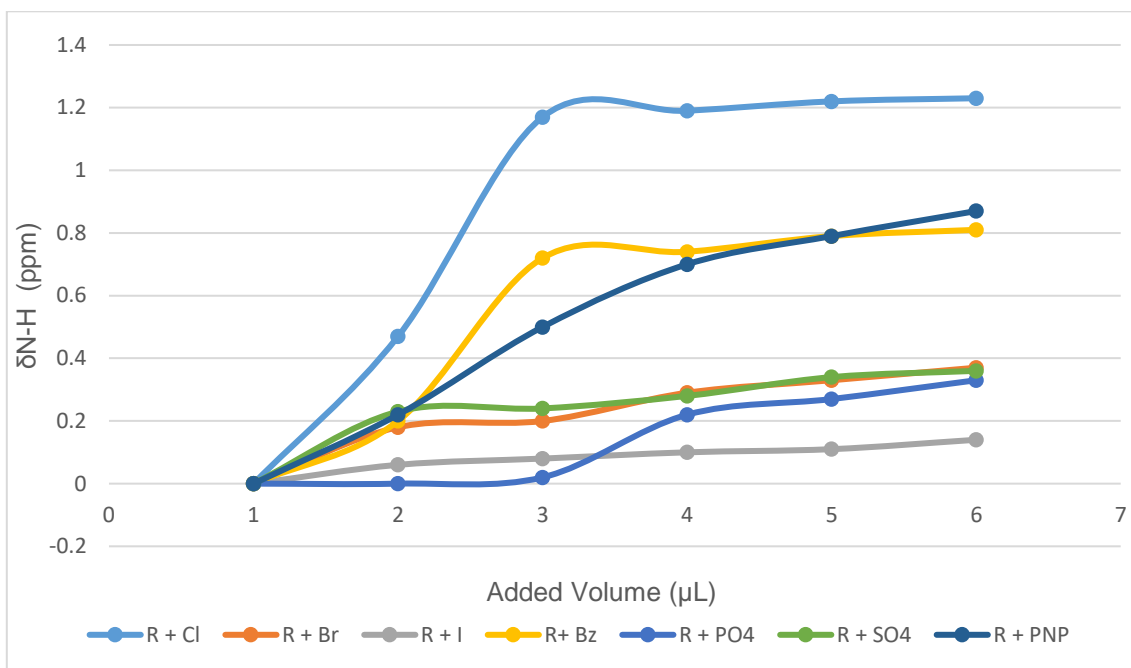
Figure 5.9: The ¹H NMR spectrum for 5-acryloylamide-N,N'-dipropylamine isophthalamide monomer

5.3.5. Anion binding assay using ¹H NMR titration

Following the successful synthesis of an anion receptor based on isophthalamide **R4**, the next step was to evaluate the anion binding properties. This was carried out using a ¹H NMR titration. To study the relative affinity of receptor **R4**, a variety of anions were chosen, including chloride, bromide, iodide, benzoate, sulphate, phosphate, and phenolate. These ¹H NMR experiments were carried out using d-chloroform as solvent; the anions used were in the form of their tetrabutyl ammonium salts.

Each titration solution began with 1 mL of the host species in an NMR tube at a concentration of 20 mg/mL. Then, 10 to 50 μL aliquots of an anion stock solution of the same concentration were added to the NMR tube and the spectrum recorded. The chemical shifts (ppm) of the NH protons

and the proton H_a with reference to the carbonyl group were monitored. After each addition of the anionic guest, the NH and H_a protons were observed to shift downfield. The data for various anions is illustrated in Graph 5.1, which shows that increasing anion concentration leads to an increase in $\Delta\delta$, due to hydrogen bonding between the isophthalamide receptor and the anions. Thus, the ^1H NMR titration analysis confirms that the synthesised core would bind anions.



Graph 5.1: ^1H NMR data obtained from titration of receptor **R4** against chloride, bromide, iodide, benzoate, phosphate, and sulphate anions.

This data indicates that receptor **R4** binds the chloride anion most strongly. Bromide and iodide binding was lower, which was due to their large size. Receptor **R4** had less ability to coordinate with tetrahedral anions such as phosphate and sulphate. The next step was to investigate a colourimetric displacement approach using Uv-Vis measurements and a complex of receptor **R4** with 4-nitrophenolate, which can be used to measure binding of other anions.

5.3.6 Displacement approach using UV-Vis spectroscopy

An investigation into whether the complex between receptor **R4** and phenolate would be broken via competitive binding with other anions was conducted as when binding takes place, the phenolate is released, producing a colour change that can be used as the basis for a colourimetric displacement assay. The colourimetric properties of this complex were studied using UV-Vis spectroscopy.

The addition of **R4** (1×10^{-2} M) to a solution of TBA-PNP (0.6×10^{-5} M) in CH_2Cl_2 at room temperature caused a significant decrease in intensity of the phenolate peak at 432 nm (Figure 5.10). This colour change was attributed to the formation of a new receptor complex (**R5**).

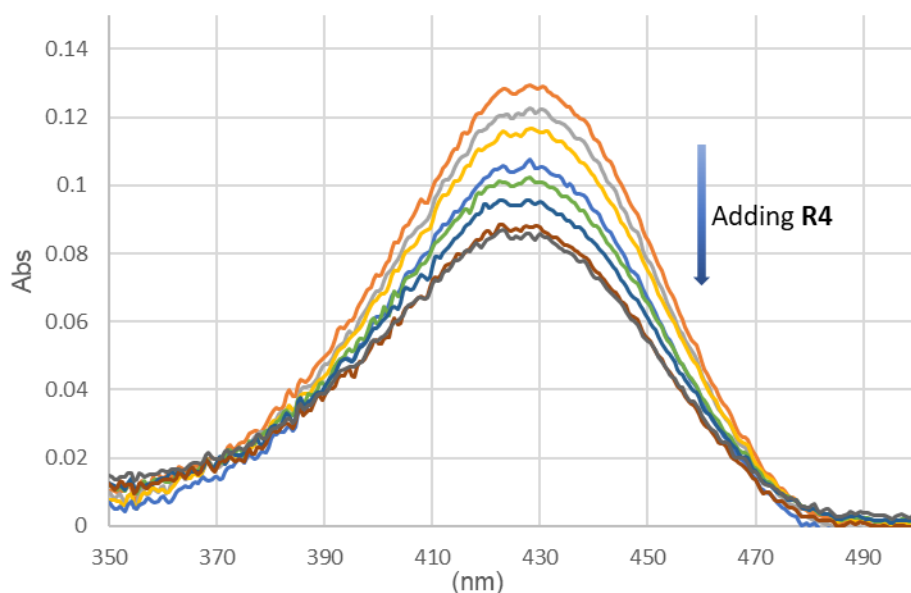
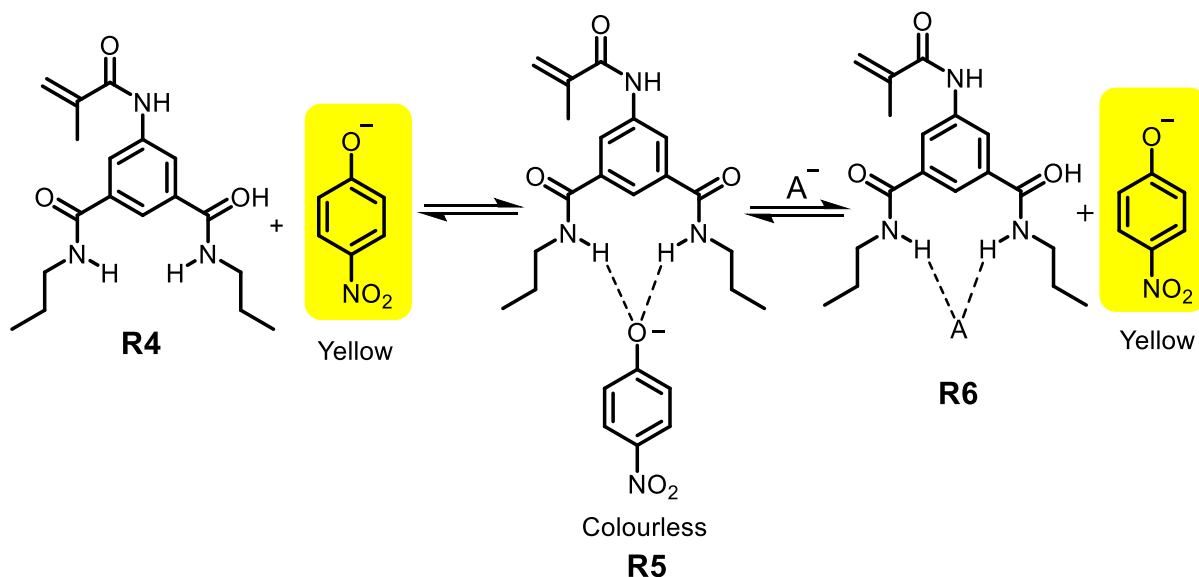


Figure 5.10: Decreasing absorbance of 4-nitrophenolate anion upon addition of **R4** in CH_2Cl_2 .

This solution was studied as a probe/sensor for anions. Specifically, when other anions are added to this colourless solution, they can compete for binding to the receptor and release phenolate. At this point the colour will return, as shown in Scheme 5.14.



Scheme 5.14: Addition of anions to solutions of ion sensor complex causing the yellow colour of the *p*-nitrophenolate anion to return as it is displaced from the **R4** anion binding site

The experiment was carried out by adding solutions of tetrabutylammonium chloride, bromide, benzoate, phosphate, and sulphate (1×10^{-3} M in all cases) to the PNP complex **R5** (1×10^{-4} M). The resultant absorption at the PNP λ_{max} were recorded. All experiments were repeated three times and the data averaged. (Figure 5.11).

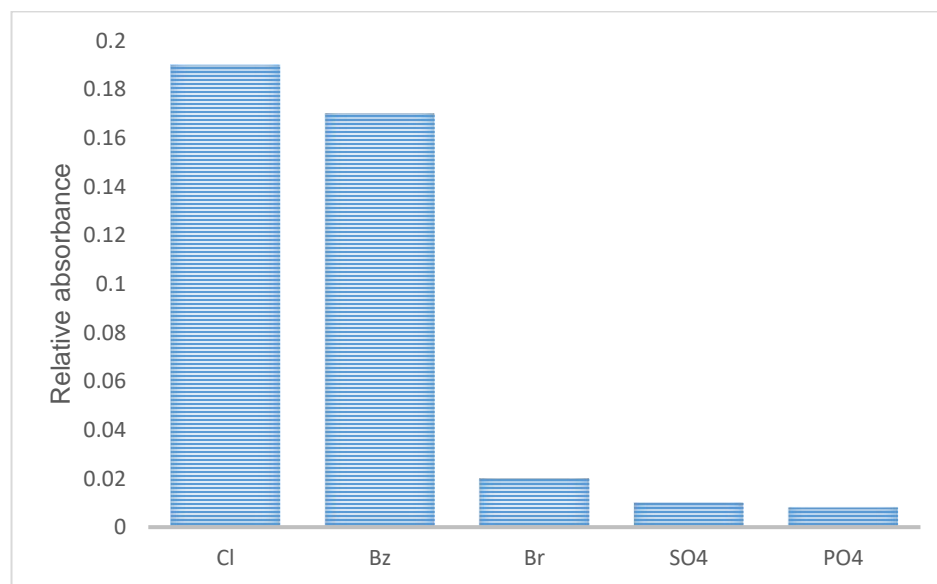


Figure 5.11: Relative absorbance of solutions containing **R4**, PNP, and various anions in DCM.

The relative absorbance values for each anion indicated that the strongest absorbance occurred with chloride, followed by benzoate. This trend reflects the relative affinities of receptor **R4** for these particular anions. The success of using receptor **R4** as an anion sensor allowed the project overall to continue, and the next step was synthesis of functionalized amphiphilic polymer that could self-assemble into a water based anion binding system.

5.3.7 Copolymerisation of methyl methacrylate and receptor **R4** using ATRP

Amphiphilic block copolymers such as mPEG-*b*-PS, can be synthesised using a standard radical method.²⁰⁵⁻²⁰⁸ However, conventional radical polymerisation methods can form large quantities of homo polymers or diblocks of inconsistent chain length.²⁰⁹ ATRP techniques are preferred, as they allow the preparation of polymers with greater control over chain length, thus reducing the quantity of homo polymers. This is particularly important when attempting to synthesise diblocks for use in self-assembly.

This copolymer of **R4** and MMA was synthesised in toluene using mPEG-Br as an initiator, with CuBr and N,N,N',N'',N''-pentamethyldiethylenetriamine (PMDETA) as a homogenous catalyst and ligand, respectively. A freeze-pump thaw cycle technique was used to deoxygenate the reaction flask to begin polymerisation, then after 15 hours, the mixture was cooled, diluted with DCM, and passed through a short Al₂O₃ column to remove the copper catalyst. The product was then obtained by precipitation with ether. After the reaction, the ¹HNMR results showed that the only product was mPEG-*b*-PMMA (Figure 4.12), and that no receptor had been incorporated.

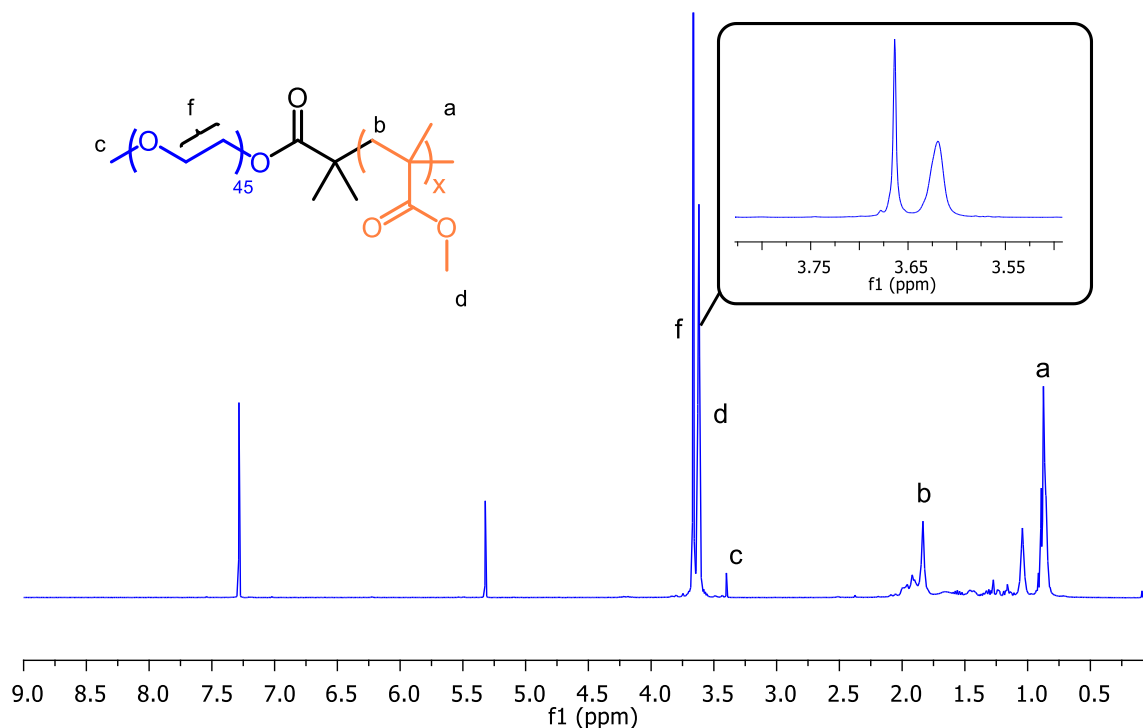


Figure 5.12: ¹H NMR in CDCl₃ of the polymer obtained by ATRP.

It was decided to repeat polymerisation using high oxidative state of the metal catalyst with reducing agent tin(II) 2-ethylhexanoate to avoid the oxygen sensitivity, which might increase the anion receptor content. Different ratios of MMA to receptor **R4** were used and the time of polymerisation increased to 24 hours. The reaction temperature was also increased to encourage the macroinitiator to be more reactive. However, the only polymer obtained in all cases was mPEG-*b*-PMMA. The crystals of receptor **R4** were then analysed using X-ray crystallography to determine whether anything about its structure might be preventing polymerisation (steric or geometric issues). However, the X-ray structure (Figure 5.13) did not show anything that might prevent polymerisation. At this point, it was assumed that the problem was due to reduced reactivity in receptor **R4**.

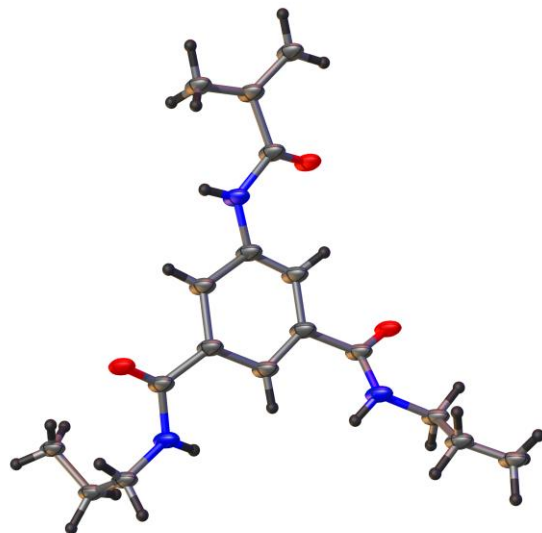


Figure 5.13: X-ray crystal structure of receptor **R4**.

However, on one occasion (21st attempt), some of receptor **R4** was observed in the polymer, albeit with low degree of polymerisation, as determined by ¹HNMR (Figure 5.14). An attempt was made to form a micelle from the product, but no signs of self-assembly was observed. Specifically, nothing was detected by DLS or CMC. At this stage, the work was halted due to time restrictions.

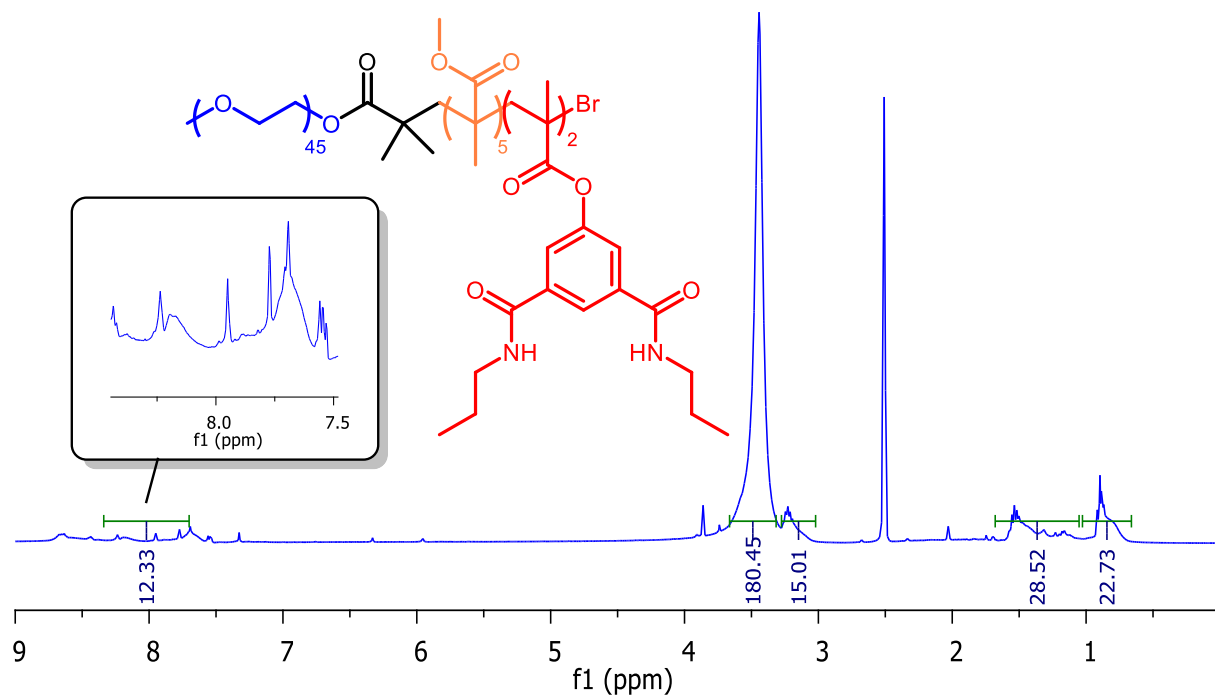


Figure 5.14: ¹HNMR in CDCl₃ of the polymer obtained by AGET ATRP.

5.5.4 Conclusion

For this project, it was necessary to bind anions in water. To achieve this, the search was made to find a way to encapsulate receptors within the hydrophobic core of a polymeric micelle. Specifically, it was important to covalently incorporate binding sites as co-monomers during controlled synthesis of an amphiphilic diblock polymer. This polymer would consist of a PEG block and a second block containing both the copolymer of methyl methacrylate and an anion receptor.

First, receptor **R3** (aromatic isophthalamide receptor) was synthesised. However, the lack of solubility of this receptor in most of organic solvents had prevented NMR binding study to be carried out. For this reason, an amide-linkage receptor with alkyl chain (**R4**) was synthesised using acid chloride and diisobutyl(amino)aluminium (DIBALH). Second, the binding studies was conducted with variety of anions using ¹HNMR. The data indicates that receptor **R4** binds the chloride anion most strongly. Displacement approach using Uiv-Vis measurements revealed that adding receptor **R4** to phenolate will decrease the intensity of yellow colour and forming receptor complex **R5**. Receptor complex **R6** was also formed as a results of adding variety of anions to the receptor complex **R5**, which makes the colour to come back. Finally, ATRP was used to synthesis the copolymer of methyl methacrylate and receptor **R4** using mPEG-Br as an initiator. Although, many attempts of polymerisation were conducted but low polymerisation degree of **R4** content within the copolymer was achieved.

5.5 Experimental

5.5.1 Chemicals and Instrumentation

Solvents and reagents

All chemicals and reagents were obtained from commercial supplier (primarily Sigma-Aldrich) and were used without further purification unless otherwise stated.

Nuclear magnetic resonance spectroscopy (NMR)

All NMR samples were prepared using deuterated solvents supplied by Sigma Aldrich. ^1H NMR and ^{13}C NMR spectra were recorded using a Bruker AV1400 MHz machine. The NMR spectra were analysed using Topspin 3.2 NMR software. Shifts are quoted as ppm and couplings quoted in Hertz.

Fourier transform infrared spectroscopy (FTIR)

FTIR spectroscopy was performed in the solid state (in reflectance mode) using Perkin Elmer Spectrum RX FT-IR System in the range of 700 to 4000 cm^{-1} .

UV-Vis spectroscopy

The ultraviolet absorbance was recorded on an Analytik Jena AG Specord s600 UV/Vis Spectrometer and analyzed using its attached Software (WinASPECT).

Fluorescence Spectroscopy

Fluorescence results were obtained using a HORIBA Scientific Fluoromax-4 spectrofluorometer using its attached software (FluorEssence V3).

Mass spectrometry

The form of ionisation used was dependent on the molecular weight of the sample in question. For samples with a low molecular weight, an Electrospray ionisation (ES) was used to record spectra. The instrument used was a WATERS LCT mass spectrometer. For samples with a high molecular weight, Matrix assisted laser desorption ionisation (MALDI) was required. The instrumentation used was a Bruker Reflex III MALDI -ToF mass spectrometer.

pH measurement

The pH of the buffer solutions prepared was substantiated using a pH 210 Microprocessor pH Meter from Hanna Instruments Ltd. (Leighton Buzzard, UK). The device was calibrated using pH 4.0 and pH 7.0 standard solutions, prepared with buffer tablets (Sigma-Aldrich, Poole, UK).

Dynamic light scattering (DLS)

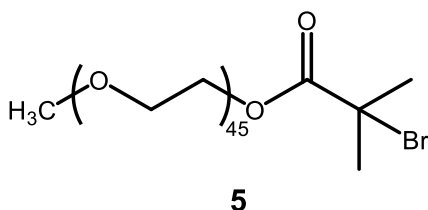
DLS results were obtained using the Brookhaven instrument 90 Plus Particle Size Analyser (Holtsville, NY, USA) 35 mW solid state standard laser. This instrumentation was used to determine the hydrodynamic diameter of nanoparticles. Particle sizing software 9kpsdw32.exe.ver.3.80 was used for characterisation. Light was scattered at an angle of 90 ° with each run lasting 2 minutes at a temperature of 37.5 °C. Samples were filtered using Whatman® GD/X syringe filters with a pore size of 0.45 µm, prior to analysis. Results reported are based upon volume distribution.

Gel Permeation Chromatography/ Size Exclusion Columns

Analytical THF GPC data was obtained at room temperature using either a high molecular weight column (3x300 mm PL gel 10 µm mixed-B), or a low molecular weight column (2x600 mm PL gel 5µm (500 Å) mixed-E). Calibration was achieved by using polystyrene standards (Mn 220-1,

1,000,000 Da) and molecular weights are thus reported relative to these specific standards used. The samples were run using Fisher GPC grade THF as a solvent stabilised with 0.025 % BHT (which was supplied to the columns by a Waters 515 HPLC Pump at 1.00 mLmin⁻¹). Toluene was added to prepared sample as a flow marker, before injection through a 200 μ L sample loop with a Gilson 234 Auto Injector. The concentration of a sample was studied using an Erma ERC-7512 refractive index detector and, where applicable, by UV using a Waters Millipore Lambda Max 481 LC Spectrophotometer. Aqueous GPC data was acquired using a Millipore Waters Lambda-Max 481 LC spectrometer with a LMW/HMW column. The eluent which was used was NaNO₃/NaH₂PO₄ (pH=7) buffer solution (unless stated otherwise). The data attained was then analysed using GPC-online software. Samples were filtered using Whatman® GD/X syringe filters with a pore size of 0.45 μ m prior to analysis.

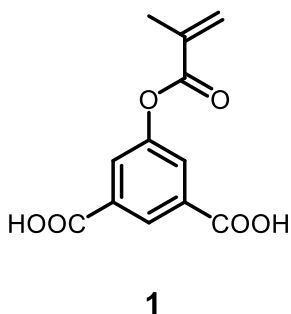
5.5.2 Synthesis of mPEG macroinitiator (5)



A solution of mPEG₂₀₀₀ (10 g, 5.0 mmol) and TEA (1.4 mL, 10 mmol) in 80 mL anhydrous toluene was cooled in an ice-water bath. 2-Bromoisobutyryl bromide (1.2 mL, 10 mmol) was then slowly added over 30 min via syringe to the reaction under continuous stirring and nitrogen bubbling. The reaction was warmed up to room temperature and further stirred for 2 days. After the reaction, the solution was filtered to remove the by-product triethylamine hydrobromide precipitate. The solvent was half evaporated and then the polymer was precipitated in a 10 fold excess of cold diethyl ether. The resulting product was dissolved in CH₂Cl₂ and extracted with alkaline water. The organic layer was harvested and dried over MgSO₄, then the solvent was removed under reduced pressure and the product obtained was dried in vacuum oven (at 38 °C). Yield 3 g, (60%).

$^1\text{H NMR}$ (CDCl_3 , 400 MHz) δ : 4.31 (t, 2H); 3.64 (m, 178H); 3.39 (s, 3H); 1.95 (s, 6H). FTIR (cm^{-1}): 2867 (s, aliphatic C-H), 1636, 1461 (C-O). Mass spec (MALDI): 2142.

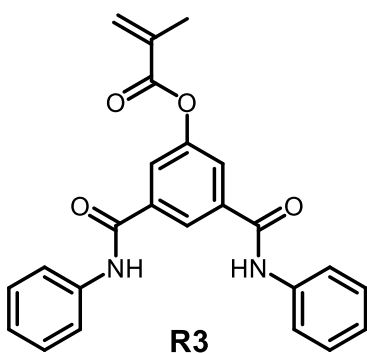
5.5.3 Synthesis of 5-methacryloyloxy isophthalic acid (1)



5-Hydroxy-isophthalic acid (1.0 g, 5.4 mmol) was dissolved in 10 mL water and NaOH (0.68 g, 16.2 mmol) was then added. This suspension was cooled using ice bath and within 2 hours a solution of methacryloyl chloride (0.62 mL, 5.4 mmol) in 5 mL diethyl ether was added. The reaction solution was stirred overnight at room temperature. After the reaction, the organic phase was separated and the crude product was precipitated out of the aqueous phase after adding dilute HCl (10:1). The product was washed with water several times and dried. Yield 0.87 g (87%).

$^1\text{H NMR}$ (CD_3SOCD_3), δ : 13.52 ppm (s, 2H); 8.36 (s, 1H); 7.97 (s, 2H); 6.33 (s, 1H); 5.91 (s, 1H); 2.01 (s, 3H). $^{13}\text{C NMR}$ (CDCl_3 , 400 MHz, δ : 18.3, 120.9, 125.3, 132.4, 140.3, 166.9, and 167.5. Mass spec (MH^+): 251, m.p. = 254-256 $^\circ\text{C}$.

5.5.4 Synthesis of 5-methacryloyloxy isophthaloyl-N,N'-diphenyl amine monomer (R3)

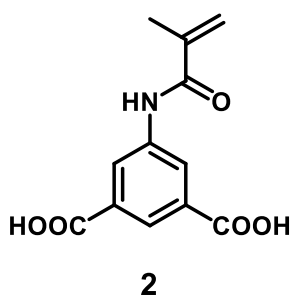


A one-neck round bottom flask was charged with freshly distilled aniline (1.25 g, 5 mmol) and 4-DMAP (1.3 g, 10 mmol) then dissolved in 100 mL anhydrous THF. The reaction mixture was cooled to 0-5 C with ice water bath. After degassing for 10min, a mixture of 5-methacryloyloxy isophthalic acid (0.93 mL, 10 mmol) and EDC (2.1 g, 1.0 mmol) were dissolved in anhydrous THF and then were added to solution. After stirring for 2h, the reaction mixture was stirred overnight at room temperature. 20-30 mL distilled water was added, then the THF was evaporated under

reduced pressure. The resulting precipitate was filtered and washed twice with water dried at room temperature. Further purification was conducted by flash column chromatography using $\text{CH}_2\text{Cl}_2/\text{acetonitrile}$ (10:1) as the eluent to give the white product. Yield 1.0 g, 80%.

^1H NMR (DMSO- d_6 , 400 MHz) δ : 10.50 (s, 2H) 8.50 (s, 1H) 8.01 (s, 2H), 7.80 (m, 4H), 7.40 (t, 4H), 7.13 (t, 2H), 6.37 (s, 1H), 5.99 (s, 1H), 2.06 (s, 3H). ^{13}C NMR (DMSO- d_6 , 400 MHz) δ : 18.4, 120.8, 124.9, 129.1, 137.2, 137.7, 139.3, 164.2, and 165.4. Mass spec (MH^+): 401.2.

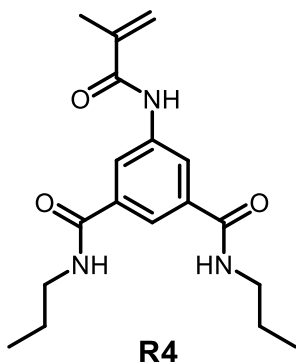
5.5.5 Synthesis of 5-methacrylamide isophthalic acid (2)



A mixture of 5-amino-isophthalic acid (1.8 g, 10 mmol), and TEA (1.4 mL) in 50 mL of toluene was given a dropwise addition of methacryloyl chloride (1.3 g, 12.5 mmol) over the course of 30 min at 0-5 °C. The reaction was stirred for further 6 hours. The filtrate was washed free of triethylamine hydrochloride with 500-600 mL of 3 N aqueous HCl. The product obtained was dried and recrystallized from 30% aqueous ethanol. Yield 1.4 g (80%).

^1H NMR (DMSO- d_6 , 400 MHz) δ : 13.10 (br,s, 2H), 10.80 (s, 1H), 8.02 (s, 1H), 7.92 (s, 2H), 5.70 (s, 1H); 5.40 (s, 1H); 1.98 (s, 3H). ^{13}C NMR (DMSO- d_6 , 400 MHz) δ : 18.3, 120.9, 125.3, 132.4, 140.3, 166.9, and 167.4. Mass spec (MH^+): 250.

5.5.6 Synthesis of 5-methacrylamide-N,N'-dipropyl isophthalamide (R4)



Three necked round bottom flask equipped with a magnetic stirrer, nitrogen inlet, and a condenser was charged with 5-methacrylamide isophthalic acid **11** (1.0 g, 4.4 mmol), freshly distilled thionyl chloride (10.0 mL) and 5.0 mL of DMF. The flask was stirred at room temperature for 30 min and then gently heated up to 60 °C for 6 h. Excess of amount

of thionyl chloride and solvent was then distilled off. The resulting pale yellow product the bis acyl chloride was used directly for the next reaction.

First procedure followed for amide formation by different bases (pyridine, TEA and excess of amine): To the residue, 20.0 mL of CHCl_3 and 2.2 mL of base (TEA) were added. After the solution was cooled down to 0-5 °C, a twofold amount of n-propylamine was added slowly and stirred for 2 h. The reaction solution was then evaporated and the crude product was purified by silica gel column chromatography using ethyl acetate/ hexane (1:1) as eluent to give a white solid product; yield 0.21 g (21%).

Second procedure followed for amide formation using DIBALH: A dried and argon flushed flask equipped with a magnetic stirrer was charged with propylamine (1.47 mL) and 10 mL of THF. After cooling to 0 °C, DIBALH (15.6 mL, 1.1 M in hexane) was added dropwise. The reaction was stirred for 3 h at room temperature and then a solution of isophthaloyl chloride solution was added slowly over 10 min and stirred for further 10 min. the reaction was stopped by adding 10 mL of 1N HCl and water. The product was separated with diethyl ether (2 x 10 mL) and the organic layers were dried over MgSO_4 , then filtered and concentrated under reduced pressure. The resulting product was purified by column chromatography on silica gel; yield 0.7 g, (70%)

^1H NMR (CDCl_3), δ ppm: 8.87 (s, 1H); 8.29 (s, 2H); 7.93 (s, 1H); 6.80 (s, 2H); 5.87 (s, 1H); 5.49 (s, 1H); 3.36 (q, 4H); 2.05 (s, 3H); 1.61 (m, 4H); 0.95 (t, 6H). ^{13}C NMR (CDCl_3 , 400 MHz, δC): 11.9, 19.1, 22.8, 41.7, 120.9, 121.0, 122.3, 136.0, 139.6, 140.6, 166.1, and 167.0. Mass spec (MH^+): 332, m.p. = 128-130 °C.

5.5.7 ATRP (General procedure)

A Schlenk flask with a magnetic stir bar and a rubber septum was charged with mPEG-Br (3 g, 1.5 mmol), MMA (0.15 mL, 1.5 mmol), receptor **12** (0.6 g, 1.5 mmol), PMDETA (0.52 mL, 3 mmol) and toluene (20 mL). The flask was deoxygenated by three freeze-pump thaw cycles, backfilled

with nitrogen, and then CuBr (0.22 g, 1.50 mmol) was introduced into the flask under the protection of nitrogen flow. Finally, the reaction mixture was degassed with another three freeze pump thaw cycles, and then sealed followed by immersing the flask into an oil bath and stirred at 70 °C to start the polymerisation. After reaction overnight, the flask was taken away from the bath, and the reaction mixture was cooled to room temperature; the reaction mixture was diluted with DCM (10 mL) and then passed through a short Al₂O₃ column (basic, activated) to remove the copper catalyst. The resulting solution was concentrated and poured into anhydrous ethyl ether to precipitate the product. The product was separated by filtration and further purified by redissolving/precipitating with DCM/ethyl ether, and finally dried in vacuum for 3 days.

5.5.8 AGET ATRP (General procedure)

All polymerisation procedures were conducted in a Radleys Carousel 12 place Reaction Station. The general procedure in the presence of air was as follows; mPEG-Br (3 g, 1.5 mmol), CuBr (0.22 g, 1.5 mmol), PMDETA (0.52 mL, 3 mmol), MMA (0.15 mL, 1.5 mmol), receptor **12** (0.6 g, 1.5 mmol), and DMF (20 mL) were added into a dry Schlenk tube under stirring. The flask was thoroughly purged by vacuum and flushed with nitrogen (three cycles). 300 µL of tin(II) 2-ethylhexanoate (Sn(Oct)₂) was added to the reaction mixture via syringe. The mixture was bubbled with nitrogen for 10 min. The reaction flask was then in a Radleys Carousel 12 place Reaction Station at 90 °C. After a definite time, the tube was placed in an ice bath to stop the reaction. The resultant mixture was then poured into methanol for precipitation. The polymer was obtained by filtration, washing and drying in vacuum for two days.

¹HNMR (CDCl₃), δ ppm: 7.6-7.54(br m, 3H), 3.45 (s, 180H), 3.23 (t, 3H), 1.55-1.47 (br m 2H), 0.9 (m, 3H).

References

- (1) Bianchi, A.; Bowman-James, K.; García-España, E. *Supramolecular Chemistry of Anions*; Vch Pub, 1997.
- (2) Christianson, D. W.; Lipscomb, W. N. Carboxypeptidase A. *Acc. Chem. Res.* **1989**, *22* (2), 62–69.
- (3) Puglisi, J. D.; Chen, L.; Frankel, A. D.; Williamson, J. R. Role of RNA Structure in Arginine Recognition of TAR RNA. *Proc. Natl. Acad. Sci.* **1993**, *90* (8), 3680–3684.
- (4) Berg, J. M. Zinc Finger Domains: From Predictions to Design. *Acc. Chem. Res.* **1995**, *28* (1), 14–19.
- (5) Haridas, V.; Sahu, S.; Kumar, P. P. P.; Sapala, A. R. Triazole: A New Motif for Anion Recognition. *RSC Adv.* **2012**, *2* (33), 12594–12605.
- (6) Caputo, A.; Hinzpeter, A.; Caci, E.; Pedemonte, N.; Arous, N.; Di Duca, M.; Zegarra-Moran, O.; Fanen, P.; Galiotta, L. J. V. Mutation-Specific Potency and Efficacy of Cystic Fibrosis Transmembrane Conductance Regulator Chloride Channel Potentiators. *J. Pharmacol. Exp. Ther.* **2009**, *330* (3), 783–791.
- (7) Grasemann, H.; Ratjen, F. Emerging Therapies for Cystic Fibrosis Lung Disease. *Expert Opin. Emerg. Drugs* **2010**, *15* (4), 653–659.
- (8) Gelboin, H. V.; Battula, N.; Gonzalez, F. J.; Moss, B. Recombinant Vaccinia Virus Encoding Cytochromes P-450. Google Patents April 9, 1996.
- (9) Glidewell, C. Nitrate/Nitrite Controversy. *Chem. Br.* **1990**, *26*, 137–140.
- (10) Beer, P. D.; Gale, P. A. Anion Recognition and Sensing: The State of the Art and Future Perspectives. *Angew. Chemie Int. Ed.* **2001**, *40* (3), 486–516.
- (11) Shannon, R. D. Revised Effective Ionic Radii and Systematic Studies of Interatomic Distances in Halides and Chalcogenides. *Acta Crystallogr. A* **1976**, *32* (5), 751–767.
- (12) Pascal Jr, R. A.; Spergel, J.; Van Engen, D. Synthesis and X-Ray Crystallographic

- Characterization of a (1, 3, 5) Cyclophane with Three Amide NH Groups Surrounding a Central Cavity. A Neutral Host for Anion Complexation. *Tetrahedron Lett.* **1986**, 27 (35), 4099–4102.
- (13) Valiyaveetil, S.; Engbersen, J. F. J.; Verboom, W.; Reinhoudt, D. N. Synthese Und Komplexierungsverhalten Ungeladener Anionen-Rezeptoren. *Angew. Chemie* **1993**, 105 (6), 942–944.
- (14) Valiyaveetil, S.; Engbersen, J. F. J.; Verboom, W.; Reinhoudt, D. N. Synthesis and Complexation Studies of Neutral Anion Receptors. *Angew. Chemie Int. Ed. English* **1993**, 32 (6), 900–901.
- (15) Raposo, C.; Pérez, N.; Almaraz, M.; Mussons, M. L.; Caballero, M. C.; Morán, J. R. A Cyclohexane Spacer for Phosphate Receptors. *Tetrahedron Lett.* **1995**, 36 (18), 3255–3258.
- (16) Bisson, A. P.; Lynch, V. M.; Monahan, M. C.; Anslyn, E. V. Recognition of Anions through NH \cdots π Hydrogen Bonds in a Bicyclic Cyclophane—Selectivity for Nitrate. *Angew. Chemie Int. Ed. English* **1997**, 36 (21), 2340–2342.
- (17) Kelly, T. R.; Kim, M. H. Relative Binding Affinity of Carboxylate and Its Isosteres: Nitro, Phosphate, Phosphonate, Sulfonate, and δ -Lactone. *J. Am. Chem. Soc.* **1994**, 116 (16), 7072–7080.
- (18) Bühlmann, P.; Nishizawa, S.; Xiao, K. P.; Umezawa, Y. Strong Hydrogen Bond-Mediated Complexation of H₂PO₄⁻ by Neutral Bis-Thiourea Hosts. *Tetrahedron* **1997**, 53 (5), 1647–1654.
- (19) Gale, P. A.; Sessler, J. L.; Kral, V.; Lynch, V. Calix [4] Pyrroles: Old yet New Anion-Binding Agents. *J. Am. Chem. Soc.* **1996**, 118 (21), 5140–5141.
- (20) Sessler, J. L.; Gale, P. A.; Genge, J. W. Calix [4] Pyrroles: New Solid-phase HPLC Supports for the Separation of Anions. *Chem. Eur. J.* **1998**, 4 (6), 1095–1099.
- (21) Sessler, J.; Bleasdale, E.; Gale, P. Anthracene-Linked Calix [4] Pyrroles: Fluorescent

Chemosensors for Anions. *Chem. Commun.* **1999**, No. 17, 1723–1724.

- (22) Sessler, J. L.; Gebauer, A.; Gale, P. A. Anion Binding and Electrochemical Properties of Calix [4] Pyrrole Ferrocene Conjugates. *Gazz. Chim. Ital.* **1997**, *127*, 723–726.
- (23) Andrievsky, A.; Ahuis, F.; Sessler, J. L.; Vögtle, F.; Gudat, D.; Moini, M. Bipyrrrole-Based [2] Catenane: A New Type of Anion Receptor. *J. Am. Chem. Soc.* **1998**, *120* (37), 9712–9713.
- (24) Park, C. H.; Simmons, H. E. Macrobicyclic Amines. III. Encapsulation of Halide Ions by in, in-1,(K+ 2)-Diazabicyclo [Klm] Alkane Ammonium Ions. *J. Am. Chem. Soc.* **1968**, *90* (9), 2431–2432.
- (25) Hosseini, M. W.; Lehn, J. M. Anion Receptor Molecules. Chain Length Dependent Selective Binding of Organic and Biological Dicarboxylate Anions by Ditopic Polyammonium Macrocycles. *J. Am. Chem. Soc.* **1982**, *104* (12), 3525–3527.
- (26) Hosseini, M. W.; Lehn, J. Anion Coreceptor Molecules. Linear Molecular Recognition in the Selective Binding of Dicarboxylate Substrates by Ditopic Polyammonium Macrocycles. *Helv. Chim. Acta* **1986**, *69* (3), 587–603.
- (27) Bauer, V. J.; Clive, D. L. J.; Dolphin, D.; Paine III, J. B.; Harris, F. L.; King, M. M.; Loder, J.; Wang, S. W. C.; Woodward, R. B. Sapphyrins: Novel Aromatic Pentapyrrolic Macrocycles. *J. Am. Chem. Soc.* **1983**, *105* (21), 6429–6436.
- (28) Sessler, J. L.; Cyr, M. J.; Lynch, V.; McGhee, E.; Ibers, J. A. Synthetic and Structural Studies of Sapphyrin, a 22- π -Electron Pentapyrrolic "Expanded Porphyrin". *J. Am. Chem. Soc.* **1990**, *112* (7), 2810–2813.
- (29) Sessler, J. L.; Cyr, M.; Furuta, H.; Král, V.; Mody, T.; Morishima, T.; Shionoya, M.; Weghorn, S. Anion Binding: A New Direction in Porphyrin-Related Research. *Pure Appl. Chem.* **1993**, *65* (3), 393–398.
- (30) Echavarren, A.; Galan, A.; Lehn, J. M.; De Mendoza, J. Chiral Recognition of Aromatic

- Carboxylate Anions by an Optically Active Abiotic Receptor Containing a Rigid Guanidinium Binding Subunit. *J. Am. Chem. Soc.* **1989**, *111* (13), 4994–4995.
- (31) Inoue, Y.; Hakushi, T.; Liu, Y.; Tong, L.; Shen, B.; Jin, D. Thermodynamics of Molecular Recognition by Cyclodextrins. 1. Calorimetric Titration of Inclusion Complexation of Naphthalenesulfonates with. Alpha.-, Beta.-, and. Gamma.-Cyclodextrins: Enthalpy-Entropy Compensation. *J. Am. Chem. Soc.* **1993**, *115* (2), 475–481.
- (32) Steed, J. W.; Johnson, C. P.; Juneja, R. K.; Atwood, J. L.; Burkhalter, R. S. Anion Inclusion within the Cavity of π -Metalated Pt-Butylcalix [5] Arene. *Supramol. Chem.* **1996**, *6* (3–4), 235–238.
- (33) Staffilani, M.; Hancock, K. S. B.; Steed, J. W.; Holman, K. T.; Atwood, J. L.; Juneja, R. K.; Burkhalter, R. S. Anion Binding within the Cavity of π -Metalated Calixarenes. *J. Am. Chem. Soc.* **1997**, *119* (27), 6324–6335.
- (34) Watson, J. D.; Milner-White, E. J. A Novel Main-Chain Anion-Binding Site in Proteins: The Nest. A Particular Combination of ϕ , ψ Values in Successive Residues Gives Rise to Anion-Binding Sites That Occur Commonly and Are Found Often at Functionally Important Regions. *J. Mol. Biol.* **2002**, *315* (2), 171–182.
- (35) Afzal, A. M.; Al-Shubailly, F.; Leader, D. P.; Milner-White, E. J. Bridging of Anions by Hydrogen Bonds in Nest Motifs and Its Significance for Schellman Loops and Other Larger Motifs within Proteins. *Proteins Struct. Funct. Bioinforma.* **2014**, *82* (11), 3023–3031.
- (36) Milner-White, E. J.; Russell, M. J. Sites for Phosphates and Iron-Sulfur Thiolates in the First Membranes: 3 to 6 Residue Anion-Binding Motifs (Nests). *Orig. Life Evol. Biosph.* **2005**, *35* (1), 19–27.
- (37) Ramakumar, S.; Ramagopal, U. A.; Inai, Y.; Goel, S.; Sahal, D.; Chauhan, V. S. De Novo Design and Characterization of a Helical Hairpin Eicosapeptide: Emergence of an Anion Receptor in the Linker Region. *Structure* **2004**, *12* (3), 389–396.

- (38) Bianchi, A.; Giorgi, C.; Ruzza, P.; Toniolo, C.; Milner-White, E. J. A Synthetic Hexapeptide Designed to Resemble a Proteinaceous P-loop Nest Is Shown to Bind Inorganic Phosphate. *Proteins Struct. Funct. Bioinforma.* **2012**, *80* (5), 1418–1424.
- (39) Denessiouk, K. A.; Johnson, M. S.; Denesyuk, A. I. Novel Ca²⁺ Structural Motif for Protein Recognition of Phosphate Ions. *J. Mol. Biol.* **2005**, *345* (3), 611–629.
- (40) Sheet, T.; Banerjee, R. Sulfate Ion Interaction with ‘Anion Recognition’ Short Peptide Motif at the N-Terminus of an Isolated Helix: A Conformational Landscape. *J. Struct. Biol.* **2010**, *171* (3), 345–352.
- (41) Sheet, T.; Supakar, S.; Banerjee, R. Conformational Preference of ‘Ca²⁺’ Short Peptide Motif towards Recognition of Anions. *PLoS One* **2013**, *8* (3), e57366.
- (42) Aguilar-Barajas, E.; Díaz-Pérez, C.; Ramírez-Díaz, M. I.; Riveros-Rosas, H.; Cervantes, C. Bacterial Transport of Sulfate, Molybdate, and Related Oxyanions. *Biometals* **2011**, *24* (4), 687–707.
- (43) Koropatkin, N. M.; Pakrasi, H. B.; Smith, T. J. Atomic Structure of a Nitrate-Binding Protein Crucial for Photosynthetic Productivity. *Proc. Natl. Acad. Sci.* **2006**, *103* (26), 9820–9825.
- (44) Koropatkin, N. M.; Koppelaar, D. W.; Pakrasi, H. B.; Smith, T. J. The Structure of a Cyanobacterial Bicarbonate Transport Protein, CmpA. *J. Biol. Chem.* **2007**, *282* (4), 2606–2614.
- (45) Niemann, V.; Koch-Singenstreu, M.; Neu, A.; Nilkens, S.; Götz, F.; Unden, G.; Stehle, T. The NreA Protein Functions as a Nitrate Receptor in the Staphylococcal Nitrate Regulation System. *J. Mol. Biol.* **2014**, *426* (7), 1539–1553.
- (46) Hollenstein, K.; Comellas-Bigler, M.; Bevers, L. E.; Feiters, M. C.; Meyer-Klaucke, W.; Hagedoorn, P.-L.; Locher, K. P. Distorted Octahedral Coordination of Tungstate in a Subfamily of Specific Binding Proteins. *JBIC J. Biol. Inorg. Chem.* **2009**, *14* (5), 663–672.
- (47) Aryal, B. P.; Brugarolas, P.; He, C. Binding of ReO₄⁻ with an Engineered MoO₄²⁻

- Binding Protein: Towards a New Approach in Radiopharmaceutical Applications. *JBIC J. Biol. Inorg. Chem.* **2012**, *17* (1), 97–106.
- (48) Famulok, M.; Mayer, G.; Blind, M. Nucleic Acid Aptamers from Selection in Vitro to Applications in Vivo. *Acc. Chem. Res.* **2000**, *33* (9), 591–599.
- (49) Ellington, A. D.; Szostak, J. W. In Vitro Selection of RNA Molecules That Bind Specific Ligands. *Nature* **1990**, *346* (6287), 818.
- (50) Tuerk, C.; Gold, L. Systematic Evolution of Ligands by Exponential Enrichment: RNA Ligands to Bacteriophage T4 DNA Polymerase. *Science* (80-.). **1990**, *249* (4968), 505–510.
- (51) Seetharaman, S.; Zivarts, M.; Sudarsan, N.; Breaker, R. R. Immobilized RNA Switches for the Analysis of Complex Chemical and Biological Mixtures. *Nat. Biotechnol.* **2001**, *19* (4), 336.
- (52) Li, J.; Lu, Y. A Highly Sensitive and Selective Catalytic DNA Biosensor for Lead Ions. *J. Am. Chem. Soc.* **2000**, *122* (42), 10466–10467.
- (53) Srinivasan, J.; Cload, S. T.; Hamaguchi, N.; Kurz, J.; Keene, S.; Kurz, M.; Boomer, R. M.; Blanchard, J.; Epstein, D.; Wilson, C. ADP-Specific Sensors Enable Universal Assay of Protein Kinase Activity. *Chem. Biol.* **2004**, *11* (4), 499–508.
- (54) Sazani, P. L.; Larralde, R.; Szostak, J. W. A Small Aptamer with Strong and Specific Recognition of the Triphosphate of ATP. *J. Am. Chem. Soc.* **2004**, *126* (27), 8370–8371.
- (55) Song, Y.; Zhao, C.; Ren, J.; Qu, X. Rapid and Ultra-Sensitive Detection of AMP Using a Fluorescent and Magnetic Nano-Silica Sandwich Complex. *Chem. Commun.* **2009**, No. 15, 1975–1977.
- (56) Li, Y.; Geyer, R.; Sen, D. Recognition of Anionic Porphyrins by DNA Aptamers. *Biochemistry* **1996**, *35* (21), 6911–6922.
- (57) Kwon, H.; Jiang, W.; Kool, E. T. Pattern-Based Detection of Anion Pollutants in Water with DNA Polyfluorophores. *Chem. Sci.* **2015**, *6* (4), 2575–2583.

- (58) Selman Garcia, M. Management of Low Radioactive Waste.-Comparative Analysis from the Norwegian Oil and Gas Industry. Høgskolen i Molde 2011.
- (59) Liland, A.; Strand, P.; Amundsen, I.; Natvig, H.; Nilsen, M.; Lystad, R.; Frogg, K. E. Advances in NORM Management in Norway and the Application of ICRP's 2007 Recommendations. *Ann. ICRP* **2012**, *41* (3–4), 332–342.
- (60) Barescut, J.; Eriksen, D. Ø.; Sidhu, R.; Ramsøy, T.; Strålberg, E.; Iden, K. I.; Rye, H.; Hylland, K.; Ruus, A.; Berntssen, M. H. G. Radioactivity in Produced Water from Norwegian Oil and Gas Installations—Concentrations, Bioavailability, and Doses to Marine Biota. *Radioprotection* **2009**, *44* (5), 869–874.
- (61) Wakoff, B.; Nagy, K. L. Perrhenate Uptake by Iron and Aluminum Oxyhydroxides: An Analogue for Per technetate Incorporation in Hanford Waste Tank Sludges. *Environ. Sci. Technol.* **2004**, *38* (6), 1765–1771. <https://doi.org/10.1021/es0348795>.
- (62) Katayev, E. A.; Kolesnikov, G. V.; Sessler, J. L. Molecular Recognition of Per technetate and Perrhenate. *Chem. Soc. Rev.* **2009**, *38* (6), 1572–1586. <https://doi.org/10.1039/b806468g>.
- (63) Cornes, S. P.; Sambrook, M. R.; Beer, P. D. Selective Perrhenate Recognition in Pure Water by Halogen Bonding and Hydrogen Bonding Alpha-Cyclodextrin Based Receptors. *Chem. Commun.* **2017**, *53* (27), 3866–3869. <https://doi.org/10.1039/c7cc01605k>.
- (64) Ali, A. H.; Mheemmed, A. K.; Hassan, H. I. Concentration Measurements of Uranium, Thorium and Their Daughter Products in Water Produced from and near Oil Fields in North of Iraq Using SSNTRD's Passive Method. *J. Radioanal. Nucl. Chem.* **2015**, *303* (1), 959–965.
- (65) Evans, N. H.; Beer, P. D. Advances in Anion Supramolecular Chemistry: From Recognition to Chemical Applications. *Angew. Chemie Int. Ed.* **2014**, *53* (44), 11716–11754.
- (66) Langton, M. J.; Serpell, C. J.; Beer, P. D. Anion Recognition in Water: Recent Advances

- from a Supramolecular and Macromolecular Perspective. *Angew. Chemie Int. Ed.* **2016**, *55* (6), 1974–1987.
- (67) Kawaguchi, T.; Moore, J. S.; Walker, K. L.; Wilkins, C. L. Double Exponential Dendrimer Growth. *J. Am. Chem. Soc.* **1995**, *117* (8), 2159–2165. <https://doi.org/10.1021/ja00113a005>.
- (68) Hult, A.; Johansson, M.; Malmström, E. Hyperbranched Polymers. In *Branched Polymers II*; Springer, 1999; pp 1–34.
- (69) Voit, B. I. Hyperbranched Polymers: A Chance and a Challenge. *Comptes Rendus Chim.* **2003**, *6* (8–10), 821–832. <https://doi.org/10.1016/j.crci.2003.07.004>.
- (70) Kowsari, E. Synthesis and Applications of Hyperbranched Polymers. *Polym. Synth.* **2011**, *40*, 99–111. <https://doi.org/10.1016/j.eurpolymj.2004.02.007>.
- (71) Flory, P. J. Molecular Size Distribution in Three Dimensional Polymers. VI. Branched Polymers Containing A-R-Bf-1 Type Units. *J. Am. Chem. Soc.* **1952**, *74* (11), 2718–2723. <https://doi.org/10.1021/ja01131a008>.
- (72) Kim, Y. H.; Webster, O. W. Water-Soluble Hyperbranched Polyphenylene; “A Unimolecular Micelle”? *J. Am. Chem. Soc.* **1990**, *112* (11), 4592–4593. <https://doi.org/10.1021/ja00167a094>.
- (73) Hawker, C. J.; Lee, R.; Fréchet, J. M. J. One-Step Synthesis of Hyperbranched Dendritic Polyesters. *J. Am. Chem. Soc.* **1991**, *113* (12), 4583–4588. <https://doi.org/10.1021/ja00012a030>.
- (74) Liu, M.; Vladimirov, N.; Fréchet, J. M. J. A New Approach to Hyperbranched Polymers by Ring-Opening Polymerization of an AB Monomer: 4-(2-Hydroxyethyl)-ε-Caprolactone. *Macromolecules* **1999**, *32* (20), 6881–6884. <https://doi.org/10.1021/ma990785x>.
- (75) Karak, N. *Fundamentals of Polymers: Raw Materials to Finish Products*; PHI Learning Pvt. Ltd., 2009.
- (76) Voit, B. New Developments in Hyperbranched Polymers. *J. Polym. Sci. Part A Polym.*

- Chem.* **2000**, 38 (14), 2505–2525. [https://doi.org/10.1002/1099-0518\(20000715\)38:14<2505::AID-POLA10>3.0.CO;2-8](https://doi.org/10.1002/1099-0518(20000715)38:14<2505::AID-POLA10>3.0.CO;2-8).
- (77) Kim, Y. H. Hyperbranched Polymers 10 Years After. *J. Polym. Sci. Part A Polym. Chem.* **1998**, 36 (11), 1685–1698. [https://doi.org/10.1002/\(SICI\)1099-0518\(199808\)36:11<1685::AID-POLA1>3.0.CO;2-R](https://doi.org/10.1002/(SICI)1099-0518(199808)36:11<1685::AID-POLA1>3.0.CO;2-R).
- (78) Uhrich, K. E.; Hawker, C. J.; Fréchet, J. M. J.; Turner, S. R. One-Pot Synthesis of Hyperbranched Polyethers. *Macromolecules* **1992**, 25 (18), 4583–4587. <https://doi.org/10.1021/ma00044a019>.
- (79) Spindler, R.; Fréchet, J. M. J. Synthesis and Characterization of Hyperbranched Polyurethanes Prepared from Blocked Isocyanate Monomers by Step-Growth Polymerization. *Macromolecules* **1993**, 26 (18), 4809–4813. <https://doi.org/10.1021/ma00070a013>.
- (80) Fréchet, J. M. J.; Henmi, M.; Gitsov, I.; Aoshima, S.; Leduc, M. R.; Grubbs, R. B. Self-Condensing Vinyl Polymerization: An Approach to Dendritic Materials. *Science* (80-.). **1995**, 269 (5227), 1080–1083. <https://doi.org/10.1126/science.269.5227.1080>.
- (81) Hawker, C. J.; Dao, J.; Fréchet, J. M. J.; Grubbs, R. B. Preparation of Hyperbranched and Star Polymers by a “Living”, Self-Condensing Free Radical Polymerization. *J. Am. Chem. Soc.* **1995**, 117 (43), 10763–10764. <https://doi.org/10.1021/ja00148a027>.
- (82) Suzuki, M.; Atsuhiko, L.; Saegusa, T. Multibranching Polymerization: Palladium-Catalyzed Ring-Opening Polymerization of Cyclic Carbamate To Produce Hyperbranched Dendritic Polyamine. *Macromolecules* **1992**, 25 (25), 7071–7072. <https://doi.org/10.1021/ma00051a055>.
- (83) Sunder, A.; Hanselmann, R.; Frey, H.; Mu, R. Controlled Synthesis of Hyperbranched Polyglycerols by Ring-Opening Multibranching Polymerization. *Society* **1999**, 4240–4246. <https://doi.org/10.1021/ma990090w>.

- (84) Stiriba, S. E.; Kautz, H.; Frey, H. Hyperbranched Molecular Nanocapsules: Comparison of the Hyperbranched Architecture with the Perfect Linear Analogue. *J. Am. Chem. Soc.* **2002**, *124* (33), 9698–9699. <https://doi.org/10.1021/ja026835m>.
- (85) Burakowska, E.; Quinn, J. R.; Zimmerman, S. C.; Haag, R. Cross-Linked Hyperbranched Polyglycerols as Hosts for Selective Binding of Guest Molecules. *J. Am. Chem. Soc.* **2009**, *131* (30), 10574–10580. <https://doi.org/10.1021/ja902597h>.
- (86) Stiriba, S. E.; Frey, H.; Haag, R. Dendritic Polymers in Biomedical Applications: From Potential to Clinical Use in Diagnostics and Therapy. *Angew. Chemie - Int. Ed.* **2002**, *41* (8), 1329–1334. [https://doi.org/10.1002/1521-3773\(20020415\)41:8<1329::AID-ANIE1329>3.0.CO;2-P](https://doi.org/10.1002/1521-3773(20020415)41:8<1329::AID-ANIE1329>3.0.CO;2-P).
- (87) Liu, C.; Gao, C.; Yan, D. Synergistic Supramolecular Encapsulation of Amphiphilic Hyperbranched Polymer to Dyes. *Macromolecules* **2006**, *39* (23), 8102–8111. <https://doi.org/10.1021/ma0608065>.
- (88) Chen, Y.; Shen, Z.; Pastor-Pérez, L.; Frey, H.; Stiriba, S. E. Role of Topology and Amphiphilicity for Guest Encapsulation in Functionalized Hyperbranched Poly(Ethylenimine)S. *Macromolecules* **2005**, *38* (2), 227–229. <https://doi.org/10.1021/ma047837p>.
- (89) Lin, Y.; Liu, X.; Dong, Z.; Li, B.; Chen, X.; Li, Y. S. Amphiphilic Core-Shell Nanocarriers Based on Hyperbranched Poly(Ester Amide)-Star-PCL: Synthesis, Characterization, and Potential as Efficient Phase Transfer Agent. *Biomacromolecules* **2008**, *9* (10), 2629–2636. <https://doi.org/10.1021/bm800607a>.
- (90) Kirkorian, K.; Ellis, A.; Twyman, L. J. Catalytic Hyperbranched Polymers as Enzyme Mimics; Exploiting the Principles of Encapsulation and Supramolecular Chemistry. *Chem. Soc. Rev.* **2012**, *41* (18), 6138–6159. <https://doi.org/10.1039/c2cs35238a>.
- (91) Gittins, P. J.; Twyman, L. J. Postsynthetic Modification at the Focal Point of a

- Hyperbranched Polymer. *J. Am. Chem. Soc.* **2005**, *127* (6), 1646–1647.
<https://doi.org/10.1021/ja043909g>.
- (92) Burnett, J.; King, A. S. H.; Twyman, L. J. Probing the Onset of Dense Shell Packing by Measuring the Aminolysis Rates for a Series Amine Terminated Dendrimers. *React. Funct. Polym.* **2006**, *66* (1), 187–194. <https://doi.org/10.1016/j.reactfunctpolym.2005.07.022>.
- (93) Gittins, P. J.; Alston, J.; Ge, Y.; Twyman, L. J. Total Core Functionalization of a Hyperbranched Polymer. *Macromolecules* **2004**, *37* (20), 7428–7431.
<https://doi.org/10.1021/ma049149b>.
- (94) Kokan, Z.; Chmielewski, M. J. A Photoswitchable Heteroditopic Ion-Pair Receptor. *J. Am. Chem. Soc.* **2018**, *140* (47), 16010–16014. <https://doi.org/10.1021/jacs.8b08689>.
- (95) Painter, G. R.; Pressman, B. C. Dynamic Aspects of Ionophore Mediated Membrane Transport. *Top. Curr. Chem.* **1982**, *101*, 83–110. https://doi.org/10.1007/3-540-11103-4_7.
- (96) Reviews, B. Elementary Kinetics of Membrane Carrier Transport. *Comp. Biochem. Physiol. Part B Comp. Biochem.* **1974**, *47* (1), 233. [https://doi.org/10.1016/0305-0491\(74\)90109-6](https://doi.org/10.1016/0305-0491(74)90109-6).
- (97) Karabulut, S.; Namli, H.; Kurtaran, R.; Yildirim, L. T.; Leszczynski, J. Modeling the Intermolecular Interactions: Molecular Structure of N-3-Hydroxyphenyl-4-Methoxybenzamide. *J. Mol. Graph. Model.* **2014**, *48*, 1–8.
<https://doi.org/10.1016/j.jmgm.2013.11.001>.
- (98) Mann, G. Exploiting the Architectural Features of Various Macromolecules for Biomimetic Applications. *PhD Thesis* **2013**, No. September, 169–178.
- (99) Kavallieratos, K.; Bertao, C. M.; Crabtree, R. H. Hydrogen Bonding in Anion Recognition: A Family of Versatile, Nonpreorganized Neutral and Acyclic Receptors. *J. Org. Chem.* **1999**, *64* (5), 1675–1683. <https://doi.org/10.1021/jo982382l>.
- (100) Turner, S. R.; Voit, B. I.; Mourey, T. H. All-Aromatic Hyperbranched Polyesters with Phenol and Acetate End Groups: Synthesis and Characterization. *Macromolecules* **1993**, *26*

- (17), 4617–4623. <https://doi.org/10.1021/ma00069a031>.
- (101) Feast, W. J.; Stainton, N. M. Synthesis, Structure and Properties. **1995**, 5 (3), 405–411.
- (102) Adam Ellis- PhD.
- (103) Walbridge, D. J. Chain Polymerization II. **1989**, 4.
- (104) Szwarc, M. M. Szwarc, Nature, 1956, 178, 1168-1169. *Nature* **1956**, 1168–1169.
- (105) Denev, I.; Christova, D.; Markova, I. Synthesis of Diblock Copolymers for Obtaining Functionalized Nanoparticles. *J. Univ. Chem. Technol. Metall.* **2009**, 44 (1), 24–28.
- (106) Fontaine, L. Handbook of Ring-Opening Polymerization. Edited by Philippe Dubois, Olivier Coulembier and Jean-Marie Raquez. *Angew. Chemie Int. Ed.* **2009**, 48 (52), 9780–9780. <https://doi.org/10.1002/anie.200904840>.
- (107) Dechy-Cabaret, O.; Martin-Vaca, B.; Bourissou, D. Controlled Ring-Opening Polymerization of Lactide and Glycolide. *Chem. Rev.* **2004**, 104 (12), 6147–6176. <https://doi.org/10.1021/cr040002s>.
- (108) Labet, M.; Thielemans, W. Synthesis of Polycaprolactone: A Review. *Chem. Soc. Rev.* **2009**, 38 (12), 3484–3504. <https://doi.org/10.1039/b820162p>.
- (109) Albertsson, A. C.; Varma, I. K. Recent Developments in Ring Opening Polymerization of Lactones for Biomedical Applications. *Biomacromolecules* **2003**, 4 (6), 1466–1486. <https://doi.org/10.1021/bm034247a>.
- (110) Fiscaro, E.; Compari, C.; Braibanti, A. Entropy/Enthalpy Compensation: Hydrophobic Effect, Micelles and Protein Complexes. *Phys. Chem. Chem. Phys.* **2004**, 6 (16), 4156–4166. <https://doi.org/10.1039/b404327h>.
- (111) Smart, T.; Lomas, H.; Massignani, M.; Flores-Merino, M. V.; Perez, L. R.; Battaglia, G. Block Copolymer Nanostructures. *Nano Today* **2008**, 3 (3–4), 38–46. [https://doi.org/10.1016/S1748-0132\(08\)70043-4](https://doi.org/10.1016/S1748-0132(08)70043-4).
- (112) Sakaia, K.; Smith, E. G.; Webber, G. B.; Wanless, E. J.; Bütün, V.; Armes, S. P.; Biggs, S.

- Effects of Copolymer Concentration and Chain Length on the PH-Responsive Behavior of Diblock Copolymer Micellar Films. *J. Colloid Interface Sci.* **2006**, *303* (2), 372–379. [https://doi.org/10.1016/S0960-0779\(02\)00434-4](https://doi.org/10.1016/S0960-0779(02)00434-4).
- (113) Nose, T. Polymers in Solution. *Reports Prog. Polym. Phys. Japan* **2000**, *43*, 43–60. <https://doi.org/10.1088/0953-8984/2/1/001>.
- (114) Sakai, K.; Smith, E. G.; Webber, G. B.; Schatz, C.; Wanless, E. J.; Bütün, V.; Armes, S. P.; Biggs, S. PH-Responsive Diblock Copolymer Micelles at the Silica/Aqueous Solution Interface: Adsorption Kinetics and Equilibrium Studies. *J. Phys. Chem. B* **2006**, *110* (30), 14744–14753. <https://doi.org/10.1021/jp062830q>.
- (115) Steed, J. W. JL Atwood in Supramolecular Chemistry. *John Wiley&Sons* **2009**.
- (116) Mourya, V. K.; Inamdar, N.; Nawale, R. B.; Kulthe, S. S. Polymeric Micelles: General Considerations and Their Applications. *Indian J. Pharm. Educ. Res.* **2011**, *45* (2), 128–138.
- (117) Doncom, K. E. B.; Blackman, L. D.; Wright, D. B.; Gibson, M. I.; O'Reilly, R. K. Dispersity Effects in Polymer Self-Assemblies: A Matter of Hierarchical Control. *Chem. Soc. Rev.* **2017**, *46* (14), 4119–4134. <https://doi.org/10.1039/c6cs00818f>.
- (118) Lo, C. L.; Lin, K. M.; Huang, C. K.; Hsiue, G. H. Self-Assembly of a Micelle Structure from Graft and Diblock Copolymers: An Example of Overcoming the Limitations of Polyions in Drug Delivery. *Adv. Funct. Mater.* **2006**, *16* (18), 2309–2316. <https://doi.org/10.1002/adfm.200500627>.
- (119) Zhang, Y.; Li, X.; Zhou, Y.; Wang, X.; Fan, Y.; Huang, Y.; Liu, Y. Preparation and Evaluation of Poly(Ethylene Glycol)-Poly(Lactide) Micelles as Nanocarriers for Oral Delivery of Cyclosporine A. *Nanoscale Res. Lett.* **2010**, *5* (6), 917–925. <https://doi.org/10.1007/s11671-010-9583-4>.
- (120) Wang, J.; Wang, Y.; Liang, W. Delivery of Drugs to Cell Membranes by Encapsulation in PEG-PE Micelles. *J. Control. Release* **2012**, *160* (3), 637–651.

<https://doi.org/10.1016/j.jconrel.2012.02.021>.

- (121) Ma, G.; Zhang, C.; Zhang, L.; Sun, H.; Song, C.; Wang, C.; Kong, D. Doxorubicin-Loaded Micelles Based on Multiarm Star-Shaped PLGA–PEG Block Copolymers: Influence of Arm Numbers on Drug Delivery. *J. Mater. Sci. Mater. Med.* **2016**, *27* (1), 1–15. <https://doi.org/10.1007/s10856-015-5610-4>.
- (122) Sinha, V. R.; Bansal, K.; Kaushik, R.; Kumria, R.; Trehan, A. Poly- ϵ -Caprolactone Microspheres and Nanospheres: An Overview. *Int. J. Pharm.* **2004**, *278* (1), 1–23. <https://doi.org/10.1016/j.ijpharm.2004.01.044>.
- (123) Zabidi, M. A. Bin. Branched Polymers and Self-Assembled Polymer Complexes for Use As Artificial Blood. University of Sheffield 2015.
- (124) Kwon, G.; Naito, M.; Yokoyama, M.; Okano, T.; Sakurai, Y.; Kataoka, K. Micelles Based on AB Block Copolymers of Poly(Ethylene Oxide) and Poly(β -Benzyl L-Aspartate). *Langmuir* **1993**, *9* (4), 945–949. <https://doi.org/10.1021/la00028a012>.
- (125) Ananthapadmanabhan, K. P.; Goddard, E. D.; Turro, N. J.; Kuo, P. L. Fluorescence Probes for Critical Micelle Concentration. *Langmuir* **1985**, *1* (3), 352–355. <https://doi.org/10.1021/la00063a015>.
- (126) Chen, W. Y.; Alexandridis, P.; Su, C. K.; Patrickios, C. S.; Hertler, W. R.; Hatton, T. A. Effect of Block Size and Sequence on the Micellization of ABC Triblock Methacrylic Polyampholytes. *Macromolecules* **1995**, *28* (25), 8604–8611. <https://doi.org/10.1021/ma00129a020>.
- (127) Shin, I. G.; Kim, S. Y.; Lee, Y. M.; Cho, C. S.; Sung, Y. K. Methoxy Poly(Ethylene Glycol)/ ϵ -Caprolactone Amphiphilic Block Copolymeric Micelle Containing Indomethacin. I. Preparation and Characterization. *J. Control. Release* **1998**, *51* (1), 1–11. [https://doi.org/10.1016/S0168-3659\(97\)00164-8](https://doi.org/10.1016/S0168-3659(97)00164-8).
- (128) Astafieva, I.; Zhong, X. F.; Eisenberg, A. Critical Micellization Phenomena in Block

- Polyelectrolyte Solutions. *Macromolecules* **1993**, *26* (26), 7339–7352.
<https://doi.org/10.1021/ma00078a034>.
- (129) Zhao, C. Le; Winnik, M. A.; Riess, G.; Croucher, M. D. Fluorescence Probe Techniques Used To Study Micelle Formation in Water-Soluble Block Copolymers. *Langmuir* **1990**, *6* (2), 514–516. <https://doi.org/10.1021/la00092a038>.
- (130) R. Pecora. Dynamic Light Scattering Measurement of Nanometer Particles in Liquids. *J. Nanoparticle Res.* **2000**, *2*, 123–131.
- (131) Kaszuba, M.; McKnight, D.; Connah, M. T.; McNeil-Watson, F. K.; Nobbmann, U. Measuring Sub Nanometre Sizes Using Dynamic Light Scattering. *J. Nanoparticle Res.* **2008**, *10* (5), 823–829. <https://doi.org/10.1007/s11051-007-9317-4>.
- (132) Fiscaro, E.; Compari, C.; Duce, E.; Biemmi, M.; Peroni, M.; Braibanti, A. Thermodynamics of Micelle Formation in Water, Hydrophobic Processes and Surfactant Self-Assemblies. *Phys. Chem. Chem. Phys.* **2008**, *10* (26), 3903–3914. <https://doi.org/10.1039/b719630j>.
- (133) Topel, Ö.; Çakir, B. A.; Budama, L.; Hoda, N. Determination of Critical Micelle Concentration of Polybutadiene-Block- Poly(Ethyleneoxide) Diblock Copolymer by Fluorescence Spectroscopy and Dynamic Light Scattering. *J. Mol. Liq.* **2013**, *177*, 40–43. <https://doi.org/10.1016/j.molliq.2012.10.013>.
- (134) Lavasanifar, A.; Samuel, J.; Kwon, G. S. Poly(Ethylene Oxide)-Block-Poly(L-Amino Acid) Micelles for Drug Delivery. *Adv. Drug Deliv. Rev.* **2002**, *54* (2), 169–190. [https://doi.org/10.1016/S0169-409X\(02\)00015-7](https://doi.org/10.1016/S0169-409X(02)00015-7).
- (135) Jin, R. H. Controlled Location of Porphyrin in Aqueous Micelles Self-Assembled from Porphyrin Centered Amphiphilic Star Poly(Oxazolines). *Adv. Mater.* **2002**, *14* (12), 889–892. [https://doi.org/10.1002/1521-4095\(20020618\)14:12<889::AID-ADMA889>3.0.CO;2-6](https://doi.org/10.1002/1521-4095(20020618)14:12<889::AID-ADMA889>3.0.CO;2-6).
- (136) Mahou, R.; Wandrey, C. Versatile Route to Synthesize Heterobifunctional Poly(Ethylene

- Glycol) of Variable Functionality for Subsequent Pegylation. *Polymers (Basel)*. **2012**, *4* (1), 561–589. <https://doi.org/10.3390/polym4010561>.
- (137) Mishra, P.; Nayak, B.; Dey, R. K. PEGylation in Anti-Cancer Therapy: An Overview. *Asian J. Pharm. Sci.* **2016**, *11* (3), 337–348. <https://doi.org/10.1016/j.ajps.2015.08.011>.
- (138) Holtsberg, F. W.; Ensor, C. M.; Steiner, M. R.; Bomalaski, J. S.; Clark, M. A. Poly(Ethylene Glycol) (PEG) Conjugated Arginine Deiminase: Effects of PEG Formulations on Its Pharmacological Properties. *J. Control. Release* **2002**, *80* (1–3), 259–271. [https://doi.org/10.1016/S0168-3659\(02\)00042-1](https://doi.org/10.1016/S0168-3659(02)00042-1).
- (139) Whitesides, G. M.; Boncheva, M. Beyond Molecules: Self-Assembly of Mesoscopic and Macroscopic Components. *Proc. Natl. Acad. Sci. U. S. A.* **2002**, *99* (8), 4769–4774. <https://doi.org/10.1073/pnas.082065899>.
- (140) Chen, D.; Jiang, M. Strategies for Constructing Polymeric Micelles and Hollow Spheres in Solution via Specific Intermolecular Interactions. *Acc. Chem. Res.* **2005**, *38* (6), 494–502. <https://doi.org/10.1021/ar040113d>.
- (141) Yan, D.; Zhou, Y.; Hou, J. Supramolecular Self-Assembly Of. **2004**, *303* (January), 65–68.
- (142) Kawasaki, T.; Tokuhira, M.; Kimizuka, N.; Kunitake, T. Hierarchical Self-Assembly of Chiral Complementary Hydrogen-Bond Networks in Water: Reconstitution of Supramolecular Membranes. *J. Am. Chem. Soc.* **2001**, *123* (28), 6792–6800. <https://doi.org/10.1021/ja010035e>.
- (143) Jehng, J. M.; Chen, C. M. Amination of Polyethylene Glycol to Polyetheramine over the Supported Nickel Catalysts. *Catal. Letters* **2001**, *77* (1–3), 147–154. <https://doi.org/10.1023/A:1012782927451>.
- (144) Runeberg, J.; Baiker, A.; Kijenski, J. Applied Catalysis, 17 (1985) 309-319. *Appl. Catal.* **1985**, *17*, 309–319.
- (145) Zhang, L.; Zhang, P.; Zhao, Q.; Zhang, Y.; Cao, L.; Luan, Y. Doxorubicin-Loaded

- Polypeptide Nanorods Based on Electrostatic Interactions for Cancer Therapy. *J. Colloid Interface Sci.* **2016**, *464*, 126–136. <https://doi.org/10.1016/j.jcis.2015.11.008>.
- (146) Rich, R. R. L.; Myszka*, D. G.; Myszka, D. G. Survey of the Year 2005 Commercial Optical Biosensor Literature. *J. Mol. Recognit.* **2006**, *19* (March), 478–534. <https://doi.org/10.1002/jmr>.
- (147) Chmielewski, M. J.; Charon, M.; Jurczak, J. 1,8-Diamino-3,6-Dichlorocarbazole: A Promising Building Block for Anion Receptors. *Org. Lett.* **2004**, *6* (20), 3501–3504. <https://doi.org/10.1021/ol048661e>.
- (148) Molina, L.; Moreno-Clavijo, E.; Moreno-Vargas, A. J.; Carmona, A. T.; Robina, I. Synthesis of a C3-Symmetric Furyl-Cyclopeptide Platform with Anion Recognition Properties. *European J. Org. Chem.* **2010**, No. 21, 4049–4055. <https://doi.org/10.1002/ejoc.201000219>.
- (149) Dunetz, J. R.; Magano, J.; Weisenburger, G. A. Large-Scale Applications of Amide Coupling Reagents for the Synthesis of Pharmaceuticals. *Org. Process Res. Dev.* **2016**, *20* (2), 140–177. <https://doi.org/10.1021/op500305s>.
- (150) Bi, Y.; Yan, C.; Shao, L.; Wang, Y.; Ma, Y.; Tang, G. Well-Defined Thermoresponsive Dendritic Polyamide/Poly(N-Vinylcaprolactam) Block Copolymers. *J. Polym. Sci. Part A Polym. Chem.* **2013**, *51* (15), 3240–3250. <https://doi.org/10.1002/pola.26716>.
- (151) Valeur, E.; Bradley, M. Amide Bond Formation: Beyond the Myth of Coupling Reagents. *Chem. Soc. Rev.* **2009**, *38* (2), 606–631. <https://doi.org/10.1039/b701677h>.
- (152) Takeda, H.; Goshima, N.; Nomura, N. Chapter 8 Resonance. No. 3, 131–145. <https://doi.org/10.1007/978-1-60761-670-2>.
- (153) Martínez-Máñez, R.; Sancenón, F. *Fluorogenic and Chromogenic Chemosensors and Reagents for Anions*; 2003; Vol. 103. <https://doi.org/10.1021/cr010421e>.
- (154) Jung, H. S.; Park, M.; Han, D. Y.; Kim, E.; Lee, C.; Ham, S.; Kim, J. S. Cu²⁺ Ion-Induced Self-Assembly of Pyrenylquinoline with a Pyrenyl Excimer Formation. *Org. Lett.* **2009**, *11*

- (15), 3378–3381. <https://doi.org/10.1021/ol901221q>.
- (155) Zhang, R.; Tang, D.; Lu, P.; Yang, X.; Liao, D.; Zhang, Y.; Zhang, M.; Yu, C.; Yam, V. W. W. Nucleic Acid-Induced Aggregation and Pyrene Excimer Formation. *Org. Lett.* **2009**, *11* (19), 4302–4305. <https://doi.org/10.1021/ol901607g>.
- (156) Shao, J.; Lin, H.; Lin, H. A Novel Chromo- and Fluorogenic Dual Responding H₂PO₄ - Receptor Based on an Azo Derivative. *Dye. Pigment.* **2009**, *80* (2), 259–263. <https://doi.org/10.1016/j.dyepig.2008.07.012>.
- (157) Jang, H. H.; Yi, S.; Kim, M. H.; Kim, S.; Lee, N. H.; Han, M. S. A Simple Method for Improving the Optical Properties of a Dimetallic Coordination Fluorescent Chemosensor for Adenosine Triphosphate. *Tetrahedron Lett.* **2009**, *50* (46), 6241–6243. <https://doi.org/10.1016/j.tetlet.2009.09.016>.
- (158) Colorimetric, E.; Han, M. S.; Kim, D. H. <Naked-Eye Detection of Phosphate Ions in.Pdf>. **2002**, *2* (3800), 3809–3811.
- (159) Henderson, L. C.; Li, J.; Nation, R. L.; Velkov, T.; Pfeffer, F. M. Developing an Anion Host for Lipid A Binding and Antibacterial Activity. *Chem. Commun.* **2010**, *46* (18), 3197–3199. <https://doi.org/10.1039/b925135a>.
- (160) Davis, J. T.; Gale, P. A.; Okunola, O. A.; Prados, P.; Iglesias-Sánchez, J. C.; Torroba, T.; Quesada, R. Using Small Molecules to Facilitate Exchange of Bicarbonate and Chloride Anions across Liposomal Membranes. *Nat. Chem.* **2009**, *1* (2), 138–144. <https://doi.org/10.1038/nchem.178>.
- (161) Swinburne, A. N.; Paterson, M. J.; Beeby, A.; Steed, J. W. Fluorescent “twist-on” Sensing by Induced-Fit Anion Stabilisation of a Planar Chromophore. *Chem. - A Eur. J.* **2010**, *16* (9), 2714–2718. <https://doi.org/10.1002/chem.200903293>.
- (162) Duke, R. M.; O’Brien, J. E.; McCabe, T.; Gunnlaugsson, T. Colorimetric Sensing of Anions in Aqueous Solution Using a Charge Neutral, Cleft-like, Amidothiourea Receptor: Tilting

- the Balance between Hydrogen Bonding and Deprotonation in Anion Recognition. *Org. Biomol. Chem.* **2008**, *6* (22), 4089–4092. <https://doi.org/10.1039/b807579d>.
- (163) Dos Santos, C. M. G.; Gunnlaugsson, T. Exploring the Luminescent Sensing of Anions by the Use of an Urea Functionalised 1,10-Phenanthroline (Phen)-Based (3:1) Eu(III) Complex. *Supramol. Chem.* **2009**, *21* (1–2), 173–180. <https://doi.org/10.1080/10610270802588285>.
- (164) Liu, Y. L.; Palacios, M. A.; Anzenbacher, P. The Power of the Weak: Recognition of Ion Pairs in Water Using a Simple Array Sensor. *Chem. Commun.* **2010**, *46* (11), 1860–1862. <https://doi.org/10.1039/b925506k>.
- (165) Massue, J.; Quinn, S. J.; Gunnlaugsson, T. Lanthanide Luminescent Displacement Assays: The Sensing of Phosphate Anions Using Eu(III)-Cyclen-Conjugated Gold Nanoparticles in Aqueous Solution. *J. Am. Chem. Soc.* **2008**, *130* (22), 6900–6901. <https://doi.org/10.1021/ja800361e>.
- (166) Gale, P. A.; Tong, C. C.; Haynes, C. J. E.; Adeosun, O.; Gross, D. E.; Karnas, E.; Sedenberg, E. M.; Quesada, R.; Sessler, J. L. Octafluorocalix [4] Pyrrole : A Chloride / Bicarbonate Antiport Agent. **2010**, No. 3, 3240–3241.
- (167) Duke, R. M.; Veale, E. B.; Pfeffer, F. M.; Kruger, P. E.; Gunnlaugsson, T. Colorimetric and Fluorescent Anion Sensors: An Overview of Recent Developments in the Use of 1,8-Naphthalimide-Based Chemosensors. *Chem. Soc. Rev.* **2010**, *39* (10), 3936–3953. <https://doi.org/10.1039/b910560n>.
- (168) Beer, P. D. Anion Selective Recognition and Optical/Electrochemical Sensing by Novel Transition-Metal Receptor Systems. *Chem. Commun.* **1996**, No. 6, 689–696. <https://doi.org/10.1039/cc9960000689>.
- (169) Sessler, J. L.; Anzenbacher, P.; Miyaji, H.; Jursikova, K.; Bleasdale, E. R.; Gale, P. A. Modified Calix[4]Pyrroles. *Ind. Eng. Chem. Res.* **2000**, *39* (10), 3471–3478. <https://doi.org/10.1021/ie000102y>.

- (170) Beer, P. D.; Keefe, A. D. A New Approach to the Coordination of Anions, Novel Polycobalticinium Macrocyclic Receptor Molecules. *J. Organomet. Chem.* **1989**, 375 (1), 1–3. [https://doi.org/10.1016/0022-328X\(89\)85105-8](https://doi.org/10.1016/0022-328X(89)85105-8).
- (171) Metzger, A.; Anslyn, E. V. A Chemosensor for Citrate in Beverages. *Angew. Chemie - Int. Ed.* **1998**, 37 (5), 649–652. [https://doi.org/10.1002/\(SICI\)1521-3773\(19980316\)37:5<649::AID-ANIE649>3.0.CO;2-H](https://doi.org/10.1002/(SICI)1521-3773(19980316)37:5<649::AID-ANIE649>3.0.CO;2-H).
- (172) Sessler, J. L.; Tvermoes, N. A.; Davis, J.; Anzenbacher, P.; Jursíková, K.; Sato, W.; Seidel, D.; Lynch, V.; Black, C. B.; Try, A.; et al. Expanded Porphyrins. Synthetic Materials with Potential Medical Utility. *Pure Appl. Chem.* **1999**, 71 (11), 2009–2018. <https://doi.org/10.1351/pac199971112009>.
- (173) Kubot, M. Colorimetric Chiral Recognition NH (Yt :’ OH (NoH. **1996**, 382 (June), 522–524.
- (174) Gale, P. A.; Twyman, L. J.; Handlin, C. I.; Sessler, J. L. A Colourimetric Calix[4]pyrrole-4-Nitrophenolate Based Anion Sensor. *Chem. Commun.* **1999**, 2 (18), 1851–1852. <https://doi.org/10.1039/a905743i>.
- (175) Amendola, V.; Bergamaschi, G.; Boiocchi, M.; Fabbrizzi, L.; Mosca, L. The Interaction of Fluoride with Fluorogenic Ureas: An ON 1-OFF-ON2 Response. *J. Am. Chem. Soc.* **2013**, 135 (16), 6345–6355. <https://doi.org/10.1021/ja4019786>.
- (176) Heon Oh, S.; Ryoo, R.; Shik Jhon, M. Iodine-127 and Potassium-39 NMR Study of the Interaction of Ions with Water-Soluble Polymers. *Macromolecules* **1990**, 23 (6), 1671–1675. <https://doi.org/10.1021/ma00208a019>.
- (177) Song, J. D.; Ryoo, R.; Jhon, M. S. Anion Binding Properties of Poly(Vinylpyrrolidone) in Aqueous Solution Studied by Halide NMR Spectroscopy. *Macromolecules* **1991**, 24 (8), 1727–1730. <https://doi.org/10.1021/ma00008a006>.
- (178) Zhang, Y.; Furyk, S.; Bergbreiter, D. E.; Cremer, P. S. Specific Ion Effects on the Water

- Solubility of Macromolecules: PNIPAM and the Hofmeister Series. *J. Am. Chem. Soc.* **2005**, *127* (41), 14505–14510. <https://doi.org/10.1021/ja0546424>.
- (179) Rembert, K. B.; Okur, H. I.; Hilty, C.; Cremer, P. S. An NH Moiety Is Not Required for Anion Binding to Amides in Aqueous Solution. *Langmuir* **2015**, *31* (11), 3459–3464. <https://doi.org/10.1021/acs.langmuir.5b00127>.
- (180) Kim, H.; Kim, Y.; Chang, J. Y. Polymers for Luminescent Sensing Applications. *Macromol. Chem. Phys.* **2014**, *215* (13), 1274–1285. <https://doi.org/10.1002/macp.201400128>.
- (181) Zhao, X.; Schanze, K. S. Fluorescent Ratiometric Sensing of Pyrophosphate via Induced Aggregation of a Conjugated Polyelectrolyte. *Chem. Commun.* **2010**, *46* (33), 6075–6077. <https://doi.org/10.1039/c0cc01332c>.
- (182) Li, E.; Lin, L.; Wang, L.; Pei, M.; Xu, J.; Zhang, G. Synthesis of a New Cationic Polythiophene Derivative and Its Application for Colorimetric and Fluorometric Detection of Iodide Ion and Anionic Surfactants in Water. *Macromol. Chem. Phys.* **2012**, *213* (9), 887–892. <https://doi.org/10.1002/macp.201200100>.
- (183) Fonseca, S. M.; Galvão, R. P.; Burrows, H. D.; Gutacker, A.; Scherf, U.; Bazan, G. C. Selective Fluorescence Quenching in Cationic Fluorene-Thiophene Diblock Copolymers for Ratiometric Sensing of Anions. *Macromol. Rapid Commun.* **2013**, *34* (9), 717–722. <https://doi.org/10.1002/marc.201200734>.
- (184) Chen, X.; Gao, B.; Kops, J.; Batsberg, W. Preparation of Polystyrene-Poly(Ethylene Glycol) Diblock Copolymer by “living” Free Radical Polymerisation. *Polymer (Guildf)*. **1998**, *39* (4), 911–915. [https://doi.org/10.1016/S0032-3861\(97\)00341-8](https://doi.org/10.1016/S0032-3861(97)00341-8).
- (185) Matyjaszewski, K. Radical Nature of Cu-Catalyzed Controlled Radical Polymerizations (Atom Transfer Radical Polymerization). *Macromolecules* **1998**, *31* (15), 4710–4717. <https://doi.org/10.1021/ma980357b>.
- (186) Li, Q.; Zhang, L.; Bai, L.; Miao, J.; Cheng, Z.; Zhu, X. Atom Transfer Radical

- Polymerization. *Prog. Chem.* **2010**, 22 (11), 2079–2088. <https://doi.org/10.1021/cr940534g>.
- (187) Giacomelli, C.; Borsali, R. ATRP of Silylated Glycerol Monomethacrylate in Organic Medium for Convenient Synthesis of Amphiphilic Copolymers. *Macromol. Rapid Commun.* **2008**, 29 (7), 573–579. <https://doi.org/10.1002/marc.200700803>.
- (188) Peng, Z.; Li, G.; Liu, X.; Tong, Z. Synthesis, PH-and Temperature-induced Micellization and Gelation of Doubly Hydrophilic Triblock Copolymer of Poly (N, N-dimethylamino-2-ethylmethacrylate)-b-poly (Ethylene Glycol)-b-poly (N, N-dimethylamino-2-ethylmethacrylate) in Aqueous Solutions. *J. Polym. Sci. Part A Polym. Chem.* **2008**, 46 (17), 5869–5878.
- (189) Wang, J. S.; Matyjaszewski, K. Controlled/“Living” Radical Polymerization. Atom Transfer Radical Polymerization in the Presence of Transition-Metal Complexes. *J. Am. Chem. Soc.* **1995**, 117 (20), 5614–5615. <https://doi.org/10.1021/ja00125a035>.
- (190) Beers, K. L.; Gaynor, S. G.; Matyjaszewski, K.; Sheiko, S. S.; Moeller, M. Synthesis of Densely Grafted Copolymers by Atom Transfer Radical Polymerization. *Macromolecules* **1998**, 31 (26), 9413–9415. <https://doi.org/10.1021/ma981402i>.
- (191) Matyjaszewski, K. Atom Transfer Radical Polymerization and the Synthesis of Polymeric Materials - Patten - 1999 - Advanced Materials - Wiley Online Library. *Adv. Mater.* **1998**, 901–915. [https://doi.org/10.1002/\(SICI\)1521-4095\(199808\)10:12<901::AID-ADMA901>3.3.CO;2-2](https://doi.org/10.1002/(SICI)1521-4095(199808)10:12<901::AID-ADMA901>3.3.CO;2-2).
- (192) Matyjaszewski, K. Transition Metal Catalysis in Controlled Radical Polymerization: Atom Transfer Radical Polymerization. *Chem. - A Eur. J.* **1999**, 5 (11), 3095–3102. [https://doi.org/10.1002/\(SICI\)1521-3765\(19991105\)5:11<3095::AID-CHEM3095>3.0.CO;2-#](https://doi.org/10.1002/(SICI)1521-3765(19991105)5:11<3095::AID-CHEM3095>3.0.CO;2-#).
- (193) Min, K.; Jakubowski, W.; Matyjaszewski, K. AGET ATRP in the Presence of Air in Miniemulsion and in Bulk. *Macromol. Rapid Commun.* **2006**, 27 (8), 594–598.

<https://doi.org/10.1002/marc.200600060>.

- (194) Kwiatkowski, P.; Jurczak, J.; Pietrasik, J.; Jakubowski, W.; Mueller, L.; Matyjaszewski, K. High Molecular Weight Polymethacrylates by AGET ATRP under High Pressure. *Macromolecules* **2008**, *41* (4), 1067–1069. <https://doi.org/10.1021/ma702770u>.
- (195) Oh, J. K.; Min, K.; Matyjaszewski, K. Preparation of Poly(Oligo(Ethylene Glycol) Monomethyl Ether Methacrylate) by Homogeneous Aqueous AGET ATRP. *Macromolecules* **2006**, *39* (9), 3161–3167. <https://doi.org/10.1021/ma060258v>.
- (196) Patten, T. E.; Matyjaszewski, K. Copper(I)-Catalyzed Atom Transfer Radical Polymerization. *Acc. Chem. Res.* **1999**, *32* (10), 895–903. <https://doi.org/10.1021/ar9501434>.
- (197) Lu, G.; Li, Y. M.; Lu, C. H.; Xu, Z. Z.; Zhang, H. AGET ATRP of Methyl Methacrylate by Silica-Gel-Supported Copper(II) Chloride/2-(8-Heptadecenyl)-4,5-Dihydro-1H-Imidazole-1-Ethylamine. *Des. Monomers Polym.* **2010**, *13* (6), 509–522. <https://doi.org/10.1163/138577210X530585>.
- (198) Hu, J.; Zhang, G.; Geng, Y.; Liu, S. Micellar Nanoparticles of Coil-Rod-Coil Triblock Copolymers for Highly Sensitive and Ratiometric Fluorescent Detection of Fluoride Ions. *Macromolecules* **2011**, *44* (20), 8207–8214. <https://doi.org/10.1021/ma201777p>.
- (199) Harris, M. J.; Zalipsky, S. Sherman, 1997.Pdf. *Poly(ethylene glycol) Chemistry and Biological Applications*. 1997.
- (200) Detrembleur, C.; Mazza, M.; Lou, X.; Halleux, O.; Lecomte, P.; Mecerreyes, D.; Hedrick, J. L.; Jérôme, R. New Functional Aliphatic Polyesters by Chemical Modification of Copolymers of ϵ -Caprolactone with γ -(2-Bromo-2-Methylpropionate)- ϵ -Caprolactone, γ -Bromo- ϵ -Caprolactone, and a Mixture of β - and γ -Ene- ϵ -Caprolactone. *Macromolecules* **2000**, *33* (21), 7751–7760. <https://doi.org/10.1021/ma000488o>.
- (201) Mecerreyes, D.; Atthoff, B.; Boduch, K. A.; Trollsås, M.; Hedrick, J. L. Unimolecular

- Combination of an Atom Transfer Radical Polymerization Initiator and a Lactone Monomer as a Route to New Graft Copolymers. *Macromolecules* **1999**, *32* (16), 5181–5182. <https://doi.org/10.1021/ma982005a>.
- (202) Wei, H.; Ravarian, R.; Dehn, S.; Perrier, S.; Dehghani, F. Construction of Temperature Responsive Hybrid Crosslinked Self-assemblies Based on PEG-b-P (MMA-co-MPMA)-b-PNIPAAm Triblock Copolymer: ATRP Synthesis and Thermoinduced Association Behavior. *J. Polym. Sci. Part A Polym. Chem.* **2011**, *49* (8), 1809–1820.
- (203) Abdul Aziz, A. Micromolecular Approaches to Protein Binding. University of Sheffield 2019.
- (204) Park, J. K.; Shin, W. K.; An, D. K. New and Efficient Synthesis of Amides from Acid Chlorides Using Diisobutyl(Amino)Aluminum. *Bull. Korean Chem. Soc.* **2013**, *34* (5), 1592–1594. <https://doi.org/10.5012/bkcs.2013.34.5.1592>.
- (205) Yu, K.; Zhang, L.; Eisenberg, A. Novel Morphologies of “Crew-Cut” Aggregates of Amphiphilic Diblock Copolymers in Dilute Solution. *Langmuir* **1996**, *12* (25), 5980–5984. <https://doi.org/10.1021/la960894u>.
- (206) Yu, K.; Hurd, A. J.; Eisenberg, A.; Brinker, C. J. Syntheses of Silica/Polystyrene-Block-Poly(Ethylene Oxide) Films with Regular and Reverse Mesostructures of Large Characteristic Length Scales by Solvent Evaporation-Induced Self-Assembly. *Langmuir* **2001**, *17* (26), 7961–7965. <https://doi.org/10.1021/la0113724>.
- (207) Khan, T. N.; Mobbs, R. H.; Price, C.; Quintana, J. R.; Stubbersfield, R. B. Synthesis and Colloidal Behaviour of a Polystyrene-b-Poly(Ethylene Oxide) Block Copolymer. *Eur. Polym. J.* **1987**, *23* (3), 191–194. [https://doi.org/10.1016/0014-3057\(87\)90072-3](https://doi.org/10.1016/0014-3057(87)90072-3).
- (208) Jialanella, G. L.; Firer, E. M.; Piirma, I. Synthesis of Polystyrene-block-polyoxyethylene for Use as a Stabilizer in the Emulsion Polymerization of Styrene. *J. Polym. Sci. Part A Polym. Chem.* **1992**, *30* (9), 1925–1933. <https://doi.org/10.1002/pola.1992.080300915>.

- (209) Jankova, K.; Truelsen, J. H.; Chen, X.; Kops, J.; Batsberg, W. Controlled/"living" Atom Transfer Radical Polymerization of Styrene in the Synthesis of Amphiphilic Diblock Copolymers from a Poly(Ethylene Glycol) Macroinitiator. *Polym. Bull.* **1999**, *42* (2), 153–158. <https://doi.org/10.1007/s002890050447>.